Dissecting the multispecies interaction network at the *A. thaliana* root-soil interface

Inaugural – Dissertation

zur
Erlangung des Doktorgrades
der Mathematisch-Naturwissenschaftlichen Fakultät
der Universität zu Köln

vorgelegt von

Paloma Durán Ballesteros

aus Madrid, Spanien

Köln, Juli 2019

Berichterstatter: Prof. Dr. Paul Schulze-Lefert
Prof. Dr. Marcel Bucher
Prüfungsvorsitz: Prof. Dr. Gunther Döhlemann

Tag der Disputation: 30. Juli 2018

MAX-PLANCK-GESELLSCHAFT

Die vorliegende Arbeit wurde am Max-Planck-Institut für Pflanzenzüchtungsforschung in Köln in der Abteilung für Pflanzen-Mikroben Interaktionen (Direktor Prof. Dr. Paul Schulze-Lefert) angefertigt.

Abstract

In nature, healthy and asymptomatic plants cohabit with a variety of microbes, such as bacteria, fungi, and oomycetes, forming complex microbial consortia that interact with each other and likely provide fitness benefits to the host plant. Advances in culture-independent methods have deepened our understanding on microbial communities' distribution in nature and the environmental factors shaping these communities. However, there is still a lack of consensus between studies and a more holistic approach is needed, by studying several microbial groups under a variety of environmental conditions. Importantly, there is a significant part of the microbial variance that remains unexplained in host-associated microbiota studies. Decades of research have shown that microbes interact with each other, indicating that microbe-microbe interactions might represent a major, yet poorly described, force driving microbial community establishment in and outside plant roots. In order to assess microbial communities´ functions and assembly rules, microbiota reconstitution experiments in gnotobiotic plant systems are needed. By linking microbial community profiling data from natural *Arabidopsis thaliana* populations (chapter I) with reconstruction experiments with synthetic microbial communities and germ-free plants (chapter II), I provide novel insight into how environment, host-microbe and microbe-microbe interactions affect microbial community structure and plant health in nature.

In the first chapter, I analyzed bacterial, fungal and oomycetal communities associated with *Arabidopsis thaliana* roots from seventeen natural populations across a European transect, for three consecutive years. By developing a fractionation protocol that distinguishes four microbial niches (Soil, Rhizosphere, Rhizoplane and Root), I dissected the relevance of host compartment, host species, biogeography, harvesting year, and soil characteristics on microbial communities' distribution at a continental scale. I showed that bacterial, fungal and oomycetal communities are primarily shaped by different factors, including the host niche for bacteria, the site for fungi, and the year for oomycetes. Also, I identified an *A.thaliana* root-associated core microbiota, resilient across harvesting years and locations. Furthermore, reciprocal transplant experiments conducted in natural and controlled conditions uncovered the important role of climate as well as the climate-dependent host genotype effect on microbial communities' distribution.

In the second chapter, I utilized a gnotobiotic plant system for reconstituting multispecies synthetic microbial communities, which revealed the relevance of multi-kingdom microbe-microbe interactions for plant health and microbial communities' assembly. In these experiments the bacterial microbiota is essential for plant survival and protection against detrimental activities of root-derived filamentous eukaryotes. Moreover, I revealed that microbial load only partially drives plant health and that disease protection of bacterial root commensals is a redundant trait needed to maintain microbial interkingdom balance for plant health. Finally, I investigated the dynamics of microbiota establishment and explored the importance of the host for microbiota establishment.

Zusammenfassung

In der Natur leben gesunde Pflanzen mit einer Vielzahl verschiedener Mikroorganismen wie Bakterien, Pilzen und Oomyzeten zusammen, welche komplexe mikrobielle Gemeinschaften bilden, und deren Mitglieder miteinander interagieren. Das Zusammenleben mit diesen Mikroorganismen verleiht der Wirtspflanze wahrscheinlich einen Fitnessvorteil. Fortschritte bei Forschungsmethoden, welche nicht auf die Kultivierung von Mikroorganismen angewiesen sind, haben unser Wissen über die Verteilung von Mikroorganismen in der Natur und die Faktoren, welche ihre Gemeinschaften beeinflussen, vergrößert. Allerdings weisen entsprechende Studien einen Mangel an Übereinstimmung auf. Daher ist ein holistischer Ansatz nötig, der Gruppen verschiedener Mikroorganismen in unterschiedlichen Umweltbedingungen untersucht. Es ist wichtig zu beachten, dass ein signifikanter Anteil der mikrobiellen Vielfalt in Studien über wirtsassoziierte Mikroorganismen unerklärt bleibt. Jahrzehnte an Forschung haben gezeigt, dass Mikroorganismen miteinander interagieren, was darauf hinweist, dass diese Interaktionen eine bedeutende, aber bis jetzt wenig beschriebene Antriebskraft sind, die auch für die Entstehung von mikrobiellen Gemeinschaften in und an Pflanzenwurzeln verantwortlich sein könnte. Um die Entstehung und Funktionen dieser Gemeinschaften von Mikroorganismen beschrieben zu können, sind Experimente mit gnotobiotischen Pflanzensystemen notwendig. Durch die Verknüpfung von Daten zu mikrobiellen Gemeinschaften innerhalb natürlich vorkommender *Arabidopsis thaliana* Populationen (Kapitel I) mit Experimenten, welche mit synthetischen mikrobiellen Gemeinschaften und keimfreien Pflanzen durchgeführt wurden (Kapitel II), liefere ich neue Erkenntnisse darüber, wie Umwelteinflüsse, Wirt-Mikrobiom und Mikrobiom-Mikrobiom Interaktionen den Aufbau mikrobieller Gemeinschaften und die Gesundheit der Wirtspflanze beeinflussen.

In Kapitel 1 habe ich Bakterien-, Pilz- und Oomyzetengemeinschaften, welche mit den Wurzeln von 17 natürlich vorkommenden, über Europa verteilten *Arabidopsis thaliana* Populationen assoziiert sind, über einen Zeitraum von drei Jahren hinweg analysiert. Mit der Entwicklung eines Fraktionierungsprotokolls, dass vier mikrobielle Nischen (Erde, Rhizosphäre, Rhizoplane und Wurzeln) separiert, habe ich den Einfluss von Wirtsnischen, Wirtsspezies, Biogeographie, Erntejahr und Erdcharakteristika auf die Verteilung von Mikroorganismengemeinschaften auf kontinentaler Ebene untersucht. Ich habe gezeigt, dass die Gemeinschaften von Bakterien, Pilzen und Oomyceten hauptsächlich von unterschiedlichen Faktoren beeinflusst werden, wie die Wirtsnische für

Bakterien, der Standort für Pilze und das Jahr für Oomyzeten. Des Weiteren habe ich einen Kern an *A. thaliana* wurzelassoziierten Mikroorganismen identifiziert, welcher robust gegenüber den Einflüssen von Erntejahr und Standort ist. Reziproke Transplantationsexperimente, welche in natürlichen sowie kontrollierten Bedingungen durchgeführt wurden, haben die wichtige Rolle des Klimas als auch des klima-abhängigen Wirtsgenotypen auf die Verteilung der mikrobiellen Gemeinschaften aufgedeckt.

In Kapitel 2 habe ich ein gnotobiotisches Pflanzensystem für die Analyse synthetischer mikrobieller Gemeinschaften genutzt, welches die Relevanz mikrobieller Interaktionen über höhere taxonomische Gruppen hinweg für die Gesundheit der Wirtspflanze und den Aufbau der mikrobiellen Gemeinschaften aufgezeigt hat. Bei diesen Experimenten hat sich herausgestellt, dass das bakterielle Mikrobiom essentiell für das Überleben der Pflanze und die Verteidigung gegen schädliche Einflüsse von wurzelassoziierten, filamentösen Eukaryoten ist. Zudem habe ich herausgefunden, dass die Anzahl der Mikroorganismen nur zu einem Teil die Gesundheit der Pflanze beeinflusst, und dass der Schutz vor Krankheiten durch bakterielle Wurzelkommensale, eine redundante Eigenschaft ist. Zuletzt habe ich die Dynamiken der Etablierung des Mikrobioms untersucht, und die Wichtigkeit des Wirtes dabei untersucht.

Table of Contents

Abstract I

Zusammenfassung III

Table of Contents V

CHAPTER I 1

Characterization of *A. thaliana* root-associated microbial communities in natural populations across a continental transect 1

1. INTRODUCTION 1

- 1.1 The holobiont concept 1
- 1.2 Soil microbiota 2
- 1.3 Plant-associated microbiota 3
  - 1.3.1 The bacterial microbiota of plants 5
  - 1.3.2 The fungal microbiota of plants 6
  - 1.3.3 Protists associated with plants 8
- 1.4 Amplicon sequencing for an integrated view of plant microbiota structure 9
- 1.5 Thesis aims (Chapter I) 10

2. RESULTS 11

- 2.1 Structure of root-associated microbial communities at a continental scale 11
  - 2.1.1 Experimental set-up 11
  - 2.1.2 Fractionation protocol 12
  - 2.1.3 Bacterial communities profile 16
  - 2.1.4 Fungal communities profile 21
  - 2.1.5 Oomycetal communities profile 24
  - 2.1.6 Microbial site-dependent signatures 26
  - 2.1.7 The Arabidopsis root core microbiota at the European scale 27
- 2.2 Influence of stable environmental factors on microbial communities’ composition 28
- 2.3 Influence of climate and host genotype on microbial communities’ composition . 31
- 2.4 Comparison of bacterial and fungal profiles using different amplification regions 36

3. DISCUSSION 41

- 3.1 Distinct root-associated compartments are potential microbial niches 41
- 3.2 Only a specific fraction of the soil microbiota can colonize root endosphere 41
- 3.3 Microbial beta-diversity is driven by environmental factors and the host plant´s effect 42
- 3.4 Microbial communities´ composition is host species dependent 43
- 3.5 Bacterial communities are stable across years 44

3.6 Reduced but stable *A. thaliana* root-associated core microbiota 45
3.7 Specific soil characteristics have a small but significant impact on root microbiota establishment 46
3.8 Climate is a major driver of root-associated microbial composition 47
3.9 Bacterial and fungal communities profiling is essentially comparable between amplification methods 48
3.10 Conclusions and future perspectives 49
3. MATERIALS AND METHODS 51
4.1 Materials 51
4.1.1 Plant material 51
4.1.2 Oligonucleotides 51
4.1.3 Enzymes 51
4.1.4 Chemicals 51
4.1.5 Buffers and solutions 52
4.2 Methods 52
4.2.1 Experimental set-up and sample collection in natural sites 52
4.2.2 Root compartments fractionation protocol 52
4.2.3 Fractionation protocol validation 53
4.2.4 Transplantation experiment set-up 55
4.2.5 Microbial community profiling 57
CHAPTER II 63
Microbiota reconstitution in *A. thaliana* plants to understand the role of interkingdom microbe-microbe interactions for the establishment of microbial communities and host fitness 63
1. INTRODUCTION 63
1.1 Microbial interactions in nature 63
1.1.1 Cooperative interactions 63
1.1.2 Competitive interactions 65
1.2 Microbial interactions shaping plant-associated microbial communities 68
1.2.1 The mycosphere 68
1.2.2 Influence of pathogen invasion on the plant microbiota 70
1.2.3 Microbial hubs as modulators of plant-associated microbial communities 71
1.3 Consequences of intermicrobial interactions on plant growth and health 72
1.3.1 Intermicrobial interactions and plant growth promotion 72
1.3.2 Disease suppression 73
1.3.3 Disease facilitation 74
1.4 Thesis aims (Chapter II) 76

2. RESULTS 77

2.1 Synthetic microbial communities reconstitution as a tool to understand microbial interactions and their role for plant health 77

2.1.1 Multi-kingdom microbial synthetic communities 77

2.1.2 Effect of multi-kingdom microbe-microbe interactions on microbial community structure and plant growth 80

2.1.3 Microbiota perturbation experiments 87

2.1.4 Root microbiota dynamics 92

3. DISCUSSION 97

3.1 Microbial communities composition correlates with host plant health 97

3.2 Most root-associated fungi isolated from healthy plants are pathogenic 98

3.3 Microbial load is partially responsible for plant health 99

3.4 Bacterial-driven disease suppression is a redundant trait within bacterial communities 100

3.5 Microbial communities are established over time and host plant health is impacted by different microbiota age 101

3.6 Concluding remarks and future perspectives 104

4. MATERIALS AND METHODS 107

4.1 Materials 107

4.1.1 Microbial culture collections 107

4.1.2 Plant material 107

4.1.3 Oligonucleotides 107

4.1.4. Enzymes 107

4.1.5. Chemicals and antibiotics 107

4.1.6. Buffers and solutions 108

4.2 Methods 108

4.2.1 Microbial strains storage 108

4.2.3 Gnotobiotic experiments 109

4.2.4 Microbial community profiling 115

Abbreviations 119

References 123

Supplementary figures and tables 143

Erklaerung 163

Acknowledgements 165

Curriculum vitae 166

Annex 167

CHAPTER I

Characterization of *A. thaliana* root-associated microbial communities in natural populations across a continental transect

1. INTRODUCTION

1.1 The holobiont concept

Microbes, including bacteria, archaea, fungi, and protists, have colonized most surfaces on the planet. These microbes can inhabit most environments on Earth, including soil, air and oceans, as well as other living organisms, from human skin to plant tissues. Microorganisms have been traditionally considered as individual entities that engage in interactions with other micro- or macro-organisms found in the surrounding environment. Cell number of these microbes, however, usually compares to the cell number of the macrobe they are associated with (1:1 compared to human cells, Sender *et al.,* 2016), and each of these microbes brings along their own genetic repertoire. In many occasions, the genetic load of these microbes will provide their host with functions otherwise inaccessible for them. For example, termites host a gut microbiota that allows them degrade cellulose very efficiently (Brune, 2014); bacterial communities in the soil drive fungal biocontrol together with their host plants (Chapelle *et al.,* 2016); others, facilitate acquisition of otherwise unavailable nutrients for their host, for example, through the formation of plant root-mycorrhiza symbiosis (Bonfante and Genre, 2010). Furthermore, such interactions can also happen between microbes; for example, between the fungus *Rhizopus sp*. and its bacterial endosymbiont, which produces an endotoxin necessary for the fungus to infect its host plant (Partida-Martinez and Hertweck, 2005). These and many other examples in nature highlight that these microbes can no longer be considered as organisms interacting with macrobes in an isolated manner, but rather as an extension of them. This relationship has been referred as the holobiont concept (Bordenstein and Theis, 2015), i.e.: “biomolecular networks composed of the host plus its associated microbes”. As such, it is very likely that the holobiont components share a very close evolutionary history and have developed and adapted responses to their surrounding environment in parallel. This joint adaptation has presumably been especially favorable to plants, which are not capable of actively migrating from a stressful environment, as animals could, and therefore have been able to expand their resources to face environmental stresses. It is relevant to note, however, that not all microorganisms within a plant holobiont have an impact on plant evolution and, more importantly, that not all partners in a holobiont impact positively each other (Moran and Sloan, 2015).

1.2 Soil microbiota

Although plant microbiota members can derive from various sources (air, animals, rainwater, etc.), the major pool for plant-associated microbiota is soil-borne microbes. Microbial load in soil has been estimated to be as numerous as 10^8 cells per gram of soil (Raynaud and Nunan 2014). The major bacterial inhabitants of soil are members of the Acidobacteria, Bacteroidetes, Firmicutes, Actinobacteria, and Proteobacteria phyla; from the fungal side, Basidiomycota, Ascomycota, Mortierellomycotina, and Mucoromycotina are the major soil-inhabiting groups (Fierer *et al.,* 2007; Tedersoo *et al.,* 2014). Despite the staggering bacterial diversity found across soils around the world, 2% of the bacterial phylotypes actually account for half of soil communities worldwide (Delgado-Baquerizo *et al.,* 2018), suggesting that soil microbiota holds stable roles within the soil ecosystem. Indeed, microbes are essential in certain soil processes, such nitrogen, carbon and phosphorus cycling, organic matter decomposition, regulation of plant diversity, or soil aggregation processes (Van der Heijden, 2008). On the other hand, the microbial composition is strongly related to the physical, chemical and biological characteristics of the ecosystem. Specifically, bacterial and fungal communities are correlated to soil pH composition (Fierer and Jackson 2006; Lauber *et al.,* 2009; Rousk *et al.,* 2010; Tedersoo *et al.,* 2014). By profiling the bacterial communities present in 88 soil across the American continent, it was possible to observe that pH-dependency in bacterial communities is mainly driven by changes on specific bacterial groups (Actinobacteria, Bacteroidetes and Acidobacteria) (Lauber *et al.,* 2009). Similarly, fungal communities are also impacted by soil pH, although it is more notable at lower taxonomic levels. For example, the abundance of members of the Ascomycota phylum, Hypocreales and Helotiales in particular, is strongly correlated to pH variation across soils (Rousk *et al.,* 2010). Metagenomic comparative analysis of desert soil with non-desert soil suggests that there are other soil factors driving microbial community composition and functions, such as lower soil moisture and plant biomass. Furthermore, soil composition will determine the microbial diversity and, therefore, the competition between microbial members (Fierer *et al.,* 2012). Another important soil characteristic is net carbon mineralization rate, which allowed to correlate bacterial taxa abundances across 71 soils in North America (Fierer *et al.,* 2007). Specific soil nutritional content also shapes which microbial communities will inhabit certain soil, as shown for fungal communities across the globe, where soil calcium content explained 8.9% of fungal variation (Tedersoo *et al.,* 2014).

The very ancient origin of microbes on Earth, tracing back to the beginning of life more than 3.5 billion years ago, indicates that microbe-microbe interactions have continuously evolved and diversified over time, far before plants colonized land 450 Mya (Hassani *et al.,* 2018). Therefore, it is likely that both intra- and inter-kingdom microbial interactions represent strong drivers of the establishment of microbial consortia in soil. However, the contribution of competitive and cooperative microbe-microbe interactions to the overall microbial community structure remains difficult to evaluate in nature due to the strong environmental noise. As a first approach, co-occurrence network analysis of prokaryotic microbes within 151 soils across the world shows that indeed there is a non-random microbial community assembly, suggesting that soil microorganisms tend to co-occur, and presumably interact, more than expected by chance (Barberán *et al.,* 2012). In conclusion, the combination of abiotic factors (environment) and biotic factors (microbe-microbe interactions) model microbial communities present in a given soil, which will then be the microbial input that a new plant seed will encounter and will interact with, in order to shape its own microbiota.

1.3 Plant-associated microbiota

In nature, healthy plants interact and cohabit with diverse microorganisms such as bacteria, archaea, fungi, and protists, collectively referred to as the plant microbiota. Microbiota members distribute on and within all plant tissues and compartment-specific microbial communities signatures have been reported for rhizosphere (Bulgarelli *et al.,* 2013), phyllosphere (Rastogi *et al.,* 2013) and endosphere plant niches (Lundberg *et al.,* 2012; Bulgarelli *et al.,* 2012). As discussed above, microbiota members colonizing plant tissues mainly come from the surrounding bulk soil, but it is important to note that plant seeds are not sterile when they fall to the ground. Vertical transmission of microbiota is a very important driver of the initial seed microbiota, as well as the quick microbial shifts upon emergence (Barret *et al.,* 2015; Barret *et al.,* 2016). Microbial communities interacting with plants can be beneficial and promote plant growth and adaptation to the environment, but specific members can also cause plant diseases in a context-dependent manner (Buée *et al.,* 2009). A great body of studies in the literature have focused on the beneficial effects that microbes have on plants. For example, it has been postulated that pathogen interaction with the plant host induces changes on its associated microbial communities that will, in turn, restrict pathogen infection (Mendes *et al.,* 2011; Chapelle *et al.,* 2015; Santhanam *et al.,* 2015; Ritpitakphong *et al.,* 2016a). Plant-associated microbiota members, such *Pseudomonas fluorescens* WCS417r, can prime the plant immune system by targeting specific transcription factors and preventing infections by various pathogens (Van der Ent *et al.,* 2009; Stringlis *et al.,* 2018). Importantly, plant microbiota members are capable of promoting increased nutrient acquisition in plants. For example, Zamioudis *et al.,* 2015 showed that, upon co-inoculation with *P. fluorescens* WCS417r, *Arabidopsis thaliana* roots trigger an iron-deficiency-like responses, correlated with its capacity to induce systemic resistance. Also, well-known plant symbiotic microbial members are mycorrhiza and nitrogen-fixing bacteria that help the plant with phosphorus and nitrogen uptake, respectively (Berendsen *et al.,* 2012; van der Heijden *et al.,* 2016). In this respect, third microbial partners might play an important role in promoting such interactions. For example, helper bacteria are capable of assisting mycorrhizal formation and improve the functioning of the symbiosis (Frey-Klett *et al.,* 2007). In order to face environmental stresses, plants engage in tight interactions with microbial partners. For example, a subset of microbial strains isolated from rootstocks of grapevine were able to secrete mucilaginous material, which improved the water-holding capacity of the soil and decreased water loss during desiccation, both under greenhouse and outdoors conditions (Rolli *et al.,* 2015). Interestingly, microbial beneficial effects can be dependent of environmental conditions. Specifically, it has been shown that, different *A. thaliana* accessions accommodate differently Pseudomonadaceae species, which correlates with the Pseudomonas-driven plant growth promotion. This effect, however, is reversed under stress conditions, suggesting that the plant host has adapted its interaction capacity with certain members, which might be beneficial in stressful environments, such in nutrient-depleted environments, but not in normal conditions (Haney *et al.,* 2015).

Most of this host-microbe interactions knowledge, however, has been traditionally studied as one-to-one interactions, obviating other microbial members playing a role, or environmental conditions that shape these interactions. In order to address this limitation, research has been moving towards an understanding of plant-microbe interactions as holobiont interactions (concept introduced above), where both host-microbe and microbe-microbe interactions likely affect microbial community establishment and plant health. Such advance has been possible due to the rapid development of high-throughput sequencing technologies, by which microbial communities can be easily profiled from a wide variety of environments. In the next paragraphs I will outline the current knowledge about plant microbiota composition, regarding the major microbial groups (bacteria, fungi and protists).

1.3.1 The bacterial microbiota of plants

It is now widely accepted that bacterial community establishment on plants is not random but rather controlled by specific assembly rules, as reviewed by Bulgarelli *et al.,* 2013 and Reinhold-Hurek *et al.,* 2015. As discussed before, soil composition is an important factor driving bacterial communities' structure. Indeed, growing sterile *A. thaliana* plants in natural soils, showed that one of the major drivers of root-associated microbial communities was the soil characteristics (Bulgarelli *et al.,* 2012; Lundberg *et al.,* 2012). Secondly, plant compartment plays an important role shaping bacterial communities, where bacterial members are taxonomically very similar between plant tissues (i.e. roots and leaves), but differ in structure and functions (Bodenhausen *et al.,* 2013; Bai *et al.,* 2015; Wagner *et al.,* 2016). Thus, reconstitution experiments using leaf- and root-derived bacteria showed that these microbes are specialized to their respective niche (Bai *et al.,* 2015). Such compartment specialization is not only valid for *A. thaliana* plants, but also for other plant species, for example *Ginkgo biloba* trees (Leff *et al.,* 2015), grapevine (Zarraonaindia *et al.,* 2015) or rice (Edwards *et al.,* 2015). In the latter, it was also possible to describe another bacterial niche between the rhizosphere and the root endosphere: the rhizoplane, which accounts for the microbes inhabiting the root surface. Plant-associated bacterial communities also differ depending on their host species and, in a lesser extent, on the host genotype, based on multiple comparisons of species and accessions in the literature: 56 tree species (Redford *et al.,* 2010), 600 *A. thaliana* accessions (Lundberg *et al.,* 2012), 27 maize accessions (Peiffer *et al.,* 2013), *A. thaliana* and relatives (Schlaeppi *et al.,* 2014; Dombrowski *et al.,* 2017), wild and domesticated barley (Bulgarelli *et al.,* 2015) and several lettuce accessions (Cardinale *et al.,* 2015), among other studies. Nevertheless, despite host-genotype-dependent variation, by using a tropical soil chronosequence it was possible to identify a root core microbiota of phylogenetically very distant plants, accounting for up to 33% of the bacterial abundance. This suggests that, even though each host plant has its own microbial-recruitment signature, especially notable between different plant species, root microbiomes could have evolved with plants at least since the divergence of lycopods ~400 million years ago (Yeoh *et al.,* 2017). By screening 196 *A. thaliana* accessions in the field, it was possible to highlight which host genomic characteristics are important for abundant microbes' assembly on plant leaves. Thus, cell-wall-integrity related genes and ABC transporters (that could be related to pathogen resistance) are part of the most significantly correlated plant genes with microbial communities' composition (Horton *et al.,* 2014). Using a reductionist approach, a similar conclusion was reached, where cuticle-related genes and ethylene signaling are important for bacterial community establishment (Bodenhausen *et al.,* 2014). Furthermore, plant immune system seems to be an important modulator of root-associated bacterial communities, as *A. thaliana* mutants impaired in salicylic acid signaling cannot assemble a normal root microbiota (i.e. same as wild type) (Lebeis *et al.,* 2015). Other plant traits can also change bacterial communities, as wood density, leaf mass or leaf nutrient content (Kembel *et al.,* 2014). Importantly, plant undergo several developmental stages during their life cycle, during which they might have different secretion signatures that impact the composition of bacterial communities or their colonization capacity. Indeed, inspection of rhizosphere-associated bacterial communities of *A. thaliana* plants at four developmental stages showed that specific microbial members, such Acidobacteria, Actinobacteria, Bacteroidetes and Cyanobacteria, structure differently throughout plant growth (Chaparro *et al.,* 2014). These changes, however, seem to be notable only at early developmental points (from seedling to vegetative), and not later in the life cycle. Such observation was done by comparative analysis of an *Arabis alpina* non-flowering mutant (*pep1*) to its wild type, showing non-significant differences in bacterial communities' composition upon flowering (Dombrowski *et al.,* 2017). On the other hand, from year to year it is possible to observe bacterial shifts associated with leaves and roots of perennial plants (Wagner *et al.,* 2016). Furthermore, seasonality can also be a trigger of bacterial communities' shifts, as shown for leaves of *Populus deltoides* (Redford and Fierer 2009), 106 field-grown lettuce plants (Rastogi *et al.,* 2012), greenhouse-grown *A. thaliana* plants (Maignien *et al.,* 2014), leaves of common bean, soybean and canola planted in field locations (Copeland *et al.,* 2015) and in roots of *Avena fatua* grown in greenhouse (Shi *et al.,* 2015). Also, in response to environmental changes, such drought, plants are capable of specifically changing its associated microbiota; for example, sorghum roots drive enrichment of monoderm bacterial strains (Xu *et al.,* 2018). Despite the large number of bacterial phyla described in nature and the multiple factors that affect these communities, the bacterial microbiota of plants is dominated by three major phyla (Proteobacteria, Actinobacteria, and Bacteroidetes) in both above- and belowground plant tissues (Bulgarelli *et al.,* 2013; Hacquard *et al.,* 2015), suggesting that there are either very conserved taxonomic-dependent plant-bacteria interactions over evolutionary history, or a lack of host ability to engage into tight interactions with more diverse bacterial taxa.

1.3.2 The fungal microbiota of plants

Even though less attention has been paid to the fungal microbiota of plants, culture-independent community profiling has revealed a staggering diversity of fungi colonizing both above- and belowground plant tissues, mainly belonging to two major phyla: Ascomycota and Basidiomycota (Jumpponen and Jones, 2009; Toju *et al.,* 2013; Hardoim *et al.,* 2015). In roots, although arbuscular- (Glomeromycota phylum) and ectomycorrhizal fungi have been mostly studied, recent community profiling data indicate that other endophytic fungi also represent an important fraction of the fungal root microbiota (Toju *et al.,* 2013; Bonito *et al.,* 2014). In non-mycorrhizal plant species such as *A. thaliana*, *A. alpina*, or *Microthlaspi*, it has been proposed that they might compensate for the lack of mycorrhizal partners (Glynou *et al.,* 2016; Hiruma *et al.,* 2016; Almario *et al.,* 2017). Similarly to bacteria, the structure of plant-associated fungal communities is not random and varies depending on soil type, plant compartment, plant species, or seasons, although local environment appears to be a more impacting factor for fungal communities than for bacterial (Hacquard, 2016). Whether this pattern is accentuated by the different taxonomic resolutions resulting from 16S rRNA and ITS marker loci utilized for culture-independent surveys, remains to be clarified (Peay *et al.,* 2016). Study of phyllospheric fungal composition in European beeches (*Fagus sylvatica*) across an elevation gradient (up to 1000 meters), shows that only 7% of the fungal OTUs (Operational Taxonomic Units) are shared across all sites surveyed and, furthermore, one of the major factors separating samples clusters was the sampling date (from one year to another) (Cordier *et al.,* 2012). Profiling of rhizosphere and phyllosphere of three *Agave* species showed that biogeography accounts for up to 71% of the fungal community variation, whereas plant compartment explains 8% of the community variance (Coleman-Derr *et al.,* 2016). Similarly, profiling of root fungal communities associated with 23 *Populus deltoides* showed 14% of variance explained by geography, and 9.8% of variance explained by soil type. Furthermore, soil components such as calcium, manganese and moisture content significantly correlated with fungal communities' distribution, whereas host genotype had no effect (Shakya *et al.,* 2013). Compared to the bacterial microbiota, fungal communities established in soil and on plant roots seem to be more subjected to stochastic variations. In a disturbance experiment in the field, where grasses were removed and grinded, fungal communities proved to be resilient to disturbance, so that similar OTUs re-colonized the disturbed area, although distribution of these OTUs across the experimental site was unpredictable (Lekberg *et al.,* 2012). On the contrary, bacterial communities have been proven to significantly deviate from stochastic expectation curve (Wang *et al.,* 2013). Also, as described above, fungal and bacterial communities respond differently to environmental factors (Rousk *et al.,* 2010; Shakya *et al.,* 2013; Hacquard, 2016). Consequently, mainly dispersal limitation and climate explain the global biogeographic distribution of fungi and have been suggested to constrain fungal dispersal, favoring high endemism in fungal populations. For example, by studying the fungal microbiota in 600 soil samples, in forest areas of Pinaceae trees, 50% of the variance could be explained due geographical distribution of the samples, but also within relatively close areas, which the authors discuss as a possible correlation with the dispersal barriers (Talbot *et al.,* 2014).

1.3.3 Protists associated with plants

A recent study, targeting all major groups of small soil eukaryotes (fungi, green algae, protists) and mesofauna (Nematoda, Annelida and Collembola) suggested that their spatial structure in soil is mostly stochastic due to high dispersal and drift in their local environment (Bahram *et al.,* 2016). More particularly, protists have been shown to be abundant plant microbiota members in both the rhizosphere and the phyllosphere (Bonkowski, 2004; Ploch *et al.,* 2016). Network analysis of *A. thaliana* leaves-associated microbiota showed that certain microbes occupy a more central position within the interaction network, suggesting their importance for microbiota stability. This was further tested under a controlled environment, where an oomycetal and fungal members, *Albugo laibachii* and *Dioszegia sp*. respectively, strongly affected phyllosphere communities (Agler *et al.,* 2016a). In contrast with the rich diversity of fungi and bacteria detected in or outside plant tissues, oomycetes (protists of the Oomycota lineage) seem to be less diverse and few host-adapted members belonging to the genera *Pythium*, *Phytophthora*, *Peronospora* or *Albugo* are found living in association with plant roots or leaves (Coince *et al.,* 2013; Kamoun *et al.,* 2015; Agler *et al.,* 2016a). Notably, the vast majority of oomycete species described so far are destructive plant pathogens that have major impact on plant productivity worldwide (Kamoun *et al.,* 2015). Nonetheless, comparative analysis of root infection by closely related *Pythium spp*. or leaf infection by *Phytophthora infestans* isolates suggests very different levels of pathogenicity on plants (Day *et al.,* 2004; Van Buyten and Hofte, 2013). Importantly, oomycetes can be also detected or isolated from the roots of healthy and asymptomatic plants (Benhamou *et al.,* 2012; Coince *et al.,* 2013), suggesting that some members can establish non-pathogenic interactions within plant tissues (Sapp *et al.,* 2018) or that their pathogenicity observed in laboratory conditions with germ-free plants is reduced in a community context. Given the fact that protists can impact plant growth (Bonkowski, 2004; Krome *et al.,* 2009) and are active drivers of soil- and root-associated bacterial communities structure (Murase *et al.,* 2006; Rosenberg *et al.,* 2009; Flues *et al.,* 2017), further investigations are needed to better understand 1) the diversity of protists that associate with plants, 2) the factors shaping protist assemblages and 3) their ecological/functional roles in the rhizosphere and the phyllosphere.

1.4 Amplicon sequencing for an integrated view of plant microbiota structure

While soil characteristics, host species and biogeography represent important drivers structuring root-associated bacterial and fungal communities, most of the variance observed in microbiome studies remains to be explained (Shakya *et al.,* 2013; Hacquard, 2016). Part of these unexplained factors may relate to complex interactions existing between microbial communities, where the distribution and functioning of taxa co-regulate each other. The importance of microbe-microbe interactions for structuring and stabilizing plant-associated microbial communities has been so far neglected but recently emerged as a an important trait of the phyllosphere microbiota. In this work, Agler *et al.,* (2016a) surveyed bacterial, fungal and oomycete communities associated with *A. thaliana* leaves and found that microbe-microbe interactions can play a major role in shaping the structure of the phyllosphere microbiota and that few "hub" (or keystone) microbes can severely affect community structure (Agler *et al.,* 2016a). These hub species are active drivers of community structure mediating microbial community shifts either directly via microbe-microbe interactions and/or indirectly through 1) cascade modifications in the interconnected microbial network or 2) alteration of the host immune system. Particularly, authors showed that the oomycete *Albugo sp*. represents a hub microbe on *A. thaliana* leaves, and its presence negatively impacts phyllosphere bacterial diversity (Agler *et al.,* 2016a). This comprehensive survey shed new light on the complexity of microbial interactions in the phyllosphere and revealed how microbe-microbe interactions can sculpt microbial assemblages on plant leaves. Agler *et al.,* recently developed a comprehensive and effective amplicon-based pipeline for multiple microbial loci profiling, using MiSeq-based technology (Agler *et al.,* 2016b; Caporaso *et al.,* 2010). This pipeline was further validated by using a complex mock community, including bacterial, fungal and oomycetal strains. Thus, this pipeline will be very useful in order to study in depth structure of different groups of microbial communities interacting together with a host plant in nature, and therefore disentangle the effect of microbe-microbe interactions in microbial communities' structure.

1.5 Thesis aims (Chapter I)

Recent studies have advanced our knowledge about microbial communities associated with plants and environmental factors shaping these communities, but it is difficult to cross-compare between different techniques and experimental set-ups, in order to describe a microbial communities' composition working model (Thompson *et al.,* 2017). Although the structure of the bacterial root microbiota has been extensively described in *A. thaliana* and Brassicaceae relatives at a local scale (Schlaeppi *et al.,* 2014), fungal community profiling has never been used to characterize root-associated fungi in this model plant species, for which the signaling pathways required for establishing mutualistic interactions with mycorrhizal fungi have been lost. Therefore, as first thesis aim, I will survey *A. thaliana* bacterial, fungal, and oomycetal communities associated with distinct root compartments, across a wide geographical area, that comprises very distant latitudinal locations. This survey will contain very different climatic and soil properties, so that it will be possible to correlate these with microbial communities' composition and distribution. Also, plants will be harvested in three consecutive years, to test for resilient microbes associated with *A. thaliana* roots, as well as neighboring plants, in order to assess the microbial plant species specificity. Finally, in order to fully disentangle the geographical effect into 1) host/accession genotype, 2) climate and 3) soil properties effects, soil and climate transplantation experiments will be performed. Thus, the following questions will be addressed through this thesis chapter:

1) What is the composition of the *A. thaliana* root-associated bacterial, fungal and oomycetal communities at a continental scale?
2) Is there resilient or "core" bacterial, fungal and oomycetal communities associated with *A. thaliana* roots?
3) How do stable environmental factors shape microbial communities at a continental scale?
4) How do climatic conditions and host genotype structure microbial communities at a continental scale?
5) Are microbial profiles impacted by the amplification primers utilized?

2. RESULTS

2.1 Structure of root-associated microbial communities at a continental scale

2.1.1 Experimental set-up

The aim of this project was to explore the robustness of *A. thaliana* root-associated microbial communities across various environmental conditions and different soil types, including geographically very distant locations. Thus, seventeen sites were selected across a gradient of climates within Europe, from Sweden to Spain, which included five distinct soil textures, as well as anthropized and non-anthropized areas. Most of these *A. thaliana* populations had been previously surveyed for plant population genetic studies by our collaborators (Jon Ågren from University of Uppsala, in Sweden; Eric Kemen, University of Tuebingen in Germany; Fabrice Roux from INRA Toulouse, in France; and Carlos Alonso Blanco, from CSIC-CNB Madrid, in Spain, **Figure 1**, **Annex: Table 1**).

A. thaliana plants were harvested in a period from February to May, in order to match the bolting and flowering time of each geographic region (Boyes *et al.,* 2001). Albeit no differences between late developmental stages have been previously observed in root microbial communities of *A. thaliana* relatives (Dombrowski *et al.,* 2017), it was intended to harvest every plant at the same developmental stage to avoid possible variability. In order to learn more about microbial resilience over time, plant and soil samples were harvested three consecutive years during the same period each time. Further, in order to ensure high quality and quantity of DNA after sample processing, at least four individual plants were pooled to form one technical replicate and four technical replicates were taken in total. Since this pooling could mask the plant-to-plant microbial community variation, four plants were also harvested individually per site. Because we observed very low differences between pooled and single plants during the first harvesting year (see below), we therefore reduced the number of technical replicates from four to one individual plant in subsequent years. Finally, to assess species-specific effect on microbial communities, neighboring grass plants were also harvested. In total, 285 plants were harvested across sites and years.

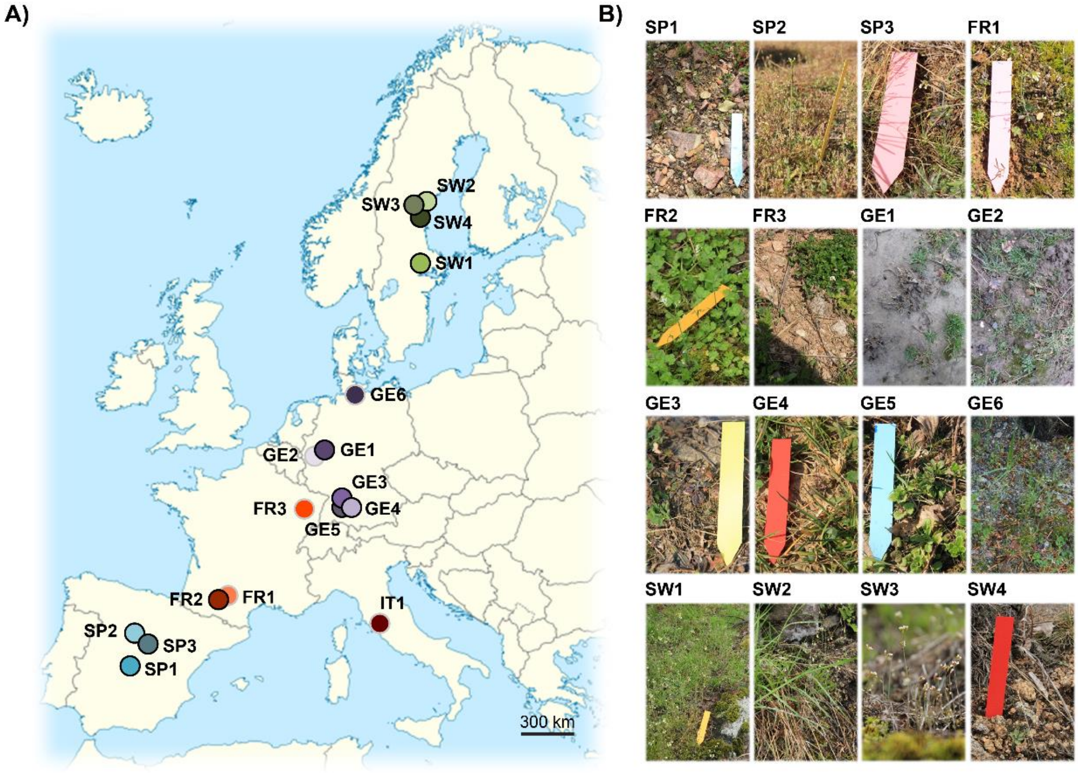

Figure 1: European transect of 17 natural *A. thaliana* populations. A) European map, depicting each of the studied sites and accessions: SP1, SP2, SP3 (IP-Mar-1, Ip-Cdc-3, Leo-1, respectively, Alonso-Blanco *et al.,* 2016), FR1 and FR2 (Bartoli *et al.,* 2018), FR3 (Saint-Die, Duran *et al.,* in preparation), GE1, GE2 (Pulheim and Geyen, respectively, Duran *et al.,* in preparation), GE3 (K6910, Agler *et al.,* unpublished), GE4, GE5 (PFN and JUG, respectively, Agler *et al.,* 2016), GE6 (This study), SW1 (Tos-82-393, Alonso-Blanco *et al.,* 2016), SW2, SW3, (Ellis and Agren, unpublished), SW4 (Rödåsen, Agren & Schemske 2012), IT1 (Castelnuovo, Agren & Schemske 2012). Color-code matches colors in next figures. Dots with black stroke were harvested over three consecutive years. **B)** Representative images of natural *A. thaliana* accessions.

2.1.2 Fractionation protocol

It has been previously reported that bacterial communities associated with plant roots have a strong compartmentalization along the soil-root continuum, and it has been shown that specific microbes are enriched in certain root niches (Bulgarelli *et al.,* 2012; Edwards *et al.,* 2015). Also, it has been proposed that bacteria are selected by plant roots following a two-step selection process (Bulgarelli *et al.,* 2013), where microbes are “filtered” from the rhizosphere to the root endophytic compartment through the rhizoplane. However, not many reports consider each soil-to-root compartment as a unique microbial niche nor they include fungal and oomycetes compartment-dependent analysis, where important information regarding plant microbiota establishment might be missing. Thus, I developed and validated a fractionation protocol, where four compartments are separated (Bulk Soil;

Rhizosphere, “RS”; Rhizoplane, “RP”, and Roots or Endophytic fraction) (**Figure 2A**) and later used this protocol to process all harvested plant roots from natural sites.

Bulk soil and rhizosphere fractions were obtained from harvested samples as already described in previous studies (Bulgarelli *et al.,* 2012). Briefly, a sample from the bulk soil was taken, making sure that no root debris was included, snap-frozen in liquid nitrogen and stored for further processing. Individual plants were manually separated from the main soil body and non-tightly adhered soil particles were removed by gently shaking the roots; these roots were then separated from the shoot using a sterile blade and placed in a 15-mL falcon with 10 mL of deionized autoclaved water, which was then inverted 10 times. Roots were transferred to another falcon and further processed, while leftover wash-off was centrifuged at 4000 xg for 10 min. Supernatant was discarded except for approximately 2 mL, which were then used to re-suspend the pellet and transfer it to a new 2-mL screw-lid tube. This tube was centrifuged at 20000 rpm for 10 minutes; the supernatant was discarded and the pellet (RS compartment) was snap-frozen in liquid nitrogen and stored for further processing.

In order to specifically separate the rhizoplane from the endophytic root compartment, I tested three methods: 1) sonication (as in Bulgarelli *et al.,* 2012 and Edwards *et al.,* 2015), 2) surface sterilization and 3) consecutive detergent washes (similarly to Agler *et al.,* 2016a). To validate that root surfaces were depleted from microbes and that a RP fraction was obtained, I printed each treated root and plated remaining washes on TSA 50%, followed by counting colony-forming units (CFUs) after three days of incubation at 37 °C. Furthermore, I took scanning-electron microscopy images (SEM) with the help of Rainer Franzen (Central Microscopy, CeMic, MPIPZ). Due to high variation between SEM images, no quantification of colonies was done and images are used to illustrate results from CFU counting (**Figure 2B**).

1. Sonication. This method was tested as described in Bulgarelli *et al.,* 2012. Although there was a trend of CFUs decrease compared to non-treated samples (Kruskal-Wallis, Dunn test *post-hoc*, non-significant, **Figure 2B**), roots looked heavily shattered and there was a strong possibility that part of the endophytic fraction could leak out, or that microbial cells would rupture as plant cells did. Furthermore, very low load of microbes was recovered in the washes post-sonication and, therefore, making this method not suitable to recover a RP fraction (**Figure 2B**).
2. Root surface sterilization. I further followed the protocol from Bulgarelli *et al.,* 2012, which includes a final step of root surface sterilization, using sodium hypochlorite

(NaClO, 3%) and ethanol (80%). Roots were sterilized with 1-minute ethanol wash, washed with NaClO for one minute and rinsed five times with deionized water. Printed roots showed the lowest CFU count compared to all other treatments (Kruskal-Wallis, Dunn test *post-hoc*, p-value<0.05); however, inspection of SEM images revealed that microbes were still present on the root surface, confirming that the sterilization process reduced the viability of microbial cells (less CFUs on plates) but did not remove the actual cells and hence their DNA from the root's surface, which would interfere with the microbial community profiling (**Figure 2B**).

3. Detergent washes. This method was tested in order to remove microbes from the root surface in a less invasive manner compared to sonication, as well as to recover as much RP-associated microbiota (modification of the protocol from Agler *et al.,* 2016a). After RS removal, roots were placed in a 15-mL falcon with 6 mL of detergent (1x TE + 0.1 % Triton® X-100) and manually shaken for 2 minutes. If further detergent washes were applied, roots were transferred to a new 15-mL falcon. As it can be observed in **Figure 2B**, printing of these roots shows that there is a trend of decreasing CFUs on root surface after three rounds of detergent washes, however no significant differences could be found due to low replication (3 data points per treatment). More importantly, the microbial recovery in the washes is the highest using this method. Therefore, this was the approach selected to capture RP-associated microbes in this fractionation protocol.

After using detergent washes to obtain the RP fraction, the remaining washes (approximately 18 mL) were filtered through a 0.22 µM-pore membrane, to capture the microbes specifically colonizing the RP fraction, and also snap-frozen in liquid nitrogen until further processing. Lastly, three-times washed roots were subjected to a further surface sterilization step to fully remove any leftover microbe from the root surface, as indicated in step 2. These roots were dried using sterile Whatman paper and snap-frozen in liquid nitrogen until further processing (Root or Endophytic fraction).

DNA from all harvested and fractionated samples (in total, 1139 samples) was isolated and subjected to microbial profiling, using specific genomic regions for each microbial group of study: 16s rRNA gene for bacterial profiling (V2-V4 region and V4-V7 region), ITS1 and ITS2 (internal transcribed spacer 1 and 2) for fungal profiling and ITS1 for oomycetal profiling (see **Methods**, **Annex: Table 2,** Agler *et al.,* 2016b). Although 16s V4-V7 and ITS1 have been widely used (Bulgarelli *et al.,* 2012; Lundberg *et al.,* 2012; Dombrowski *et al.,* 2017; Agler *et al.,* 2016b), which makes them suitable regions to cross-compare these data with previously published reports, it is of interest to profile microbial communities with another region within marker genes (16s and ITS), in order to know whether there is a profile bias depending on which DNA region is used (Birtel *et al.*, 2015; Peay *et al.*, 2016).

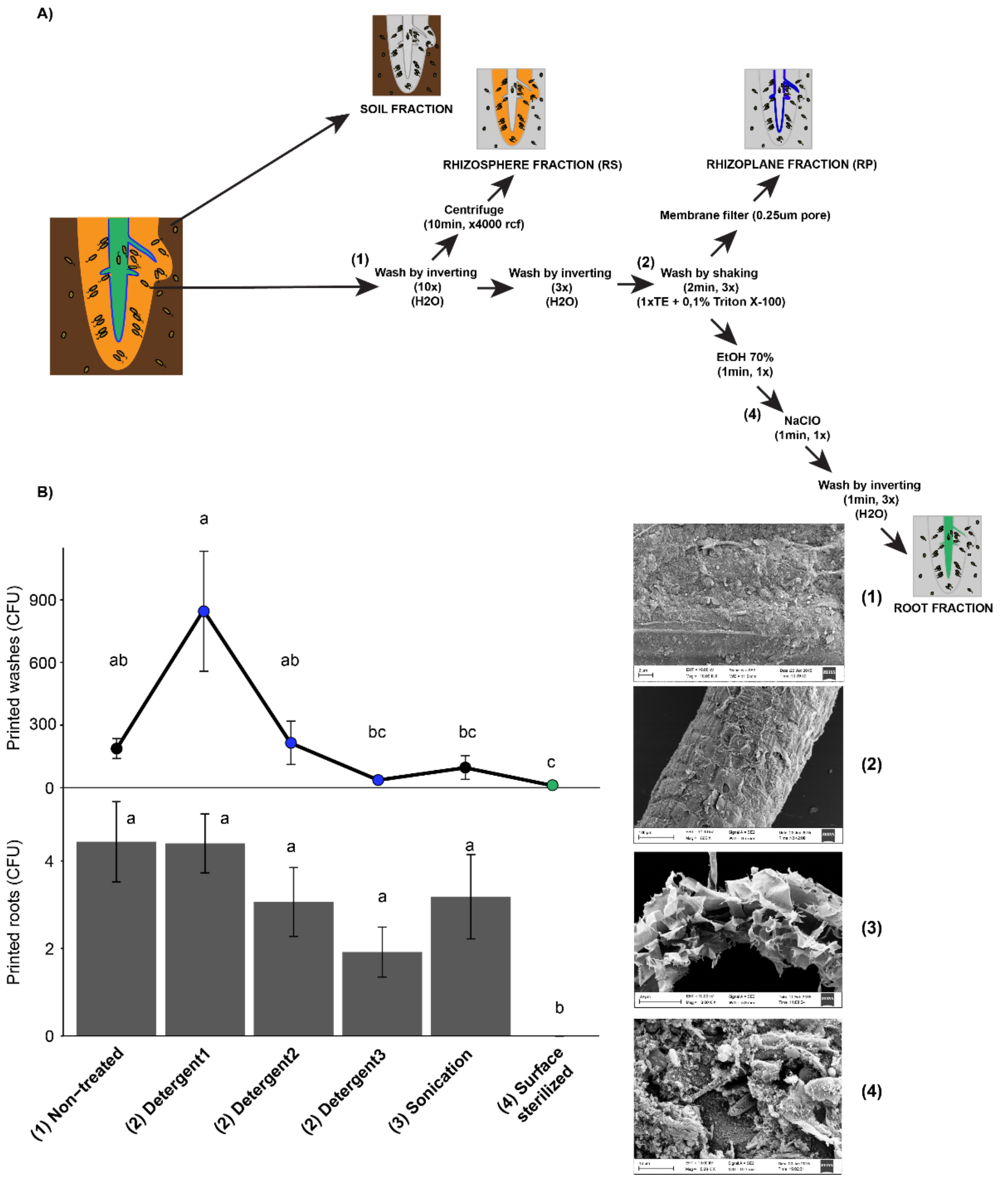
A)
SOIL FRACTION
RHIZOSPHERE FRACTION (RS)
RHIZOPLANE FRACTION (RP)
Centrifuge
(10min, x4000 rcf)
Membrane filter (0.25um pore)
(1)
Wash by inverting
(10x)
(H2O)
Wash by inverting
(3x)
(H2O)
(2)
Wash by shaking
(2min, 3x)
(1xTE + 0,1% Triton X-100)
EtOH 70%
(1min, 1x)
(4)
NaClO
(1min, 1x)
Wash by inverting
(1min, 3x)
(H2O)
ROOT FRACTION
B)
Printed washes (CFU)
900
600
300
0
a
ab
ab
bc
bc
c
Printed roots (CFU)
4
2
0
a
a
a
a
a
b
(1) Non-treated
(2) Detergent1
(2) Detergent2
(2) Detergent3
(3) Sonication
(4) Surface sterilized
(1)
(2)
(3)
(4)

Figure 2: Fractionation protocol to separate four microbial niches (Soil, Rhizosphere, Rhizoplane and Root). A) Fractionation protocol to separate Rhizosphere compartment (1), from Rhizoplane compartment (2) by using sequential detergent washes, enriching the root fraction (4) with only root-endophytic microbes. **B)** CFU counts after three days of incubation at 37 °C of leftover washes after each treatment on TSA 50 % media (line plot); and CFU counts after three days of incubation at 37 °C from roots after treating them with each of the fractionation steps, and printed on TSA 50 % media (bar plot). Significantly different values are indicated with different letters (Kruskal-Wallis, Dunn test *post-hoc*, $p<0.05$). The rightmost panel shows scanning electron microscopy (SEM) images of the same roots, to illustrate the root surface after each treatment.

2.1.3 Bacterial communities profile

Microbial alpha-diversity indicates how diverse a given microbial community is related to the number of species present within a sample. Depending on which community characteristics are taken into account, there are different indices used in the literature, including: “Observed OTUs”, which indicates the number of unique OTUs within the sample; “Chao Index” accounts for the possibility that rare OTUs could be lost due to under sampling, and the Shannon Index accounts for microbial abundance and microbial evenness (Morris *et al.*, 2014). Analysis of the bacterial alpha-diversity shows that there is a significant decrease of bacterial diversity from bulk soil samples to endophytic root samples (from an average of 430 observed OTUs in bulk soil to an average of 105 observed OTUs in root samples, Kruskal Wallis, Dunn test *post-hoc*, $p<0.05$). Furthermore, these results indicate that the fractionation protocol utilized to process the samples is successful at separating a significantly distinct bacterial niche (RP) containing an intermediate diversity between RS and the Root (**Figure 3A**, **Supplementary figure 1A**, Kruskal Wallis, Dunn test *post-hoc*, $p<0.05$).

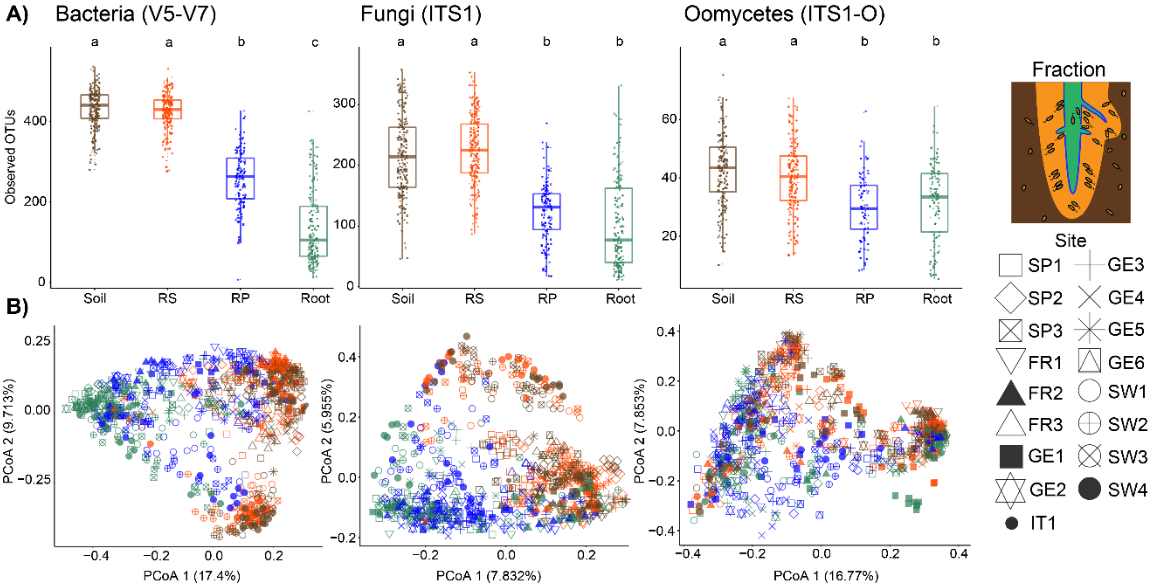

Figure 3: Structure of *A. thaliana* root-associated microbial communities at a continental scale. A) Observed OTUs in the whole dataset, for bacterial (16s rRNA region, V5/V7), fungal (ITS1) and oomycetal (ITS1) profiles, colored by fraction (Soil, RS, RP or Root fractions), matching the cartoon on the right, and shaped by site. Significant differences are depicted with letters (Kruskal Wallis, Dunn *post-hoc*, p-value< 0.05). **B)** Principal coordinates analysis (PCoA) based on Bray-Curtis dissimilarities between all samples, colored by fraction (Soil, RS, RP or Root fractions) and shaped by site. In these plots, the further away two samples cluster from each other, the more different their microbial community is.

Further analysis of the beta-diversity (microbial composition differences between samples) was performed using Bray-Curtis dissimilarity (that quantifies the composition dissimilarity between two samples, based on read counts on each sample), weighted Unifrac (which also takes into account the microbial taxonomy) and unweighted Unifrac distances (that accounts for taxonomy and absence/presence of certain OTUs) (Lozupone *et al.,* 2005) (**Figure 3B, Supplementary figure 1B**). Although each index has its benefits and added information, only the Bray-Curtis distances can be cross-compared with ITS-based profiling data due to the high variability of ITS1 and ITS2 regions for accurate phylogenetic analysis (Lindahl *et al.,* 2013).

Principal Coordinates Analysis (PCoA) showed that the factor that explains most of the bacterial community structure is fraction (first axis, 17%). Secondly, the y axis clusters apart samples from different geographical sites, specifically Swedish Soil and RS samples (second axis, 9%) (**Figure 3B**). Remarkably, despite these different bacterial soil inputs, the communities converge towards the root endophytic compartment. This evidence, together with the decrease in alpha-diversity towards the root compartment, suggests that *A. thaliana* roots play an important role in filtering specific microbial members, consistent with the two-step selection model previously proposed (Bulgarelli *et al.,* 2013), and that the structure of bacterial root microbiota is highly conserved at a continental scale, despite large geographical distances and different environmental conditions. Compartment-dependent separation is also visible with Weighted and Unweighted Unifrac measurements, although the site-dependent signature of the bacterial microbiota in soil and rhizosphere samples is lost (**Supplementary Figure 1B**). It is plausible then, that the bacterial OTUs that differentiate Swedish soil samples from the rest have very different relative abundances, but are taxonomically very similar to other sites. Another observation is that RP samples are more scattered in the plot, whereas soil, RS or root samples are tightly clustering together, which could be due to individual root-associated microbial variation, although technical variation cannot be excluded (**Figure 3B**). Separating the samples by compartment, shows that bacterial communities differentiate by site in soil and RS samples (separation of Swedish samples from the rest), whereas it is not the case in RP and Root fractions (**Figure 4A**). Indeed, permutational multivariate analysis of variance (PERMANOVA, p-value<0.001) indicates that "Site" variance decreases from soil to root compartment (37.2% to 15.3%, respectively) (**Figure 4E**, **Table 3**).

The relative abundance of each OTU within each sample was calculated by removing OTUs with less than 1% representation in the whole dataset, to account for sequencing biases towards rare taxa (Bulgarelli *et al.,* 2012). Reflecting the previous observation that bacterial communities distribute in a compartment-dependent manner, high-taxonomic-level representation of the OTUs (phylum and class-level) shows a clear compartmentalization pattern (**Figure 5A**).

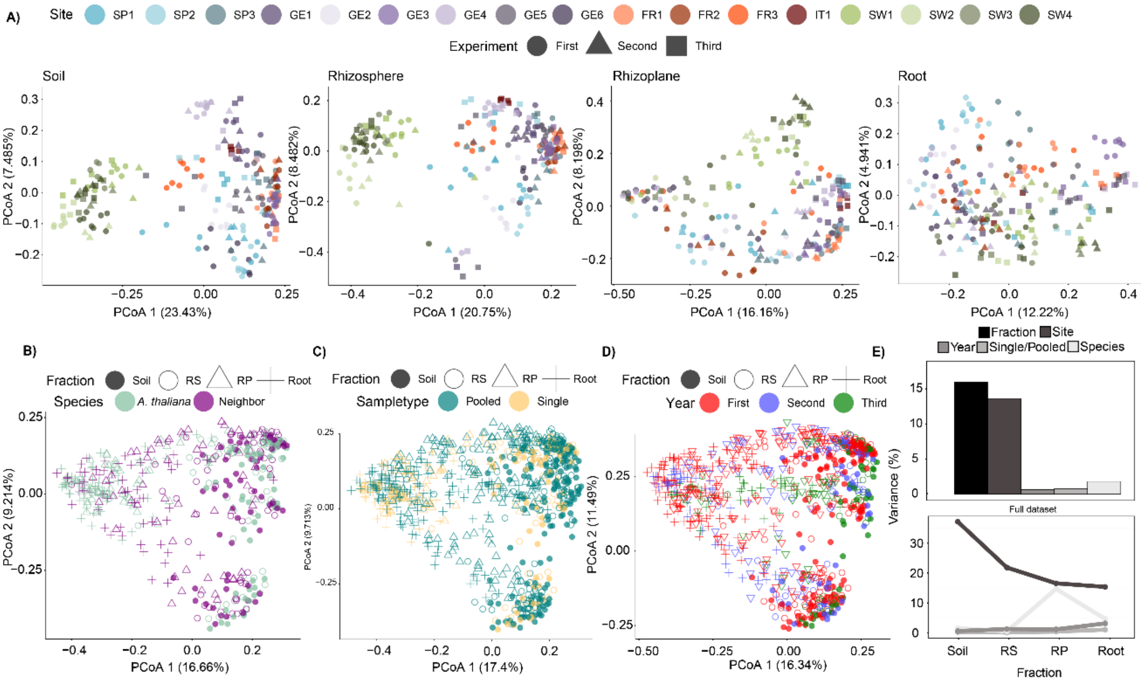

Figure 4: Different factors shape bacterial communities composition. A) PCoA plots showing Bray-Curtis dissimilarities between Soil, Rhizosphere, Rhizoplane and Root samples separately, colored by “Site” and shaped by “Year” of harvest. **B)** PCoA plot containing a subset of the samples (all individually harvested roots and all neighboring plants, which were plants growing in the surrounding area to *A. thaliana* plants, belonging to the Poaceae family), to show the species-dependent sample clustering. **C)** PCoA containing the full dataset, to show clustering differences between harvesting type (Pooling four plants together or Single plant individuals). **D)** PCoA containing samples harvested in all three years (12 sites, out of 17), to show the year-dependent sample clustering. **E)** Variance explained by each of the plotted variables in A, B, C and D, calculated using permutation analysis (999 permutation, $p<0.001$), in the full or subsetted dataset (upper plot) and in each root-associated compartment (lower plot).

The most abundant bacterial members are part of the Proteobacteria, Actinobacteria, Bacteroidetes and Firmicutes phyla, as well as some less abundant groups such as Acidobacteria, Gemmatimonadetes, Chloroflexi and Verrucomicrobia. Furthermore, consistent with previous observations, members of the Proteobacteria family are more abundant towards root samples, whereas Actinobacteria and Acidobacteria increase towards RS and soil samples. It is interesting to observe that, despite the remarkable consistency of bacterial profiles across seventeen European sites, it is possible to highlight site-dependent signatures. For example, many sites (such as SP1, SP2 or GE3) have very low representation of Firmicutes members, in comparison with other sites; also, Swedish sites have higher representation of Acidobacterial members, in comparison with any other harvested sites. Regarding the latter observation, it is likely that the separate clustering of Swedish samples in the PCoA plot is due an increase of the relative abundance of Acidobacteria (**Figure 3B**). Remarkably, 90% of the relative abundances across samples are composed of known and abundant bacterial members, whereas only 10% of the reads belong to rare or very low abundant taxa (**Figure 5A**).

Factor	**Fraction**	**Bacteria (V5/V7)**	**Fungi (ITS1)**	**Oomycetes (ITS1)**
Site	All	13.62	18.04	11.34
	Soil	37.22	40.22	15.12
	Rhizosphere	21.85	39	18.5
	Rhizoplane	16.56	17.76	15.94
	Root	15.38	13.98	13.49
Fraction		15.95	8.16	2.97
Single/Pooled	All	0.75	0.54	0.44
	Soil	0.21	0.28	0.16
	Rhizosphere	0.07	0.46	0.67
	Rhizoplane	0.38	0.82	0.88
	Root	1.03	0.4	0.16
Year	All	0.64	5.05	12.77
	Soil	0.55	1.13	5.88
	Rhizosphere	1.24	1.19	6
	Rhizoplane	1.13	2.08	2.4
	Root	3.12	9.14	6.46
Species (*Arabidopsis*/ Neighbors)	Soil	1.52	0.52	0.88
	Rhizosphere	0.44	0.52	0.89
	Rhizoplane	14.7	4.47	3.66
	Root	4.63	1.17	3.14

Table 3: Factors driving microbial composition at a continental scale. PERMANOVA analysis (999 permutations, p-value<0.001). Full dataset was used to calculate "Site", "Fraction" and "Single/Pooled" effects; only samples harvested all three years were used to calculate "Year" effect; a subset containing single and neighboring plants was used to calculate "Species" effect. Green-colored cells have a significant p-value<0.001; grey-colored boxes have a non-significant p-value>0.001.

With such an strong root compartment signal, it was interesting to explore the possibility that *A. thaliana* plants in nature select a species-specific set of microbes, regardless of the environment, compared to phylogenetically unrelated neighboring plants. For this purpose, together with *A. thaliana* plants, I harvested grasses growing in close vicinity (grasses were selected due their high presence in every site and their phylogenetic distance with *A. thaliana*; Du *et al.,* 2016) (three individuals in the first year and one in the following harvesting rounds), and subjected them to the same fractionation protocol described above. In order to make a fair comparison, neighboring plants data was compared only to the *A.thaliana* samples with one single individual, since neighboring plants were not pooled together. PCoA analysis of all compartments did not show a different clustering pattern from the one observed for the *A. thaliana*-only dataset (**Figure**

4B), and fraction is also the main driver explaining the structure of grass-root-associated bacteria (first axis, 16%), followed by site (second axis, 9%). These data were separated by fraction, in order to disentangle at which root-associated compartment soil microbiota might be impacted by different plant species. Thereby, PERMANOVA analysis on each fraction, comparing neighboring and *A.thaliana* plants, showed that in soil and RS compartments, the species effect was non-significant, whereas in RP and root fractions, neighboring plants recruited significantly different bacterial communities compared to *A. thaliana* plants (14% and 4%, p<0.001, respectively) (**Figure 4E, Table 3**). It is likely that exudates released by different plant species at the root vicinity, or other species-specific features, contribute to the recruitment of distinct RP- and root-associated bacteria between *A. thaliana* and grasses.

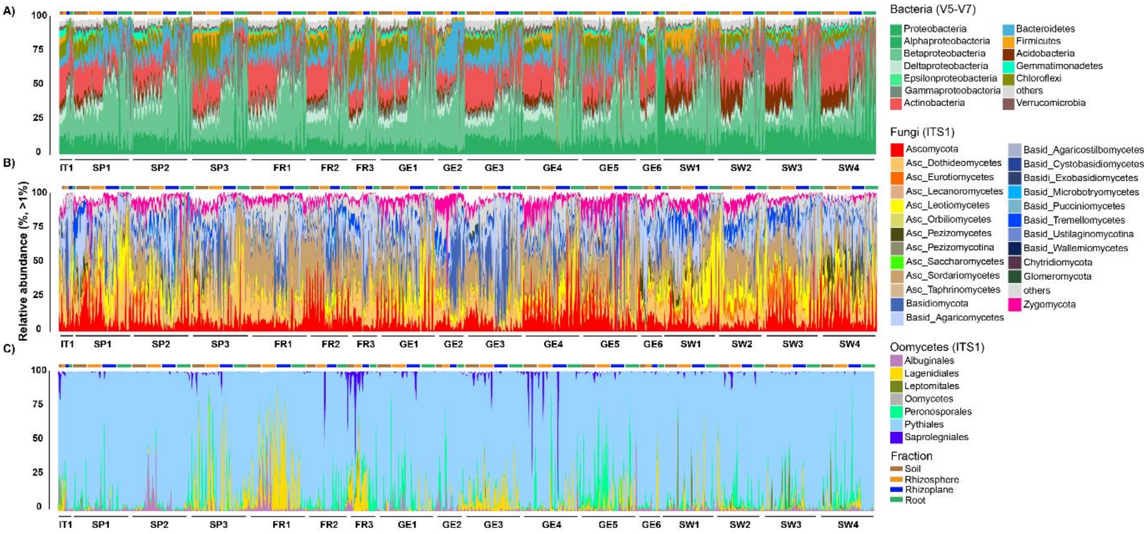

Figure 5: Microbial abundances profiles at a continental scale. Phylum and class-level OTU relative abundances of bacterial **(A)** and fungal profiles **(B)**, and at order level for oomycetal **(C)** profiles, of the whole dataset. Relative abundance is shown for OTUs with >1% relative abundance within each sample. Samples are organized by site (x axis labels) and, within each site, by Fraction (Soil, RS, RP, Root; lines on top of the plot depict which fraction each group of samples belongs to).

As mentioned in the **Experimental set-up** section, most of the harvested plants were pooled in order to obtain enough DNA material. However, this could lead to a masking of individual-to-individual root-associated microbial composition differences. In order to assess this issue, single plants were also harvested in the first two years. Processing of these samples showed that 0.75% (p-value<0.001, PERMANOVA test) of the variation in the full dataset was due to the differences between pooled- or individually-harvested plants (**Figure 4E**). Consistent with that, PCoA of Bray-Curtis dissimilarities shows no species-dependent clustering (**Figure 4C, Table 3**). Detailed evaluation of this effect in each root-associated fraction shows that bacterial communities are slightly, but significantly, impacted by the pooling strategy in the root endophytic samples (1.03%, p-value<0.001), but not in other fractions. Therefore, taking into account this very small variation, pooled samples were preferred for further analysis, due to the low DNA read counts produced by single root samples (**Annex: split_libraries**).

An important output of this dataset was to study the variability of root-associated microbial communities across different years. Therefore, most samples were harvested in three consecutive harvesting rounds, from February to May of 2015, 2016 and 2017. No harvesting was made between June and January, and therefore no seasonal variation could be addressed. A subset of the samples that included samples harvested in all three years (12 out of the 17 sites) was selected to monitor the resilience of microbial communities over time. Although Bray-Curtis dissimilarities show a higher variability for second and third year samples, the overall year variance is only 0.64%. Furthermore, only root samples display a significant variance due to harvesting time (3.12%, p<0.001), whereas bacterial communities in Soil, RS and RP samples remain remarkably stable throughout sampling years (**Figure 4D and E, Table 3**). Thus, it could be concluded that bacterial communities in the studied sites display very robust and stable patterns across successive years.

2.1.4 Fungal communities profile

Fungal communities' data analysis included the same steps as for bacteria. Thus, profiling of the ITS1 of fungal communities shows a similar range of observed OTUs compared to bacterial profiles (between 20 and 500 for a given sample), but, unlike bacteria, fungal communities do not show a significantly different number of OTUs in RP samples compared to root samples (**Figure 3A**, Kruskal Wallis, Dunn test *post-hoc*, p<0.05). Further, the sample variability is much higher between fungal samples than for bacterial samples. Interestingly, if another alpha-diversity index is used, such the Shannon Index, a statistically significant difference can be observed (**Supplementary Figure 2A**). Because the Shannon index takes into account abundance and evenness of species, this suggests that the number of OTUs is overall similar between these two compartments, but that their relative abundance is markedly different. Due to their eukaryotic nature and the fact that fungi form hyphae, it is plausible that fully separating such filamentous organisms growing in a continuum from the soil towards the root is not possible. Therefore, and unlike bacterial community profiles, it is not possible to differentiate the RP fraction from the root in the majority of alpha-diversity indices.

PCoA analysis of the fungal profiles also showed a compartment-dependent distribution, with two main clusters separating the soil and RS samples from the RP and root samples (x axis, 7.8%). In this case, fungal samples appear to have a stronger geographical signature, as clear site-dependent clusters can be observed (for example, clusters of Swedish or Spanish sites) (**Figure 3B**). Indeed, PERMANOVA analysis of the dataset shows that “Site” has the strongest impact on fungal communities, while “Fraction” is the second factor driving fungal communities’ distribution (18.04% and 8.16%, respectively, p-value<0.001; **Table 3**). This site-dependency for fungal samples is even more notable if the dataset is subsetted according to the fraction (**Figure 6A**). In this case, site-specific fungal community clusters can be observed for soil and RS samples. Although still visible in RP and to a lesser extent in root samples, this signature is largely absent in the latter fractions, similarly to bacterial community profiles. PERMANOVA analysis of the “Site” effect on each fraction shows a significant effect for all four fractions, with a gradual decrease from soil to root compartments (from 40.2% in soil to 13.9% in roots, p<0.001, **Figure 6E and Table 3**). This suggests that fungal distribution in soils is strongly impacted by the environment, but, similarly to bacterial communities, host plant roots are also capable of determining fungal communities in root-associated tissues.

The main fungal taxa found in root-associated compartments are Ascomycota, Basidiomycota and Zygomycota members, but also, although less abundant, Chytridiomycota and Glomeromycota, as already shown for other plant species (**Figure 5B,** Coleman-Derr *et al.,* 2016). Unlike bacterial profiles, no clear fraction-dependent patterns were observed at the phylum or class level for fungi. Thus, OTUs’ relative abundances shows a high variability across all sites, with certain taxonomic signatures in each location. For example, in GE2 and GE3, Basidiomycota are more abundant than in other sites; or Pezizomycetes, that are abundant in SW4 but less represented in other sites. Also, fungal profiles contain up to 20% of reads assigned to rare or low abundant taxa (**Figure 5B**).

In order to know whether the roots of phylogenetically-unrelated neighboring plants recruit different fungal taxa, fungal community profiles of a subset of individually harvested *A. thaliana* roots were compared to those of neighboring grasses. PCoA analysis of the Bray-Curtis dissimilarities does not show species-specific clusters (**Figure 6C**). Furthermore, PERMANOVA analysis indicates no statistically significant variance across most root-associated fractions, with the exception of the RP (4.47%, p<0.001, **Figure 6E and Table 3**). This lack of host species-dependent variance in fungal community profiles for endosphere root samples suggests that while bacterial communities have evolved closer host-specific interactions, fungal communities are mainly impacted by environmental factors, although are still driven by root secretions (significant variance in RP samples).

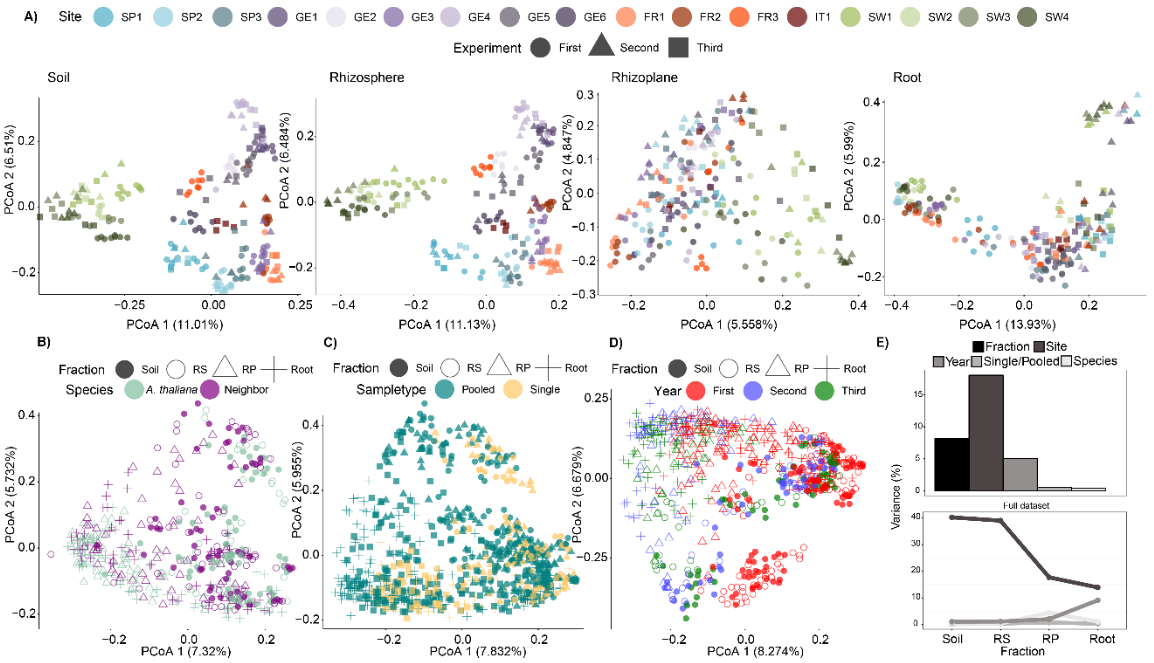

Figure 6: Different factors shape fungal communities composition. A) PCoA plots showing Bray-Curtis dissimilarities between Soil, Rhizosphere, Rhizoplane and Root samples separately, colored by Site and shaped by Year of harvest. **B)** PCoA plot containing a subset of the samples (all individually harvested roots and all neighboring plants, which were plants growing in the surrounding area to *A. thaliana* plants, belonging to the Poaceae family), to show the species-dependent sample clustering. **C)** PCoA containing the full dataset, to show clustering differences between harvesting type (Pooling four plants together or Single plant individuals). **D)** PCoA containing samples harvested in all three years (12 sites, out of 17), to show the year-dependent sample clustering. **E)** Variance explained by each of the plotted variables in A, B, C and D, calculated using permutation analysis (999 permutation, p<0.001), in the full or subsetted dataset (upper plot) and in each root-associated compartment (lower plot).

Comparison of pooled versus individually harvested roots shows no specific cluster due to the sampling method in the PCoA visualization; furthermore, PERMANOVA analysis indicates that fungal communities are not significantly different between roots of single and pooled individuals, suggesting low individual-to-individual variation in fungal communities associated with *A. thaliana* roots. (**Figure 6C and E, Table 3**).

Fungal community stability across successive years has not been thoroughly explored in natural plant populations (Cordier *et al.,* 2012). Thus, as for bacterial profiles, fungal profiles were compared between sites harvested every year. Such analysis shows a differential cluster of samples in the PCoA analysis, with a similar profile across year but with a slight shift from one year to the next (**Figure 6D**). Analysis of the variance shows that fungal communities in all fractions are significantly impacted by the year of harvest, although with an increasing gradient from soil to root samples (from 1.13% in soil to 9.14% in roots, p<0.001, **Figure 6E**, **Table 3**). Such gradient could be indicative of the local adaptation of fungi, where they respond robustly to environmental changes in soil over time and colonize differently plant hosts over successive years.

2.1.5 Oomycetal communities profile

Although most oomycetes described to date are highly destructive plant pathogens, it remains unclear whether healthy plants engage in intimate association with oomycetal species in their natural habitats (Kamoun *et al.,* 2015). Examination of the alpha-diversity showed that oomycetal communities contain only up to 76 OTUs per sample, with root samples containing very low number of observed OTUs (6 to 65), which contrasts with root-associated bacterial (12-425) and fungal (11-331) communities' profiles (**Figure 3A**). Similarly to fungi, the number of observed OTUs are overall similar in RP and Root samples, but significantly lower than in RS and soil samples (Kruskal Wallis, Dunn test *post-hoc*, $p<0.05$). However, because Shannon and Chao indices are significantly higher and lower, respectively, for RP samples than for root samples (**Supplementary Figure 2B**), it is likely that both OTU relative abundances and rare OTU taxa influence alpha-diversity indices in RP samples. This suggests that, very low number of oomycetes can actually colonize root-associated compartments, but that this low amount of oomycetes members are very abundant at the root vicinity, prior colonization (in RP compared to root fraction).

Inspection of oomycetal beta-diversity using PCoA of a Bray-Curtis dissimilarity matrix did not show a clear compartment-specific distribution. Although a slight separation in the second axis can be observed from soil and RS samples to RP and root samples, the oomycetal dataset appears to be very variable overall, especially in RP and root samples (**Figure 3B**). In fact, both "Site" and "Fraction" have lower impact on oomycetal communities compared to either fungal or bacterial communities (11.34% and 2.97% respectively in oomycetal communities, compared to 18.04% and 8.16% respectively in fungal communities, or 13.62% and 15.95% respectively in bacterial communities, PERMANOVA analysis, p-value<0.001, **Table 3**). Different visualization of the dataset and subsetting of the samples according to the fraction, shows a site-dependent clustering in soil and RS samples, slightly decreasing towards the root samples (PERMANOVA analysis, from 15.12% in soil to 13.49% in roots, p-value<0.001, **Figure 7A and E, Table 3**). In contrast to bacterial and fungal community profiles, a strong year-dependent clustering can be observed, which explains most of the variance observed in oomycetal communities distribution (12.77%, p-value<0.001) (**Figure 7A, D and E, Table 3**). Altogether, oomycetal communities are impacted strongly by environmental and year-dependent variation, which is not reduced in root-associated tissues, suggesting a less tight association with the host plant, compared to other microbial groups.

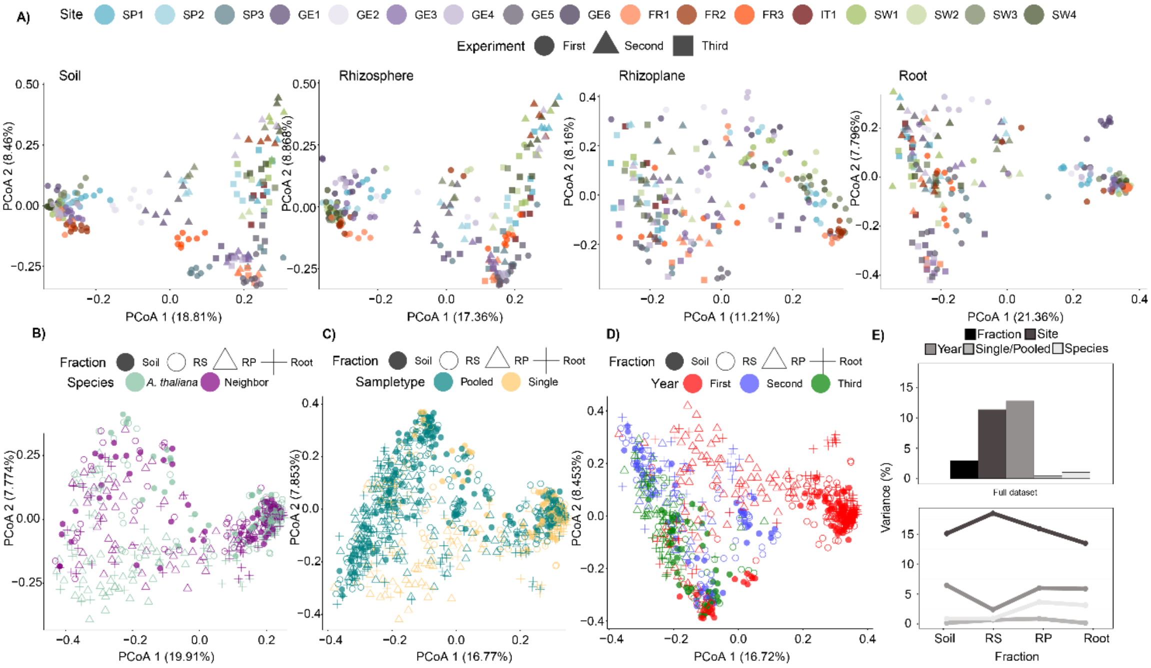

Figure 7: Different factors shape oomycetal communities composition. A) PCoA plots showing Bray-Curtis dissimilarities between Soil, Rhizosphere, Rhizoplane and Root samples separately, colored by Site and shaped by Year of harvest. **B)** PCoA plot containing a subset of the samples (all individually harvested roots and all neighboring plants, which were plants growing in the surrounding area to *A. thaliana* plants, belonging to the Poaceae family), to show the species-dependent sample clustering. **C)** PCoA containing the full dataset, to show clustering differences between harvesting type (Pooling four plants together or Single plant individuals). **D)** PCoA containing samples harvested in all three years (12 sites, out of 17), to show the year-dependent sample clustering. **E)** Variance explained by each of the plotted variables in A, B, C and D, calculated using permutation analysis (999 permutation, $p<0.001$), in the full or subsetted dataset (upper plot) and in each root-associated compartment (lower plot).

Relative abundances of oomycetal OTUs at the order level is dominated by taxa belonging to the Pythiales group. As it was the case for fungal members, there is no clear compartment-dependent signature; however, it is possible to distinguish specific oomycetal profiles for each site (**Figure 5C**). For example, Albuginales members are abundant in soils of SP2 and FR1, but very low abundant in most of the other sites; also, the Lagenidiales group is very abundant in FR1, FR3 and GE3 samples, but very seldom present in other sites. Notably, although most of the OTUs present in the oomycetes profiles come from the Pythiales group, almost 100% of the reads are assigned to an abundant taxonomic order, in contrast to fungal profiles (**Figure 5B and C**).

Comparative analysis of *A. thaliana* and neighboring plants' oomycetal profiles shows no species-specific clustering in the full dataset. However, RP and root samples are significantly impacted by the different plant species (3.66% and 3.14%, respectively, PERMANOVA analysis, p-value<0.001, **Figure 7B, Table 3**). These differential oomycetes profiles, as for bacterial and fungal communities, could be explained by species-specific secretion or certain root features.

Comparison between pooled roots and individually harvested roots showed similar results in oomycetal profiles, comparable to either bacterial or fungal profiles. Thereby, no specific clustering could be observed in the full dataset, although it was noticeable that single samples appear more scattered in the PCoA representation, indicating a possible higher variability between single roots or a lower sequencing depth due to lower sample quality (**Figure 7C, Annex: split_libraries**). Still, this suggests a very low individual-to-individual variation in root-associated oomycetal communities.

2.1.6 Microbial site-dependent signatures

As shown above, microbial communities are heavily impacted by their local environment and the distance to the root, although at different extents, depending of the microbial group of study. Therefore, it is plausible to hypothesize that root-associated microbial communities will have members that are specifically more abundant in certain locations, in comparison to any other site. In order to test whether root-associated bacterial, fungal, and oomycetal OTUs show contrasting enrichment patterns across sites, I performed site-dependent enrichment tests in root samples using a Generalized Linear Model. This shows a subset of root-associated OTUs significantly more abundant in one of the sites, compared to the other 16 (Generalized Linear Model, p.adj.method=FDR, p-value<0.05, **Figure 8**). These OTUs are taxonomically very diverse and, in some cases, very abundant within one site. This is the case, for example, of the OTU belonging to the Alphaproteobacteria class in the site GE6, which accounts for more than the 60% of the total read count in plant root samples from that site. This is also the case for certain root-associated fungal or oomycetal OTUs, belonging to the Ascomycota and Lagenidales groups, respectively, that account for 10-15% of the total abundances profiles in their respective sites (**Figure 8B and C**). Notably, there is a reduced number of root-associated bacterial OTUs specifically enriched in each site (average of 10 enriched bacterial root OTUs), compared to either fungal or oomycetal OTUs (average of 22 and 34 enriched fungal and oomycetal OTUs, respectively). These results corroborate the finding that a substantial proportion of fungal and oomycetal OTUs detected in plant roots are site-specific, whereas root-associated bacterial OTUs are more conserved across sites (**Figure 8**).

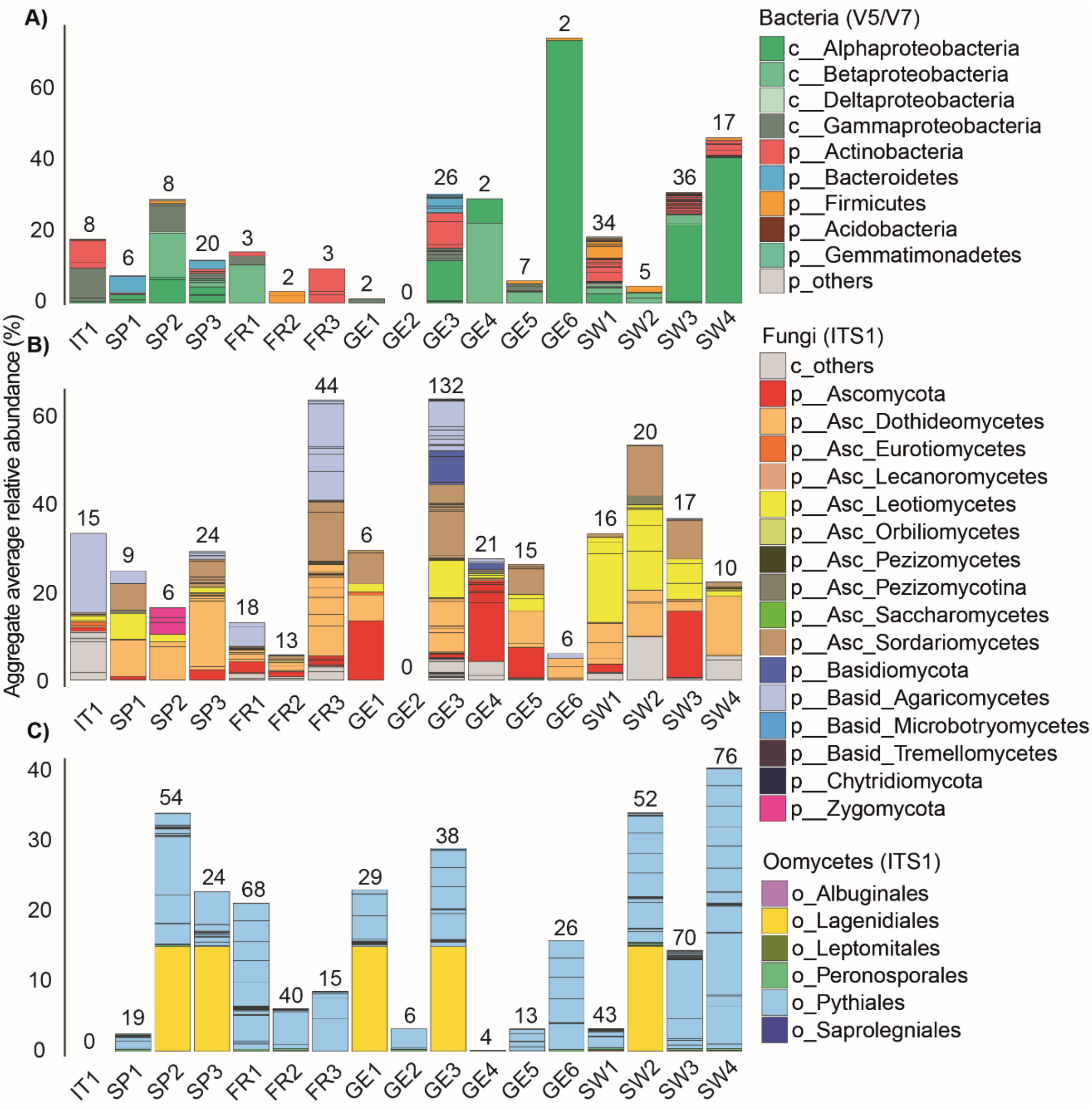

Figure 8: European site-specific microbial signatures. Site enriched OTUs in root endophytic compartments (Generalized linear model, GLM, p.adj.method=FDR<0.05), shown as aggregate average relative abundance, for bacterial **(A)**, fungal **(B)** and oomycetal **(C)** profiles. Each block within each bar corresponds to one single OTU (numbers on top of group of bars indicates the number of OTUs enriched in a given site). Color-code of the bar is based on OTU taxonomic assignment (phylum- and class- level for bacterial samples, class level for fungal samples, and order level for oomycetal samples).

2.1.7 The Arabidopsis root core microbiota at the European scale

The high distance between sites, the successive sampling over years, and the large number of replicates in the current dataset, provide a unique opportunity to determine whether root-associated microbiota members are consistently and robustly found within *A. thaliana* root tissues across Europe. In order to address this question, I subsetted the data to pooled root samples that were harvested across all three years (namely, FR1, SP1, SP2, SP3, GE1, GE3, GE4, GE5, SW1, SW2, SW3 and SW4). Then, I calculated which OTUs were present in at least half of the samples of each site. Based on these calculations, only 13 bacterial OTUs, 5 fungal OTUs, and 3 oomycetal OTUs that were present in all sites across three successive years could be identified (**Figure 9**). Remarkably, the relative abundance of resilient root-associated bacterial OTUs range between 25 and 55%, indicating that these few core OTUs represent a large fraction of the endosphere bacterial root microbiota. These belong to the four most representative phyla found in plant roots: Proteobacteria (members of the Bradyrhizobiaceae, Rickettsiales, Comamonadaceae, Oxalobacteraceae, Bulkholderiaceae, and Pseudomonadaceae groups), Actinobacteria (Mycobacteriaceae family), Bacteroidetes (Flavobacteriaceae family) and Firmicutes (Bacillaceae family), suggesting that the "core" root microbiota requires a minimal bacterial diversity for stability. Regarding the fungal and oomycetal OTUs, these belong to the Ascomycota (*Ilyonectria*, *Fusarium*, *Tetracladium* and *Plectosphaerella* genera) and the Zygomycota (*Mortierella* genus), and to the Pythiales (*Pythium* genus) and Albuginales (*Albugo* genus) which are also part of the most abundant taxa in root-associated microbiota. By looking at the OTUs that are conserved in at least 75% of the sites, many more OTUs were identified compared to those present in 100% of the sites (333 bacterial, 15 fungal and 8 OTUs, **Supplementary Figure 3**). Since the initial method was very stringent, the OTUs present in 100% of the sites should be also found in every other studied site. Indeed, all "core" OTUs can also be found in root samples of the sites that were not included for the initial calculation (namely, IT1, FR2, FR3, GE1 and GE6), suggesting that these microbial groups are in fact part of the *A. thaliana* root microbiota across Europe (**Supplementary Figure 4**).

2.2 Influence of stable environmental factors on microbial communities' composition

Microbial communities are impacted by their local environment, at different extents depending on which microbial group is analyzed, as shown above. It is has been previously reported that soil composition is a major driver of soil microbiota composition and, therefore, a major driver of the microbial input that will finally colonize plant roots (Lauber *et al.,* 2009; Rousk *et al.,* 2010). Since the current dataset includes several soil textures and very different concentrations of nutritional elements (**Annex: Table 1**), I used this information to correlate how different soil characteristics and the interactions between these components impact microbial communities' composition across European sites. Due to the lack of certain soil nutritional values for the IT1 samples, these were removed for the current analysis. Samples belonging to different root-associated compartments were analyzed together, since even though soil composition will have more impact on soil communities, this impact should also be visible in other fractions. Permutational Multivariate Analysis Of Variance Using Distance Matrices (*adonis* formula in R, see **Methods**) was used to calculate the effect of individual soil nutritional elements on bacterial, fungal and oomycetal communities, but also the effect of the interaction of each nutrient combination (**Figure 10**). Based on this analysis, the overall major driver of microbial communities is pH (5.95%, 3.57%, and 1.43%, p-value<0.001, in bacterial, fungal and oomycetal community profiles, respectively) (Lauber *et al.,* 2009; Rousk *et al.,* 2010), but also iron for bacterial (4.8%, p-value<0.001) and fungal communities (2.83%, p-value<0.001), and manganese for oomycetes (1.95%, p-value<0.001). Interestingly, Swedish soils are very rich in iron, compared to any other site (**Annex: Table 1**). Thus, it is very likely that this is one of the main reasons driving the separation of Swedish sites observed above (**Figure 3A**). Also, while bacterial communities appear to be impacted by only a subset of soil nutrients, such Boron (3.31%, p-value<0.001) or Reserve Calcium (2.98%, p-value<0.001), fungal and oomycetal communities have more soil-nutrients-dependent profiles, indicating that local soil nutritional characteristics influence fungal and oomycetal biogeography and contribute to the strong site-specific microbial signatures observed in natural *A. thaliana* populations. Interestingly, some soil nutrients display higher impact on microbial communities only in combination with others. For example, Available Calcium together with Reserve Magnesium have a higher impact on both bacterial and fungal communities than each separately (interaction: 3.64% and 2.31%, in bacterial and fungal communities, compared to 2.48% and 1.08% respectively for bacterial communities, and 2% and 1.61% respectively for fungal communities, **Figure 10**), suggesting that interactions between soil geochemical characteristics are key factors to account for when studying microbial communities composition in nature.

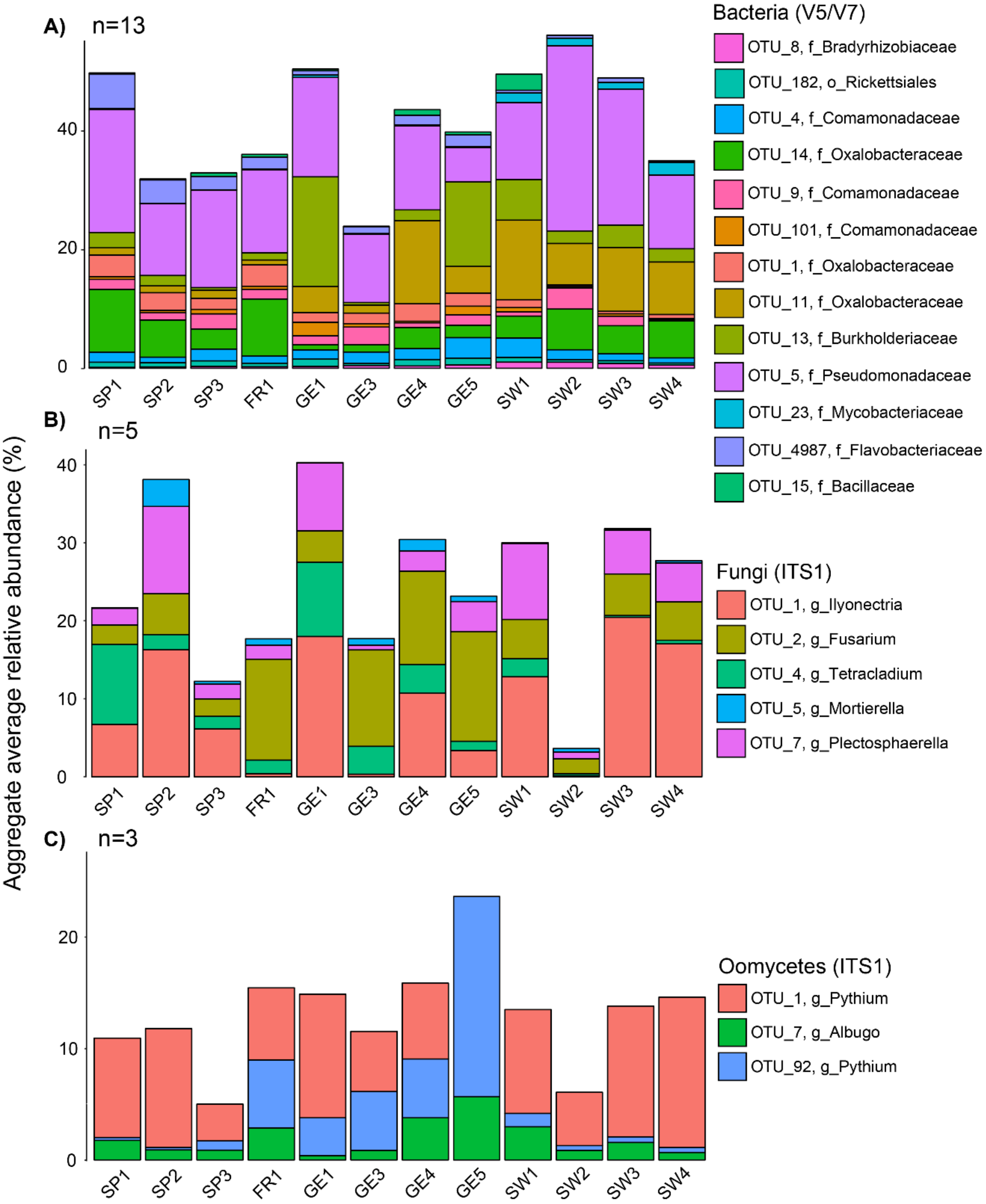

Figure 9: The Arabidopsis root core microbiota across Europe. Aggregate average relative abundances of the bacterial **(A)**, fungal **(B)** and oomycetal **(C)** OTUs present all harvested years and in at least 50% of the samples of each site* (*oomycetal OTUs are present at least in 50% of the samples of 92% of the sites). (”n” represents the number of OTUs that are present in all sites per microbial group). Each OTU has the lowest taxonomic assignment possible for each microbial group (family for bacterial profile, and genus for fungal and oomycetal profiles).

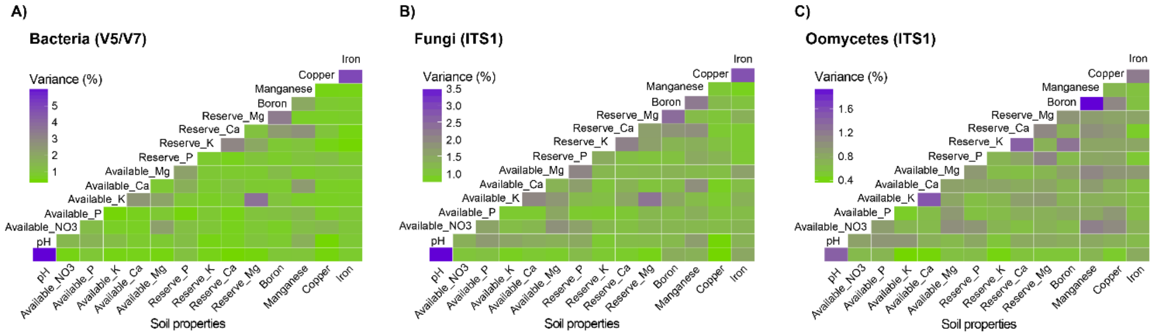

Figure 10: Soil properties driving microbial communities' composition. Heatmaps illustrating variance explained by soil properties in bacterial **(A)**, fungal **(B)** and oomycetal **(C)** communities, and the variance explained by the interaction of each of these soil properties (*adonis* test, p-value<0.001). Color code reflects the variance level (purple color shows higher variance, green color shows lower variance). Note that for each microbial group, there is a legend with different variance limits.

2.3 Influence of climate and host genotype on microbial communities' composition

Microbial communities are highly impacted by the factor "Site", which includes numerous environmental parameters, including soil characteristics but also climatic conditions. Soil properties, however, appear to have a reduced impact on microbial distribution, compared to the overall geographical effect. The impact of climatic conditions could not be addressed in the previous experimental set-up since samples were harvested at a given day and time, which is not representative of the overall climate in every site. Therefore, in collaboration with Prof. Dr. Jon Ågren and Dr. Thomas Ellis, we set up several experiments to address the following questions: 1) how does the climate shape microbial communities? 2) how do specific *A. thaliana* accessions shape their own root microbiota? and 3) is the soil microbiota relevant for local plant adaptation? In order to answer these questions, a common-garden experiment in the field and, in parallel, another common-garden experiment under controlled laboratory conditions were performed (see **Methods** for details).

First, two sites with contrasting climatic conditions were selected out of the 17, namely IT1 (Castelnuovo di Porto, Italy, **Annex: Table 1**) and SW4 (Rödåsen, Sweden, **Annex: Table 1**). At these sites, a transplantation experiment was set up where Swedish and Italian soils were transferred in trays and placed at each site. Then, seedlings of Italian accessions (It15, It24, It32, It41) and Swedish accessions (Sw7, Sw11, Sw43, Sw47) pre-germinated in agar plates were transferred to the trays in Italy and Sweden. In this way, we could assess climate and genotype effect on soil and root-associated microbial communities, as well as the impact of climate and soil on plant fitness (**Supplementary Figure 5**). The experiment started during October 2016 and plants were harvested in March 2017 (IT1) and May 2017 (SW4), so that plants would go through a full life cycle and that they would be at similar developmental stage (i.e. flowering). Harvesting consisted of taking each plant and their surrounding soil, removing as much soil attached to the root as possible and keeping this root as a technical replicate (this made between 6 and 12 technical replicates per condition, depending on plant survival). Then, a soil sample was taken from the remaining in the well. Due to the size of the well (20x20mm), the roots would occupy the majority of the space and, therefore, these soil samples would be mostly rhizospheric samples (**Supplementary Figure 5**). Also, root samples would still contain the RP fraction as no fractionation protocol was performed. These root and soil samples were snap-frozen in dry ice and transported to the laboratory, where DNA extraction and library preparation was performed (see **Methods**). Due to high plant mortality, especially at the Swedish site, where no Italian accession survived (**Supplementary Figure 6**), unplanted soil samples were taken, as well as planted soil samples where the *A. thaliana* plant had died. In total, 144 root and soil samples were processed.

The first output of this experimental set-up was the plant survival rate before the winter period (to score plant establishment at each site), and plant fitness as number of fruits per reproductive adult (i.e.: that had flowers at the counting time) shortly before root and soil harvesting. Survival of plants before winter already showed a local adaptation dependency for both Italian and Swedish lines. Swedish plants grown in Swedish soil in Sweden had significantly higher survival rate than Italian plants in the same conditions and *vice versa* (Italian plants in Italian soil in Italy had significantly higher survival rate than Swedish plants under the same conditions) (**Supplementary Figure 6A and B**). After winter time, overall plant survival in SW4 was very low and, furthermore, almost no Italian plants were alive at scoring time. Therefore, no fitness data is available for this site. Nevertheless, in the Italian site, we observed that Italian plant genotype produced significantly more fruits in the Italian soil than Swedish plants, but also that Swedish plants produced significantly more fruits in the Swedish soil than in the Italian soil (**Supplementary Figure 6D**). These results suggest that there is a climate dependency for plant fitness, but also a soil dependency.

Microbial profiling of the field common-garden experiment (including V5/V7 for bacterial profiling and ITS1 for fungal and oomycetal profiling) showed that alpha-diversity of microbial communities does not consistently vary across conditions. Only bacterial communities in root samples show a significant decrease in diversity upon Climate x

Genotype change in Italian soil. In contrast, these bacterial root communities show a significant diversity increase in Swedish soil. Fungal and oomycetal communities show no significant changes, probably due to the high variability across samples (**Supplementary Figure 7**).

Bray-Curtis dissimilarities analysis, by calculating the distance between clusters (considering soil as the stable parameter and "changed conditions" each of the clusters, namely "Control", "Climate", "Genotype" and "Climate x Genotype" or "CxG") it was notable how, from the Control cluster (for example, Italian soil with an Italian genotype in Italy), Climate and CxG clusters significantly separated, whereas the Genotype cluster does not significantly shift apart from the Control cluster (Kruskal Wallis, Dunn test *post-hoc*, p-value<0.05, **Figure 11A**). This is the case for all microbial groups, for both soil types (Italian and Swedish) and for both fractions (root and soil). This result indicates that climatic changes strongly impact root- and soil-associated microbial communities but that host genotype does not drive significant changes on its surrounding microbes. It would be evident to hypothesize that the change observed in CxG conditions is a reflection of the Climate effect alone; however, deeper inspection and comparison of microbial communities related to Climate only and CxG conditions showed that this was not the case. Representation of microbial relative abundances indicated slight changes in microbial community composition upon Climate and CxG changes (**Supplementary Figure 8**). To further account for microbial differences between the Climate and CxG conditions only, samples were splitted by fraction (root and soil samples separately) and also by soil type, because, consistently with the European transect data, these are the strongest drivers of bacterial and fungal communities (**Table 4**). PERMANOVA tests of the subsetted data shows a high variance explained by changing the climate, for all microbial communities, but especially for fungi (between 16-35% for bacterial communities, between 20-40% for fungi and between 14-15% for oomycetes, **Table 4**). Notably, combination of Climate x Genotype, however, drives the highest variance for all microbial groups (up to 53% for bacteria, up to 41% for fungi and up to 29% for oomycetes). Furthermore, Generalized Linear Model analysis (p.adj.method=FRD, p-value<0.05) of each microbial group and each soil type separately, shows significantly enriched microbial members when comparing the two conditions, especially in bacterial community profiles (**Figure 11B**). This result indicates that there is a host genotype effect on root-associated microbial communities that is climate-dependent. There are 54 bacterial OTUs (in Swedish soil) and 15 bacterial OTUs (in Italian soil) significantly changed. These bacteria are taxonomically diverse (Proteobacteria, Actinobacteria, Bacteroidetes and other phyla, **Annex: Supplementary Table 1**), whereas the 22 fungal

OTUs (in Swedish soil) that significantly changed mostly belong to the Ascomycota phylum (**Annex: Supplementary Table 1**). Due to high variation in oomycetes profiles, no significantly different OTUs could be captured.

	Factor	**Fraction**	**Bacteria (V5/V7)**	**Fungi (ITS1)**	**Oomycetes (ITS1)**
	Soil		48.15	31.47	4.41
	Fraction		20.15	9.56	4.03
Italian soil	**Climate**	*Matrix*	30.11	39.14	15.36
		Root			
	Genotype	*Matrix*	1.11	1.27	1.73
		Root	3.18	2.82	3.83
	ClimatexGenotype	*Matrix*	38.98	41.4	19.27
		Root	53.13	27.28	22.38
Swedish soil	**Climate**	*Matrix*	35.93	40.31	19.32
		Root	16.63	20.16	14.38
	Genotype	*Matrix*	1.03	1.48	1.25
		Root			
	ClimatexGenotype	*Matrix*	45.96	37.77	29.64
		Root	26.05	20.2	16.84

Table 4: Factors driving microbial composition in transplantation experiment. PERMANOVA analysis (999 permutations, p-value<0.001). Full dataset was used to calculate "Soil" and Fraction" effects. Then, samples were separated by these factors to calculate "Climate", "Genotype" and "Climate x Genotype" effects. Green-colored cells have a significant p-value<0.001; grey-colored cells have a non-significant p-value>0.001.

In order to reduce the environmental background inherent to the previous experiment, the same experimental set-up was reconstituted in climatic chambers, located at Uppsala University (Sweden). These growth chambers mimicked very closely SW4 and IT1 climatic conditions for a period of 6 months (i.e.: day-to-day variation in light quantity, humidity, temperature, etc. See **Methods**), where the Swedish winter was shortened in order to match the Italian chamber timeline (see **Methods**). After six months of incubation in each climatic chamber, roots and surrounding soil were harvested similarly to the field experiment. Then, DNA extraction and library preparation for bacterial, fungal and oomycetal profiles were also performed. Analysis of the sequencing data showed that the overall conclusion from the field experiment remained true (Climate has a strong impact on microbial communities, CxG has the strongest, but Genotype effect remains non-significant, **Supplementary Figure 9**). Sample variability, surprisingly, was much higher in this experimental set-up than it was in the field experiment, probably due to technical reasons, such desiccation or chamber edge effect (**Supplementary Figure 9A,** see **Methods**).

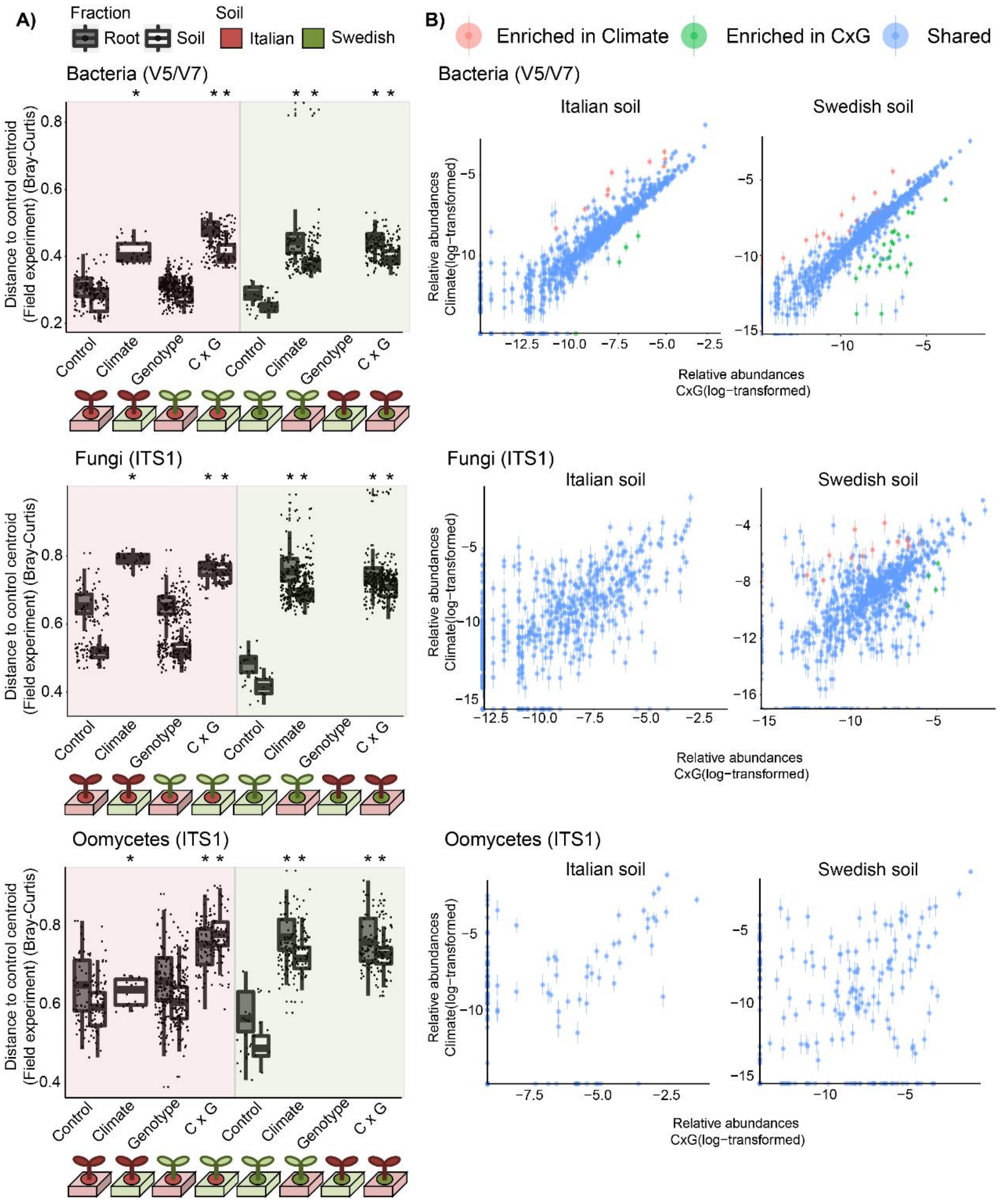

Figure 11: Microbial communities' composition in the common-garden field experiment. A) Plots depicting average Bray-Curtis distances between clusters of conditions (x axis) in root and soil samples, for bacterial, fungal and oomycetes profiles. Cartoons show which conditions are changed, while soil (either Italian -red- or Swedish -green-) remains as the constant factor. Asterisks indicate in which conditions microbial communities are significantly apart from the control cluster (Kruskal-Wallis, Dunn test *post-hoc*, $p<0.05$). **B)** Regression plots comparing the log-transformed relative abundances of bacterial, fungal and oomycetal OTUs in the conditions Climate (x axis) and CxG (y axis), for Italian soil (left panels) and Swedish soil (right panels). Red- and green-colored are OTUs significantly enriched in the Climate and CxG conditions, respectively (Generalized Linear Model, p.adj.method=FDR, p-value<0.05).

Taking these and the European transect results into account, it is plausible that most of the "Site" effect observed for microbial communities across Europe, actually arises from the climate effect on this microbiota, and that host genotype drives subtle microbial community shifts in a climate-dependent manner (i.e., climate x genotype interaction).

2.4 Comparison of bacterial and fungal profiles using different amplification regions

An important output of this project was to rule out the possibility that there are sequencing and results biases due to the amplified DNA regions used for both bacterial and fungal community profiles. Currently, a large body of literature report the structure of plant-associated microbiota (Bulgarelli *et al.,* 2013; Rastogi *et al.,* 2013) but it remains difficult to cross-reference results due to the lack of standardization and the use of different marker loci (Thompson *et al.,* 2017). Therefore, it was important to address this question with the current dataset, as it contains a large amount of samples and it compares more than one microbial group. In order to validate the sequencing results obtained for bacteria using the 16s V5/V7 and for fungi using the ITS1 region (see above), I also produced sequencing libraries using the same DNA samples but using PCR primers that target a different region of the bacterial 16s rRNA gene (region V2/V4) and of the fungal ITS-related region (ITS2).

First, I grouped OTUs by their taxonomic assignment at phylum level and compared which groups were represented by both primer pairs. Overall, V2/V4- and ITS1-derived regions capture more phylogenetic diversity compared to either V5/V7 or ITS2, (8 and 2 additional phyla detected, respectively). However, all these phyla are largely underrepresented across the dataset and contain low abundant OTUs. Therefore all taxonomic groups not shared between the two pairs of libraries (targeting V2/V4 and V5/V7 for bacteria, and ITS1 and ITS2 for fungi) were not considered for this comparative analysis. Relative abundance estimates were used at different taxonomic levels per amplifying pair. Thereby, comparison at the phylum level between the V2/V4 and V5/V7 regions of the bacterial 16s rRNA showed a very significant correlation (Pearson's correlation 0.70, p-value=9.87e-07; Mantel statistical r=0.50, p-value<0.001, **Figure 12**). However, at lower taxonomic resolution, such class or order levels, these correlations, although significant, are lower (0.41, p-value=1.15e-5 and 0.315, p-value=5.1e-5, respectively). It is important to note that at lower levels, such family or genus, the taxonomic assignment to the public database is very poor for both libraries and many OTUs are grouped as "non-assigned". This is the case for both libraries and, therefore, the high correlation values are actually reflecting the high overlap between "non-assigned" OTUs (for example, it can be observed that almost half of the phyla compared in **Figure 12A** are no longer present in the comparison of **Figure 12D)**. In the case of fungal profiles, correlation at phylum levels is very high (Pearson's correlation 0.992, p-value=1.06e-5; Mantel statistical r= 0.55, p-value<0.001, **Figure 13**), but also at lower taxonomic levels (order: 0.94, p-value=2.2e-16; family: 0.97, p-value=2.2e-16; genus: 0.98, p-value=2.2e-16, **Figure 13**). In this case, ITS1- and ITS2-based libraries appear to give very consistent taxonomic and relative abundance results.

Deeper analysis of the profiles shows first that, similarly to the V5/V7 data, root compartmentalization drives most of the bacterial variation in the V2/V4 profile, followed by biogeography and year variations (55%, 6.73% and 0.99%, respectively, p-value<0.001, PERMANOVA analysis, **Supplementary Table 2**). Interestingly, fraction-dependent variance is greatly magnified in V2/V4 (from 15.95% in V5/V7 to 38.24% in V2/V4 profile, **Table 3**, **Supplementary Table 2, Supplementary Figure 10A**). Distribution of the samples in the plot is very similar between the two datasets, where Swedish soil and RS samples cluster separately from other sites, and there is a convergence at the root fraction (**Supplementary Figure 10A**). Maybe due to the higher number of rare taxa found in V2/V4, soil samples amplified with this region display higher variance explained by the different years of harvesting (non-significant, 0.55 in V5/V7 and 3.69%, p-value<0.001 in V2/V4). Similar species-dependent variance can be observed between the two datasets (14.7% and 4.63% in Rhizoplane and Root samples, respectively, in V5/V7, compared to 9.12% and 2.94% in Rhizoplane and Root samples, respectively, in V2/V4, p-value<0.001, PERMANOVA analysis, **Table 3**, **Supplementary Table 2**). Although both V2/V4 and V5/V7 regions provide overall similar information regarding community diversity and structure, as well as regarding the factors that shape these communities, the V2/V4 region appears to provide a better resolution for low abundant OTUs (**Figure 12**).

In the case of ITS1 and ITS2, the main variables impacting ITS1 profiles remain correct for ITS2 profiles. Thus, "Site" is the most important factor driving fungal communities distribution, followed by fraction and year of harvesting (18.04%, 8.16% and 5.05, respectively, in ITS1 and 14.82%, 5.33% and 9.9% in ITS2, PERMANOVA analysis, p-value<0.001, **Table 3**, **Supplementary Table 2**). By looking at the PCoAs of the ITS1 and ITS2 profiles, a very similar distribution pattern can be observed, although the ITS2 clusters are tighter together, compared to the ITS1 clusters (**Supplementary Figure 10B**). Further, ITS2 profiles only appear to be slightly more impacted by the species-specific effect in RP samples compared to ITS1 (9.94% in ITS2 and 4.47% in ITS1 profiles, p-value<0.001). In conclusion, fungal community profiles are highly consistent between both ITS regions, and, therefore, either of them will be suitable for further analysis.

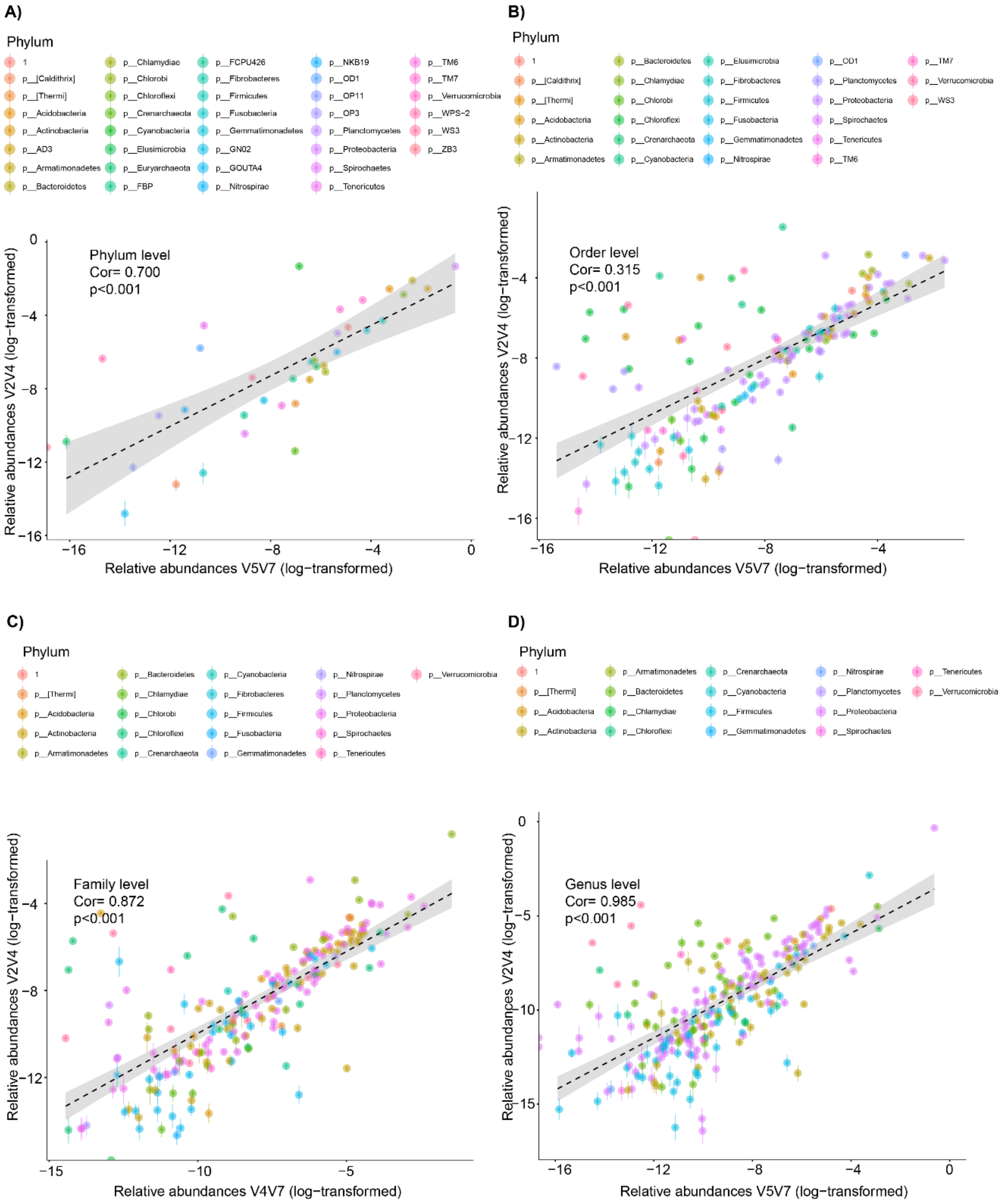

Figure 12: Bacterial profiles amplified with two different loci in the 16s region (V5-V7 and V2-V4). Plots showing the taxonomic overlap between log-transformed relative abundances of bacterial OTUs obtained using V2V4 and V5V7 from the bacterial 16s rRNA region amplification, at phylum **(A)**, order **(B)**, family **(C)** and genus **(D)** levels. (Pearson's correlation test, p-value<0.001). Grey area along the regression line denotes the smoothed conditional means. Note that due to the low taxonomic assignment at the species level, correlation levels are inflated.

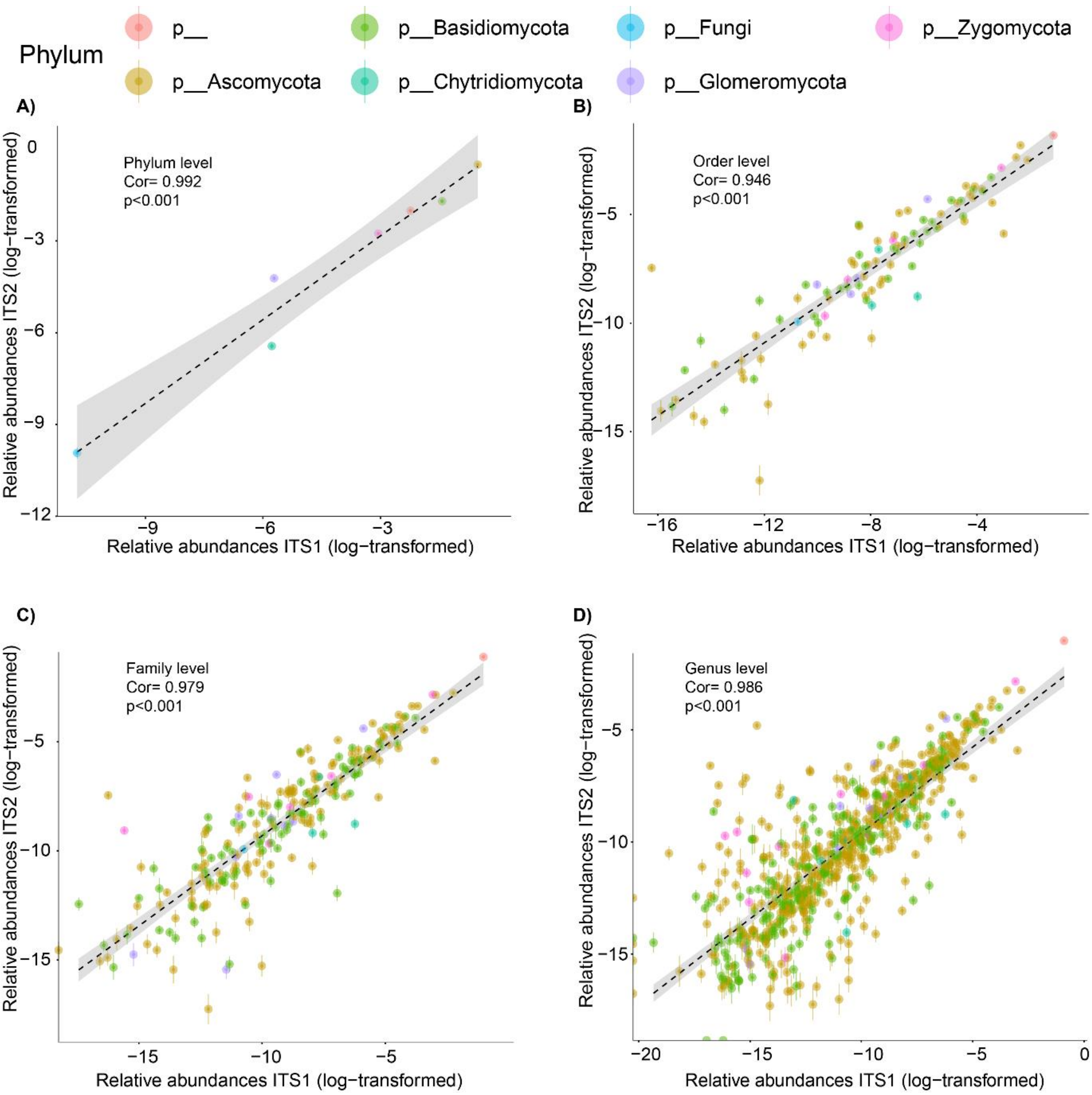

Figure 13: Fungal profiles amplified with two ITS regions (ITS1 and ITS2). Plots showing taxonomic overlap between log-transformed relative abundances of fungal OTUs obtained amplifying ITS1 and ITS2 fungal regions, at phylum **(A)**, order **(B)**, family **(C)** and genus **(D)** levels. (Pearson's correlation test, p-value<0.001). Grey area along the regression line denotes the smoothed conditional means.

3. DISCUSSION

3.1 Distinct root-associated compartments are potential microbial niches

Previous studies already determined that bacterial and fungal communities are strongly impacted by the root compartment (Bulgarelli *et al.,* 2013; Edwards *et al.,* 2015). Therefore, it was important for the aim of this project to establish a fractionation protocol that selectively separates distinct root niches colonized by epiphytic and endophytic microbes. More importantly, this protocol had to be adapted for distinct microbial groups to allow comparative analysis between microbial profiles. Bulk soil and RS fractions were obtained as described previously (Bulgarelli *et al.,* 2012); further, it was noted that, in rice roots, RP is an important fraction where microbes that will colonize the root interior are filtered (Edwards *et al.,* 2015). The protocol initially utilized in this study included a sonication step in order to harvest RP-associated microbes. However, this sonication treatment heavily shattered *A. thaliana* roots (**Figure 2B**) and these sonicated roots, printed on TSA 50% did not show significantly lower number of CFUs compared to untreated roots (Kruskal-Wallis, Dunn test *post-hoc*, p-value<0.05, **Figure 2B**). Furthermore, I hypothesized that the same damage observed on root surface upon sonication, could affect fungal and oomycetal hyphae which, therefore, makes this step not suitable for the purpose of this project. Using an adapted protocol from Agler *et al.,* 2016a, where they could recover specific microbes inhabiting the leaf surface, I tested whether sequential detergent washes would efficiently recover microbiota from the RP and enrich for root endophytes. Subsequent detergent washes showed a trend of increasing removal of microbes from the root surface, but not significantly. However, this method showed the highest recovery of RP microbes (**Figure 2B**). Therefore, this final fractionation protocol was the one incorporated for the next steps in this project (**Figure 2A**).

3.2 Only a specific fraction of the soil microbiota can colonize root endosphere

Bacterial communities have been described to decrease gradually their species diversity from bulk soil to endosphere root compartments (Bulgarelli *et al.,* 2012; Lundberg *et al.,* 2012; Edwards *et al.,* 2015). Such observation is also true for fungal communities, although compartment-driven variance is much lower than for bacterial communities (Coleman-Derr *et al.,* 2016; Hacquard, 2016). Alpha-diversity analysis of the full dataset showed significant decrease of bacterial communities from soil samples to root endophytic fraction, with a significantly different fraction between RS and root compartments: the rhizoplane (RP) (**Figure 3A,** Edwards *et al.,* 2015). Although the species diversity also decreased for fungal and oomycetal communities, the RP fraction did not harbor a significantly different number of fungal and oomycetal OTUs compared to the endophytic fraction. In the case of fungal communities, the Shannon Index highlights a significant difference between RP and roots samples, suggesting that, even though OTU number and assignment are very similar, their relative abundances change from the root surface towards the root interior (**Supplementary Figure 2A**). Nevertheless, and as already mentioned in the **Results** section, it is very likely that the fractionation protocol, although successful separating compartments, it captures the same eukaryotic microbes that grow in a continuum from the soil to the plant root. Still, it can be concluded that the microbial communities studied here are filtered towards the root compartment, with more or less specificity depending on the microbial group of study. On the other hand, it would also be plausible to consider that only a small fraction (<25%) of the soil bacterial microbiota is adapted to colonize the root endophytic environment, whereas a larger fraction (50%) of soil-borne filamentous eukaryotes colonize the plant endosphere, as well as the rhizoplane fraction.

3.3 Microbial beta-diversity is driven by environmental factors and the host plant´s effect

Using the Bray-Curtis dissimilarities, it was possible to observe how bacterial, fungal and oomycetal samples cluster apart from each other. Thereby, analysis of the current dataset highlighted that, while bacterial communities' distribution is mainly determined by the root compartment, fungal and oomycetal communities have a more complex distribution patterns (**Figure 3B, Figure 4A, Figure 6A, Figure 7A**). PERMANOVA analysis indeed showed that bacterial communities are impacted by compartment, site and year of harvesting, in this order (15%, 13% and 0.6%, respectively, p-value<0.001, **Table 3, Figure 4**). Fungal communities, on the other hand, are primarily impacted by site, fraction and year of harvesting (18%, 8% and 5%, respectively, p-value<0.001, **Table 3, Figure 6**). And, finally, oomycetal communities are mainly impacted by the year of harvesting, followed by site and fraction (12%, 11% and 3%, respectively, p-value<0.001, **Table 3, Figure 7**). These results highlighted the necessity to analyze each of these microbial groups under the same environmental conditions, the same fractionation protocol and within the same survey, as stated by Thompson *et al.,* 2017. Otherwise, it would not have been possible to assess how the microbiota localized in the exact same habitat responds very differently to environmental inputs and to the host plant. Furthermore, these data are consistent with previous reports. Thus, bacterial compartment-driven distribution resembles the one described by Bulgarelli *et al.,* 2012 or Edwards *et al.,* 2015 (**Figure 9**), as well as fungal site-distribution (**Figure 8B**), as pointed out by Shakya *et al.,* 2013 and Coleman-Derr *et al.,* 2016. The results from my dataset, however, are remarkable due to the higher number of root-associated samples and sites used for these comparisons (17 sites/soils, only comparable to the Earth Microbiome Project, Thompson *et al.,* 2017). I concluded that despite the large geographical distances and the different bacterial soil inputs, *A. thaliana* roots are colonized by remarkably similar bacterial communities at a European scale, underlining the strong root filtering effect. In contrast, root-associated fungal and oomycetal communities resemble more those of the surrounding soil, suggesting they do not form taxonomically structured communities in plant roots at the European scale (Talbot *et al.,* 2014). The observation that root-associated oomycetal communities resemble more fungal communities' behavior and display a stronger seasonality effect suggests that distinct factors shape fungal and oomycetal communities at the continental scale (Bahram *et al.,* 2016). Although different marker loci were used between bacteria and filamentous eukaryotes, potentially inflating these observations (Peay *et al.,* 2016), the use of the same locus to target fungal and oomycetal community structure (e.g. ITS1) indicates that at least fungi and oomycetes clearly respond differently to the tested variables.

3.4 Microbial communities´ composition is host species dependent

As in previous reports, bacterial *A. thaliana* root-associated communities were mainly composed of Proteobacteria, Actinobacteria, Bacteroidetes and Firmicutes (Bulgarelli *et al.,* 2013; Hacquard *et al.,* 2015; **Figure 5A**). Also, the fungal taxa colonizing plant roots mainly belong to the phyla Ascomycota and Basidiomycota (Jumpponen and Jones, 2009; Toju *et al.,* 2013; Hardoim *et al.,* 2015; **Figure 5B**), as well as Zygomycota phylum. Members of the Brassicaceae family do not engage in symbiotic associations with mycorrhizal fungi (mostly belonging to the Glomeromycota phylum) and, consistent with that, relative abundance of this group is highly reduced across this dataset (**Figure 5B**). Thus, is very likely that other fungal members provide other beneficial traits in *A. thaliana* plants, as previously shown (Hiruma *et al.,* 2016; Hacquard *et al.,* 2016; Almario *et al.,* 2017). Regarding oomycetal communities, these were mainly composed by members of the Pythiales order, although, depending of the site of study, Albuginales, Lagenidiales and Saprolegniales were also represented (**Figure 5C, Figure 8C**). Interestingly, almost all oomycetes described to date are pathogens (Kamoun *et al.,* 2015), raising the possibility that the roots of healthy *A.thaliana* are colonized by pathogenic oomycetes that remain non-pathogenic in a community context.

In order to decipher whether these microbial communities are similar between *A. thaliana* plants and other plant species growing in close vicinity, I also harvested grasses, belonging to the Poaceae family, from all sites, for three consecutive years. PERMANOVA analysis of the comparison between *A. thaliana* root-associated samples from single roots, with grasses-associated samples showed that bacterial and fungal soil and RS communities are not significantly different between the species. However, the strongest host-dependent effect can be observed in RP samples (14% of the variation explained in bacterial communities, 4% in fungal communities and 3% in oomycetal communities, p-value<0.001, **Table 3**). Further, bacterial and oomycetal communities are still impacted at the root fraction (4% and 3%, respectively, p-value<0.001), whereas that is not the case for fungal communities. Such host-dependent changes have been previously observed for different plant species (Redford *et al.,* 2010; Schlaeppi *et al.,* 2014; Coleman-Derr *et al.,* 2016; Fitzpatrick *et al.,* 2018, among others) and it is tempting to speculate that different root exudate chemistry or root architectural features (Chaparro *et al.,* 2014; Kembel *et al.,* 2014; Zhalnina *et al.,* 2018) contribute to the striking differences observed between plant species in the RP fraction.

3.5 Bacterial communities are stable across years

The current dataset includes samples harvested at the same plant developmental stage, across three consecutive years. Therefore, it was possible to assess whether *A. thaliana* root-associated microbiota members establish stable associations throughout time. Bacterial and fungal communities were more stable in soil-related compartments, than in the root (0.55% in soil, non-significant, compared to 3.12% in roots, for bacterial communities; and 1.13% in soil, compared to 9.14% in root-associated fungal communities, PERMANOVA, p-value<0.01, **Table 3, Figure 4D and E, Figure 6D and E**). This suggests that the observed change in root-associated communities may be driven by plant responses to other environmental factors such as precipitation or temperature (Wagner *et al.,* 2016). Soil microbiota strongly depends on soil composition (van der Heijden, 2008), which is not expected to change significantly over time. However, although soil bacterial communities do not vary significantly across years (PERMANOVA, 0.55%, non-significant), fungal and oomycetal soil-associated communities are significantly different from one year to the next (1.13% and 5.88% variance, respectively, p-value<0.001, **Table 3, Figure 6D and E, Figure 7D and E**), suggesting that soil composition might be variable across years, impacting fungal and oomycetal communities, which might be more responsive to environmental variations in soils or persist poorly in soils (Lekberg *et al.,* 2012). On the other hand, the host plant, in this case *A. thaliana*, is an annual plant, with a new generation each year. Assuming the host genotype is on driver of bacterial communities (Horton *et al.,* 2014; Bodenhausen *et al.,* 2014), then a new individual plant each year should recruit a slightly different microbiota to its parental lines, but more similar than compared to another species (3% year-to-year variation, compared to 4% species variation, respectively, **Table 3**).

3.6 Reduced but stable *A. thaliana* root-associated core microbiota

As reported previously (Lundberg *et al.,* 2012; Yeoh *et al.,* 2017; Hamonts *et al.,* 2018; Fitzpatrick *et al.,* 2018), it is important to determine whether root samples harbor a core group of microbes across host genotypes or species that could be relevant for plant fitness in their natural habitats. The difference with these studies is that I harvested the same plant species, *A. thaliana*, in very contrasted environments and soil types across years. Further, this screen includes several microbial groups that, if are part of the *A. thaliana* root microbiota, it can be assumed they robustly interact across environments and years. Bacterial resilient OTUs, robustly colonizing plant roots across all sites and years, belong to the four most representative phyla found in plant roots: Proteobacteria (members of the Bradyrhizobiaceae, Rickettsiales, Comamonadaceae, Oxalobacteraceae, Bulkholderiaceae, and Pseudomonadaceae groups), Actinobacteria (Mycobacteriaceae family), Bacteroidetes (Flavobacteriaceae family) and Firmicutes (Bacillaceae family), suggesting that the “core” root microbiota requires certain bacterial diversity for stability (**Figure 9A**). Comparison of these core members with other publications showed that most of these groups can be also found in other wild species and crops (Yeoh *et al.,* 2017; Hamonts *et al.,* 2018; Fitzpatrick *et al.,* 2018). This suggests that an evolutionary conserved core microbiota has evolved with terrestrial plants (Yeoh *et al.,* 2017). Notably, this *A. thaliana* bacterial core microbiota is dominated by four proteobacterial OTUs (OTU_5, OTU_11, OTU_13 and OTU_14). This is remarkable because this extremely reduced number of OTUs accounts for 14-47% of the root endosphere 16s rRNA reads at each site, suggesting that they have evolved strategies to efficiently colonize and persist within root tissues, despite large geographical distances (**Figure 9A**). Regarding the fungal and oomycetal OTUs, these belong to the Ascomycota (*Ilyonectria*, *Fusarium*, *Tetracladium* and *Plectosphaerella* genera) and the Zygomycota (*Mortierella* genus) phyla, and to the Pythiales (*Pythium* genus) and Albuginales (*Albugo* genus) orders which are also part of the most abundant taxa in root-associated microbiota, as also observed for bacterial and fungal core OTUs of sugarcane (**Figure 9B and C**, Hamonts *et al.,* 2018). It is tempting to speculate that these microbes have been engaging in robust and consistent interactions within *A. thaliana* root tissues, and that they provide certain beneficial function to its host, or to their microbial partners. Interestingly, most of these microbial core members are actually culturable (Bai *et al.,* 2015; Duran *el al.,* in preparation), so that it would be very interesting to test the previous hypothesis using these strains and co-inoculating them under controlled conditions with germ-free plants.

3.7 Specific soil characteristics have a small but significant impact on root microbiota establishment

As introduced before, soil microbiota plays a very important role for nutrient cycling and soil stability (van der Heijden, 2008), but these microbes are also strongly affected by the soil nutritional composition itself. The current dataset, due to the great variety of soil compositions and soil textures that it comprises, gave the opportunity to analyze the effect of soil properties on bacterial, fungal and oomycetal communities. As previously reported, pH is the major soil property that impacts both bacterial and fungal communities (5.95% and 3.57%, respectively, p-value <0.001, **Figure 13**, Lauber *et al.,* 2009; Rousk *et al.,* 2010). The strongest soil property driver for oomycetal communities, however, is manganese (Mn) (1.95%, p-value<0.001, **Figure 13**). Although not much is known about oomycetal distribution drivers, it has been shown that utilization of Mn, together with potassium (K) in phosphite-based treatments, alleviates the damping-off of *Pythium* species on soybean seeds (Carmona *et al.,* 2018), which could suggest that these nutrients will have a negative effect on oomycetes distribution. In fact, Mn levels negatively correlates with oomycetal diversity in the current dataset (Pearson’s correlation= -0.15, p-value= 2.523e-05). Iron is another important soil nutrient for microbial communities (4.8% for bacteria, 2.83% for fungi, 1.2% for oomycetes, p-value< 0.001, **Figure 13**). This could be due to the link between microbial-driven iron reduction and carbon cycles in soils (competition for electron acceptors), which then indirectly impacts the rest of the microbial community (Dubinsky *et al.,* 2010). Notably, Acidobacteria are more represented in Swedish soils, where iron levels are very high (337-1647 mg/kg *versus* 8.1-343 mg/kg in other sites, **Annex: Table 1**). Since Acidobacteria are well known to grow in iron rich mine environments, they likely play an important role in iron redox reactions in soils (Ward *et al.,* 2009). Other soil nutrients also have an impact on bacterial communities’ distribution, such as Boron (3.31%). Boron at high concentrations is a toxic element for most bacterial members, although some isolates have been described to display high tolerance (Ahmed *et al.,* 2007). Further, inspection of the pH-boron-salinity effect on cucumber growth and rhizospheric bacterial communities showed that, although pH and salinity are the major determinants, boron has a key role at early plant growth stages on bacterial communities' richness (Ibekwe *et al.,* 2010). Related to this, some soil nutrients display higher impact on microbial communities only in combination with others. For example, Available Calcium together with Reserve Magnesium have a higher impact on both bacterial and fungal communities than each separately (Available Calcium x Reserve Magnesium: 3.64% and 2.31%, for bacterial and fungal communities, respectively, **Figure 13**). Overall, microbial communities' distribution have significant but small effects driven by soil composition. These effects are probably nested within each other and it is difficult to fully disentangle each soil properties' effect on each microbial group. Therefore, it will be interesting to build a model based on single taxa correlations with each soil property, in order to find which combination of soil characteristics actually drives most of microbial communities' composition.

3.8 Climate is a major driver of root-associated microbial composition

Biogeography and soil are major drivers of microbial communities in nature, as shown in previous studies (Bulgarelli *et al.,* 2012; Talbot *et al.,* 2014). Because soil properties are predicted to have significant but small impacts on microbial communities, other biogeography-related variables must have more pronounced effect on microbial composition across Europe. In each of the harvested sites, locally adapted *A. thaliana* accessions could be found, which were different in each site. Therefore, no *A. thaliana*-related genotype effect could be separated from biogeography, although it has been shown to be a significant driver of bacterial communities' composition (Lundberg *et al.,* 2012). Further, climatic conditions in each site are probably major determinants of host responses, soil composition and overall microbial communities (Xu *et al.,* 2018). In order to disentangle the effect of each of these factors on microbial community structure, I selected the two contrasted IT1 and SW4 populations for reciprocal transplantation experiments in the field but also under controlled laboratory conditions. In the field experiment, plant survival and fruit production was already a proxy of how important climatic and soil adaptation is for host performance. Thereby, plants growing in their adapted climate and soil, had a significantly higher survival rate than non-adapted host (**Supplementary Figure 8**). This suggests local adaptation of the local genotype to its own soil and climate. Further, microbial communities profiling showed a strong climate effect on all microbial groups in all soils (15-40%), but no genotype effect (**Figure 14A**,

Table 4, Supplementary Figure 10). Interestingly, the strongest effect came from the interaction between climate and genotype effects (**Table 4, Supplementary Figure 10**). Enrichment tests showed that taxonomically distinct bacterial members and specific fungal members are responsible for the climate-driven genotype effect, suggesting that, indeed, under specific climatic conditions, the host plant can recruit genotype-specific microbiota members (**Figure 14B**; Xu *et al.,* 2018; Fitzpatrick *et al.,* 2018).

3.9 Bacterial and fungal communities profiling is essentially comparable between amplification methods

Using different DNA regions for microbial profiling can lead to slightly different results depending on the region of choice, and also to inflations of certain results, as well as new information (Peay *et al.,* 2016; Wang *et al.,* 2016). Thus, I profiled bacterial and fungal communities using a second genomic region (V2/V4 within the 16s rRNA region for bacterial communities, and ITS2 for fungal communities), similarly to Agler *et al.,* 2016b. Comparison of the bacterial profiles (V5/V7 vs V2/V4) shows a very significant overlap between OTU relative abundances at high taxonomic levels, which decreased at lower taxonomic levels. Overall distribution patterns remain very similar, although slightly inflated in V2/V4 (**Table 3, Annex: Supplementary Table 1, Supplementary Figure 3A**). This is probably due to the higher taxonomic assignment to rare taxa in V2/V4 compared to V5/V7. Thereby, relative abundances are decompensated between the two datasets. The presence of rare taxa, however, is likely not due to sequencing bias, as OTUs with less than 1% representation in the dataset were removed for the comparison (see **Methods**). Also, it is important to note that both profiles lack good taxonomic assignment at lower levels than family. Thus, V2/V4 can bring an additional information about taxa not usually captured by V5/V7, but a parallel profiling using a second region within the conserved gene can complement a bacterial communities profiling (Wang *et al.,* 2016; Agler *et al.,* 2016b). Fungal profiles, on the other hand, are very significantly correlated at all taxonomic levels (Pearson's correlation at phylum: 0.992, p-value=1.06e-5, order: 0.94, p-value=2.2e-16; family: 0.97, p-value=2.2e-16; genus:0.98, p-value=2.2e-16, **Figure 11**), as well as overall fungal communities' distribution patterns (**Table 3, Annex: Supplementary Table 1, Supplementary Figure 3B**). Therefore, either fungal ITS region will be suitable for further analysis.

3.10 Conclusions and future perspectives

Recent studies have advanced our knowledge about microbial communities associated with plants and environmental factors shaping these communities, but it is difficult to cross-compare between different techniques and experimental set-ups, in order to describe a microbial communities' composition working model. Although the structure of the bacterial root microbiota has been extensively described in *A. thaliana* and Brassicaceae relatives at a local scale, fungal community profiling has never been used to characterize root-associated fungi in this model plant species, in which the signaling pathways required for establishing mutualistic interactions with mycorrhizal fungi have been lost. Therefore, first, I surveyed *A. thaliana* bacterial, fungal, and oomycetal communities associated with distinct root compartments, across a wide geographical area. Also, I could reveal that microbial communities are very differently impacted by environmental cues depending on the microbial group of study. Thus, bacterial communities' distribution is impacted by plant compartment, geographic location and year, in that order; fungal communities are impacted by location, compartment and year and, oomycetes communities, by year, location and compartment (**Figure 14**). I showed that a very reduced but robust group of core microbes can be consistently found within *A.thaliana* root tissues across Europe, but also that *A.thaliana* in each location has a very specific microbial footprint. Secondly, in order to fully disentangle the geographical effect into 1) host/accession genotype, 2) climate and 3) soil properties effects, soil and climate transplantation experiments were performed, showing that soil is the major driver of microbial composition, but that climate is a very important fraction of the geographic location effect, by directly impacting microbial communities composition, but also indirectly through the host genotype (**Figure 14**). Importantly, individual soil characteristics have small but significant impacts on microbial communities, which cannot be separated from the overall soil and climate effect. Therefore, separation of soil biotic from abiotic components will be key to learn the specific effect of soil composition on microbial communities. Thus, transplantation experiments of soil slurries under different climatic conditions will allow to understand these soil-microbes interactions and their effect on plant performance.

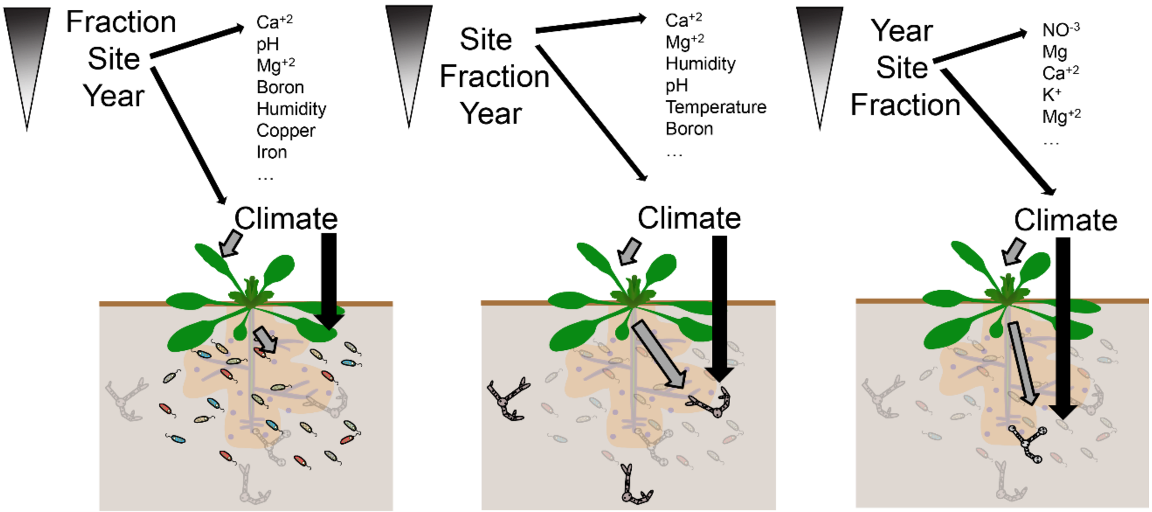
Fraction
Site
Year
Ca+2
pH
Mg+2
Boron
Humidity
Copper
Iron
…
Climate
Site
Fraction
Year
Ca+2
Mg+2
Humidity
pH
Temperature
Boron
…
Climate
Year
Site
Fraction
NO-3
Mg
Ca+2
K+
Mg+2
…
Climate

Bacteria **Fungi** **Oomycetes**

Figure 14: Schematic representation of environmental drivers of *A. thaliana* root-associated microbial communities' composition in nature. The major drivers of microbial communities' composition and distribution in nature are root fraction or root vicinity, site or geographic location and year or seasonality. These environmental factors, however, have different impact grades on bacterial, fungal and oomycetal communities. Further, geographic location comprises several factors: soil composition, climate and host genotype. Soil composition also has a variable effect on microbial communities depending on the microbial group of study. Climatic conditions are a key driver of microbial composition, which directly impacts communities' distribution or indirectly, through the host genotype.

3. MATERIALS AND METHODS

4.1 Materials

4.1.1 Plant material

A. thaliana accessions were harvested from natural populations described in the following studies: SP1, SP2, SP3 (IP-Mar-1, Ip-Cdc-3, Leo-1 respectively, Alonso-Blanco *et al.,* 2016), FR1 and FR2 (Bartoli *et al.,* 2018), FR3 (Saint-Die, Duran *et al.,* in preparation), GE1, GE2 (Pulheim and Geyen, respectively, Duran *et al.,* in preparation), GE3 (K6910, Agler *et al.,* unpublished), GE4, GE5 (PFN and JUG, respectively, Agler *et al.,* 2016a), GE6 (This study), SW1 (Tos-82-393, Alonso-Blanco *et al.,* 2016), SW2, SW3, (Ellis and Ågren, unpublished), SW4 (Rödåsen, Ågren & Schemske 2012), IT1 (Castelnuovo, Ågren & Schemske 2012).

Italian and Swedish *A. thaliana* accessions utilized in transplantation experiments were provided by Prof. Dr. Jon Ågren and Dr. Thomas Ellis, University of Uppsala. The accessions utilized were It15, It24, It32, It41 (from Italian parental lines) and Sw7, Sw11, Sw43, Sw47 (from Swedish parental lines) (Agren & Schemske 2012).

4.1.2 Oligonucleotides

Oligonucleotides used for PCR amplification are listed in **Annex: Table 2** and were purchased from Metabion (Steinkirchen, Germany) or Sigma-Aldrich (Hamburg, Germany).

4.1.3 Enzymes

DNA-free DFS Taq polymerase was purchased from Bioron (Ludwigshafen, Germany). Antarctic phosphatase and Exonuclease I were acquired from New England Biolabs (Frankfurt, Germany).

4.1.4 Chemicals

Laboratory grade chemicals and reagents are described within each method.

4.1.5 Buffers and solutions

Buffers and solutions used in this study are described within each method. If not stated otherwise, buffers were prepared in deionized H_2O and aqueous solutions were sterilized by autoclaving at 121 °C for 20 min.

4.2 Methods

Brands and manufacturer's information of each material will be indicated only the first time they are mentioned.

4.2.1 Experimental set-up and sample collection in natural sites

Seventeen sites were selected across a gradient of climates within Europe, from Sweden to Spain, which included five distinct soil textures (**Figure 1, Annex: Table 1**), where *A. thaliana* populations naturally occur. This project was done in collaboration with Jon Ågren from Uppsala Universitet, in Sweden; Eric Kemen, University of Tuebingen in Germany; Fabrice Roux from INRA Toulouse, in France; and Carlos Alonso Blanco, from CSIC-CNB Madrid, in Spain, **Annex: Table 1**). *A.thaliana* plants were harvested from February to May, intending to harvest every plant at the same developmental stage (mainly flowering stage, for an easier plant identification), for three consecutive years. Plants were identified in the field with the help of collaborators.

Plants were harvested with their surrounding soil with a hand shovel, trying not to disturb the plant root system, transferred to 7x7 greenhouse pots and transported to a laboratory (either Max Planck Institute for Plant Breeding Research or collaborator's laboratory) for further processing. Single plant individuals were harvested. Four plant individuals pooled together were considered as one pooled-plant technical replicate (4 technical replicates). In addition, four plants were not pooled and kept individually as single-plant replicates. Three neighboring plants growing in the surrounding area from *A. thaliana* and belonging to the Poaceae family were harvested in a similar manner as *A.thaliana* plants. In total, 285 plants were harvested.

4.2.2 Root compartments fractionation protocol

In order to separate four potential microbial niches, plants and respective roots were taken out from the pot. Samples from the leftover bulk soil were taken, making sure that no root debris was included, snap-frozen in liquid nitrogen and stored for further processing. Individual plants were manually separated from the main soil body and non-tightly adhered soil particles were removed by gently shaking the roots; these roots were then separated from the shoot using a sterile blade and placed in a 15-mL falcon (Corning, USA) with 10 mL of deionized water, which was then inverted 10 times. Roots were transferred to another falcon and further processed, while leftover wash-off (containing more tightly adhered soil particles) was centrifuged at 4000 xg for 10 min (5810R, Eppendorf, Hamburg, Germany). Supernatant was discarded except for approximately 2 mL, which were then used to resuspend the pellet and transfer it to a new 2-mL screw-cap tube. This tube was centrifuged at 20000 rpm for 10 minutes (5424, Eppendorf, Hamburg, Germany); the supernatant was discarded and the pellet (Rhizosphere compartment) was snap-frozen in liquid nitrogen and stored for further processing. As described in the **Results** section, sequential detergent washes were utilized to obtain the Rhizoplane fraction and enrich the root tissue with root endophytes. After RS removal, roots were placed in a 15-mL falcon with 6 mL of detergent (1xTE + 0.1% Triton® X-100; Tris-EDTA buffer solution 100x, T9285-100mL, Sigma, Hamburg, Germany; Serva, Heidelberg, Germany, respectively) and manually shaken for 2 minutes. This step was repeated to a total of three detergent washes, in between which, roots were transferred to a new 15-mL falcon with new detergent. After these washes, roots were transferred to a new 15-mL falcon. The remaining washes (approximately 18 mL) were transferred to a 20 mL syringe (Mediware, berlin, Germany) and filtered through a 0.22 µM-pore membrane (47 mm, MCE, Millipore, USA), utilizing a membrane holder with an luer adaptor for the syringe (Swinnex-25, Millipore, USA). The membrane was then snap-frozen in liquid nitrogen until further processing. Lastly, three-times washed roots were subjected to a further surface sterilization step to fully remove any leftover microbe from the root surface. Roots were sterilized with 1-minute ethanol wash (Ethanol absolute, VWR Chemicals, USA), washed with NaClO (Sodium hypochlorite solution 6-14%, Honeywell Fluka, USA) for one minute and rinsed five times with deionized water. These roots were dried using sterile Whatman paper (Whatman® glass microfiber filters, Grade GF/B, Sigma-Aldrich, Hamburg, Germany) and snap-frozen in liquid nitrogen until further processing (Root or Endophytic fraction) (**Figure 2A**). In total, 1139 samples were produced after fractionation.

4.2.3 Fractionation protocol validation

4.2.3.1 Sonication

Sonication was done as described in Bulgarelli *et al.,* 2012. Briefly, after Rhizosphere removal, *A. thaliana* roots were transferred to a new 15-mL falcon tube and sonicated 10 times at 160 W with 30-second brakes (Bioruptor Next Gen UCD-300, Diagenode, Liège, Belgium).

4.2.3.2 Root printing

In order to validate removal of microbes from the root surface, roots were printed on TSA 50 % (Tryptic Soy Broth, Sigma-Aldrich, Hamburg, Germany) containing 10 % agar (Difco Agar, Granulated, VWR, USA) after each step of the fractionation protocol. After Rhizosphere removal (1), after each detergent wash (2), after sonication (3) and after surface sterilization (4) (**Figure 2B**), roots were dried with a sterile Whatman paper and shortly placed on TSA 50 % (10-30 seconds approximately) and then removed. Plates were incubated for 3 days at 25 ºC and CFU counts were done after this time. CFU counts were plotted using *ggplot2* in R, and significant differences were calculated with Kruskal Wallis, Dunn test *post-hoc*, $p<0.05$ (**Figure 2B**).

4.2.3.3 Washes printing

In order to test the microbial recovery after each step of the fractionation protocol, leftover washes were collected and plated on TSA 50 %, containing 10 % agar. After Rhizosphere removal (1), after each detergent wash (2), after sonication (3) and after surface sterilization (4) (**Figure 2B**), washes were serially diluted (1:1, 1:10, 1:100) and 20 µL of each dilution was placed on a TSA 50 % plate. Plates were incubated for 3 days at 25 ºC and CFU counts were done after this time. CFU counts were plotted using *ggplot2* in R, and significant differences were calculated with Kruskal Wallis, Dunn test *post-hoc*, $p<0.05$ (**Figure 2B**).

4.2.3.4 SEM imaging

To evaluate the efficiency of each fractionation step, roots of *A. thaliana* were collected after Rhizosphere removal (1), after each detergent wash (2), after sonication (3) and after surface sterilization (4) (**Figure 2B**), and stored in 1x PBS (8 g/L NaCl, 0.2 g/L KCl, 1.44 g/L Na2HPO4, 0.24 g/L KH2PO4) until further usage. Root material was further processed for SEM by Rainer Franzen at the Central Microscopy group at the Max Planck Institute for Plant Breeding Research, Cologne. Briefly, samples were fixed in 4% glutaraldehyde (Roth, Karlsruhe, Germany) in 1x PBS at 4 °C overnight. Afterwards, roots were washed twice with 1x PBS for 30 minutes and washed with increasing ethanol concentrations (30 % ethanol for 30 minutes, 50 % ethanol for 30 minutes, 70 % ethanol for 30 minutes, 90 % ethanol for 30 minutes, 96 % ethanol for 60 minutes, 96 % ethanol for 60 minutes). To remove remaining water, root material was incubated in dried ethanol at 4 °C overnight. Afterwards, samples were dried using a critical point dryer (CPD30;

BALTEC, Wetzlar, Germany). During this procedure ethanol was exchanged 10 times against liquid CO_2. Then, samples were spattered using the Polaron Sputter Coater 7600 using a platinum target. Microscopy pictures were taken with a Supra 40VP (Zeiss, Munich, Germany).

4.2.4 Transplantation experiment set-up

4.2.4.1 Field transplantation experiment

Swedish (from SW4) and Italian (from IT1) soils were planted in four 299-well trays (Pluggbrätten, DAN QPD299W, 310x530 mm, Trädgårdsteknik AB, Sweden) with their adapted genotype (It15, It24, It32, It41, for Italian soil, and Sw7, Sw11, Sw43, Sw47 for Swedish soil, randomly distributed) and the reciprocal genotypes, in IT1 (Castelnuovo di Porto, Italy) and in SW4 (Rödåsen, Sweden). *A. thaliana* plants underwent a full life cycle (from October 2016 to March 2017 in Italy, and to May 2017 in Sweden). After this period, plants and their surrounding soil were harvested on site by taking the whole soil plug. Soil was separated from the roots manually and a soil sample was taken. Loosely adhered soil particles were removed by gently shaking the roots. Then, roots were placed in a 15-mL falcon and washed by inverting with 10 mL of deionized water and surface-sterilized as indicated in **4.2.2**. Twelve samples were harvested per soil, genotype and site. Samples were stored in dry ice and shipped to the Max Planck Institute for Plant Breeding Research, were they were stored at -80°C until further processing. Plant fitness was assessed by scoring mature fruit production at the end of the experiment by Dr. Thomas Ellis and Prof. Dr. Jon Ågren, from University of Uppsala (**Supplementary Figure 6**). In total, 144 soil and root samples were harvested, from which microbial communities profiling was performed, including V5/V7 16s rRNA for bacterial communities profiling, and ITS1 for fungal and oomycetal communities profiling.

4.2.4.2 Chamber transplantation experiment

Swedish (from SW4) and Italian (from IT1) soils were planted in 299-well trays cut up into 42-well trays which were then placed into 17x21x6 cm plastic tupperware tubs (Förvaringslådor SmartStore, 2362001, Office Depot, Sweden). Seeds of each line were sown on sterilized petri dishes with media consisting of Gambog’s B-5© nutrient mix, Bacto© Agar and ultrapure water. Dishes were wrapped in parafilm and cold-stratified in the dark at 4 °C for 5 days to break seed dormancy. Native populations in both Italy and Sweden experience cold periods at or below this temperature in the field during germination. Afterwards, the dishes were moved into a growth chamber with a constant temperature of 22 °C, 16 h days, and a photosynthetically active radiation (PAR) level of

125 lmol m^2s^{-1} using a combination of fluorescent and incandescent lights. The dishes were randomized throughout the chamber every day. After 8–10 days in the chambers, seedlings were transplanted into Italian and Swedish soils. Half of the boxes were incubated for six months in a chamber resembling climatic conditions in IT1 (Castelnuovo di Porto, Italy), and the other half in a chamber resembling climatic conditions of SW4 (Rödåsen, Sweden) (BioChambers Inc. Model# GC-20), similarly to Dittmar *et al.,* 2014. The temperatures used are based on data recorded by two data loggers (HOBO Pro Data Logger Series H08-031-08) at each site for the winter 2005/2006. For each calendar day, the daily maxima and minima recorded for air and soil temperature was taken and the average was utilized. To determine photoperiod data on times for sunrise and sunset in 2005/6 for Sundsvall and Rome were taken from timeanddate.com. Data on photosynthetically active radiation (PAR, measured in µEinsteins) are taken from data logger recordings for 2014/2015. Two loggers at each site record PAR every minute. For each calendar day every record for the times between sunrise and sunset for that day was taken and averaged across these values. Each day has six time points. Temperatures began to rise from the daily minimum two hours before dawn, reaching their daily maximum two hours after dawn. Likewise, temperatures began to fall two hours before sunset and reached the next daily minimum two hours after sunset. The growth chambers at Uppsala University can be programmed to ramp the temperature smoothly throughout this time period. In order to shorten the schedule in the Swedish chamber to under six months the 121 days from December to March were contracted into 31 days by sampling for every fourth day.

After six months, plants and their surrounding soil were harvested by taking the whole soil plug. Soil was separated from the roots manually and a soil sample was taken. Loosely adhered soil particles were removed by gently shaking the roots. Then, roots were placed in a 15-mL falcon and washed by inverting with 10 mL of deionized water and surface-sterilized as indicated in **4.2.2**. Four samples were harvested per soil, genotype and site, by pooling roots of four separate plugs, due to the small size of the plants in this experiment. In total, 132 root and soil samples were harvested. Samples were stored in dry ice and shipped to the Max Planck Institute for Plant Breeding Research, where they were stored at -80°C until further processing. Microbial communities profiling was performed, including V5/V7 16s rRNA for bacterial communities profiling, and ITS1 for fungal and oomycetal communities profiling.

4.2.5 Microbial community profiling

4.2.5.1 Library preparation and sequencing

DNA isolation was performed from Bulk Soil, Rhizosphere, Rhizoplane and Root samples harvested as described above, using the FastDNA ® SPIN for soil kit (MP Biomedicals, Solon, USA). Before DNA isolation, frozen Rhizoplane samples were manually crushed with a sterile forceps and snap-frozen again in liquid nitrogen. Buffers were added to Bulk soil, Rhizosphere and Rhizoplane samples and were homogenized once using the Precellys®24 tissue lyzer (Bertin Technologies, Montigny-le-Bretonneux, France) at 6,500 rpm for 30 seconds. Root samples were homogenized twice without buffers at 6,500 rpm for 30 seconds each time, then buffers were added and samples were homogenized a third time at 6,500 rpm for 30 seconds each time. Afterwards, DNA was extracted using the FastDNA ® SPIN for soil kit according to the manufacturer's instructions. DNA concentration was calculated using the Quant-iT™ PicoGreen dsDNA assay kit (Life Technologies, Darmstadt, Germany). 40 µL of a 1:200 dilution of PicoGreen was added to 4 µL of DNA in a 96 well plate. To calculate the DNA concentration a dilution series of standard lambda DNA, ranging from 0.5 to 20 ng/µL, was included on the same plate. Fluorescence was measured using the IQ5 real-time PCR Thermocycler (Biorad, Munich, Germany; 30 sec at 25°C, 3x30 seconds at 25°C for measuring fluorescence, 30 seconds at 15°C). DNA concentration was adjusted to 3.5 ng/ µL.

PCR amplicon libraries were generated using primers 799F-1192R (V5/V7 region of 16s rRNA) and 341F-806R (V2/V4 region of 16s rRNA) for bacterial communities profiling, ITS1F-ITS2 (ITS1) and fITS7-ITS4 (ITS2) for fungal community profiling, and ITS1o-5.8s-o-Rev for oomycetal community profiling (**Annex: Table 2**, Agler *et al.,* 2016b). Libraries were prepared in parallel for each amplicon. PCRs were performed by using 3 µL of the adjusted DNA in a total volume of 25 µL, including 1.25 U DFS-Taq DNA Polymerase (Bioron, Ludwigshafen, Germany), 1x incomplete reaction buffer, 0.3 % BSA, 2 mM of $MgCl_2$, 200 µM of dNTPs and 400 nM of each primer. To minimize PCR bias three independent PCR reactions using one master mix were prepared. The PCR reaction was pipetted in a laminar flow and PCR amplified (94 °C/2 minutes, 94 °C/30 seconds, 55 °C/30 seconds, 72° C/30 seconds, 72 °C/10 minutes for 25 cycles), using the same PCR parameters for all primer pairs. Afterwards, single stranded DNA and proteins were digested by adding 1 µl of Antarctic phosphatase, 1 µl Exonuclease I and 2.44 µl Antarctic phosphatase buffer to 20 µl of the pooled PCR product. Samples were incubated at 37 °C for 30 minutes and enzymatic activity was deactivated at 85 °C for 15 minutes. Samples were centrifuged for 10 minutes at 4,000 rpm and the supernatant was transferred to a new plate. 3 µl of this reaction was used for a second PCR with primers that included barcodes and Illumina adaptors (B5-barcodes and B3-barcodes for bacteria, Ft-barcodes and OF2-barcodes for fungi, Ot-barcodes for oomycetes, **Annex: Table 2**). PCR reactions were prepared using the same protocol described above, and the number of PCR-cycles were reduced to 10. PCR performance was assessed by loading 5 µL of PCR products of the three-replicates pool with 5 µL of Gel Loading Dye, Orange G (6X, Sigma, Hamburg, Germany) run on a 1 % agarose gel for 30 minutes, and by checking that no band could be observed in the microbe-free controls. Each bacterial reaction (70 µL approximately) were mixed with 20 µL Gel Loading Dye, Orange G and loaded in a 1.5 % agarose gel and ran for approximately 2 hours at 80 V. Bands with the correct size of ~500 bp were cut and purified using the QIAquick gel extraction kit (Qiagen, Hilden, Germany) and eluted in 60 µL of nuclease-free water (Qiagen, Hilden, Germany). DNA concentration was determined using the PicoGreen assay as described before. Fungal and oomycetal reactions were purified using Agencourt® AMPure® XP (Beckman Coulter, Krefeld, Germany) following manufacturer' instructions and eluting the PCR product in 70 µL of nuclease-free water. Equal amounts (ng) of purified PCR products were pooled, each microbial library separately. Pooled libraries were purified twice using Agencourt AMPure XP PCR Purification kit (brand) following manufacturer' instructions and eluting the PCR product in decreasing amounts of nuclease-free water (that is, 120 µL in the first round and 90 µL in the second round). Purified libraries' concentration was assessed using Quantus^{TM} Fluorometer (Promega, Manheim, Germany), by mixing 100 µL of a 1:200 dilution of Quantifluor® dsDNA dye (in 1xTE) with 2 µL and 98 µL of 1xTE in a 0.5-mL tube (Promega, Manheim, Germany), thoroughly mixing by pipetting and incubating for 5 minutes under the dark. Then, equal amounts of each library were pooled together. Final library concentration was assessed using Quantus^{TM} Fluorometer. Paired-end Illumina sequencing was performed with the MiSeq sequencer at the Department of Plant-Microbe Interactions, Max Planck Institute for Plant Breeding Research, following manufacturer' instructions.

4.2.5.2 Sequencing data analysis

Sequencing data analysis was performed using bioinformatic pipelines developed by Dr. Rubén Garrido-Oter and Dr. Thorsten Thiergart. Fourteen MiSeq libraries were processed, including five amplicon libraries each (V5/V7 and V2/V4 for bacterial libraries, ITS1 and ITS2 for fungal libraries, and ITS1 for oomycetal libraries), which contained 73851097 reads.

The paired 16s rRNA amplicon sequencing reads were joined (join_paired_ends.py, QIIME, default parameters) and the joined reads were then quality filtered and demultiplexed (split_libraries_fastq.py, QIIME, with maximum barcode errors 1 and phred score of 30) (Caporaso *et al.,* 2010). The filtered reads were dereplicated (usearch, –derep_fulllength) and sorted according to their copy number (only reads >2 copies were retained) (Edgar, 2010). These reads were clustered using the usearch algorithm (Edgar, 2010) at 97% sequence identity to form OTUs. Clustered reads were checked for chimeras using usearch (usearch –uchime_ref, Gold Database). All retained OTUs were aligned to the Greengenes Database (DeSantis 2006) using PyNAST (Caporaso *et al.,* 2010). Those that did not align to the database were removed. To each OTU a taxonomic classification was assigned using QIIME (assign_taxonomy.py, uclust algorithm with default parameters, Greengenes Database). OTUs were checked for those assigned as mitochondria. Out of the remaining sequences, an OTU table was build (usearch_global 97%, and uc2otutab.py) (**Annex: otu_tables**).

ITS reads were joined and demultiplexed as for 16s rRNA reads. In addition, also the forward reads were demultiplexed and filtered. For those reads where no joined pair of reads exist, the forward reads were kept. The combined reads were trimmed to an equal length of 220 bp. Reads were de-replicated and sorted (keeping only those with >2 copies). All reads were checked with ITSx (Bengtsson-Palme *et al.,* 2013) if ITS sequences are present. Those reads that contain ITS sequences were then clustered at 97% using usearch. Fungal OTUs were checked for chimeric sequences using (uchime_ref) against a dedicated chimera detection database (Nilsson *et al.,* 2015, UNITE). Oomycetal OTUs were checked using the -chime_denovo function from usearch. To check for non-fungal / non-oomycetal sequences the remaining OTU sequences were blasted against an ITS-sequence database. For this purpose, all available ITS sequences (search term “internal+transcribed”, for plants, animals, fungi, oomycetes and protists) were received from NCBI nucleotide database (January/February 2016). All OTU sequences whose best blast hit (bbh) was not annotated as a fungal / oomycetal sequence were removed. In addition, all sequences that show more hits in non-fungal / non-oomycetal sequences (out of max. 10 hits) were also removed. Taxonomic classification was done via RDP classifier (Wang *et al.,* 2007) using the Warcup database for fungal OTUs (Deshpande *et al.,* 2016) and a self-established database for oomycetal OTUs. The latter one was constructed out of NCBI derived ITS sequences. These ITS sequences were checked with ITSx for containing ITS sequences, and then used to train the RDP classifier.

4.2.5.3 Microbial ecology analysis

4.2.5.3.1 Alpha- and beta-diversities

To assess the alpha-diversity within natural samples, OTU-tables were rarefied to 1000 reads. Alpha-diversity indices (Shannon index, Chao index and number of observed species) were calculated using QIIME (alpha_diversity.py, **Figure 3, Supplementary Figure 1, Supplementary Figure 2, Supplementary Figure 7**). Alpha-diversities were plotted using *ggplot2* in R and Kruskal-Wallis test and Dunn test *post-hoc* were used to calculate significant differences between medians.

To estimate the beta-diversity, OTU-tables were normalized using the cumulative –sum scaling (CSS) method (Paulson *et al.,* 2013). Bray-Curtis distances between samples were used as an input for principal coordinate analysis (PCoA, done via *cmdscale* function in R) (**Figure 3, Figure 4, Figure 6, Figure 7, Supplementary Figure 1, Supplementary Figure 10)**. Full *A.thaliana*-associated samples were utilized to produce **Figure 3, Figure 4C and D**, **Figure 6C and D** and **Figure 7C and D**. Samples from each compartment were separately represented in **Figure 4A**, **Figure 6A** and **Figure 7A**. Single *A. thaliana*-associated and neighboring plants-associated samples were used to produce **Figure 4B**, **Figure 6B** and **Figure 7B.**

To visualize the distance between clusters in the transplantation experiment, average Bray-Curtis distances were calculated, normalized to control cluster (e.g.: (Control-Climate/Control-Control)) and plotted with *ggplot* in R (**Figure 11A**, **Supplementary Figure 9**).

4.2.5.3.2 Analysis of the variance

To test the effect of different factors on the microbial communities' variance, PERMANOVA analysis was performed (using *adonis* or *capscale* functions from vegan R package, with 999 permutations **Table 3, Table 4, Figure 4E, Figure 6E, Figure 7E, Figure 10, Supplementary Figure 9**). Samples were subsetted as indicated in section **4.3.3.1**. Results were represented in tables or using *ggplot2* in R.

4.2.5.3.3 Microbial relative abundances

Relative abundances plots were produced from relative OTU counts (relative abundances(%)) per sample and plotted using *ggplot2* in R (**Figure 5**, **Figure 8**, **Figure 9**, **Supplementary Figure 3**, **Supplementary Figure 4**, **Supplementary Figure 8**)

4.2.5.3.4 Root site-specific microbiota

Only *A.thaliana* roots samples were used. For each OTU, the enrichment in one site compared to the other 16 was tested using a linear model (log2, > 5 ‰ threshold) using the script described in Bulgarelli *et al.,* 2015 (developed from the R package *limma*). Using this method, it was tested if the relative abundance of one OTU within a given site was significantly higher compared to all other 16 sites (**Figure 8**). Then, the average relative abundance of each enriched OTU was calculated and represented using *ggplot2* in R.

4.2.5.3.5 *A. thaliana* root core microbiota

Only root samples from sites harvested across three years were used (SP1, SP2, SP3, FR1, GE1, GE3, GE4, GE5, SW1, SW2, SW3. SW4). Then, OTUs present in 100% (**Figure 9, Supplementary Figure 4**) or 75% (**Supplementary Figure 3**) of the sites in at least half of the samples of each site was considered as a core OTU.

4.2.5.3.6 OTUs enrichment test

To analyze differentially enriched OTUs between conditions, a linear model was used (log2, > 5 ‰ threshold) using the script described in Bulgarelli *et al.,* 2015 (developed from the R package *limma*). Using this method for each OTU it was tested if the relative abundance within conditions was significantly higher than compared to another condition (**Figure 11B**).

4.2.5.3.7 Comparison of bacterial and fungal libraries

OTUs produced by each library (V5/V7 and V2/V4 for bacteria, and ITS1 and ITS2 for fungi) were grouped by their taxonomic assignment at phylum level. Groups represented by both primers pairs were kept for the next step. Relative abundance estimates (log-transformed) were used at different taxonomic levels per region pair. Mean and standard deviation of each taxonomic group were plotted using *ggplot2* in R. Pearson's correlation between relative abundances and Mantel test between Bray-Curtis distances were calculated using *vegan* in R, and plotted using *ggplot2* in R (**Figure 12**, **Figure 13**).

CHAPTER II

Microbiota reconstitution in *A. thaliana* plants to understand the role of interkingdom microbe-microbe interactions for the establishment of microbial communities and host fitness

1. INTRODUCTION

1.1 Microbial interactions in nature

The very ancient origin of microbes on Earth, tracing back to the beginning of life more than 3.5 billion years ago, suggests that microbe-microbe interactions have continuously evolved and diversified over time, long before plants started to colonize land 450 million years ago (Hassani *et al.,* 2018). Therefore, it is likely that both intra- and inter-kingdom microbial interactions represent strong drivers of the establishment of plant-associated microbial consortia at the soil-root interface. Consistent with this, many reports have shown how much of the microbiota variation in natural samples is explained by environmental factors. However, still a great fraction of the variance remains undetermined, which could potentially be due to microbe-microbe interactions (Shakya *et al.,* 2013; Hacquard, 2016). Nonetheless, it remains unclear to what extent these interactions in the rhizosphere/phyllosphere and in endophytic plant compartments (i.e., within the host) shape microbial assemblages in nature and whether microbial adaptation to plant habitats drive habitat-specific microbe-microbe interaction strategies that impact plant fitness. Furthermore, the contribution of competitive and cooperative microbe-microbe interactions to the overall community structure remains difficult to evaluate in nature due to the strong environmental noise. To mitigate these technical hurdles, reductionist approaches have been primarily used to identify several of the diverse and sophisticated molecular mechanisms used by microbes to cooperate and compete on plant tissues and persist as complex microbial consortia, as reviewed by Whipps 2001, Frey-Klett *et al.,* 2011 or Kemen, 2014.

1.1.1 Cooperative interactions

Cooperative interactions are those in which microbial partners improve each other’s survival chances in nature, for example by enhancing nutritional potential (Morris *et al.,* 2012; Ponomarova and Patil 2015). In this sense, it has been traditionally hypothesized that very similar microbes will not occupy the same niche, due to exclusion competition. However, by analyzing microbial communities of 261 species from various environments, Zelezniak *et al.,* (2015) could show that, not only microbes with similar metabolic capabilities share niche very often, presumably to better use environmental resources, but that these metabolic dependencies drive microbial co-occurrence in many habitats. Deeper understanding of these metabolic interactions is however still needed. Combination of -omics technologies has proven to be very helpful at deciphering how microbial interactions affect microbial partners; for example, how the electron workflow affects two different microbes in a syntrophic association (Nagarajan *et al.,* 2013). Microbes can also promote other members' nutrition by expanding their fundamental niches, where certain nutrients are lacking or by removing compounds that might be harmful (Harcombe, 2010). For example, the rhizobacterium *Bacillus cereus* UW85 tightly associates with and stimulates the growth of bacteria from the Cytophaga-Flavobacterium group (CF, Bacteroidetes) in the soybean rhizosphere. The growth-promoting mechanism likely involves bacterial cell wall components, since peptidoglycan isolated from *B. cereus* cultures stimulated the growth of the CF rhizosphere bacterium *Flavobacterium johnsoniae in vitro* (Peterson *et al.,* 2006). Further, physical expansion of microbial partners is another form of cooperation. It has been well demonstrated that specific bacteria can use hyphae of filamentous eukaryotes as a vector, the so-called "fungal highway," giving them a selective advantage to spread in their environments (Worrich *et al.,* 2016). Particularly, motile bacteria use fungal mycelium hydrophobicity to solubilize and reach faster pollutants, which opens a promising branch of research for bioremediation purposes (Kohlmeier *et al.,* 2005, Wick *et al.,* 2007). According to Zhang *et al.,* (2018), it is also likely that fungal networks established along the soil-root continuum may also favor the growth of motile over non-motile bacteria at the root vicinity. Another mode of microbial cooperation is through formation of biofilms, which provide selective advantage for microbes, such as protection from competitors and antimicrobial molecules (Van Acker *et al.,* 2014), activation of enzymatic processes that require high cellular density (Nadell *et al.,* 2009) or acquisition of new genes via horizontal gene transfer (Zhang *et al.,* 2014). As an example of this, it has been shown that biofilm-mediated microcolonies formed on root hairs of finger millet by a root-inhabiting bacterial endophyte (*Enterobacter sp*.) confer a physical and chemical barrier that prevents root colonization by the pathogen *Fusarium graminearum* (Mousa *et al.,* 2016). Importantly, bacterial traits related to motility, attachment, and biofilm formation are needed for the anti-*Fusarium* activity *in planta.* These results suggest that a complex interplay takes place between the bacterium and root-hair cells, leading to the formation of this specialized killing microhabitat (Mousa *et al.,* 2016). Other ways microbes have to cooperate is by secreting molecules to communicate. One of the most described mechanisms is known as quorum sensing, which is used by several Gram-negative bacteria to monitor their own population densities through the production of the signaling molecule N-acyl-l-homoserine lactone (AHL) (Eberl, 1999). Different bacterial taxa can produce the same signal molecule type and cooperate or interfere (quorum quenching) with other unrelated taxa. This crosstalk phenomenon is supported by the fact that 8 to 12% of isolates from rhizobacterial libraries can activate AHL-specific reporter strains (biosensor) in vitro (Steidle *et al.,* 2001). In their study, Steidle *et al.,* (2001) suggest that AHLs serve as a universal language for bacteria-bacteria communication in the rhizosphere. Importantly, quorum sensing is likely also important for inter-kingdom communication between bacteria and plant-associated fungi, as reviewed in the animal field (Jarosz *et al.,* 2011). One of the most specialized microbial cooperative interactions is endosymbiosis, specifically the interaction that occurs between plant-associated fungi and their bacterial endosymbionts (Kobayashi *et al.,* 2009). The bacteria, which are detected in the fungal cytoplasm, can be actively acquired from the environment (Moebius *et al.,* 2014) and, in most cases, vertically inherited via fungal spores (Bianciotto *et al.,* 2000; Partida-Martinez *et al.,* 2007). Several examples of bacterial endosymbionts that live in intimate association with plant-associated fungi (e.g., *Rhizophagus*, *Gigaspora*, *Laccaria*, *Mortierella*, *Ustilago* and *Rhizopus sp*.) have been reported and mostly belong to the families Burkholderiaceae or related (Bianciotto *et al.,* 2000; Partida-Martinez *et al.,* 2005; Sato *et al.,* 2010), Bacillaceae (Bertaux *et al.,* 2003; Ruiz-Herrera *et al.,* 2015), or are Mollicutes-related endobacteria (Naumann *et al.,* 2010). Such interactions can impact the reproductive fitness of both members. For example, the bacterial endosymbiont (*Burkholderia sp*.) of a pathogenic *Rhizopus* fungus produces a toxin that provides fitness benefit to the fungus and is required for successful fungal colonization of rice plants (Partida-Martinez *et al.,* 2005). This bacterium is also required for fungal reproduction, and its absence impairs fungal spore formation (Partida-Martinez *et al.,* 2007). Interestingly, spores of the arbuscular mycorrhizal fungus *Gigaspora margarita* can host both Burkholderia- and Mollicutes-related endobacteria, supporting the idea that some root-associated fungi have their own intracellular bacterial low-diversity microbiome (Desiro *et al.,* 2014).

1.1.2 Competitive interactions

Microbes can use indirect mechanisms to compete with other microbes, such as rapid and efficient utilization of limiting resources. For instance, bacteria have evolved sophisticated strategies to sequestrate iron via secretion of siderophores, subsequently altering the growth of opponent microbes in their immediate vicinity (Wandersman *et al.,* 2004; Joshi *et al.,* 2006). Nutrient sequestration is also recognized as an important trait of biocontrol agents to out-compete pathogens (Whipps *et al.,* 2001). For example, the secretion of iron-chelating molecules by beneficial *Pseudomonas spp*. has been linked to the suppression of diseases caused by fungal pathogens (Mercado-Blanco and Bakker, 2007). Furthermore, it has been shown that resource competition is an important factor linking bacterial community composition and pathogen invasion in the rhizosphere of tomato plants (Wei *et al.,* 2015), which indicates that this type of microbial competition is also relevant for plant health. Plant-associated bacteria can engage in direct antagonistic interactions mediated by contact-dependent killing mechanisms. These are largely mediated by the bacterial type VI secretion system, a molecular weapon deployed by some bacteria (mostly Proteobacteria) to deliver effectors/toxins into both eukaryotic and prokaryotic cells (Records, 2011). For example, the plant pathogen *Agrobacterium tumefaciens* uses a puncturing type VI secretion system to deliver DNase effectors upon contact with a bacterial competitor *in vitro* and in the leaves of *Nicotiana benthamiana*. Remarkably, this contact-dependent antagonism provides a fitness advantage for the bacterium only *in planta*, underlining its specific importance for niche colonization (Ma *et al.,* 2014). In addition, the essential role of the bacterial type III secretion system for bacterial-fungal and bacterial-oomycetal interactions has been illustrated several times in the literature, suggesting that bacteria use this strategy to successfully colonize a broad range of eukaryotic hosts (plants, animals, small eukaryotes) (Rezzonico *et al.,* 2005; Lackner *et al.,* 2011; Cusano *et al.,* 2011; Yang *et al.,* 2016). For instance, it has been reported that *Burkholderia rhizoxinica* utilizes this secretion system apparatus to control the efficiency of its symbiosis with the fungal host, *Rhizopus microsporus*, and that mutants defective in such secretion system display a lower intracellular survival and fail to provoke fungal sporulation (Lackner *et al.,* 2011). Other mode of microbial competition is by secretion of antimicrobials. Filamentous eukaryotes are well known to produce a multitude of low-molecular-weight secondary metabolites that have antifungal activities against phylogenetically unrelated microbes (such as acetylgliotoxin and hyalodendrin) (Coleman *et al.,* 2011). These secondary metabolites are often silent in pure culture and only activated in co-culture or in a community context (Schroeckh *et al.,* 2009; Nutzmann *et al.,* 2011; Netzker *et al.,* 2015). Bacteria also produce different metabolites, including antibiotics and enzymes that exhibit broad-spectrum activity against phylogenetically unrelated fungal plant pathogens (Hass and Défago, 2005; Raaijmakers *et al.,* 2002). Antagonistic interactions among bacteria have been reported to be important in the structuring of soil-, coral-, or plant-associated bacterial communities (Rypien *et al.,* 2010; Tyc *et al.,* 2014; Maida *et al.,* 2016). Further, the study of antagonistic interactions among bacterial isolates from the rhizosphere, the roots, and the phyllosphere of the medicinal plant *Echinacea purpurea* suggests that plant-associated bacteria compete against each other through the secretion of antimicrobials (Maida *et al.,* 2016). Interestingly, bacteria from different plant compartments showed different levels of sensitivity to antagonistic activity, thereby indicating that antagonistic interactions might play an important role in shaping the structure of the plant microbiota (Maida *et al.,* 2016). In addition to antibiotic production, different bacteria (*Pseudomonas, Serratia, Stenotrophomonas, Streptomyces*) can also produce Volatile Organic Compounds (VOCs) that act as infochemicals within and between microbial groups and have been shown to inhibit the growth of a broad diversity of plant-associated fungi and oomycetes (Tyc *et al.,* 2017; Song *et al.,* 2015). It has been shown that bacterial VOCs also drive species-specific bacteria-protist interactions and likely serve as signals for protists to sense suitable prey. Notably, a *Collimonas pratensis* mutant, defective in terpene production, lost the ability to affect protists activity, indicating that terpenes represent key components of VOC-mediated communication between bacteria and protists (Schutz-Bohm *et al.,* 2017). Although the VOC activity of fungi/oomycetes towards bacteria has been less investigated, recent data indicate that soil filamentous microbes can also produce volatile blends that are perceived by bacteria. Schmidt *et al.,* (2016) identified over 300 VOCs from soil and rhizospheric fungi/oomycetes and demonstrated that some can be sensed by bacteria, thereby influencing their motility. Soil bacteria have also been shown to produce VOCs (Tyc *et al.,* 2017). The best illustrated example is the genus *Streptomyces*, which is known to produce sesquiterpenes exhibiting antimicrobial activity (Gürtler *et al.,* 1994). More recently, the comparative genomic analysis of the six strains of *Collimonas* have revealed that *C. pratensis* harbors functional terpene synthase genes responsible for the biosynthesis of a blend of sesquiterpenes with antimicrobial properties (Song *et al.,* 2015). All these examples suggest that VOCs from different microbial members could play a role as an additional defense line against other microbes and are also likely important for long distance structuring of the microbial communities (Tyc *et al.,* 2017). Microbes can also interfere with other microbes' survival by direct feeding. For instance, bacterial mycophagy consists on bacteria's ability to actively grow at the expense of living fungal hyphae (de Boer *et al.,* 2004; Leveau and Preston, 2008). Recently, it has been suggested that diverse mycophagous bacteria colonize saprotrophic rhizosphere fungi and feed as secondary consumers on root-derived carbon (Rudnik *et al.,* 2015). Some fungal or oomycetal species belonging to the genus *Trichoderma* or *Pythium*, respectively, can parasite or antagonize other fungi or oomycetes and can be used as biocontrol agents for plant protection, since they can also intimately interact with plant roots without causing disease symptoms (Benhamou *et al.,* 2012; Howell, 2003; Benitez *et al.,* 2004). Root-associated bacteria can also prey on other bacteria as described for *Bdellovibrio spp*. Phylogenetic and prey range analyses suggested that root-associated *Bdellovibrio spp*. differ from those in the soil, likely because these bacteria are best adapted to prey on root-associated bacteria (Jurkevitch *et al.,* 2000). Protist predation on bacteria has been also well documented, and recent microbiota reconstitution experiments in microcosm indicate a clear effect of Cercomonads (Rhizaria: Cercozoa) grazing on the structure and function of the leaf microbiota (Flues *et al.,* 2017). Their results indicate that Alpha- and Betaproteobacteria are less resistant to grazing and that predation restructures the bacterial network in leaves, influencing bacterial metabolic core functions (Flues *et al.,* 2017).

As exemplified in this section, microbes have evolved a great variety of mechanisms to interact with other microbial members in their environment. These interaction can be either beneficial or deleterious for the microbial partners, but it remains to be solved whether all these interactions happen in the same manner in a community context. Further, it will be key to understand whether the final community output is actually the result of multiple cascading interactions within the microbiota, or rather the result of a dominant interaction that will drive the establishment of the microbial communities (for example, the specific interaction between plant host and certain microbial members, that will determine other interactions in the system).

1.2 Microbial interactions shaping plant-associated microbial communities

The various mechanisms employed by microbes to cooperate and compete on plant tissues suggest that microbe-microbe interactions play fundamental roles in shaping and structuring microbial networks in nature. Therefore, the combination of host-microbe and microbe-microbe interactions is likely critical for the establishment of complex and diverse multi-kingdom plant-associated microbiota (Hunter *et al.,* 2010; Bakker *et al.,* 2014). However, the mechanistic understanding of the intermicrobial interactions in a community context as well as their functional impacts on plant-associated microbial communities remains sparse.

1.2.1 The mycosphere

As part of the mycosphere, fungal hyphae or fruiting bodies have been recognized for a long time as important niches that can be colonized, both externally and internally, by specific bacterial taxa, including *Pseudomonas* strains and bacteria from the Oxalobacteraceae, Bacillaceae, and Burkholderiaceae families, among others. (Andrade *et al.,* 1997; Warmink and Van Elsas, 2009; Hoffman and Arnold, 2010; Arendt *et al.,* 2016). For example, *in vitro* cultures of the AMF *Glomus intraradices* and *Glomus proliferum*, co-inoculated with a soil bacterial “tea”, showed that bacterial communities that attach to growing hyphae are significantly different to the bacterial inoculum (specifically, members of the *Streptomyces* genus and the Oxalobacteraceae family) and also different to the bacterial communities attaching to glass wool, suggesting a fungal-mycelia-specific bacterial community (Scheublin *et al.,* 2010). Fungal exudates seem to play a specific role for mycosphere colonization by stimulating the growth of specific bacteria or inducing changes in bacterial community structure (Filion *et al.,* 1999; Toljander *et al.,* 2007; Warmink *et al.,* 2009). Specifically, exudates produced by the arbuscular mycorrhizal fungus *Rhizophagus irregularis* have been shown to stimulate bacterial growth and modify bacterial community structure, which is marked by an increased abundance of several Gammaproteobacteria (Toljander *et al.,* 2007). Notably, bacterial ability to colonize the mycosphere correlates with their ability to use particular carbonaceous compounds abundantly found in mycosphere exudates such as l-arabinose, l-leucine, m-inositol, m-arabitol, d-mannitol, and d-trehalose (Warmink *et al.,* 2009). Analysis of the soil bacterial community in the presence and absence of the arbuscular mycorrhizal fungus *Glomus hoi* using a microcosm experiment also revealed the significant effect of the fungus on bacterial community structure, suggesting that nitrogen export by the fungus is an important driving force explaining bacterial community shift (Nuccio *et al.,* 2013).

Recent studies have analyzed the bacterial diversity associated with mycorrhizal root tips, revealing the complexity of the interactions between mycorrhizal fungi and their associated bacterial microbiota in the mycorrhizosphere (Vik *et al.,* 2013; Nguyen *et al.,* 2015; Uroz *et al.,* 2012; Marupakula *et al.,* 2016). Specifically, some bacterial orders (Burkholderiales and Rhizobiales) were reproducibly found within ectomycorrhizal root tips, indicative of a tight fungal-bacterial association (Nguyen *et al.,* 2015). Using microcosm experiments and germ-free *Pinus sylvestris*, Marupakula *et al.,* (2016) recently found that root tips colonized by three different ectomycorrhizal fungi host statistically distinct bacterial communities. Although all three mycorrhizal types tightly associate with high abundance of *Burkholderia*, specific bacterial signatures could be detected for each fungus (Marupakula *et al.,* 2016). Similar to the mechanisms described for the mycorrhizosphere (Johansson *et al.,* 2004), it is therefore likely that numerous plant-associated fungi could indirectly impact bacterial communities by different means such as changes in nutrient availability, modulation of environmental pH, production of fungal exudates, or nutrient competition.

1.2.2 Influence of pathogen invasion on the plant microbiota

Plant infection by pathogenic microbes often correlates with microbial community shifts in different plant compartments, including seeds (Rezki *et al.,* 2016), roots (Xue *et al.,* 2015), wood (Bruez *et al.,* 2015), and leaves (Agler *et al.,* 2016a). Analysis of the impact of two microbial invaders, the bacterial strain *Xanthomonas campestris* pv. *campestris* (*Xcc*) 8004 and the fungal isolate *Alternaria brassicicola* (Ab) Abra43 on the structure of seed-associated microbial assemblages in *Raphanus sativus*, indicates the different effects on the endogenous seed microbiota. The bacterial strain *Xcc* 8004 has no effect on microbial assemblages, whereas seed invasion by the fungal pathogen massively perturbs the resident fungal seed microbiota. Seed invasion by the pathogenic fungus explains ~ 60% of the variation of fungal communities observed between infected and non-infected seeds, likely due to fungal-fungal competition for resources and space (Rezki *et al.,* 2016). Infection of oak leaves by the obligate filamentous pathogens *Erysiphe alphitoides* (powdery mildew fungus) or *A. thaliana* leaves by *Albugo sp*. (oomycete) is accompanied by significant changes in the composition of the phyllosphere microbiota (Jakuschkin *et al.,* 2016; Agler *et al.,* 2016a, respectively). Notably, the pathogen *Albugo* has strong effects on epiphytic and endophytic bacterial colonization by decreasing species richness and stabilizing the community structure, which has been validated by manipulation experiments under controlled laboratory conditions (Agler *et al.,* 2016a). Based on microbial correlation networks, Jakuschkin *et al.,* (2016) identified 13 bacterial and fungal Operational Taxonomic Units (OTUs) that significantly associate, either negatively or positively, with powdery mildew disease. Although the protective activities conferred by the corresponding microbes have not been validated yet, a direct antagonistic effect of *Mycosphaerella punctiformis* on *E. alphitoides* has been suggested (Jakuschkin *et al.,* 2016). Significant associations were also found between the composition of the endogenous fungal microbiota in poplar leaves and rust symptom severity, suggesting that resident foliar fungal endophytes can enhance or attenuate disease severity in wild trees (Busby *et al.,* 2016). Taken together, these data indicate a tight link between pathogen invasion and the microbial community structure *in planta* that likely results from the combined effect of microbe-microbe and microbe-host interactions.

1.2.3 Microbial hubs as modulators of plant-associated microbial communities

Microbial network analysis represents an elegant way to identify specific microbes that have a more central position in a microbial network, often defined as “keystone” species or “hubs.” These microbes frequently co-occur with other taxa (highly connected to other microbes within the network) and likely exert a strong influence on the structure of microbial communities (Agler *et al.,* 2016a; Layeghifard *et al.,* 2016). A comprehensive survey of bacterial, fungal, and oomycetal communities associated with the leaves of *A. thaliana* revealed the presence of few microbial hubs, such as the obligate biotrophic oomycete pathogen *Albugo* sp. and the basidiomycete yeast fungus *Dioszegia sp*., that act by suppressing the growth and diversity of other microbes. Other candidate bacterial hubs (members of the family Comamonadaceae) were also found to positively control the abundance of numerous phyllosphere bacteria (Agler *et al.,* 2016a). Specific leaf-associated Cercomonads (Protists: Rhizaria: Cercozoa) were also recently shown to exert a significant effect on bacterial community composition. A less complex bacterial correlation network with a higher proportion of positive correlations was observed in the presence of protists, underlining the importance of predator-prey interactions for bacterial community structure (Flues *et al.,* 2017). In plant roots, Niu *et al.,* (2017) have recently employed a simplified seven-species synthetic community that is representative of the maize root microbiota to study the role of *in planta* interspecies interactions in altering the host health and the establishment of root-associated bacterial communities. Notably, the removal of one community member, *Enterobacter cloaceae*, caused a significant reduction in species richness indicating that *E. cloaceae* plays the role of “keystone” species within the seven-species community. In perennial plants, network analysis of mycorrhizal and endophytic fungi from beech trees (*Fagus sp*.) revealed the presence of two distinct microbial networks, consisting of diverse functional groups of mycorrhizal and endophytic fungi. Importantly, a different fungal hub dominates in each module (either *Oidiodendron sp*. or *Cenococcum sp*.), suggesting that diverse fungal hubs can differentially sculpt microbial assemblages within a single plant population (Toju *et al.,* 2016). However, microbial hub species identified through co-occurrence network analysis could simply represent generalist microbes that are reproducibly and abundantly found in plant tissues. Validating the functional role of microbial hubs and determining the molecular mechanisms used by these microbes to modulate microbial community structure will be key to fully understand microbial communities’ establishment.

1.3 Consequences of intermicrobial interactions on plant growth and health

Although competitive and cooperative interactions significantly impact plant-associated microbial assemblages, these microbial interactions might also alter plant growth and fitness in beneficial or deleterious ways. Although some correlations were observed between microbial community composition and plant host phylogeny (Bouffaud *et al.,* 2014; Schlaeppi *et al.,* 2014; Yeoh *et al.,* 2017), it is likely that a core plant microbiota has evolved with terrestrial plants (lycopods, ferns, gymnosperms, and angiosperms) over 450 million years (Yeoh *et al.,* 2017). Therefore, it is plausible that these co-occurring core microbiota members have evolved, in parallel, niche-specific inter-microbial interactions strategies that impact plant growth and health.

1.3.1 Intermicrobial interactions and plant growth promotion

Bacterial-mycorrhizal-plant relationships have been intensively studied due to the capacity of this microbial interplay to provide a direct benefit for the host plant (Bonfante and Anca, 2009). The interaction between mycorrhizal fungi and specific rhizobacteria promotes the establishment and functioning of mycorrhizal symbioses with the plant host, including both endo- and ectomycorrhizal interactions (Frey-Klett *et al.,* 2007, Labbé *et al.,* 2014). These so-called “helper” bacteria are able to act at several levels: (1) they increase the receptivity of the root to mycorrhizal fungi, (2) enhance soil conduciveness to the fungus, (3) promote germination of fungal spores, and (4) enhance mycelium survival (Frey-Klett *et al.,* 2007). Furthermore, this relationship appears to be specific, since some bacteria isolated from specific mycorrhizal fungi have antagonistic activities towards other phylogenetically unrelated fungi (Frey-Klett *et al.,* 2007). Beyond mycorrhiza helper bacteria, some bacterial endosymbionts of root-associated fungi also directly affect the plant host, as demonstrated for *Rhizobium radiobacter* F4. This *Serendipita indica*’s (formerly *Piriformospora indica*) endosymbiont is able to grow in the absence of its fungal host and can promote plant growth and resistance to plant leaf pathogens independently from *S. indica*, suggesting that *S. indica*-mediated plant growth promotion is partly mediated by its bacterial endosymbiont (Sharma *et al.,* 2008; Glaeser *et al.,* 2016) or by other bacterial members influencing fungal growth (Bhuyan *et al.,* 2015). In nature, most land plants are co-colonized by fungal and bacterial symbionts, as well as a staggering diversity of endophytic and pathogenic microbes (Toju *et al.,* 2013; Bonito *et al.,* 2014). However, it remains unclear how the competing demand of multiple partners is balanced in plant roots to maintain a beneficial output. A focus of interest is the cooperation between mycorrhizal fungi and nitrogen-fixing bacteria. These important members of the root microbiota are widespread and co-occur in the roots of many plant species (Artursson *et al.,* 2006). Interestingly, it has been recently shown that these microbes can complement each other to maximize nutrient acquisition in the host and act synergistically to promote plant diversity and productivity (van der Heijden *et al.,* 2016). Although the direct role of microbe-microbe interaction in this process is likely minor, mixed microbial consortia could, nonetheless, indirectly stimulate ecosystem functioning and plant productivity through different resource use strategies.

1.3.2 Disease suppression

Soil bacterial communities from different taxonomic groups have an important biocontrol potential in the so-called “disease-suppressive” soils. In these soils, plants are less affected by pathogenic microbes due to the effect of their surrounding microbiota. Specifically, it has been proposed that oxalic acid produced by the fungal root pathogen *Rhizoctonia solani,* or compounds released from plant roots under attack, promote the growth of particular bacterial families (Oxalobacteraceae and Burkholderiaceae), leading to a bacterial community shift and the activation of bacterial stress and antagonistic responses that restrict the growth of the fungal pathogen (Mendes *et al.,* 2011; Chapelle *et al.,* 2016). Furthermore, it has been shown that *Streptomyces* strains isolated from disease-suppressive soils can produce different VOCs with antifungal activity (Cordovez *et al.,* 2015). Other *Streptomyces* species have also been isolated from disease-suppressive soils from a strawberry field (Cha *et al.,* 2016). These bacteria have been found to produce an antifungal thiopeptide targeting fungal cell wall biosynthesis in *Fusarium oxysporum*, suggesting that different bacterial species use different competitive mechanisms (Cha *et al.,* 2016). Similarly, Santhanam *et al.,* (2015) have demonstrated how root-associated bacteria provide an effective rescue to *Nicotiana attenuata* from the sudden-wilt disease. Seed inoculation with a core consortium of five bacterial isolates naturally adapted to the environment provides an efficient plant protection under field conditions, underlining the importance of using locally adapted microbiota members to control plant disease. In the phyllosphere, it has been shown that the leaf surface microbiota, together with endogenous leaf cuticle mechanisms, leads to *A. thaliana* resistance against the broad host range necrotrophic fungal pathogen *Botrytis cinerea* (Ritpitakphong *et al.,* 2016). Although it is not clear whether these bacterial communities were already stable or restructured after pathogen attack, it is likely that the plant actively recruits disease-suppressive bacteria during seed production or germination (Links *et al.,* 2014; Barrett *et al.,* 2016). Interestingly, it has been also shown that soil microbiota can suppress not only plant pathogens, but also beneficial microbes, such Arbuscular Mycorrhizal Fungi (AMF) (Svenningsen *et al.,* 2018). By measuring phosphorus uptake from radioisotope-labelled soil as a proxy for extraradical mycelium activity, it was possible to observe a significant decrease of fungal activity when inoculated in 4 out of the 21 soils tested, most likely due to the higher abundances of *Weisella* and *Acidobacteriaceae* Gp1 members (Svenningsen *et al.,* 2018). Although many examples illustrate the biocontrol activity of plant-associated microbiota members, the molecular mechanisms leading to pathogen growth suppression on plant tissues remain unclear. It has been shown that the millet bacterial endophyte *Enterobacter sp*. can promote both growth and bending of millet root hairs, resulting in a multilayer root-hair endophyte stack that efficiently prevents entry by the fungal pathogen *Fusarium*. Tn5-mutagenesis further demonstrated that bacterial biocontrol activity requires c-di-GMP-dependent signaling, secretion of diverse fungicides, and resistance to a *Fusarium*-derived antibiotic (Mousa *et al.,* 2016).

Although it is known that the plant-associated microbiota can prevent disease, it remains difficult to engineer functionally reliable synthetic microbial consortia that promote plant growth and suppress disease. Reductionist approaches with synthetic microbial communities suggest that pathogen suppression increases when the diversity of the bacterial consortium increases. It has been shown that complex *Pseudomonas* species consortia better protect tomato plants against the root pathogen *Ralstonia solanacearum* than low-complexity *Pseudomonas spp*. consortia, due to the combined action of antagonistic activities and resource competition (Hu *et al.,* 2016). Similarly, Wei *et al.,* (2015) showed that disease incidence is reduced when the trophic network favors resource competition between non-pathogenic *R. solanacearum* and a pathogenic strain, due to overlap in resources acquisition (Wei *et al.,* 2015). These examples provide evidence that microbial diversity, resource competition, and inter-microbial antagonism are important factors to consider for engineering functionally relevant microbial consortia that efficiently suppress plant diseases.

1.3.3 Disease facilitation

Intermicrobial interactions do not necessarily impact plant fitness in a positive way, but can also be deleterious for the plant by enhancing disease. For instance, the bacterial plant pathogen *Clostridium puniceum* secretes clostrubins (antimicrobial polyketides) to compete against other microbial pathogens and survive in aerobic environments (Shauber *et al.,* 2015). It has been also shown that toxin production by the bacterial endosymbiont of the plant-pathogenic fungus *Rhizopus* is required for successful fungal colonization of rice plants, indicating that fungal-bacterial symbioses can also promote disease (Partida-Martinez *et al.,* 2005). Recently, high-throughput fungal profiling methods, combined with manipulative experiments, have shed new light on the ecological importance of fungal endophytes for rust disease modification in wild trees. Specifically, it has been shown that certain fungal endophytes in the poplar phyllosphere could reduce rust disease symptoms, whereas others promote susceptibility (Busby *et al.,* 2016). Taken together, these studies clearly show that intermicrobial interactions are complex and can also mediate disease facilitation.

1.4 Thesis aims (Chapter II)

Plants live in intimate association with complex and diverse microbial communities. Next-generation sequencing has already enabled us to explore different microbial groups through the targeting of specific microbial loci or using environmental metagenomes. Nonetheless, a more holistic approach is still needed to better understand the intermicrobial interactions within the microbiota of plants and to better define the functional relevance of the microbial networks for holobiont fitness (Vandenkoornhuyse *et al.,* 2015; Hacquard and Schadt, 2015). Prokaryotic and eukaryotic microbes have evolved a myriad of cooperative and competitive interaction mechanisms that shape and likely stabilize microbial assemblages on plant tissues. However, most of the data are derived from one-to-one interaction studies, and only few incorporate complex microbial communities in controlled laboratory conditions to reconstitute the plant microbiota and to understand the role of intermicrobial interactions (Vorholt *et al.,* 2017). Thus, the second aim of my thesis will be to reconstitute plant-associated microbial communities isolated from roots of healthy *Arabidopsis thaliana* plants growing in the same soil, including several microbial kingdoms and under controlled laboratory conditions, to understand the principles that govern the assembly of complex synthetic microbial communities and the maintenance of host-microbial homeostasis. In this way, I will be able to understand how different microbial kingdoms establish in the root vicinity by themselves or in combination with other microbial groups. Further, I will investigate the effect of these microbial interactions on plant growth and performance. Hence, the following questions will be addressed:

1) How do different microbial groups impact each other's establishment at *A. thaliana* roots vicinity?
2) Do these synthetic microbial communities impact *A. thaliana'*s health?
3) Do microbial communities lacking one or several microbial groups perform differently?
4) Can microbial binary assays predict microbial biocontrol activity in a community context?
5) How do microbial communities establish over time?

2. RESULTS

2.1 Synthetic microbial communities reconstitution as a tool to understand microbial interactions and their role for plant health

2.1.1 Multi-kingdom microbial synthetic communities

Studies of microbe-microbe interactions in binary systems have advanced the field in understanding how microbes might interact with each other. However, how these microbial interactions are actually happening in a community context is less understood. As reviewed by Vorholt *et al.,* (2017), a relevant approach to dissect assembly rules and functions of the plant microbiota is to deconstruct and reconstruct microbial communities under controlled laboratory conditions. It has been shown that 65% of *A. thaliana*-associated bacterial root-enriched OTUs have one or several isolates in pure culture, allowing to follow the aforementioned approach (Bai *et al.,* 2015). Thus, isolation of microbes from plant roots, followed by re-inoculation into a gnotobiotic plant system has proved to be very efficient to assess the role of plant immune system components in shaping root-associated bacterial communities, to reveal microbiota specialization in root and leaf habitats, and to dissect functional links between plant immunity, nutrition and bacterial microbiota establishment in plant roots (Lebeis *et al.,* 2015; Bai *et al.,* 2015; Castrillo *et al.,* 2017). Microbial interactions between members of different kingdoms (for example, between bacterial and fungal communities), however, remain poorly understood. In order to assess this question, Dr. Stéphane Hacquard (Department of Plant-Microbe interactions, MPIPZ) established a fungal and oomycetal culture collections from the roots of healthy *Arabidopsis thaliana* and relatives grown in GE1, GE2, and FR3 soils (from **Chapter 1**), as well as from the Cologne Agricultural Soil (CAS), the same soil that was used to establish the root-derived bacterial culture collection (Bai. *et al.,* 2015). To reconstruct a biologically significant microbiota, I selected only bacterial, fungal and oomycetal strains derived from CAS soil, and microbes that had enough sequence differences to be identified by MiSeq sequencing methods (see **Methods**). Thus, I selected 148 bacterial strains (94 Proteobacteria, 45 Actinobacteria, 1 Bacteroidetes and 8 Firmicutes), 34 fungal strains (all belonging to the Ascomycota phylum) and 8 oomycetes strains (all belonging to the Pythiaceae family) (**Figure 15, Annex: Supplementary Table 3**). Importantly, these strains largely resemble the natural taxonomic composition of the root microbiota, representing >50% of the taxa detected by culture independent community profiling. Then, a gnotobiotic plant system, the so-called FlowPots system, was used (Kremer *et al.,* 2018). FlowPots have a soil matrix (greenhouse peat) that closely resembles natural soil texture and contains complex carbon sources (**Figure 16**, based on Kremer *et al.,* 2018). Other systems were tested, such calcined clay in Magenta Boxes (Bai *et al.,* 2015), and also a liquid system, but eukaryotic microbes viability was very low or growth rate very slow, respectively, and therefore not used for the purposes of this project (data not shown).

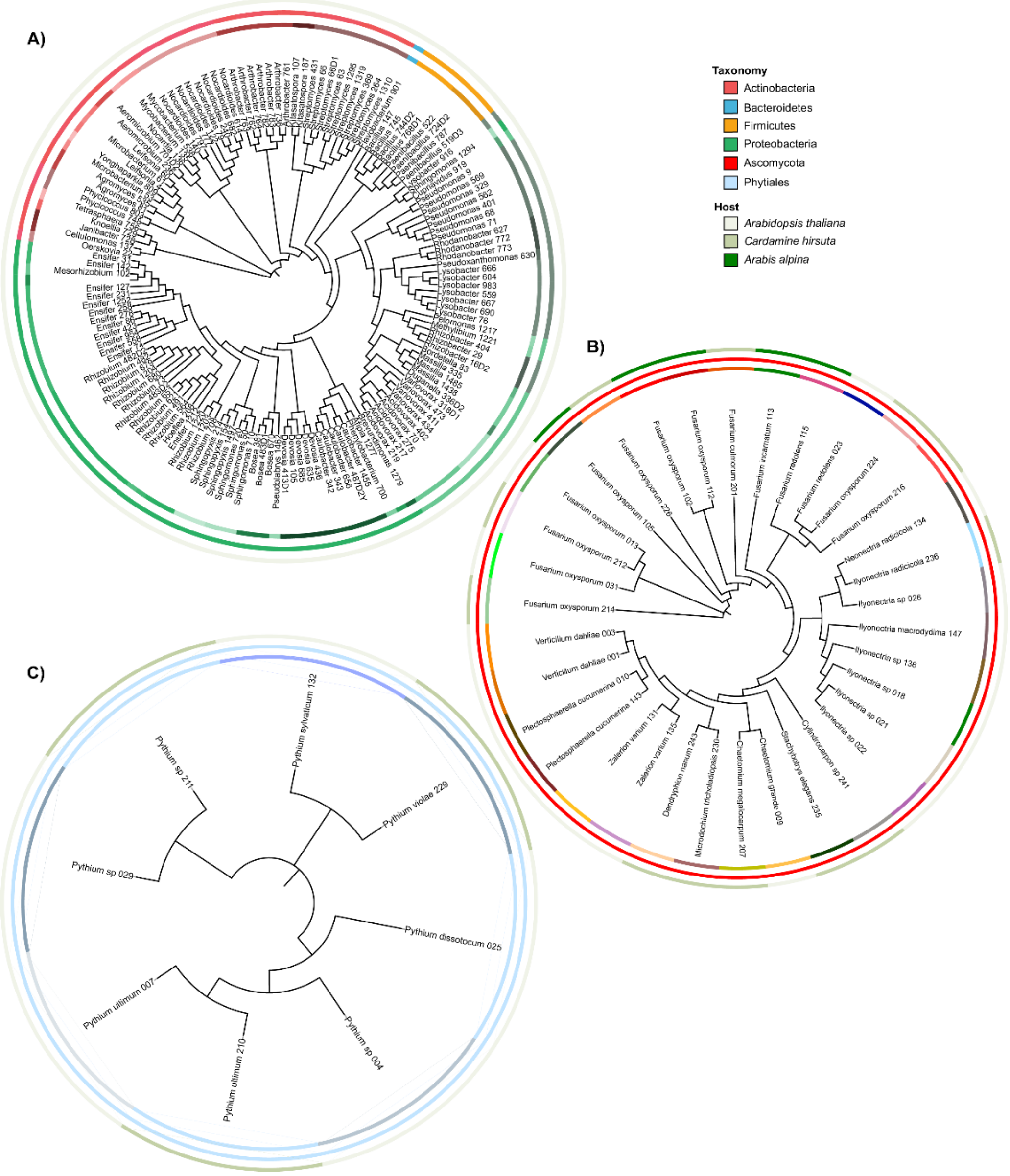
A)
Taxonomy
Actinobacteria
Bacteroidetes
Firmicutes
Proteobacteria
Ascomycota
Phytiales
Host
Arabidopsis thaliana
Cardamine hirsuta
Arabis alpina
B)
Fusarium oxysporum 102
Fusarium oxysporum 112
Fusarium culmorum 201
Fusarium incarnatum 113
Fusarium redolens 115
Fusarium redolens 023
Fusarium oxysporum 224
Fusarium oxysporum 216
Neonectria radicicola 134
Ilyonectria radicicola 236
Ilyonectria sp 026
Ilyonectria macrodydima 147
Ilyonectria sp 136
Ilyonectria sp 018
Ilyonectria sp 021
Ilyonectria sp 022
Cylindrocarpon sp 241
Stachybotrys elegans 235
Chaetomium grande 009
Chaetomium megalocarpum 207
Microdochium trichocladiopsis 230
Dendryphion nanum 243
Zalerion varium 125
Zalerion varium 131
Plectosphaerella cucumerina 143
Plectosphaerella cucumerina 010
Verticillium dahliae 001
Verticillium dahliae 003
Fusarium oxysporum 214
Fusarium oxysporum 031
Fusarium oxysporum 212
Fusarium oxysporum 013
Fusarium oxysporum 105
Fusarium oxysporum 226
C)
Pythium sylvaticum 132
Pythium violae 229
Pythium dissotocum 025
Pythium sp 004
Pythium ultimum 210
Pythium ultimum 007
Pythium sp 029
Pythium sp 211

Figure 15: Microbial culture collections for gnobotiotic experiments. Microbial members used in this study: 148 bacterial strains (**A**) (from culture collection of Bai *et al.,* (2015), 34 fungal strains (**B**); and 8 oomycetes strains (**C**) (from culture collections in Duran *et al.,* in preparation). Phylogenetic trees were constructed in the iTOL platform, by using the bacterial full 16s rRNA gene and fungal and oomycetal full ITS Sanger sequences. Each of the colored layer represents (from inner to outer layer) the genus/species levels, phylum level and plant host from which these microbes were initially isolated.

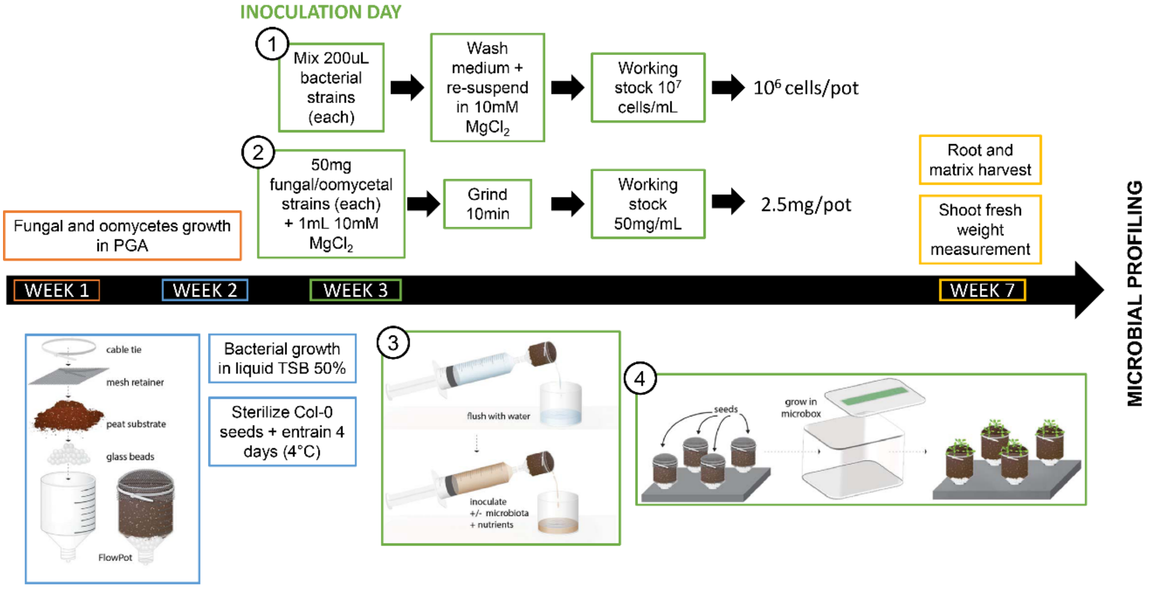
INOCULATION DAY
① Mix 200uL bacterial strains (each)
Wash medium + re-suspend in 10mM MgCl₂
Working stock 10⁷ cells/mL
10⁶ cells/pot
② 50mg fungal/oomycetal strains (each) + 1mL 10mM MgCl₂
Grind 10min
Working stock 50mg/mL
2.5mg/pot
Root and matrix harvest
Shoot fresh weight measurement
Fungal and oomycetes growth in PGA
WEEK 1
WEEK 2
WEEK 3
WEEK 7
MICROBIAL PROFILING
cable tie
mesh retainer
peat substrate
glass beads
FlowPot
Bacterial growth in liquid TSB 50%
Sterilize Col-0 seeds + entrain 4 days (4°C)
③
flush with water
inoculate +/- microbiota + nutrients
④
seeds
grow in microbox

Figure 16: Gnotobiotic experiments pipeline scheme. This scheme shows the steps followed in order to perform FlowPots-based gnotobiotic experiments. First, fungal and oomycetal strains are grown on PGA plates (Week 1) and incubated for two weeks before the inoculation day. One week after, the peat is sterilized and the FlowPots assembled. Also, bacterial strains are grown in liquid media (TSB 50 %) for one week, and the *A. thaliana* Col-0 seeds sterilized and entrained for four days at 4 °C (Week 2). On the inoculation day, 200 µL of each bacterial strain is pooled together, and re-suspended in buffer after washing off the medium. Optical density (OD) of the full mixture is measured in order to dilute it to the working stock. 50 mg of mycelium from the fungal and oomycetal strains are harvested and grinded in 1 mL of a 10 mM $MgCl_2$ buffer. Then, 900 µL of each fungal/oomycetal homogenate is pooled. Before inoculating the microbes, each FlowPot needs to be flushed with sterile water to remove toxic compounds produced by the peat from autoclaving. After microbial inoculation, seeds are sown on the surface of the FlowPots and the Microboxes incubated. After four weeks, shoot fresh weight is measured and root and matrix samples harvested for microbial community profiling. Each color matches the time point where each step is taking place. Within the inoculation day, numbers indicate the order in which step is made. FlowPots images are taken from Kremer *et al.*, (2018).

First, it was important to select a similar inoculation protocol for all microbial members. As explained in **Methods** (**Figure 16**), bacterial strains were inoculated in the system by pipetting a selected volume from liquid cultures. Fungal and oomycetal strains, on the other hand, have a very variable growth rate in liquid media, and therefore an alternative method was necessary. An option was to inoculate them as a spore suspension, but this was not viable as most of these fungi do not form spores. Instead, considering that fungi and oomycetes all grow forming mycelium, these mycelia could be harvested in similar amounts per strain and homogenized, so that they could be inoculated similarly to bacterial strains. Thereby, I tested different homogenization protocols with which fungi and oomycetes' hyphae would disrupt and could be treated similarly to bacterial inoculum (**Supplementary Figure 11A**). Thus, bead-beating of 50 mg of fungal/oomycetal mycelium for 10 minutes with 1 mL of 10 mM $MgCl_2$ and one stainless steel bead (3.2 mm of diameter) was the most effective method to disrupt the mycelium in a way that it would be possible to inoculate it in a liquid format. More importantly, this method was suitable for fungal and oomycetal survival (**Supplementary Figure 11B**).

2.1.2 Effect of multi-kingdom microbe-microbe interactions on microbial community structure and plant growth

The research questions addressed in the first experimental set-up were the following: 1) what is the individual effect of microbial groups on plant performance and 2) what is the relevance of inter-kingdom microbe-microbe interactions on microbial community establishment and plant growth. Therefore, after following the gnotobiotic experiments pipeline scheme in **Figure 16,** sterile *A. thaliana* Col-0 plants were co-incubated with different microbial combinations: bacteria only (B, 148 strains), fungi only (F, 34 strains), oomycetes only (O, 8 strains), bacteria and oomycetes (BO), bacteria and fungi (BF), fungi and oomycetes (FO) and all three groups together (BFO). Also, an un-inoculated control was included (microbe-free, MF), as well as an unplanted BFO condition, to inspect the role of the host plant presence on microbial communities. This experiment will be referred as “EXP1” in later sections of this chapter. This experiment was replicated three times, with at least three technical replicates each (two pots pooled together accounted for one technical replicate). I measured the microbial biomass inoculated in the system at the beginning of the experiment (weight of bacterial cells pellet and weight of fungal/oomycetal mycelium, respectively), and adjusted the microbial load to a final ratio that resembled previous estimations of microbial biomass in nature (Joergensen and Emerling, 2006). Thus, 6% of the inoculated biomass was bacterial and 94% shared between fungi and oomycetes.

After four weeks of microbial co-incubation with *A. thaliana* Col-0, shoot fresh weight was measured and root and matrix samples were harvested for microbial community profiling (**Figure 16**). The first output of this experiment, however, was the host survival rate, referred to as the percentage of plants that were alive at the end of the experiment, compared to the number of seeds initially sown: 10 seeds were sown per pot at the beginning of the experiment and, after one week, seedlings were thinned out to 4-5 plants per pot; from these plants, survival rate was calculated at the end of the experiment, and was strongly dependent of the community inoculated in the system. Thus, microbe-free pots had an average of 81 % survival rate, whereas, in bacterial-inoculated pots, this rate was slightly higher (B: 98 %; BO: 87 %; BF: 94 %: BFO: 100 %). Remarkably, survival rate in F-, O- or FO-inoculated pots was very low (0 %, 24 % and 0 %, respectively)

(**Figure 17**). Furthermore, shoot fresh weight assessment showed that bacterial-only inoculum (B) did not significantly improve plant growth compared to microbe-free control plants, but inoculation of either fungi-only (F) or oomycetes-only (O) decreased significantly plant growth (Kruskal Wallis, Dunn test *post-hoc*, p-value<0.05, **Figure 17**). Further, co-inoculation with fungi and oomycetes (FO) did not show different plant growth compared to the single inoculations (F, O). Fungal or oomycetal co-inoculations with bacterial communities (BF, BO), on the other hand, significantly rescued the detrimental effect that either eukaryotic microbial group had on plant growth. Remarkably, only with the full microbial inoculum (BFO) plant growth was significantly increased compared to microbe-free conditions (125% plant shoot fresh weight increase, Kruskal-Wallis, Dunn test *post-hoc*, p-value<0.05, **Figure 17**). In order to investigate whether there was a microbiota signature related to these phenotypes, I analyzed root- and matrix-associated bacterial, fungal and oomycetal community profiles. One of the first observations was that variance between biological replicates was very high, especially for bacterial and fungal communities (4.84% and 2.93%, respectively, PERMANOVA, p-value<0.001, **Table 5**, **Figure 18A**). Normalization of the Bray-Curtis dissimilarities by comparing the distance of clusters to the distance of the control cluster to itself, allowed cross-comparison between microbial conditions despite variation across biological replicates (**Figure 18B**, see **Methods**). Therefore, if samples within the control cluster (i.e., bacteria-only to bacteria-only samples (B-B), fungi-only to fungi-only samples (F-F) and oomycetes-only to oomycetes-only samples (O-O)) are significantly closer together than to cluster “X”, the microbial assemblage in cluster “X” is significantly different. Thereby, bacterial communities remained stable, compared to the control cluster, regardless of the presence of other microbial groups in the system (BF, BO, BFO), both in roots and matrix samples (**Figure 18B**). Fungal and oomycetal communities, on the other hand, were significantly different when bacterial communities were present (BF, BO, BFO), but not when oomycetes or fungi were present (FO) (Kruskal-Wallis, Dunn test *post-hoc*, p<0.05, **Figure 18B**). This was also notable by variance analysis, where fungal and oomycetal communities presence explained a small fraction of bacterial communities’ variance (3.65%, p-value=0.002, and 2.2%, p-value=0.047, PERMANOVA, **Table 5**), whereas fungal and oomycetes communities are very significantly impacted by bacterial communities (11.6% and 7.8%, respectively, PERMANOVA, p-value<0.001, **Table 5**). Remarkably, unplanted communities display very similar microbial communities compared to their planted counterpart (B-BFO UNPL., **Figure 18B**).

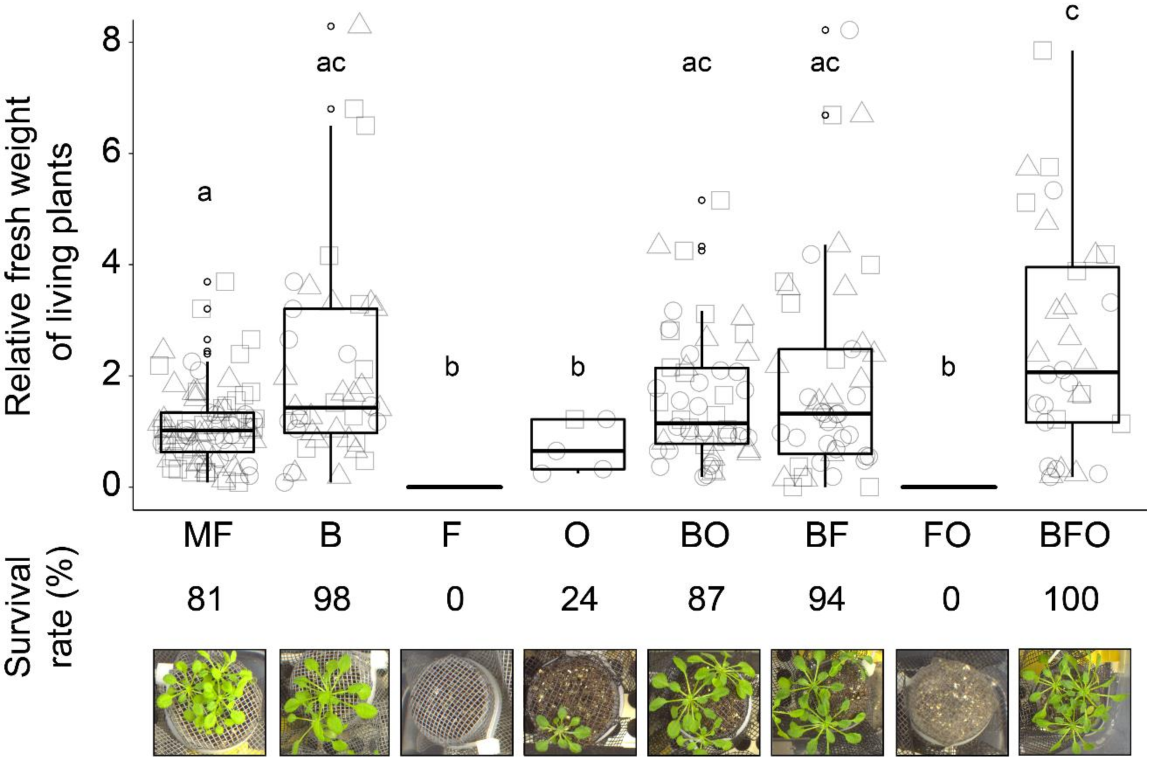

Figure 17: Multi-kingdom reconstitution experiment. Relative fresh shoot weight to microbe-free control of *A.thaliana* Col-0 plants grown with different microbial combinations (MF: Microbe Free, B: Bacteria only, F: Fungi only, O: Oomycetes only, BO: Bacteria and oomycetes, BF: Bacteria and fungi, FO: Fungi and oomycetes, BFO: full microbial community). Shoot fresh weight values are relative to the microbe-free plants in order to remove variation between biological replicates. Shapes within box plots represent each of the three biological replicates (with three technical replicates each) and statistically significant differences are depicted with letters (Kruskal-Wallis, Dunn test *post-hoc*, $p<0.05$). Survival rate values represent the number of plants that survived at end point (4 weeks), from the germinated seeds in the first week. Pictures below each label are representative of the plant phenotype at the end of the experiment.

One of the advantages of using synthetic communities for microbial reconstitution is the possibility to trace most strains after an experiment. As a comparison of microbial relative abundances across conditions, input communities (initial microbial inoculum) were also profiled. In these input samples, it was possible to observe that most of the strains inoculated can be traced back by their 16s and ITS sequences. However, by using the reference-based approach (see **Methods**), several strains may be grouped as one due to sequence similarity. Therefore, these groups of strains will be considered as Taxonomic Community Units (TCUs). Thus, 65 bacterial TCUs, 26 fungal TCUs and 6 oomycetal TCUs were identified (**Supplementary Figure 12, “Input” samples**). After four weeks of co-inoculation with *A. thaliana* plants and other microbial groups, bacterial profiles remained stable and similar across conditions. Further, as in natural communities, Proteobacteria members appear to be more abundant in root samples than in matrix/soil samples (**Figure 19A,** Bulgarelli *et al.,* 2012). Fungal and oomycetal inputs have an overrepresentation of *Fusarium* strains (102 and 216) and *Pythium* strains (210 and 227) relative abundances, respectively, which is also visible in all conditions. Nevertheless, the fungal and oomycetal community shifts observed upon bacterial co-inoculation are remarkable, where several strains show reduced relative abundance, compared to F, O or FO conditions (**Figure 19B and C**). These results indicate a clear correlation between the plant survival rate and the fungal and oomycetal community structure in the matrix. Interestingly, bacterial species diversity was maintained across all combinations, whereas fungal and oomycetal species diversity decreases upon bacterial co-inoculation, already in matrix samples (**Supplementary Figure 12**). This observation suggests that interactions between bacteria and filamentous eukaryotes take place at the soil-root interface during microbiota establishment and are maintained inside plant roots.

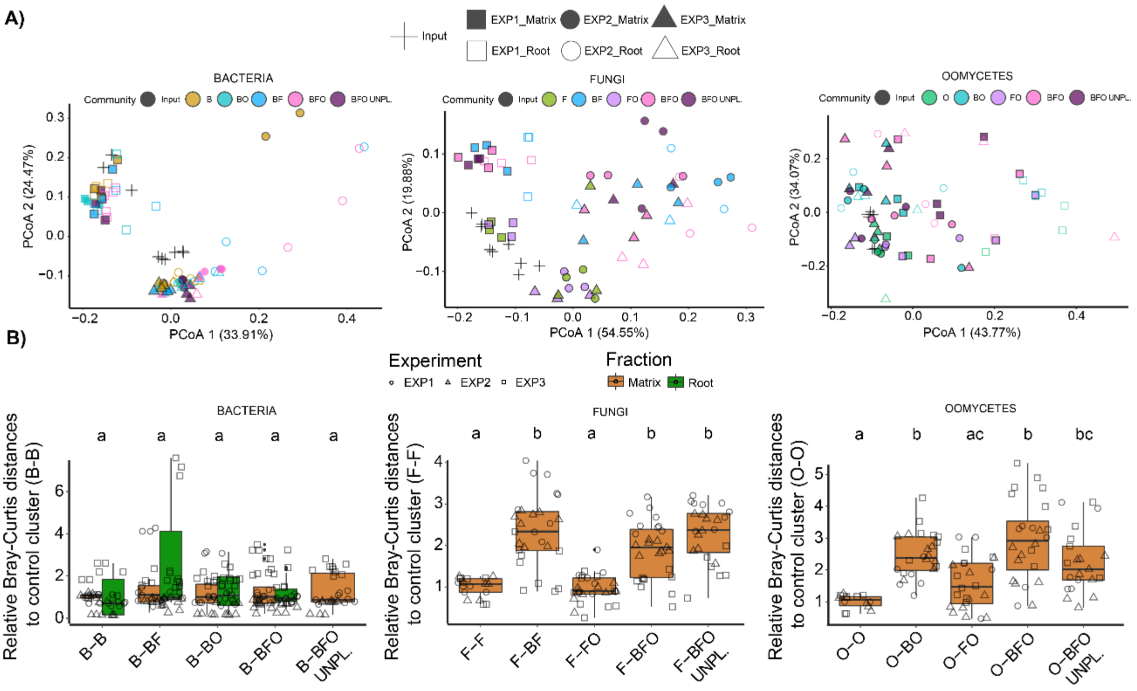

Figure 18: Microbe-microbe interactions driving microbiota establishment. A) PCoA plots of bacterial, fungal and oomycetal (from left to right) Bray-Curtis dissimilarities; shapes represent each of the three biological replicates and colors depict different microbial combinations. **B)** Relative Bray-Curtis distances between sample clusters of bacterial, fungal and oomycetes profiles (from left to right) of matrix (brown) and root (green) to the control clusters (B-B, F-F and O-O) (i.e., the closer to 1, the more similar to control cluster). Significant differences are depicted with different letter (Kruskal-Wallis, Dunn test *post-hoc*, <0.05). Shapes represent each of the three biological replicates.

Bacteria			**Fungi**			**Oomycetes**		
Factor	**Var. (%)**	**p-val.**	**Factor**	**Var.(%)**	**p-val.**	**Factor**	**Var.(%)**	**p-val.**
Fraction	8.00	0.002	**Fraction**	6.94	0.001	**Fraction**	15.12	0.001
Has_fungi	3.65	0.002	**Has_bacteria**	11.60	0.001	**Has_bacteria**	7.8	0.001
Has_oom.	2.20	0.047	**Has_oom.**	0.62	0.216	**Has_fungi**	3.02	0.029
Replicate	0.18	0.851	**Replicate**	0.50	0.307	**Replicate**	0.45	0.678
Exp.	4.84	0.002	**Exp.**	2.93	0.004	**Exp.**	1.73	0.115

Table 5: Microbial profiles variance. PERMANOVA tests were performed to study the variance explained (Var. %) by different factors on each microbial group (fraction, technical replication and biological replication (Exp.), and the presence of other microbial members).

In order to highlight the strains that significantly change upon co-inoculation with other microbes, microbial relative abundances were subjected to pairwise-comparisons between inoculated conditions using a Generalized Linear Model (p.adj.method=FDR, p-value<0.05) (see **Methods**, **Figure 20A**). Also, conditions where microbial communities and plant growth seemed similar, were compared to a third condition where these changed (for example, BF and BFO *versus* F, **Figure 20B**). Thereby, it was possible to observe that, only one bacterial member changed consistently across treatments (*Phenylobacterium*, Root1277), which was significantly more abundant in B than in any other conditions (**Figure 20A**). In the three-way comparison (B *versus* BF *versus* BFO), the same strain was significantly more abundant in B than in any of the other two conditions, suggesting that this strain is inhibited by the presence of other microbial groups. It is important to note that the high variation observed between the three biological replicates for bacteria likely led to an underestimation of the number of enriched or depleted taxa. Regarding fungal members, 18 strains have significantly different abundances across conditions, in pairwise comparisons. Specifically, the relative abundance of *Fusarium* strains (102, 112, 115, 238) is significantly higher in the presence of the bacterial root microbiota. On the other hand, the relative abundances of *Plectosphaerella cucumerina* (10 and 143), *Ilyonectria* strains (147, 18, 26, 134, 136, 22, 21), *Cylindrocarpon sp.* (241), *Dendryphion nanum*, *Microdochium bolleyi* (230), *Fusarium oxysporum* (214) and *Verticillium dahliae* (3) are significantly depleted in pairwise comparison in the presence of bacteria (**Figure 20A**). In order to highlight the fungal strains that could be correlated to the negative phenotype on plant growth, I used a more stringent test (by comparing F *versus* BF *versus* BFO), which shows that 11 of the previous 17 strains are significantly enriched in fungi-only condition (namely, *Plectosphaerella cucumerina* 10 and 143, *Microdochium bolleyi* 230, *Verticillium dahliae* 3, *Ilyonectria* strains 147, 18, 134, 136, 22 and 21, and *Fusarium oxysporum* 214 (**Figure 20B**). These fungal strains, therefore, could be the potential drivers of plant death in EXP1. Oomycetal strains also display condition-specific enrichments; however, these enrichments are not fully consistent across conditions in the pairwise comparisons and also not consistent with plant phenotype. For example, *Pythium sp*. (4) is enriched in O *versus* BO, but also in BO *versus* FO. In the three-way comparison, four oomycetal strains showed significantly higher relative abundance in O *versus* BO *versus* BFO: *Pythium ultimum* (210 and 7), *Pythium sp* 227 and *Pythium sylvaticum* 132. Therefore, a similar trend was observed for oomycetes and fungi, but the higher variability observed in oomycetal community profiles prevent to draw a general conclusion. Importantly, the effect of bacteria on oomycetal and fungal community can also arise from a decreased fungal and oomycetal load in the matrix, which cannot be quantified by community profiling. This is consistent with alpha-diversity indices (**Supplementary Figure 12**), suggesting that the combined effect of bacteria on both eukaryotic community structure and total eukaryotic biomass is needed for the rescue activity.

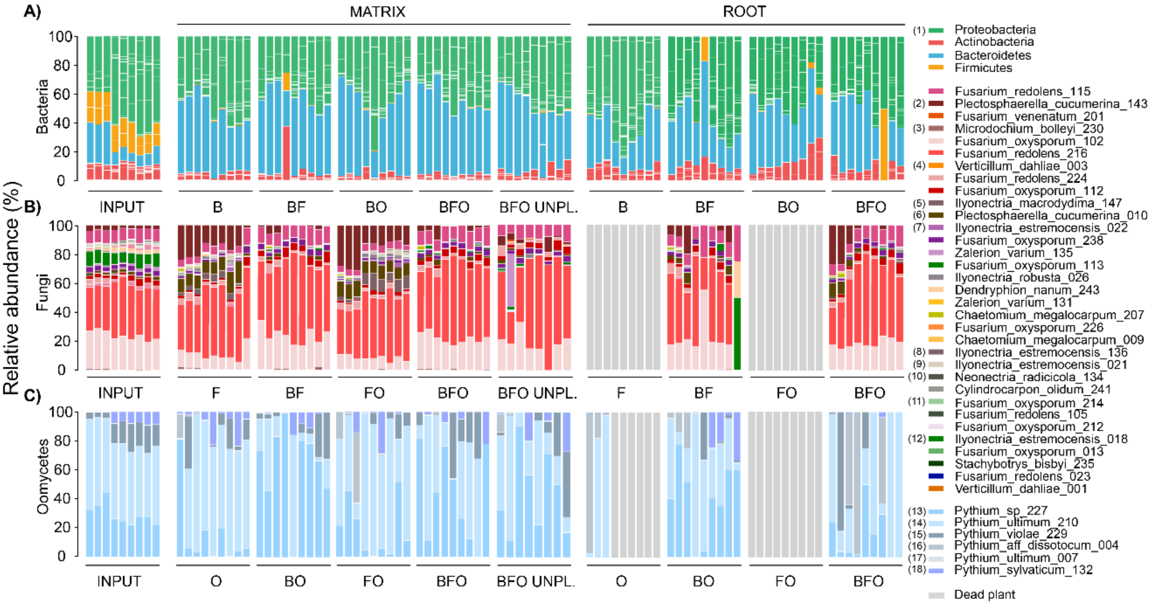

Figure 19: Microbial relative abundances in a reconstitution experiment. Relative abundances of microbial isolates in matrix and root samples after four weeks of incubation with their plant host, alone or in combination with other microbial members. (INPUT: initial microbial inoculum, mixed in a 1:1 volume ratio; B: Bacteria only, F: Fungi only, O: Oomycetes only, BO: Bacteria and oomycetes, BF: Bacteria and fungi, FO: Fungi and oomycetes, BFO: full microbial community; BFO UNPL.: full microbial community without plant), for bacterial (**A**), fungal (**B**) and oomycetal (**C**) communities. Each fungal and oomycetal strain has a different color (legend on the right side), whereas bacterial strains are grouped by the phyla they belong to, for simplicity. The abundance of strains in the legend marked with a number is significantly different between conditions (see **Figure 20**).

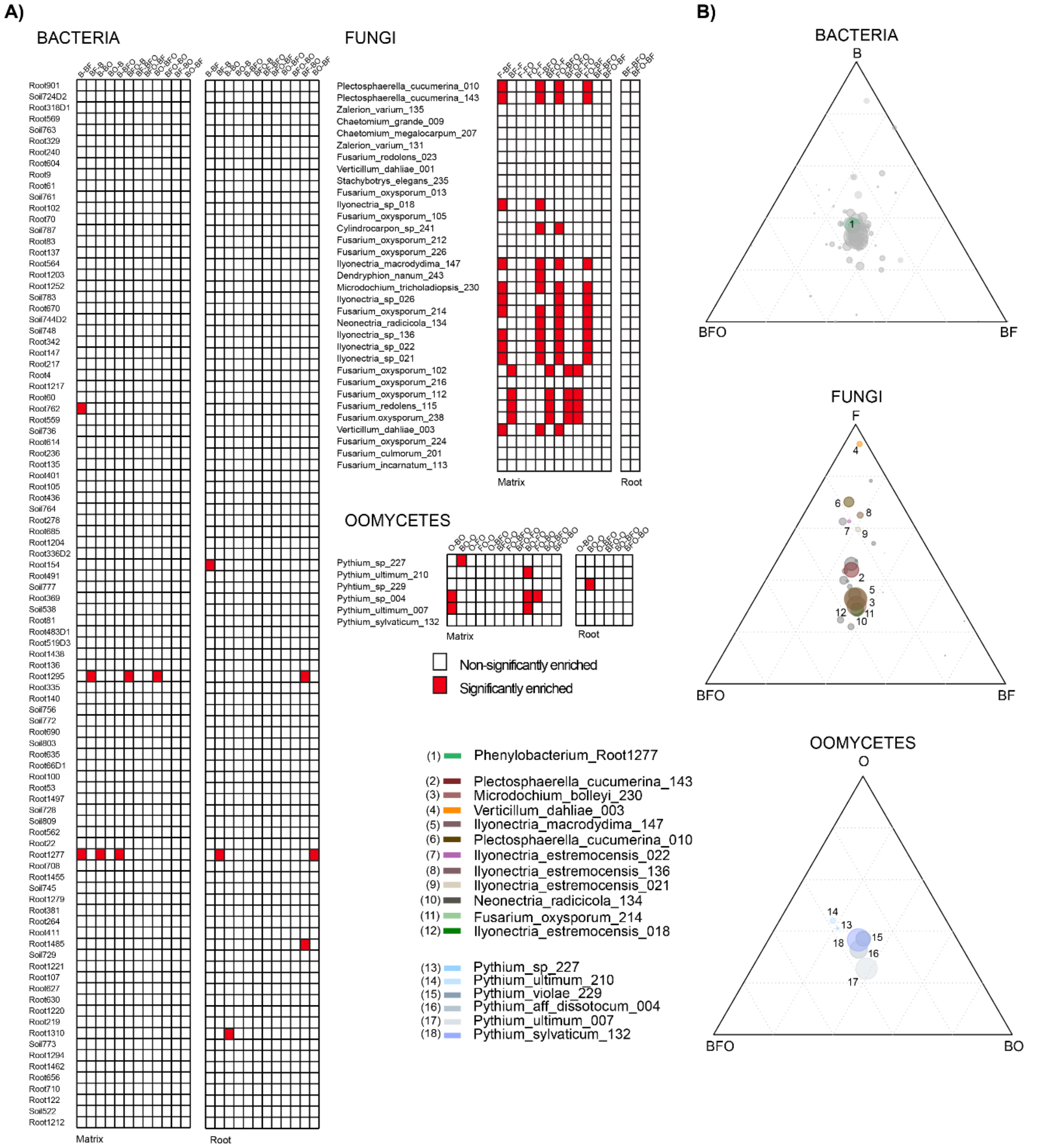

Figure 20: Microbial strains' changes upon co-inoculation with other microbial members. A) Illustration of the results from pairwise-enrichment tests for bacterial, fungal and oomycetal strains in gnotobiotic experiments (Generalized Linear Model, p.adj.method=FDR, p-value<0.05) co-inoculated in different combinations (B: Bacteria only, F: Fungi only, O: Oomycetes only, BO: Bacteria and oomycetes, BF: Bacteria and fungi, FO: Fungi and oomycetes, BFO: full microbial community). Significantly enriched strains in one combination compared to another one are depicted with a red block (e.g.: Root762 is enriched in B compared to BF). **B)** Ternary plots representing the enriched strains (colored circles) (Generalized linear model, p.adj.method=FDR <0.05) in each combination versus the other two combined (see **Annex: Supplementary Table 4**). Size of the circles depicts the relative abundance of each strain and the closeness to each edge represents the higher presence in that given condition.

2.1.3 Microbiota perturbation experiments

In EXP1 analysis it was possible to identify specific fungal strains that could be related to the detrimental effect on plant growth. This result was *per se* remarkable as all fungal strains were isolated from healthy *A. thaliana* plants, suggesting that root colonization by these strains in nature is not sufficient to provoke disease. Therefore, I hypothesized that the strains enriched in F/FO might be highly pathogenic when individually grown with the plant host. Thus, each fungal strain was separately inoculated with sterile *A. thaliana* Col-0 seeds and incubated for three weeks in the FlowPots system. This experiment will be referred as “PERT1” in later sections in this Chapter. Compared to the microbe-free control (MF), fungal strains displayed various effects on plant growth. First, it was remarkable to observe that 18 out of the 34 strains tested lead to a significant decrease on plant growth compared to microbe-free conditions (Kruskal-Wallis, Dunn test *post-hoc*, $p<0.05$, **Figure 21**). Further, these 18 strains included most of the enriched fungi in EXP1 (6 out of 18, conditions F and FO), but also other fungal strains, as *Stachybotrys bisbyi* (235) or *Fusarium redolens* (224) that were not identified as significantly enriched in the absence of the bacterial community. Moreover, some of the isolates identified as pathogenic in EXP1 F/FO, had a neutral impact on plant growth (shoot fresh weight not significantly decreased compared to microbe-free control, Kruskal-Wallis, Dunn test *post-hoc*, **Figure 21**). These observations suggest that results of enrichment tests cannot be linked with fungal pathogenic lifestyle and that bacteria do not specifically affect the growth of pathogenic fungi. Consistent with that, a 23-members fungal community lacking the 11 fungal isolates enriched in the absence of bacteria (see **Figure 20**) remains fully detrimental for plant growth.

From these results, I hypothesized that fungal communities without other microbial groups present in the system increment their biomass, which then impacts plant growth. In order to test this, I selected a subset of the tested fungal strains in PERT1 to correlate their biomass in the matrix with the plant growth phenotype. For this, with the help of Nick Dunken (Bachelor student, University of Cologne), we developed standard curves for this subset of strains, by comparing the DNA extracted from a known amount of mycelium, to the Cq reads using qPCR. In this way, we could estimate the amount of mycelium present in the system, related to the amount of DNA extracted (see **Methods**, **Supplementary Figure 13A**). This follow-up experiment will be referred as “PERT1.2” in later sections in this Chapter. Using the harvested matrix samples from PERT1, we estimated the fungal load in each sample, utilizing the standard curves produced in PERT1.2 (**Supplementary Figure 13A**). Pearson’s correlation test between estimated fungal load and plant shoot fresh weight showed no significant correlation between these two variables, suggesting that mycelial load in the matrix does not predict fungal pathogenicity on *A. thaliana* (Pearson's correlation=0.04, p-value=0.835, **Supplementary Figure 13B**).

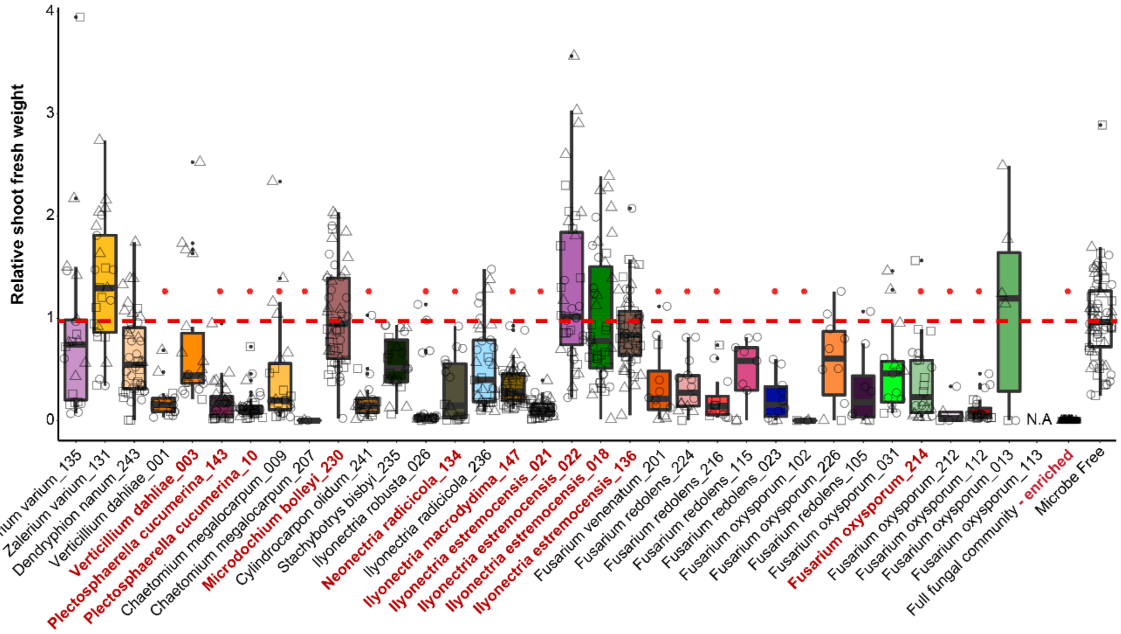

Figure 21: Individual effect of fungal strains on plant growth. Plot depicting shoot fresh weight of *A. thaliana* Col-0 plant shoots, after three weeks of incubation with individual fungal strains (same as in **Figure 18**), of three biological replicates (depicted with different shapes) with at least three technical replicates each, relative to un-inoculated control (microbe-free, MF, red dashed line). Significant differences are indicated with a red asterisk (Kruskal-Wallis, Dunn test *post-hoc*, p-value<0.05). Depletion of enriched fungal strains in **Figure 20** (strains in red) from the full fungal community did not recover plant growth (right side of the plot).

Inoculation of individual fungal isolates suggests that the detrimental activity on plant growth is mediated by multiple strains in the fungal community and that many fungal isolates retrieved from healthy plant cannot be kept at bay by the plant immune system. The next important question was to determine whether the bacterial biocontrol activity is a redundant trait in the community or a specialized mechanism that evolved in very few bacterial community members. I utilized the information from an experiment previously performed by Dr. Stéphane Hacquard (Department of Plant-Microbe interactions, MPIPZ), where the potential antagonistic effect of bacterial members on fungal growth was tested (**Supplementary Figure 14A**). In this experiment, 24 sporulating fungal members were used, including 7 used in EXP1. Thus, fungal spores were distributed in 96-well plates and incubated with or without individual bacteria members for 48 hours. Fungal growth was determined by fluorescence using a chitin binding assay (**Supplementary Figure 14A**). Using this assay, it was possible to establish a gradient of bacterial antagonistic scores (**Supplementary Figure 14B**), from which I subsetted bacterial groups to create distinct synthetic communities (SynComs, SC) that followed an antagonistic gradient (from the most antagonistic members, SC1, to the least antagonistic, SC6,

Supplementary Figure 14B). Since it has been suggested that diversity is important for plant health (Hu *et al.,* 2016), I grouped every two SynComs into a higher diversity groups (SC7, SC8 and SC9, **Supplementary Figure 14B**). Finally, to compare with EXP1, I included a SynCom containing all bacterial members (SC10). Each of these bacterial SynComs was inoculated with sterile *A. thaliana* Col-0 seeds, with or without the 34-members fungal community used in EXP1, and incubated for three weeks. After this period, shoot fresh weight was assessed (**Figure 22**). This experiment will be referred as "PERT2" in later sections of this chapter. Host shoot phenotypic results were calculated as relative plant rescue, where shoot fresh weight values were calculated relative to those of microbe-free control plants (in order to remove as much variation as possible from each biological replicate). Samples inoculated with both bacterial and fungal members were compared to bacteria-only conditions, in order to investigate the capacity of each bacterial SynCom to rescue fungal effect, compared to bacteria-only conditions (**Figure 22A**). Using this method, it was possible to observe that the SynComs SC2, SC4, SC5, SC7, CS8, SC9 and SC10 were able to rescue fungal deleterious effect on plant growth. Interestingly, the bacterial SynCom predicted to have the highest antagonistic effect (SC1, **Supplementary Figure 14**), also has a detrimental effect on plant growth *per se* (data not shown), which could suggest that these bacteria secrete toxic molecules that also affect plant development. Assessment of microbial load in matrix samples of each of the inoculated conditions shows that fungal load is high in fungi-only condition, but drastically drops in the presence of any bacterial SynCom, and especially in the presence of the full bacterial community (SC10, **Figure 22B**). Further, bacterial load is very variable, although it appears to increase together with SynCom diversity (SC7, SC8, SC9 and SC10, **Figure 22B**). Correlation analysis between microbial loads and plant growth shows that fungal load is not significantly correlated to bacterial load (Pearson's correlation, p-value=0.39, **Supplementary Figure 15A**). Also, bacterial and fungal loads independently have no correlation with plant shoot fresh weight (p-value= 0.30 and 0.11, respectively, **Supplementary Figure 15B and C**). Interestingly, fungal/bacterial ratio is correlated with plant shoot fresh weight (Pearson's correlation= - 0.28, p-value=0.04, **Supplementary Figure 15D**), which suggests that low fungal to bacterial ratio is beneficial for plant growth. Overall, bacterial rescue does not obviously correlate with the antagonistic effect observed in the binary assay, but it is notable that highly diverse bacterial consortia tend to have a more stable rescuing effect (SC7, SC8, SC9 and SC10, **Figure 22A**).

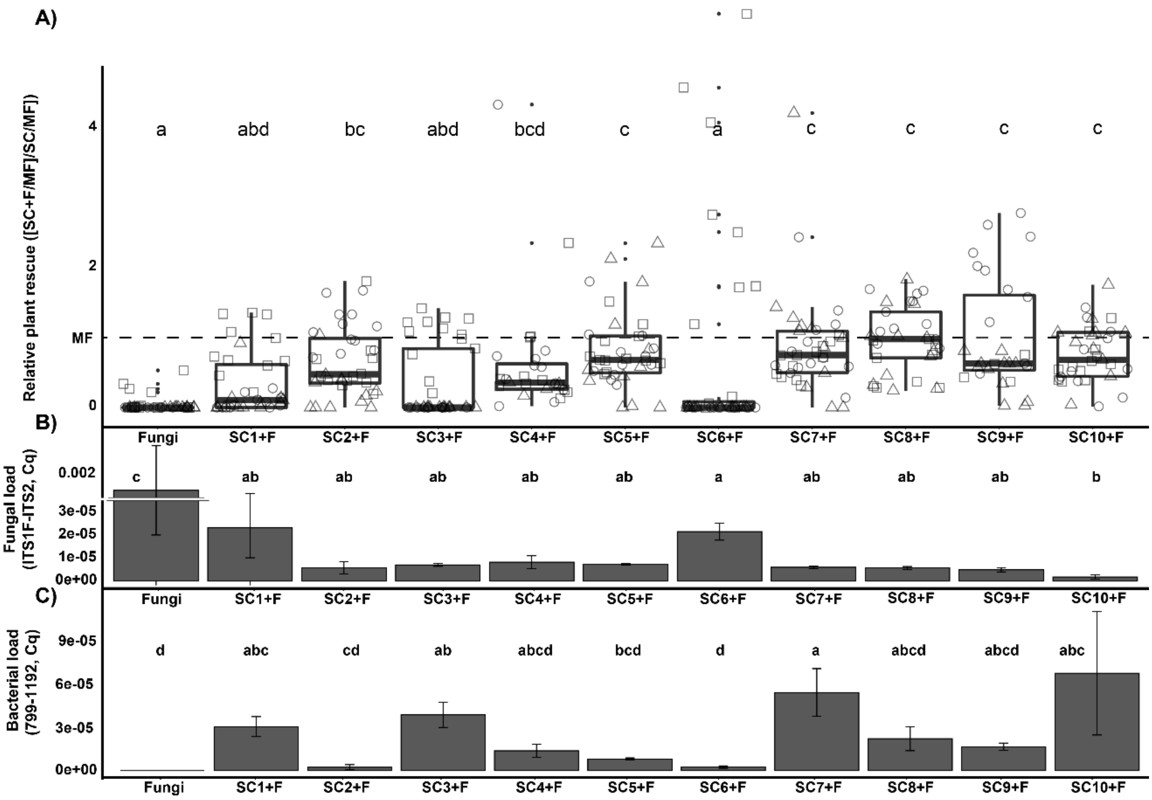

Figure 22: Bacterial antagonistic gradient against fungal overgrowth. A) Shoot fresh weight represented as the relative plant rescue (relative bacteria-only-inoculated shoot fresh weight divided by the relative bacteria-and-fungi-inoculated shoot fresh weight, [(SynCom+F/Microbe-Free)/(Syncom/Microbe-Free)]). Significant differences are depicted with different letters (Kruskal-Wallis, Dunn test *post-hoc*, p<0.05). **B** and **C)** Microbial load was estimated in matrix samples from the bacterial antagonism gradient experiment by amplifying the 16s rRNA V5/V7 and ITS1 for bacterial and fungal communities, respectively. Cq values were then normalized to the microbe-free values (MF=1, dashed line). Significantly different values are depicted with letters (Kruskal-Wallis, Dunn test *post-hoc*, p-value<0.05)

Based on the antagonistic binary assay (**Supplementary Figure 14A**), it is possible to observe that there are certain taxonomic groups with a higher fungal growth inhibition than others, namely the Comamonadaceae and Pseudomonadaceae families. Further, network analysis of culture-independent data from natural sites, highlighted Comamonadaceae as one of the major bacterial groups showing negative correlation with fungal communities (analysis by Dr. Thorsten Thiergart, Duran *et al.,* in preparation). Furthermore, Comamonadaceae family was also highlighted as a major microbial hub in phyllosphere communities of *A. thaliana* (Agler *et al.,* 2016a). Therefore, in the next approach, I hypothesized that removal of either Comamonadaceae or Pseudomonadaceae members, or removal of members from both families, might result in a complete or partial loss of bacteria-mediated plant protective activity against fungi. Therefore, four Syncoms were utilized: full bacterial community as in EXP1 and PERT2

(B), bacterial community lacking Comamonadaceae family members (B-C), bacterial community lacking Pseudomonadaceae family members (B-P), as well as bacterial community lacking members from both families (B-C-P). These Syncoms were inoculated with sterile *A.thaliana* Col-0 seeds, alone or together with the 34-members fungal community used in EXP1 (two biological replicates). After four weeks of incubation, plant shoot fresh weight was measured and root and matrix samples were harvested for bacterial and fungal communities profiling (**Figure 23**). This experiment will be referred as "PERT3" in later sections of this chapter. Remarkably, removal of either Comamonadaceae or Pseudomonadaceae families did not have a significant impact on bacterial rescue capacity against fungal members. On the contrary, removal of both groups significantly decreased plant growth in the presence of the fungal community (Kruskal-Wallis, Dunn test *post-hoc*, p<0.05, **Figure 23A**), indicating that members from these two families at least partly contribute to the plant growth rescue. However, this growth decrease did not translate into a bacterial (**Supplementary Figure 16**) nor fungal community change (PERMANOVA, 12.7% of variance, p-value=0.31, **Figure 23B**). These observations suggest that other members belonging to other families can still confer efficient plant protection against fungi. Thus, I propose that the biocontrol activity is a redundant trait and key function of the bacterial root microbiota for *A. thaliana* survival.

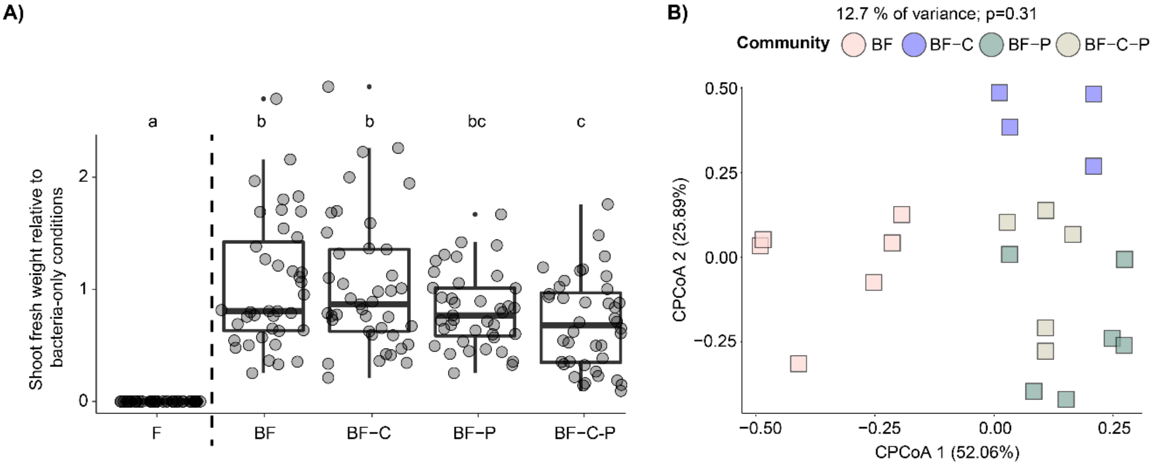

Figure 23: Taxonomy perturbation of bacterial communities. A) Shoot fresh weight of fungi-and-bacteria-inoculated plants relative to the bacteria-only-inoculated plants in depletion experiments (two biological replicates with three technical replicates each), where specific bacterial families (C: Comamonadaceae; P: Pseudomonadaceae) were removed from the full bacterial community (B/SC10) in EXP1/PERT2 to test their fungal control capacity. Shoot fresh weight of fungi-only-inoculated is shown for comparison. Significant differences are depicted with different letters (Kruskal-Wallis, Dunn test *post-hoc*, p<0.05). **B)** Constrained principal components analysis of Bray-Curtis dissimilarities of fungal communities in matrix samples. PERMANOVA analysis shows no significant differences between the distribution of sample clusters (12.7% of variance, p=0.31).

2.1.4 Root microbiota dynamics

Although the experiments described above shed new light about interkingdom microbial interactions and their effect on plant growth, relatively little is known about the dynamics of microbiota establishment in plant roots (Edwards *et al.,* 2015; van der Heijden and Schlaeppi, 2015; Zhang *et al.,* 2018). In order to investigate when microbial communities reach a stable assembly, within individual kingdoms and in the presence of other microbial groups, I performed a time-series experiment. The previously used bacterial, fungal and oomycetal communities were used (B, F, and O), as well as the full community (BFO). Using the Flowpots system, peat matrix was inoculated with each of these microbial communities and incubated for four weeks without plant host. At different time points, matrix samples were harvested in order to visualize how microbial communities change over time (0 hours/Input, 4 hours, 12 hours, 24 hours, 48 hours, 1 week and 4 weeks). This experiment will be referred as "TIME1" in later sections of this chapter. In EXP1, it was observed that unplanted BFO displayed a very similar profile to the planted counterpart (**Figure 18B**). However, it is still unclear what the host plant effect is on microbiota establishment. Thus, after each of the harvesting time points, sterile *A.thaliana* Col-0 seeds were sown and, at the end of the experiment (4 weeks after each seed sowing), shoot fresh weight was measured, and root- and matrix-associated microbial profiles were analyzed (**Figure 24**). Although this experiment is a continuation of TIME1, it will be referred as "TIME2" for clarity in later sections of this chapter. Lastly, I hypothesized that microbial impact on plant performance could also have an impact on its nutritional status. Therefore, harvested four-weeks-old shoots were subjected to ICP-MS analysis (together with Dr. Izabela Fabianska, Bucher Lab, University of Cologne).

2.1.4.1 TIME1

In TIME1, community profiling of matrix samples, harvested at different time points in the absence of the host, showed that matrix-associated microbiota has a very strong time-dependent signature. Thus, microbial communities shifted from their input community and slowly changed over time (**Supplementary Figure 17**). This dynamic assembly pattern is very clear for the bacterial community inoculated alone (B) or together with filamentous eukaryotes (BFO), both showing time-dependent community shifts (63.84% variance due to time, PERMANOVA, p-value<0.001, **Supplementary Table 5A**). Interestingly, these shifts appear to decrease towards later time points (1 week and 4 weeks), where both clusters are closer together compared to any other cluster. This suggests that bacterial community stabilization was occurring towards the end of the experiment (**Supplementary Figure 17A**). Fungal communities also show a

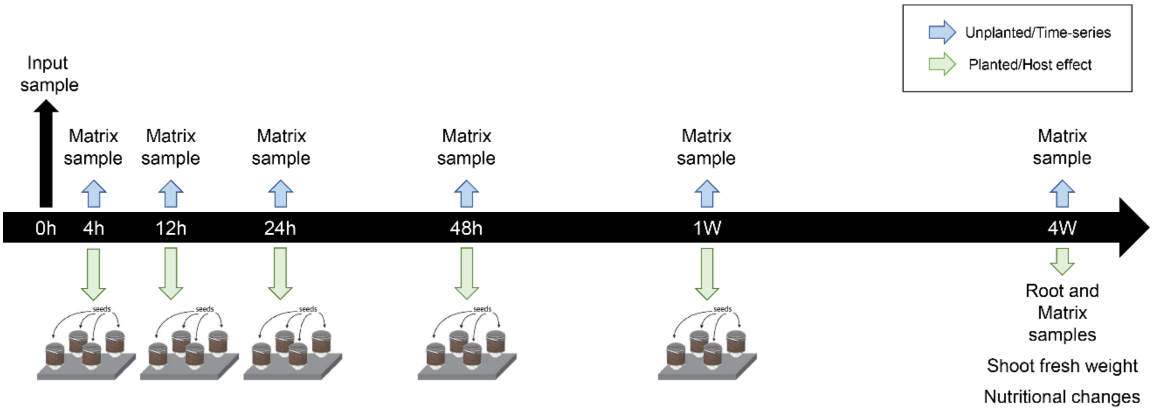

Figure 24: Experimental set-up to study microbiota dynamics. Using the Flowpots system, peat matrix was inoculated with microbial community used in EXP1 (bacteria-only (B), fungal-only (F), oomycetes-only (O) and full community (BFO)) and incubated for four weeks without plant host. At different time points, matrix samples (one technical replicate, from three biological replicates) were harvested in order to visualize how microbial communities change over time (0 hours/Input, 4 hours, 12 hours, 24 hours, 48 hours, 1 week and 4 weeks) (blue arrows). After each of the harvesting time points, sterile *A.thaliana* Col-0 seeds were sown and, at the end of the experiment (4 weeks after each seed sowing), shoot fresh weight was measured, and root- and matrix-associated microbial profiles were analyzed (green arrows) (one technical replicate from three biological replicates). Shoots were also utilized for ICP-MS analysis, to investigate microbial-driven nutritional changes over time.

time-dependent distribution in non-planted matrix samples (31.81%, p-value<0.001, **Supplementary Table 5A**), although variability across samples is higher than for bacterial communities (**Supplementary Figure 17B**). Time-dependent variability is lower for fungal communities than for bacterial communities, probably due to the microbial overlap between time points, suggesting fungal changes are slower than bacterial (Coleman, 1994). Overall, fungal communities are not significantly impacted by the presence of bacterial members in an unplanted system, except after 4 weeks, when *Plectosphaerella cucumerina* strains (143 and 010) are depleted in BFO and *Fusarium culmorum* (201) and *Zalerion varium* (135) are enriched, similarly to EXP1. These results suggest that bacterial-driven fungal community shifts occur between 1 week and 4 weeks of co-incubation. Similarly to fungal communities, oomycetes communities establishment is also time-dependent, but in a lesser manner as for bacterial communities (39.27% time-dependent variance, PERMANOVA, p-value<0.001, **Supplementary Table 5A**). Consistent with EXP1, oomycetal communities are significantly impacted by the presence of other microbial members in the absence of the plant (7.94%, p-value=0.014, **Supplementary Table 5A**).

2.1.4.2 TIME2

In TIME2, matrix samples and roots of four-weeks old plants inoculated directly with the microbiota (0h) or after microbiota establishment in the matrix (4 hours to 1 week) were harvested (**Figure 24**). Shoot fresh weight of these four weeks-old plant was utilized as a proxy of plant health. Thereby, very striking plant growth patterns could be observed depending on whether synthetic microbial communities were co-inoculated with the plant or pre-established before plant sowing. Plant growth was promoted if seeds were sown right after bacterial communities inoculations (0h), whereas sowing seeds on pre-established bacterial consortia (4h-4 weeks) resulted in similar growth patterns as microbe-free control, as observed in EXP1 (Kruskal-Wallis, Dunn test *post-hoc*, p-value<0.05, **Figure 17, Figure 25A**). The same pattern is observed upon seed sowing with fungal communities: plant growth is promoted when seeds were sown directly after fungal community inoculation (0h), but this growth is significantly decreased in plants sown 4 hours after inoculation; furthermore, the 34-member fungal community became detrimental for plant health if the fungal community was pre-established for more than 4 hours in the system (**Figure 17, Figure 25B**). This is an interesting observation, as seed sowing in the EXP1 was done between 4-5 hours after inoculation, suggesting that fungal deleterious activity on plant growth only happens after this period of time. Oomycetal communities, on the other hand, seem to have a negative effect on plant growth regardless the time of seed sowing, but are especially deleterious at 12-hours and 1-week time points (**Figure 25C**). Plants with full microbial communities (BFO) inoculation have a strong growth promotion at 0- and 4-hours time points, as in EXP1, whereas later time points show no differences to microbe-free control. Furthermore, plants sown one week after microbiota self-establishment show a reduced plant growth (**Figure 25D**).

Deeper inspection of microbial communities shows that, whereas unplanted matrices in TIME1 display clear time-dependent bacterial community shifts, the bacterial community established in the roots of the corresponding four weeks old plants is remarkably similar, suggesting a structural convergence of the bacterial root microbiota in plant roots (18.47% variance), despite different start communities in the matrix (63.84% variance) (**Figure 25A,** PERMANOVA, p-value<0.001, **Supplementary Table 5B**). Similarly to EXP1, presence of other microbial members drives a small part of the bacterial communities variance (2.38%, p-value<0.001) and, as shown several times across this thesis and in previous reports, plant compartment is one of the major drivers of bacterial communities composition (16.2%, p-value<0.001). Notably, a different pattern was observed for fungi and oomycetes, where no convergence in plant roots can be observed and communities in roots resemble more the corresponding start community in the matrix. Similarly to

EXP1, fungal communities are significantly impacted by the presence of bacteria and oomycetes (4.17%, p-value=0.006, **Supplementary Table 5B**), as well as oomycetal communities (7.37%, p-value<0.002, **Supplementary Table 5B**).

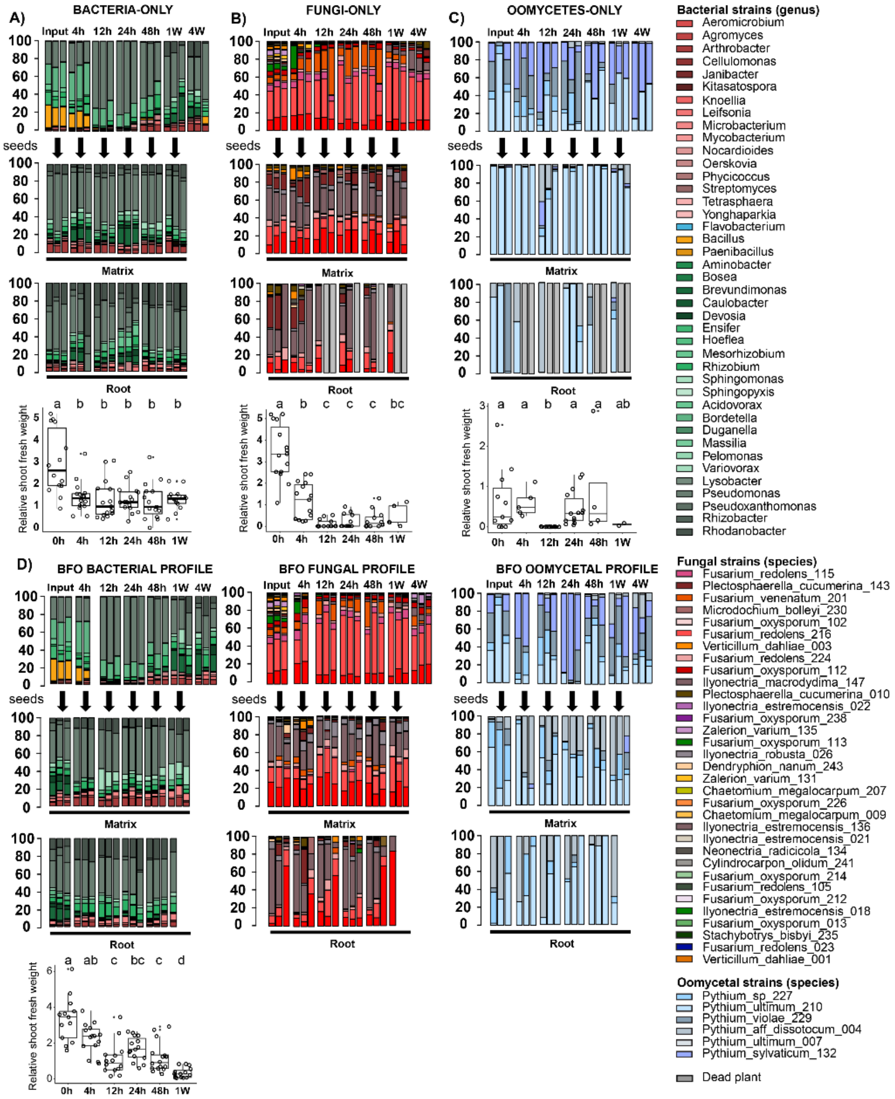

Figure 25: Microbial dynamics over time. In order to study microbial communities dynamics and the impact of a growing plant host on microbiota establishment, microbial communities without a plant host were harvested at several time points after inoculation of bacteria-only (**A**), fungi-only (**B**), oomycetes-only (**C**) and full microbial community (**D**) at 0 hours (Input community), 4 hours, 12 hours, 24 hours, 48 hours, 1 week and 4 weeks. Afterwards, *A.thaliana* Col-0 seeds were sown at the same time points; then matrix and root samples were harvested for community profiling after four weeks of incubation. Plant shoot fresh weight was used as an estimate of plant health. Here, relative strains' abundances are shown, for bacteria, fungal and oomycetal communities, in individual inoculations (**A**, **B** and **C**, respectively) and in full community inoculation. (**D**). Strains relative abundances color code is based on the legend on the right side. Relative shoot fresh weight to microbe-free control (MF=1, not shown in plot) is depicted here as box plots. Significantly different growth patterns are depicted with different letters (Kruskal-Wallis, Dunn test *post-hoc*, p-value<0.05).

2.1.4.3 Ionome analysis

In order to know whether these microbial changes impact plant health by changing their nutritional status, harvested shoots were subjected to ICP-MS analysis. Therefore, all plants shoots harvested from TIME2 were processed and analyzed. Ion concentrations were compared to microbe-free control shoots, in order to know microbiota-specific effect on the host plant ionome. Nutritional profile in bacteria-only and full community (BFO) looks very similar (increase of certain elements, such Molibden, Copper, Cadmium and Calcium in early time points, and decrease of others, such Beryllium in later time points). On the other hand, fungal communities appear to increase certain nutrients in later time points, such Cesium, Chromium, Aluminium, Aspartame or Nickel. On the contrary, oomycetes communities seem to decrease the concentration of shoot nutrients, such Vanadium, Iron, Cobalt, Cadmium and Aluminium (**Figure 26**). However, there does not seem to be a consistent time-dependent pattern of nutritional status overall, but rather a stable composition. This suggests that microbial impact on host plant in this system is through other pathways and not directly through the acquisition of specific ions.

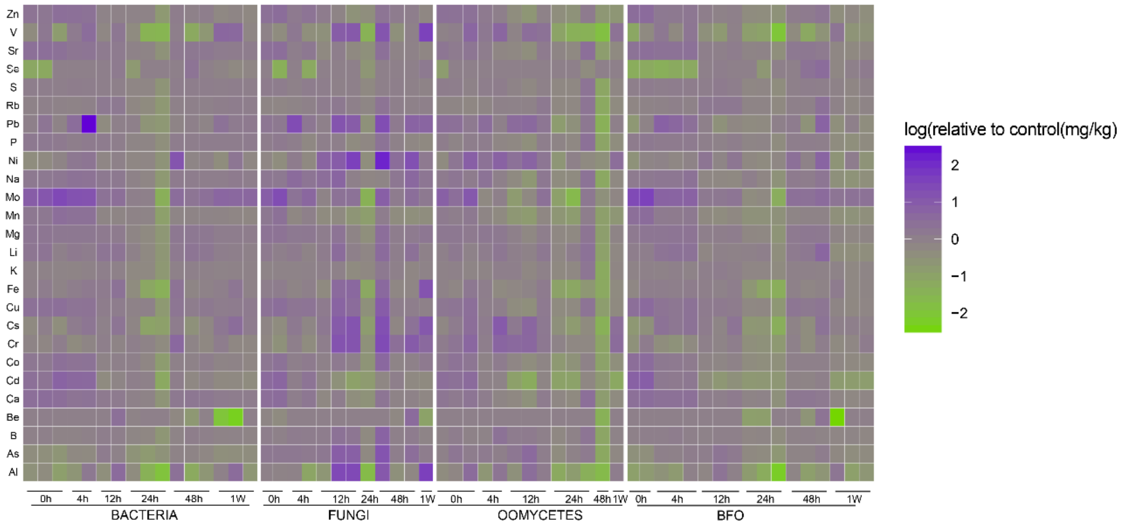

Figure 26: Microbiota and time-dependent host plant ionome. Plant nutrition slightly changes over time and in co-incubation with different microbial communities. Heat map depicting the log transformed nutritional content (mg/kg of dry tissue relative to microbe-free conditions) in shoots of plants grown with either bacteria, fungi, oomycetes or the combination of the three, at different time points, from TIME2.

3. DISCUSSION

3.1 Microbial communities composition correlates with host plant health

As introduced before, reconstitution experiments are key to fully understand how microbial communities establish and how this establishment, in turn, impacts host performance (Vorholt, 2017). Therefore, a gnotobiotic system, the FlowPots system (Kremer *et al.,* 2018), was utilized to re-populate roots of germ-free *A.thaliana* plants with mono and multi-kingdom microbial consortia (EXP1). Using this strategy, it was possible to observe that fungal and oomycetal communities without a bacterial competitors, are detrimental for plant growth (survival rate in F-, O- or FO-inoculated pots was 0 %, 24 % and 0 %, respectively), even considering that all microbes were isolated from healthy *A. thaliana* roots (**Figure 15**, **Figure 17**). Notably, only co-inoculation with bacterial members produced similar plant growth levels to microbe-free plants (**Figure 17**). Inspection of microbial profiles indicated that fungal and oomycetal communities are heavily impacted by bacterial communities (11.6 % and 7.8 %, respectively, PERMANOVA, p-value<0.001, **Table 5, Figure 18, Figure 19**) and that certain fungal and oomycetal strains are significantly more abundant when the plant survival is the lowest (F, O and FO, **Figure 19**, **Figure 20**). Previous reports indicate that the fungal and oomycetal strains identified as significantly enriched in our study in the absence of bacteria in the matrix, have a deleterious effect on diverse plant species. For example, *Plectosphaerella cucumerina* is a destructive necrotrophic fungal pathogen that causes devastating diseases in crops worldwide. This pathogen also colonizes the model plant *A. thaliana* in its natural habitat, therefore establishing the *A. thaliana - Plectosphaerella cucumerina* as a model pathosystem for studying fungal necrotrophic lifestyle and plant disease resistance (Sanchez-Vallet *et al.,* 2010). *Ilyonectria* and *Cylindrocarpon* strains are related to diseases in a wide range of plant species, such as the black foot disease of grapevine (Reis *et al.,* 2016). Also, *Dendryphion nanum* presence has been correlated with rape (*Brassica napus*) root rot (Chinn, 1973), as well as *Microdochium bolleyi* to wheat roots infection (Lascaris and Deacon, 1991), *Fusarium oxysporum* to vascular wilt in tomato (Takken and Rep, 2010), and *Verticillium dahliae* to vascular wilt diseases in a broad range of plant species (Bhat and Subbarao, 1999). Furthermore, many *Pythium* species have been described to provoke disease in many plant species (Kamoun *et al.,* 1999). Therefore, a fundamental physiological function of the bacterial root microbiota is to protect plants from the extensive colonization by root-associated filamentous eukaryotes and to promote interkingdom microbe-microbe balance for plant health. Importantly, this phenomenon is reminiscent of what has been observed for disease suppressive soils (Mendes *et al.,* 2011; Chapelle *et al.,* 2016).

The pronounced impact of root-associated bacteria on fungal and oomycetal community structure in this gnotobiotic plant system (explaining >7 and >10 % of microbial interkingdom variance, respectively) likely recapitulates microbial interactions in the natural environment that are necessary for plant survival. However, the unavailability of comprehensive microbial culture collections from unplanted CAS soil did not allow us to directly test whether the bacterial root microbiota, which is horizontally acquired from a small fraction of the bacterial soil biome (Lundberg *et al.,* 2012; Edwards *et al.,* 2015), is enriched for members that restrict root colonization by filamentous eukaryotes. I conclude that the detected microbial interkingdom interactions take place at the soil-root interface during microbiota establishment and are maintained inside plant roots. Re-colonization of *A. thaliana* with the most complex multi-kingdom microbial consortium (BFO) resulted in maximal plant growth and survival in this gnotobiotic plant system. Thus, I propose that mutual selective pressures, acting on the plant host and its associated microbial assemblage, have favored over evolutionary time scales interkingdom microbe-microbe interactions rather than associations with a single microbial class.

3.2 Most root-associated fungi isolated from healthy plants are pathogenic

Given that all bacterial, fungal, and oomycetal strains used in our study were isolated from roots of healthy *A. thaliana* plants, the contrasting effects of synthetic communities representing individual microbial kingdoms on plant health were unexpected. Loss of mycorrhiza symbiosis in *A. thaliana* or relatives appears to have been partly compensated by associations with other beneficial fungal root endophytes (Hiruma *et al.,* 2016; Hacquard *et al.,* 2016; Almario *et al.,* 2017). However, these results also show that in the absence of bacterial competitors, consortia of filamentous root-derived eukaryotes (F, O, FO) have overall detrimental activities on plant health and survival, and that >50% of the isolates restrict plant growth in mono-associations with the plant host (**Figure 21**). Similar observations were made by Kia *et al.,* (2017a), by isolating and re-inoculating root endophytic fungal strains from three different plant species (*A. thaliana*, *Microthlaspi erraticum* and *Hordeum vulgare*), where the net effect of fungal isolates was negative for plant performance. Further, they could pinpoint certain physiological fungal properties to be responsible for this effect, such hyphal growth, laccase and pectinase activities and formation of conidia (Kia *et al.,* 2017). These results suggest that the host immune system is not sufficient to control the growth of most root-associated fungi. In addition, removal of all detrimental fungi from the full fungal community, does not recover plant health (“Full fungal community-enriched”, **Figure 21**). It is possible that certain fungal members promote the negative impact of other fungal partners only in the community context, as observed by Busby *et al.,* 2016, whereas in the absence of these promoters, fungal partners might not be detrimental (as it is the case for *Ilyonectria estremocensis* strains 22, 18 and 136, or *Microdochium bolleyi* 230 in single inoculations, **Figure 21**).

3.3 Microbial load is partially responsible for plant health

Although many other competitive mechanisms have been introduced in this chapter (resource competition, nutrient sequestration, secretion of antimicrobials, among others), the complexity of the system, including a soil matrix and many microbial strains, made it difficult to assess bacterial metabolic signatures driving fungal control. Nevertheless, it is possible that bacterial control over fungal communities is due to niche competition and/or secretion of antimicrobials, thereby constraining fungal growth (Coleman, 1994). Microbial load was assessed in a subset of samples of PERT1, where fungal strains were inoculated individually, and in matrix samples of PERT2, where fungal strains were co-inoculated with bacterial SynComs with and antagonistic activity gradient. In PERT1, fungal load in matrix samples did not correlate with plant health, suggesting that fungal negative effect when inoculated individually is not dependent on the total fungal biomass in the FlowPot system, but rather on the fungal metabolic processes and virulence arsenals, as also suggested by Kia *et al.,* (2017) (**Supplementary Figure 13**). Furthermore, fungal load nor bacterial load was directly correlated with plant growth in PERT2. Remarkably, fungal/bacterial ratio was significantly correlated with plant growth (**Supplementary Figure 17**), suggesting that upon certain fungal load, bacterial communities can no longer rescue plant growth. On the other hand, fungal and bacterial loads were not correlated to each other in PERT2 (**Supplementary Figure 15A**). Irrespective of that, fungal load dramatically decreases in the presence of any bacterial SynCom (**Figure 22B**). Altogether, it is possible to conclude that the detrimental effect of fungi in this gnotobiotic plant system is likely controlled by bacteria-mediated mycelium load decrease. Whether host plant interplay with specific bacterial members is important for the final health output, as indicated in Jurkevitch *et al.,* 2000 or Chapelle *et al.,* 2015, was not assessed in this experiments and could give another layer of complexity explaining microbiota interactions and their effect on plant performance.

3.4 Bacterial-driven disease suppression is a redundant trait within bacterial communities

Bacterial community members have been recognized as drivers of plant health in a community context, by promoting mycorrhizal development (Frey-Klett *et al.,* 2007), by complementing with their fungal partners (van der Heijden *et al.,* 2016), but also by preventing microbial pathogens to affect host plant health (Chapelle *et al.,* 2016; Cha *et al.,* 2016; Santhanam *et al.,* 2015). In EXP1, it was not possible to find a group of bacteria that significantly changed their abundance in the presence of fungal or oomycetal communities (**Figure 19**, **Figure 20**) suggesting a stable bacterial community assemblage. Due to the high complexity of the microbial communities in this system and the lack of molecular tools, direct functional characterization was beyond the scope of the thesis. However, genome-resolved metatranscriptomic profiling of synthetic microbial communities are currently developed in our laboratory and will represent in the near future an important tool to dissect transcriptional reprogramming of multi-kingdom microbial consortia during colonization of plant tissues (Nobori *et al.,* 2018). To identify bacteria with high biocontrol potential, I took advantage of a previous experiment realized by Dr. Stéphane Hacquard, where bacterial antagonism (i.e. fungal growth inhibition capacity) was tested against a subset of fungal strains used in EXP1 and PERT1, from which a bacterial antagonism gradient was obtained (**Supplementary Figure 14**). Subsets of bacterial SynComs following this high-to-low antagonism gradient co-inoculated with fungal community (PERT2) did not follow the expected high-to-low plant growth rescue effect (**Figure 22A**). Instead, only certain bacterial combinations rescued fungal effect on plant growth (namely SC2, SC4 and SC5), suggesting that not only individual bacterial activity is needed to control fungal detrimental effect, but also certain bacterial community diversity. In fact, higher-diversity bacterial SynComs (SC7, SC8, SC9 and SC10), displayed higher stability at plant growth rescue, although rescue was not significantly higher compared to other bacterial combinations (**Figure 22A**). Interestingly, bacterial SynCom SC1 (predicted to have the highest fungal antagonism) also had a negative impact on plant growth when inoculated without the fungal community (data not shown). This SynCom is mostly composed by *Pseudomonas* and *Acidovorax* strains, which have been previously described as possible pathogens of plants (Xin and He. 2013; Schaad *et al.,* 2003, respectively). Although SC1 also includes few other bacterial members, it is possible that the negative impact of *Pseudomonas* and *Acidovorax* strains could not be controlled with such a low-diversity community (Hu *et al.,* 2016; Maida *et al.,* 2016). Furthermore, it is also possible that certain bacterial responses are silent in binary interaction, but are activated upon co-inoculation in a community context (Schroeckh *et al.,* 2009; Nutzmann *et al.,* 2011; Netzker *et al.,* 2015). Nonetheless, the data indicates that three out of six low diversity SynComs (< 15 members each) can rescue plant growth to control levels in the presence of the fungal community (**Figure 22A**). It remains unclear whether the observed growth rescue is mediated by one single strain or multiple strains. However, these results suggest that the observed activity is mediated by bacteria from distinct taxonomic lineages.

To test whether the presence of the most competitive bacteria belonging to the families Comamonadaceae and Pseudomonadaceae are at least partly responsible for the rescue activity, I performed depletion experiments (PERT3) in which I removed from the system all members belonging to these two families (accounting for 34% of the total relative abundance in *A. thaliana* roots, data not shown). Removal of members of both Comamonadaceae and Pseudomonadaceae families from the full bacteria consortium was sufficient to partially alter bacteria-mediated plant growth rescue in the presence of the fungal community (**Figure 23A**). However, either depletion alone (Comamonadaceae or Pseudomonadaceae) did not affect plant health nor fungal community profile, although depletion of both did lead to a decrease of plant growth. This suggests that members of the Comamonadaceae and Pseudomonadaceae families are at least partly responsible for plant health, along with other microbiota members, **Figure 23**). A final experimental approach to investigate this hypothesis will be to test whether individual strains belonging to taxonomically diverse bacterial families can provide efficient protective activity. Based on these results, it is likely that the protective activity is a redundant trait that evolved independently in distinct taxonomic lineages of the bacterial root microbiota. Consistent with that, functional and metabolic redundancy has been previously predicted (Zelezniak *et al.,* 2015) and reported for different microbial processes, such organic matter decomposition (Banerjee *et al.,* 2016) or resource utilization (Zhang *et al.,* 2016). This high redundancy in microbiota function is likely essential to provide robust host protection and to maintain host-microbiota balance in plant roots.

3.5 Microbial communities are established over time and host plant health is impacted by different microbiota age

In order to understand how microbiota interactions are shaped over time and whether they reach a stable assemblage, TIME1 experiment was performed, where different microbial groups were inoculated individually or in combination with other microbial members, in the absence of a plant host, and samples were harvested at different time points. Additionally, to understand the role of host plant in community assemblage, TIME2 experiment was used (**Figure 24**). Although the dynamics of microbial communities during plant colonization has been reported in soils under greenhouse or natural environment (Edwards *et al.,* 2015; van der Heijden and Schlaeppi, 2015; Zhang *et al.,* 2018; Edwards *et al.,* 2018), little is known regarding the assembly rules of synthetic microbial consortia in the presence and absence of a host. Previous studies have also investigated microbiota establishment after permafrost (Mackelprang *et al.,* 2011) and after perturbation with different pollutants (Kato *et al.,* 2015), which could be both considered as a resetting of the microbiota. In TIME1, bacterial, fungal and oomycetal communities drastically change from input communities in early time points (**Figure 25**). These changes are less dramatic over later time points (1 and 4 weeks), where they appear to stabilize (time-dependent variation is 63.84% for bacteria, 31.81% for fungi and 39.27% for oomycetal communities, **Supplementary Table 5A**). Interestingly, more subtle effects were observed in microbial communities due to the presence of other microbial members in the system, as observed in EXP1 (**Table 5, Figure 18B**), suggesting that 1) interkingdom microbial interactions might impact each other at later time points (4 weeks), and 2) a plant host could be important for the final microbial output by, for example, recruiting specific microbial members during seed germination (2-3 days after seed sowing) or later in the developmental process (Links *et al.,* 2014; Barrett *et al.,* 2016), that will then impact microbe-microbe interactions. Similarly, soil communities in untreated soils quickly shift in early time points but stabilizes after 3-6 weeks (Kato *et al.,* 2015), suggesting that soil microbiota interactions could reach stability after this period in different systems. Furthermore, it has been shown that certain bacterial members are mostly responsible for microbial shifts over time, including Actinobacteria and Proteobacteria, as also observed in the current dataset (Mackelprang *et al.,* 2011; Zhang *et al.,* 2018). Interestingly, these changes are even more notable in TIME1 compared to other studies, probably due to the fact that they are colonizing a sterile matrix and dynamics might be much higher.

As explained in **Figure 24**, after each matrix sample harvest in TIME1, sterile *A.thaliana* seeds were sown on the pot surface, for community profiling assessment in matrix and root samples after 4 weeks of co-incubation. Interestingly, plant growth depended on the time of seed sowing, with a significant plant growth promotion in early time points relative to bacteria- and fungi-inoculated communities, and a non-significant effect in later time points with bacterial communities. Further, either a non-significant or even a significant decrease of plant growth upon fungal, oomycetal and full microbial communities (BFO) co-incubation could be observed (**Figure 25**). Interestingly, plant phenotype in EXP1 matches 4- and 12-hour time points phenotypes in TIME2, coinciding with the time when seeds were actually sown in previous experiments, suggesting that unestablished matrix microbial communities can have very variable effect on plant growth depending on their stability stage. Such time-dependent health phenotype could be correlated to the host capacity to respond to commensal microbes at different stages of its development, as already demonstrated for *A.thaliana* interaction with *Pseudomonas simiae* WCS417 (Stringlis *et al.,* 2017). In addition, this phenotype could also be due to a time-dependent susceptibility of the host towards certain microbes (Ingle *et al.,* 2015). It is difficult, however, to directly assess such susceptibility as seeds were used in this experimental set-up instead of grown leaves or seedlings, and germination time might be slightly different from one individual plant to another. Independently of microbiota age in the matrix, microbial communities appear to converge in the presence of a plant host (**Figure 25**). This is comparable to time-dependent rice-associated microbes in vegetative state, where bacterial communities also stabilize at relatively early time-points in root compartments (Edwards *et al.,* 2018; Zhang *et al.,* 2018). Interestingly, previously identified potentially detrimental fungal members for plant growth (in EXP1, *Ilyonectria* and *Plectosphaerella* fungal strains), appear to only bloom upon plant presence, suggesting a plant-driven cue for certain microbes to thrive, which are not necessarily beneficial for plant growth (Links *et al.,* 2014; Barrett *et al.,* 2016; Zhalnina *et al.,* 2018). It is however surprising that the increase of these strains is also present in samples with healthy plants, which was not the case in EXP1 (**Figure 25, Figure 18B**). There are several explanations for this issue: 1) as mentioned in the **Methods**, certain bacterial members could not be inoculated in this experiment, which could be members responsible to keep these fungi’s relative abundances low; still, the bacterial community in TIME2 is capable of controlling fungal detrimental effect (functional redundancy observed in PERT3); 2) in PERT1, it was possible to observe that fungal strains predicted to have a negative effect on plant growth in a community context, do not show the same effect in a binary assay, which could also indicate that, at different time points, these microbes also display differential effect on plant growth; 3) in the same way that fungal communities are strongly impacted by plant presence, bacterial communities could also perceive plant cues to differentially control fungal communities (4.17% of fungal community variance explained by the presence of other microbial members in the system, upon plant presence, p-value=0.006, **Supplementary Table 5B**). Oomycetal members, unlike bacterial or fungal members, display a more stochastic effect on plant growth, suggesting that these microbial members randomly colonize the plant host and, in turn, affect its growth one way or another (**Figure 25C,** Kemen, 2014). TIME2 dataset illustrates microbiota profiles after 4 weeks post seed sowing. It would be however interesting to investigate the microbiota dynamics at different time points after seed inoculation, to further learn which microbes rapidly respond to host presence.

3.6 Concluding remarks and future perspectives

Plants live in intimate association with complex and diverse microbial communities. Although, next-generation sequencing has already enabled us to explore the composition and distribution of different microbial groups, a more holistic approach is still needed to better understand the intermicrobial interactions within the microbiota of plants and to better define the functional relevance of the microbial networks for holobiont fitness. Prokaryotic and eukaryotic microbes have evolved a myriad of cooperative and competitive interaction mechanisms that shape and likely stabilize microbial assemblages on plant tissues. However, most of the data are derived from one-to-one interaction studies, and only few incorporate complex microbial communities in controlled laboratory conditions to reconstitute the plant microbiota and to understand the role of intermicrobial interactions. Thus, the second aim of my thesis was to reconstitute plant-associated microbial communities isolated from roots of healthy *A. thaliana* plants growing in the same soil, including several microbial kingdoms and under controlled laboratory conditions.

Re-inoculation of representative root-associated bacteria, fungi and oomycetal strains allowed me to reveal that microbe-microbe interactions are crucial for microbiota assembly. Specifically, bacterial communities drive fungal and oomycetal communities' shifts that correlate with plant health and survival. Reduction of specific fungal and oomycetal strains' relative abundances in the presence of bacterial communities indicates a bacterial-driven control of host detrimental microbes. Individually inoculated fungal strains with *A. thaliana* suggested that bacterial communities might not only target potentially pathogenic fungal strains in a community context, but it is rather an overall community control. Here, I showed that *A.thaliana* immune system might not be fully capable of controlling detrimental microbiota members and that fungal/bacterial load ratio surrounding host roots could be an important driver of plant health. Further, I showed that bacterial antagonism against fungal members depends on multiple taxonomically diverse bacteria, rather than a subset of highly antagonistic members. Nevertheless, members of the Comamonadaceae or Pseudomonadaceae families were revealed as important bacterial members for plant health. In addition, I showed that soil microbiota age is an important trait for plant performance and that inter-kingdom microbe-microbe interactions effects are only visible on communities' profiles after several weeks of co-incubation.

Several questions remain open which would deepen our understanding of microbe-microbe interactions and their impact on plant health. First, bacterial-driven fungal control is a conserved trait across bacterial members, although members of the families Comamonadaceae or Pseudomonadaceae appear to have a crucial role in controlling fungal communities. Individual inoculation of each strain of these two families will shed light onto whether this feature is conserved across all members of these two families. Secondly, it remains unclear what the role of the host plant is in the control of detrimental microbiota and when this host plant is capable of restraining pathogenic members. Thus, and interesting experiment would consist of re-inoculation of microbiota members together with sterile *A.thaliana* members and study microbial community shifts after different time points. Also, utilization of immunocompromised *A.thaliana* mutants would be very useful at learning which molecular pathways are important for microbiota early establishment. Finally, it is largely unknown how these microbial members actually interact with each other in a community context. Therefore, development of genome-resolved meta-transcriptomic profiling of synthetic microbial communities will represent an important tool to dissect transcriptional reprogramming of multi-kingdom microbial consortia upon microbiota establishment and colonization of plant tissues (**Figure 27**)

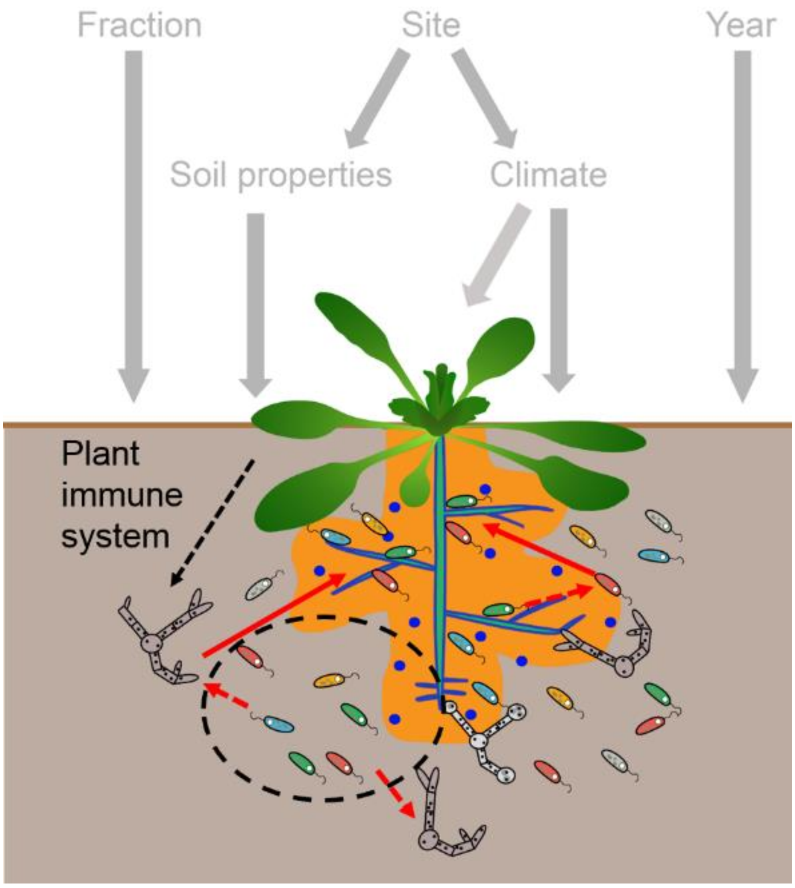

Figure 27: Scheme of microbe-microbe interactions driving plant health. Environmental factors that drive microbial communities' composition in nature (grey arrows and labels), investigated in **Chapter 1**, can be removed by utilizing gnotobiotic plant systems. Thereby, microbe-microbe interactions and their impact on plant health can be studied in depth. Throughout this chapter I could show that certain fungal members of the plant root-associated microbiota can have detrimental effects on plant growth (red arrows), which can be counteracted by bacterial communities as a whole (bacterial members surrounded with a black dashed circle), which might include all or a subset of Comamonadaceae or Pseudomonadaceae families members. These bacterial communities driving biocontrol, might also target other non-pathogenic fungi, by still unknown processes (red dashed arrows). Furthermore, bacterial members of the microbiota can also impact negatively plant growth, which might also be controlled by other bacterial members. Finally, the plant immune system might play an important role at controlling pathogenic microbiota, but it is not sufficient to control pathogenic fungi in the absence of bacterial members (black dashed line).

4. MATERIALS AND METHODS

4.1 Materials

4.1.1 Microbial culture collections

Microbial strains utilized in this chapter are listed in **Annex: Supplementary Table 3**. 148 bacterial strains were selected from the bacterial culture collection of Bai *et al.,* 2015. All these 148 strains were isolated from healthy *A. thaliana* roots growing in the Cologne Agricultural Soil (CAS) and selected depending on their full 16s rRNA gene sequence similarity. The aim was to, after sequencing, be able to separate each strain as one OTU. Similarly, 34 fungal and 8 oomycetal strains were selected from the fungal and oomycetal culture collections of Duran *et al.,* in preparation. These fungi and oomycetes were isolated from *A. thaliana*, *Cardamine hirsuta* and *Arabis alpina* roots also growing in CAS soil, and also selected based on their full ITS sequence similarity.

4.1.2 Plant material

A. thaliana plants (ecotype Columbia, Col-0) were used for this study. Seed material was provided by Dr. Stéphane Hacquard, Department of Plant-Microbe Interactions, Max Planck Institute for Plant Breeding Research.

4.1.3 Oligonucleotides

Oligonucleotides used for PCR amplification are listed in **Annex: Table 2** and were purchased from Metabion (Steinkirchen, Germany) or Sigma-Aldrich (Hamburg, Germany).

4.1.4. Enzymes

DNA-free DFS Taq polymerase was purchased from Bioron (Ludwigshafen, Germany). Antarctic phosphatase and Exonuclease I were acquired from New England Biolabs (Frankfurt, Germany).

4.1.5. Chemicals and antibiotics

Laboratory grade chemicals and reagents are described within each method. Antibiotics were purchased either from Sigma-Aldrich (Hamburg, Germany), Carl Roth (Karlsruhe, Germany) or Duchefa (Haarlem, Netherlands).

4.1.6. Buffers and solutions

Buffers and solutions used in this study are described within each method. If not stated otherwise, buffers were prepared in deionized H_2O and aqueous solutions were sterilized by autoclaving at 121 °C for 20 min.

4.2 Methods

Brands and manufacturer's information of each material will be indicated only the first time they are mentioned.

4.2.1 Microbial strains storage

Bacterial strains were stored in a glycerol stock at -80 ºC. In order to prepare this stock, under a sterile hood, one colony of each separate strain previously grown on a TSB 50% plate (Tryptic Soy Broth, Sigma-Aldrich, USA) containing 10 % agar (Difco Agar, Granulated, VWR, USA), was transferred to a well of a 96-deep-well plate (Eppendorf, Hamburg, Germany), each well containing 400 µL of TSB 50 %. This step was done in duplicate to obtain two replicates per bacterial strain. Then, each 96-deep-well plate was covered with a PCR film (Bio-Budget Technologies GmbH, Krefeld, Germany) and an sterile lid (CS/80, Eppendorf, Hamburg, Germany), and incubated for 6 days at 22 ºC, shaking at 180 rpm. After the incubation time, each 96-deep-well plate was centrifuged for 10 min at 4000 xg (5810R, Eppendorf, Hamburg, Germany). 300 µL of the supernatant were removed and the 100 µL left were utilized to resuspend the bacterial pellet. Bacterial pellets from the duplicates were mixed together. Then, 200 µL of sterile 50 % glycerol (Glycerin, 98 %, Carl Roth, Karlsruhe, Germany) were added to each bacterial pool. 100 µL of the bacterial/glycerol mixture were transferred to a new 96-well plate (96 Microwell Plates, Thermo Scientific Nunc, USA) (three replicates in three separate plates), which was covered with aluminum film (Platesealer, SilverSeal, Aluminium, 80x140mm, Greiner Bio-One, Kremsmünster, Austria) and a sterile lid and stored at -80 ºC.

Fungal strains were also stored in a glycerol stock at -80 ºC. Fungal mycelium growing on PGA plates (Potato Glucose Agar, Sigma-Aldrich, USA) was cut using sterile pipet tips into plugs of approximately 3x3 mm, and introduced in a 2 mL screw-lid tube with 1 mL 30 % glycerol. Each tube contained between 6-7 mycelium plugs, and each of these plugs was attached to the corresponding agar plug, for an easier recovery. These tubes were snap-frozen in liquid nitrogen and stored at -80 ºC.

Oomycetal strains were stored in PGA plates at 4 ºC and transferred to a new plate after 1-2 months, by cutting a 7x7 mm mycelium plug and placing it upside down (mycelia side facing the medium) in a new PGA plate.

4.2.3 Gnotobiotic experiments

4.2.3.1 FlowPots system

This system was adapted for the current project from Kremer *et al.,* 2018. Briefly, each FlowPot is prepared by adding glass beads (2.85-3.45 mm, Carl Roth, Karlsruhe, Germany) to the Luer end of a truncated syringe (Omnifix, 50 mL, Braun, USA), followed by the addition of twice-autoclaved peat (Einheits Erde Special, Sinntal-Altengronau, Germany) and vermiculite (Agra-vermiculite M3, RHP, Netherlands) mixture (2:1) (121 °C for 20 min), covered with a mesh retainer (Mesh fiberglass “Phiferglass”, 18 X 14 standard charcoal mesh, Phifer Incorporated, USA) and then secured with a cable tie. Assembled FlowPots are then autoclaved a third time (121 °C for 45 min), aseptically irrigated with sterile water, and inoculated with nutrients and any desired input microbiota by attaching a female luer adapter (Tubing silicone rubber lab tubing, T2289-25FT, Sigma, USA) and injecting the water/nutrients/microbiota with a syringe (Omnifix, 50 mL, Braun, USA). Decontaminated *A. thaliana* Col-0 seeds, stratified and imbibed with water, are sown onto each FlowPot. FlowPots are then placed into a Microbox (model TP1600+TPD1600 or OV80+OVD80, with L filter, Combiness, Nevele, Belgium) on stands. The Microboxes containing FlowPots are placed in a growth chamber or greenhouse with desired lighting and temperature conditions for plant growth (**Figure 17**).

4.2.3.2 Bacterial strains growth and inoculation

Bacterial glycerol stocks were taken from -80 ºC and placed in a polystyrene box with dry ice, to maintain the temperature of the glycerol stock. With a 96-well stamper (EnzyScreen Bv, Leiden, Netherlands), each bacterial strain was transferred simultaneously to a previously prepared 96-deep-well plate containing 400 µL of TSB 50 % in each well, by placing the stamper on each glycerol stock well and, then, stir it in the liquid media. The stamper utilized was previously sterilized by placing it in a 96-deep-well plate with 1 mL of 100 % ethanol (Ethanol absolute, VWR Chemicals, USA) and flaming it twice. Prior to storage, the stamper was sterilized twice again and flushed with bacillol (Bacillol® AF, Hartmann, Heidenheim an der Brenz, Germany). Each 96-deep-well containing bacterial strains was incubated for 6 days in a shaker, at 25 ºC.

On the inoculation day, 200 µL of each bacterial strain were pooled together in a 50-mL falcon (Corning, USA). This bacterial mixture was centrifuged for 10 min at 4000 xg and supernatant was discarded. Bacterial pellet was resuspended in 10 mM $MgCl_2$ buffer (Magnesium Chloride Hexahydrate, Merck, Darmstadt, Germany), using a final volume equal to the initial one (200 µL x number of strains pooled). A 1:4 dilution of the washed bacterial pool was used to assess bacterial OD (absorbance at 600nm, BioPhotometer Plus, Eppendorf, Hamburg, Germany) and to calculate the final dilution in order to have a 10^7 cells/mL final stock (considering that OD=1 contains $5x10^8$ bacterial cells). 1 mL of this final stock was pipetted into 50 mL of sterile ½ MS medium (Murashige and Skoog medium including vitamins, Duchefa Biochemie, Haarlem, Netherlands) + MES (MES anhydrous, BioChemica, UK) and injected as described above in one FlowPot.

Before bacterial pooling, a sterile stamper was utilized to plate bacterial strains on a plate with TSA 50%, which was then incubated for a week at 25 ºC to control for bacterial survival. By using this method, it was possible to observe that in EXP1, TIME1 and TIME2 most bacterial strains inoculated were recovered on the TSA 50% plate. However, in PERT2 and PERT3, only 89 bacterial strains out of the initial 148 were alive in the glycerol stock and therefore inoculated, which possibly impacted part of the results in these experiments.

4.2.3.3 Fungal and oomycetal strains growth and inoculation

Fungal strains were grown by taking a mycelium plug from the glycerol stock and placing it upside down on a PGA plate containing antibiotics ($Strep^{100}Kn^{50}Amp^{50}Tc^{20}Rimf^{100}$), and incubating them for 1 week at 25 ºC. Then, a piece of mycelium cut with a sterile pipet tip, was transferred to a new PGA plate and incubated for two weeks at 25 ºC. Similarly, oomycetal strains were grown by transferring a mycelium plug from the 4 ºC-stored plate to a new PGA plate, and incubated also at 25 ºC for 2 weeks.

On the inoculation day, fungal and oomycetal mycelium was harvested by utilizing a sterile pipet tip. 50 mg of mycelium per strain were separated from the agar and placed in a 2-mL screw-lid tube with 1 mL of sterile 10 mM $MgCl_2$ and one stainless steel bead (3.2 mm of diameter, Next Advance, USA). Then, each tube containing one fungal and oomycetal strain was placed in a paint shaker (SK450, Fast & Fluid Management, Sassenheim, Netherlands) and grinded for 10 min. 900 µL of fungal and oomycetal homogenates were pooled together in two final fungal and oomycetal stocks, of 50 mg/mL concentration. 50 µL of these stocks were utilized to inoculate 50 mL of ½ MS + MES, which were then injected as described above in one FlowPot. The remaining 100 µL of fungal and oomycetal homogenates were used to control for fungal and oomycetal survival, by pipetting part of this on PGA plates and incubated for a week at 25 ºC.

4.2.3.3.1 Fungal and oomycetal mycelia grinding protocol

Fungal and oomycetal homogenization was tested prior gnotobiotic experiments, by using different homogenization protocols with which fungi and oomycetes' hyphae would disrupt and could be treated similarly to bacterial inoculum. I tested two bead sizes and two beating times (**Supplementary Figure 13A**). Thereby, bead-beating of 50 mg of fungal/oomycetes for 10 minutes with 1 mL of 10 mM $MgCl_2$ and one stainless steel bead (3.2 mm of diameter) proved to be the most effective technique to disrupt the mycelium in a way that it would be possible to inoculate it in a liquid format. More importantly, this method was suitable for fungal and oomycetal survival afterwards (**Supplementary Figure 13B**). Hyphae disruption was observed by pipetting 20 µL of homogenate in a microscope slide and visualizing it at 5x augmentation (Axio Imager 2, Zeiss, Jena, Germany).

4.2.3.4 Seeds sterilization, sowing and growth

A. thaliana Col-0 seeds were sterilized and entrained prior utilization in experiments. Seed sterilization was performed by adding 600 µL of 70% ethanol (Ethanol absolute, VWR Chemicals, USA) in a 1.5-mL Eppendorf tube containing the seeds to be sterilized, and shaken in a rotator (Rotator SB3, Stuart, UK) for 10 min. Under a sterile hood, ethanol supernatant was removed by pipetting, and 600 µL of 100 % ethanol added. Tube was manually rotated for 2 min. Supernatant was again removed and 600 µL of 3 % NaClO (Sodium hypochlorite solution 6-14 %, Honeywell Fluka, USA) added and mixed for 1 min by manually rotating the tube. Supernatant was removed and 600 µL of sterile deionized water were added and mixed for 1 min 5 times to remove any NaClO traces. After the last wash, another 600 µL of sterile water were added. The Eppendorf tube was wrapped in aluminum foil and placed in the fridge (4 ºC) for at least 4 days.

After microbial inoculation (described above), seeds were taken out of the fridge and a subset of them were pipetted into a sterile petri dish with sterile deionized water, so that seeds were diluted enough to be taken one by one by pipetting. Without touching the pot surface, 10 seeds were sown per pot. Microboxes containing inoculated FlowPots with sown seeds were grown for 3-4 weeks in chamber (Panasonic; Day conditions: light intensity 4, 21ºC, 10 hours light; Night conditions: light intensity 0, 19ºC, 14 hours dark). For germination control, 20 seeds were sown on a ½ MS + MES with 1% agar and grown in the same chamber as the Microboxes.

After one week of incubation, seedlings were thinned out. Microboxes were opened under a sterile hood and, with flame-sterilized forceps, seedlings were removed from the pots to leave a minimum of 4 seedlings per pot.

4.2.3.5 Sample harvesting

After 3 or 4 weeks of incubation (depending of the experiment), plant shoots were harvested, along with root and matrix samples. First, pictures were taken to compare shoot phenotypes between conditions. Then, Microboxes were opened and harvested one by one in non-sterile conditions. First, plant shoots were cut using a sterile blade (Einmalskalpelle Cutfix Fig. 22 sterile, VWR, USA) and kept in a petri dish for later fresh shoot weight in a precision balance (ABS-N/ABJ-NM, Kern & Sohn, Balingen, Germany). Shoots were cleaned from any soil trace and quickly dried with kitchen paper to remove excess of water. Then, the content of one FlowPot was poured in a petri dish and plant roots were separated from the matrix body using flame-sterile forceps, either by manually separating the roots from the soil particles or by adding sterile water and "fishing" them out from the plate. Then, roots were thoroughly cleaned from soil and vermiculite traces in a second petri dish with clean sterile water, dried with a sterile Whatman paper (Whatman® glass microfiber filters, Grade GF/B, Sigma-Aldrich, Hamburg, Germany), placed in a 2-mL screw-lid tube and snap-frozen in liquid nitrogen for storage at -80 ºC until further processing. Matrix samples were taken from the remaining soil particles in the FlowPot, carefully making sure no root traces were taken with them. These samples were also placed in a 2-mL screw-lid tube and snap-frozen in liquid nitrogen for storage at -80 ºC until further processing.

4.2.3.6 Shoot fresh weight assessment

As mentioned in the section above, shoots were separated from roots by using a sterile blade and the shoot fresh weight was assessed by drying and cleaning plant shoots prior weighting them in a precision balance. In order to remove experiment-to-experiment variation, all shoot fresh weight values were relative to the control within one biological replicate (un-inoculated control, microbe-free, MF).

Relative shoot fresh weight = shoot fresh weight / microbe-free average shoot fresh weight

Depending of the experiment, however, additional normalization methods were utilized. Box plots were represented using *ggplot2* in R (**Figure 18, Figure 22, Figure 23, Figure 24, Figure 25, Supplementary Figure 17**).

4.2.3.6.1 EXP1, PERT1, TIME2

No additional calculations were done (**Figure 18, Figure 22, Figure 25**)

4.2.3.6.2 PERT2, PERT3

After calculating the relative shoot fresh weight to microbe-free control, shoot fresh weights were calculated as relative plant rescue. That is, relative to the bacteria-only conditions (**Figure 23, Figure 24**).

Relative plant rescue = [shoot fresh weight bacteria+fungi/ MF average shoot fresh weight] / [shoot fresh weight bacteria-only/ MF average shoot fresh weight]

4.2.3.6 Microbial load assessment

4.2.3.6.1 PERT1.2

Before assessing fungal load in matrix samples of PERT1.2, standard curves reflecting mycelium load correlated to Cq values were produced. This was done by harvesting 50 mg of fungal mycelium of the strains 243, 230, 143, 010, 026, 236, 147, 021, 022, 018, 136, as described above (4.1.2.3). DNA was isolated by using the Plant DNAeasy kit (Qiagen, Hilden, Germany), following manufacturer's instructions. DNA concentration was calculated using the Quant-iT™ PicoGreen dsDNA assay kit (Life Technologies, Darmstadt, Germany). 40 µl of a 1:200 dilution of PicoGreen was added to 4 µl of DNA in a 96 well plate. To calculate the DNA concentration a dilution series of standard lambda DNA, ranging from 0.5 to 20 ng/µL, was included on the same plate. Fluorescence was measured using the IQ5 real-time PCR Thermocycler (Biorad, Munich, Germany; 30 sec at 25 °C, 3x30 seconds at 25 °C for measuring fluorescence, 30 seconds at 15 °C). Utilizing this DNA concentration, a dilution series was performed to a final DNA concentration of 15, 10, 5, 1, and 0.5 ng/µl.

DNA isolation was performed from matrix samples of FlowPots inoculated with the previously mentioned fungal strains, from one technical replicate per biological replicate, using the FastDNA ® SPIN for soil kit (MP Biomedicals, Solon, USA). Before DNA isolation, samples were homogenized once using the Precellys®24 tissue lyzer (Bertin Technologies, Montigny-le-Bretonneux, France) at 6,500 rpm for 30 seconds. Afterwards, DNA was extracted using the FastDNA ® SPIN for soil kit according to the manufacturer's instructions. DNA concentration was calculated using the Quant-iT™ PicoGreen dsDNA assay kit (Life Technologies, Darmstadt, Germany). 40 µl of a 1:200 dilution of PicoGreen were added to 4 µl of DNA in a 96 well plate. To calculate the DNA concentration a dilution series of standard lambda DNA, ranging from 0.5 to 20 ng/µL, was included on the same plate. Fluorescence was measured using the IQ5 real-time PCR Thermocycler (Biorad, Munich, Germany; 30 sec at 25 °C, 3x30 seconds at 25 °C for measuring fluorescence, 30 seconds at 15 °C). DNA concentration was adjusted to 3.5 ng/µl. Fungal-load Cq values were measured by using the IQ5 real-time PCR Thermocycler and the ITS1 fungal primers (ITS1F-ITS2, **Annex: Table 2**). 4 µl of DNA template were mixed under sterile conditions with 7.5 µl of 1X iQ SYBR Green (Bio-Rad, Munich, Germany), 1.2 µl of forward and reverse primers and up to 15 µl final volume with sterile water (95 °C: 3 min, 95 °C: 10 sec, 60 °C: 30 sec, 72°C: 30 sec, for 40 cycles). To calculate the fungal DNA concentration, a dilution series of the standard fungal curves produced above, ranging from 15, 10, 5, 1, and 0.5 ng/µl, were included on the same plate. Fungal load was calculated utilizing the 2(-Delta Delta C(T)) method (Livak and Schmittgen, 2001), subtracting the microbe-free values.

Regression plots were performed by using *ggplot2* in R, and Pearson's correlation test was done using *cor.test* function in R (**Supplementary Figure 15**).

4.2.3.6.2 PERT2

DNA isolation was performed from matrix samples of FlowPots, from one technical replicate per biological replicate, using the FastDNA® SPIN for soil kit (MP Biomedicals, Solon, USA). Before DNA isolation, samples were homogenized once using the Precellys®24 tissue lyzer (Bertin Technologies, Montigny-le-Bretonneux, France) at 6,500 rpm for 30 seconds. Afterwards, DNA was extracted using the FastDNA ® SPIN for soil kit according to the manufacturer's instructions. DNA concentration was calculated using the Quant-iT™ PicoGreen dsDNA assay kit (Life Technologies, Darmstadt, Germany). 40 µl of a 1:200 dilution of PicoGreen were added to 4 µl of DNA in a 96 well plate. To calculate the DNA concentration a dilution series of standard lambda DNA, ranging from 0.5 to 20 ng/µL, was included on the same plate. Fluorescence was measured using the IQ5 real-time PCR Thermocycler (Biorad, Munich, Germany; 30 sec at 25 °C, 3x30 seconds at 25 °C for measuring fluorescence, 30 seconds at 15 °C). DNA concentration was adjusted to 3.5 ng/µL. Fungal- and bacterial-load Cq values were measured by using the IQ5 real-time PCR Thermocycler, together with the ITS1 fungal primers (ITS1F-ITS2, **Annex: Table 2**) and bacterial 16s rRNA primers, targeting the V5-V7 region (799F-1192R, **Annex: Table 2**), using as a comparison the targeting the 16s rRNA gene for *A. thaliana* (SH11-At16S-F :CAGGCGGTGGAAACTACCAAG; SH12-At16S-R: TACAGCACTGCACGGGTCGAT). 4 µL of DNA template were mixed under sterile conditions with 7.5 µL of 1X iQ SYBR Green (Bio-Rad, Munich, Germany), 1.2 µL of forward and reverse primers and up to 15 µL final volume with sterile water (95 °C: 3 min, 95 °C: 10 sec, 60 °C: 30 sec, 72 °C: 30 sec, for 40 cycles). Fungal and bacterial load estimation was calculated utilizing the 2(-Delta Delta C(T)) method (Livak and Schmittgen, 2001), subtracting the microbe-free values and plant 16s reads.

Regression plots and bar plots were performed by using *ggplot2* in R, and Pearson's correlation test was done using *cor.test* function in R (**Figure 23**, **Supplementary Figure 18**).

4.2.3.7 ICP-MS analysis

Shoots harvested from TIME2 were dried at 60 °C for two days. Then, the dry material was digested in 0.5 ml 67% nitric acid (Nitric acid 68 - 70%, ARISTAR® ACS, VWR, USA) and diluted with 4.5 ml of deionized water. Dilution factor was calculated to estimate ion concentration in each sample (Dilution factor: DF= final weight of the solution/ weight of the sample). Ionome analysis was performed at the Biocenter Mass Spectrometry Platform, University of Cologne. Heatmap was performed using *ggplot2* in R (**Figure 25**).

4.2.4 Microbial community profiling

4.2.4.1 Library preparation and sequencing

DNA isolation was performed from matrix and root samples harvested as described above, using the FastDNA ® SPIN for soil kit (MP Biomedicals, Solon, USA). Before DNA isolation, samples were homogenized once using the Precellys®24 tissue lyzer (Bertin Technologies, Montigny-le-Bretonneux, France) at 6,500 rpm for 30 seconds. Afterwards, DNA was extracted using the FastDNA ® SPIN for soil kit according to the manufacturer's instructions. DNA concentration was calculated using the Quant-iT™ PicoGreen dsDNA assay kit (Life Technologies, Darmstadt, Germany). 40 µl of a 1:200 dilution of PicoGreen was added to 4 µl of DNA in a 96 well plate. To calculate the DNA concentration a dilution series of standard lambda DNA, ranging from 0.5 to 20 ng/µL, was included on the same plate. Fluorescence was measured using the IQ5 real-time PCR Thermocycler (Biorad, Munich, Germany; 30 sec at 25 °C, 3x30 seconds at 25 °C for measuring fluorescence, 30 seconds at 15 °C). DNA concentration was adjusted to 3.5 ng/µL.

PCR amplicon libraries were generated using primers 799F-1192R for bacteria-containing samples, ITS1F-ITS2 for fungi-containing samples, and ITS1o-5.8s-Rev-o for oomycetes-containing samples (**Annex: Table 2**). Control samples (microbe-free, MF) were amplified with the three primer pairs to control for contaminations and possible remaining DNA in the peat. PCRs were performed by using 3 µL of the adjusted DNA in a total volume of 25 µL, including 1.25 U DFS-Taq DNA Polymerase, 1x incomplete reaction buffer, 0.3 % BSA, 2 mM of $MgCl_2$, 200 µM of dNTPs and 400 nM of each primer. To minimize PCR bias three independent PCR reactions using one master mix were prepared. The PCR reaction was pipetted in a laminar flow and PCR amplified (94 °C/2 minutes, 94 °C/30 seconds, 55 °C/30 seconds, 72 °C/30 seconds, 72 °C/10 minutes for 25 cycles), using the same PCR parameters for all primer pairs. Afterwards, single stranded DNA and proteins were digested by adding 1 µl of Antarctic phosphatase, 1 µl Exonuclease I and 2.44 µl Antarctic phosphatase buffer to 20 µl of the pooled PCR product. Samples were incubated at 37 °C for 30 minutes and enzymatic activity was deactivated at 85 °C for 15 minutes. Samples were centrifuged for 10 minutes at 4,000 xg and the supernatant was transferred to a new plate. 3 µl of this reaction were used for a second PCR with primers that included barcodes and Illumina adaptors (B5-barcodes for bacteria, Ft-barcodes for fungi, Ot-barcodes for oomycetes, **Annex: Table 2**). PCR reactions were prepared using the same protocol described above, and the number of PCR-cycles were reduced to 10. PCR performance was assessed by loading 5 µL of PCR products of the three-replicate' pool with 5 µL of Gel Loading Dye, Orange G (6X, Sigma, Hamburg, Germany) run on a 1 % agarose gel for 30 minutes, and by checking that no band could be observed in the microbe-free controls. Each bacterial reaction (70 µL approximately) were mixed with 20 µL Gel Loading Dye, Orange G and loaded on a 1.5 % agarose gel and ran for approximately 2 hours at 80 V. Bands with the correct size of ~500 bp were cut and purified using the QIAquick gel extraction kit (Qiagen, Hilden, Germany) and eluted in 60 µL of nucleases-free water (Qiagen, Hilden, Germany) DNA concentration was determined using the PicoGreen assay as described before. Fungal and oomycetal reactions were purified using Agencourt AMPure XP PCR Purification kit (brand) following manufacturer' instructions and eluting the PCR product in 70 µL of nucleases-free water. Equal amounts (ng) of purified PCR products were pooled, each microbial library separately. Pooled libraries were purified twice using Agencourt AMPure XP PCR Purification kit (Beckman Coulter, Krefeld, Germany) following manufacturer' instructions and eluting the PCR product in decreasing amounts of nucleases-free water (that is, 120 µL in the first round and 90 µL in the second round). Purified libraries' concentration was assessed using Quantus^{TM} Fluorometer (Promega, Manheim, Germany), by mixing 100 µL of a 1:200 dilution of Quantifluor® dsDNA dye (in 1xTE) with 2 µL and 98 µL of 1xTE in a 0.5-mL tube (Promega, Manheim, Germany), thoroughly mixing by pipetting and incubating for 5 minutes under dark. Then, equal amounts of each library were pooled together. Final library concentration was assessed using Quantus^{TM} Fluorometer, as described above. Paired-end Illumina sequencing was performed with the MiSeq sequencer at the Department of Plant-Microbe Interactions, Max Planck Institute for Plant Breeding Research, following manufacturer' instructions.

4.2.4.2 Reference-based sequencing data analysis

Sequencing data analysis was performed using bioinformatic pipelines developed by Dr. Rubén Garrido-Oter and Dr. Thorsten Thiergart.

The paired 16s rRNA amplicon sequencing reads were joined (join_paired_ends.py, QIIME, default parameters) and the joined reads were then quality filtered and demultiplexed (split_libraries_fastq.py, QIIME, with maximum barcode errors 1 and phred score of 30) (Caporaso *et al.,* 2010). The filtered reads were dereplicated (usearch, –derep_fulllength) and sorted according to their copy number (only reads >2 copies were retained) (Edgar, 2010). ITS reads were joined and demultiplexed as for 16s rRNA reads. In addition, also the forward reads were demultiplexed and filtered. For those reads where no joined pair of reads exist, the forward reads were kept. Demultiplexed reads were directly mapped to the reference sequences for the respective communities (using the usearch-global command from usearch, with a sequence identity threshold of 97%). From these mapped reads, OTU-tables were inferred (**Annex: otu_tables**).

To assess the alpha-diversity within samples, OTU-tables were rarefied to 1000 reads. Observed OTUs were calculated using QIIME (alpha_diversity.py, **Supplementary Figure 14**). To estimate the beta-diversity, OTU-tables were normalized using the cumulative –sum scaling (CSS) method (Paulson *et al.,* 2013). Bray-Curtis distances between samples were used as an input for principal coordinate analysis (PCoA, done via *cmdscale* function in R).

To visualize the distance between clusters of the same microbial inoculation condition (**Figure 19B**) despite experiment-to-experiment variation, average Bray-Curtis distances were calculated per biological replicate, normalized to control cluster (e.g.: (B-BF/B-B)) and plotted with *ggplot* in R.

To test the effect of different factors on the estimated explained variance PERMANOVA analysis was performed (*adonis* or *capscale* functions from vegan R package, with 999 permutations **Figure 19, Figure 24, Figure 26, Supplementary Figure 21, Table 5**).

For each OTU, the possible enrichment in certain condition was tested using a linear model (log2, > 5 ‰ threshold) using the script described in Bulgarelli *et al.,* 2015 (developed from the R package *limma*). Using this method for each OTU it was tested if the RA within conditions was significantly higher than compared to another condition (**Figure 21**). Ternary plots were constructed as previously described (Bulgarelli *et al.,* 2012, **Figure 21**).

Relative abundances plots were produced from relative OTU counts (relative abundances (%)) per sample and plotted using *ggplot2* in R (**Figure 20, Figure 25, Supplementary Figure 9**).

Due to the non-normal distribution of the data, Kruskal Wallis and Dunn test *post-hoc* were used to look for significant differences between medians.

Abbreviations

%	percent
:	to
~	approximately
<	less than
>	more than
®	registered trademark
°C	degrees Celsius
µM	micrometers
‰	permille
A. alpina	Arabis alpina
ABC	ATP-binding cassette transporter
AHL	N-acyl-l-homoserine lactone
Al	Aluminum
AMP	Arbuscular Mycorrhizal Fungi
Amp	ampicillin
As	Arsenic
B	Boron (mg/kg)
B	bacteria
B	Boron
bbh	best blast hit
Be	Beryllium
bp	base pairs
BSA	bovine serum albumin
C	Comamonadaceae
Ca	Calcium (mg/kg)
Ca	Calcium
CAS	Cologne agricultural soil
Cd	Cadmium
c-di-GMP	cyclic diguanylate
CFUs	colony forming units
CFUs	Cytophaga-Flavobacterium
cm	centimeters
Co	Cobalt
CO_2	carbon dioxide
Col	Arabidopsis thaliana ecotype Columbia
Cq	quantification cycle
Cr	Chromium
Cs	Cesium
CSIC-CNB	*Consejo Superior de Investigaciones Científicas Centro Nacional de Biotecnología*
CSS	cumulative –sum scaling
Cu	Copper (mg/kg)
Cu	Copper

CxG	ClimatexGenotype
DF	dilution factor
DNA	Deoxyribonucleic acid
dNTP	desoxynucleotide
Dr.	doctor
e.g.	for example
EDTA	ethylendiaminetetraacetic acid
et al.	and colleagues
etc.	etcetera
EXP1	experiment 1
F	forward
F	fungi
FDR	false discovery rate
Fe	Iron (mg/kg)
Fe	Iron
g	grams
h	hour
H_2O	water/Dihydrogen oxide
i.e.	that is
INRA	Institut national de la recherche agronomique
iTOL	interactive tree of life
ITS	internal transcribed spacer
K	Potassium (mg/kg)
K	Potassium
KCl	Potassium chloride
kg	kilogram
kg	kilograms
KH2PO4	Monopotassium phosphate
Kn	kanamycin
L	liter
Li	Lithium
lmol m^2s-^{1}	light intensity measurement
max.	maximum
MES	2-(N-morpholino)ethanesulfonic acid
MF	microbe-free
Mg	Magnesium (mg/kg)
Mg	Magnesium (mg/kg)
mg	miligrams
Mg	Magnesium
$MgCl_2$	magnesium chloride
min	minutes
mL	milliliters
mm	millimeters
Mn	Manganesium (mg/kg)
Mn	Manganese

Mo	Molybdenum
MPIPZ	Max Planck Institut fuer Pflanzenzuechtung Forschung
MS	Murashige and Skoog
Mya	million years ago
N.A	not available
Na	Sodium
Na2HPO4	Sodium phosphate dibasic
NaCl	Sodium chloride
NaClO	sodium hypochlorite
NCBI	National Center for Biotechnology Information
ng	nanograms
NGS	next-generation sequencing
Ni	Nickel
nM	nanomol
NO3	Nitrate (mg/kg)
O	oomycetes
OD	optical density
OTUs	operational taxonomic units
P	Phosphorous (mg/kg)
P	Pseudomonadaceae
P	Phosphorus
p.adj.method	p-value adjustment
PAR	photosynthetically active radiation
Pb	Lead
PBS	phosphate buffered saline
PCoA	Principal Coordinates Analysis
PCR	polymerase chain reaction
pep1	perpetual flowering 1
PERMANOVA	Permutational analysis of variance
PERT1	perturbation experiment 1
PERT1.2	perturbation experiment 1.2
PERT2	perturbation experiment 2
PERT3	perturbation experiment 3
PGA	Potato glucose agar
pH	negative decimal logarithm of H+ concentration
Prof.	Professor
pv.	pathovar
PyNAST	Python Nearest Alignment Space Termination
QIIME	quantitative insights into microbial ecology
qPCR	quantitative PCR
R	Coefficient of determination
R	reverse
RA	relative abundance
Rb	Rubidium
RDP	Ribosomal Database Project
Rimf	rifampicine

RP	Rhizoplane
rpm	Revolutions per minute
rRNA	ribosomal ribonucleic acid
RS	Rhizosphere
S	Sulfur
Se	Selenium
sec	seconds
SEM	scanning-electron microscopy
sp.	species (singular)
spp.	species (plural)
Sr	Strontium
Strep	stretomycin
SynCom/SC	synthetic community
Taq	Thermophilus aquaticus
Tc	tetracycline
TCUs	Taxonomic Community Units
TE	Tris-EDTA
TIME1	time-series experiment 1
TIME2	time-series experiment 2
TM	trademark
Tris	tris-(hydroxymethyl)-aminomethan
TSA	tryptic soy broth
U	units
UNITE	User-friendly Nordic ITS Ectomycorrhiza Database
V	volt
V	Vanadium
VOCs	Volatile Organic Compounds
w	watts
WGA	Wheat Germ Agglutinin
xg	times gravity
Zn	Zinc

References

Agler, M.T., Mari, A., Dombrowski, N., Hacquard, S. and Kemen, E.M. (2016) New insights in host-associated microbial diversity with broad and accurate taxonomic resolution. *bioRxiv*, 050005.

Agler, M.T., Ruhe, J., Kroll, S., Morhenn, C., Kim, S.-T., Weigel, D. and Kemen, E.M. (2016) Microbial Hub Taxa Link Host and Abiotic Factors to Plant Microbiome Variation. *PLoS Biol.*, **14**, e1002352.

Ågren, J. and Schemske, D.W. (2012) Reciprocal transplants demonstrate strong adaptive differentiation of the model organism *Arabidopsis thaliana* in its native range. *New Phytologist*, **194**, 1112–1122.

Ahmed, I., Yokota, A. and Fujiwara, T. (2007) A novel highly boron tolerant bacterium, *Bacillus boroniphilus sp. nov*., isolated from soil, that requires boron for its growth. *Extremophiles : life under extreme conditions*, **11**, 217–24.

Almario, J., Jeena, G., Wunder, J., Langen, G., Zuccaro, A., Coupland, G. and Bucher, M. (2017) Root-associated fungal microbiota of nonmycorrhizal *Arabis alpina* and its contribution to plant phosphorus nutrition. *PNAS*, **114**, E9403–E9412.

Alonso-Blanco, C., Andrade, J., Becker, C., *et al.* (2016) 1,135 Genomes Reveal the Global Pattern of Polymorphism in *Arabidopsis thaliana*. *Cell*, **166**, 481–491.

Andrade, G., Mihara, K.L., Linderman, R.G. and Bethlenfalvay, G.J. (1997) Bacteria from rhizosphere and hyphosphere soils of different arbuscular-mycorrhizal fungi. *Plant and Soil*, **192**, 71–79.

Arendt, K.R., Hockett, K.L., Araldi-Brondolo, S.J., Baltrus, D.A. and Arnold, A.E. (2016) Isolation of Endohyphal Bacteria from Foliar Ascomycota and In Vitro Establishment of Their Symbiotic Associations. *Appl. Environ. Microbiol.*, **82**, 2943–2949.

Artursson, V., Finlay, R.D. and Jansson, J.K. (2006) Interactions between arbuscular mycorrhizal fungi and bacteria and their potential for stimulating plant growth. *Environmental Microbiology*, **8**, 1–10.

Bahram, M., Kohout, P., Anslan, S., Harend, H., Abarenkov, K. and Tedersoo, L. (2016) Stochastic distribution of small soil eukaryotes resulting from high dispersal and drift in a local environment. *The ISME Journal*, **10**, 885–896.

Bai, Y., Müller, D.B., Srinivas, G., *et al.* (2015) Functional overlap of the *Arabidopsis* leaf and root microbiota. *Nature*, **528**, 364–369.

Bakker, M.G., Schlatter, D.C., Otto-Hanson, L. and Kinkel, L.L. (2014) Diffuse symbioses: roles of plant–plant, plant–microbe and microbe–microbe interactions in structuring the soil microbiome. *Molecular Ecology*, **23**, 1571–1583.

Banerjee, S., Kirkby, C.A., Schmutter, D., Bissett, A., Kirkegaard, J.A. and Richardson, A.E. (2016) Network analysis reveals functional redundancy and keystone taxa amongst bacterial and fungal communities during organic matter decomposition in an arable soil. *Soil Biology and Biochemistry*, **97**, 188–198.

Barberán, A., Bates, S.T., Casamayor, E.O. and Fierer, N. (2012) Using network analysis to explore co-occurrence patterns in soil microbial communities. *The ISME Journal*, **6**, 343–351.

Barret, M., Briand, M., Bonneau, S., Préveaux, A., Valière, S., Bouchez, O., Hunault, G., Simoneau, P. and Jacques, M.-A. (2015) Emergence Shapes the Structure of the Seed Microbiota. *Appl Environ Microbiol*, **81**, 1257–1266.

Barret, M., Guimbaud, J.-F., Darrasse, A. and Jacques, M.-A. (2016) Plant microbiota affects seed transmission of phytopathogenic microorganisms. *Molecular Plant Pathology*, **17**, 791–795.

Bartoli, C., Frachon, L., Barret, M., *et al.* (2018) In situ relationships between microbiota and potential pathobiota in *Arabidopsis thaliana*. *bioRxiv*, 261602.

Bengtsson-Palme, J., Ryberg, M., Hartmann, M., *et al.* (2013) Improved software detection and extraction of ITS1 and ITS2 from ribosomal ITS sequences of fungi and other eukaryotes for analysis of environmental sequencing data. *Methods in Ecology and Evolution*, **4**, 914–919.

Benhamou, N., Floch, G. le, Vallance, J., Gerbore, J., Grizard, D. and Rey, P. (2012) *Pythium oligandrum*: an example of opportunistic success. *Microbiology*, **158**, 2679–2694.

Benítez, T., Rincón, A.M., Limón, M.C. and Codón, A.C. (2004) Biocontrol mechanisms of *Trichoderma* strains. *Int. Microbiol.*, **7**, 249–260.

Berendsen, R.L., Pieterse, C.M.J. and Bakker, P.A.H.M. (2012) The rhizosphere microbiome and plant health. *Trends in Plant Science*, **17**, 478–486.

Bertaux, J., Schmid, M., Prevost-Boure, N.C., Churin, J.L., Hartmann, A., Garbaye, J. and Frey-Klett, P. (2003) In Situ Identification of Intracellular Bacteria Related to *Paenibacillus spp*. in the Mycelium of the Ectomycorrhizal Fungus *Laccaria bicolor* S238N. *Appl. Environ. Microbiol.*, **69**, 4243–4248.

Bhat, R.G. and Subbarao, K.V. (1999) Host Range Specificity in *Verticillium dahliae*. *Phytopathology*, **89**, 1218–1225.

Bianciotto, V., Lumini, E., Lanfranco, L., Minerdi, D., Bonfante, P. and Perotto, S. (2000) Detection and Identification of Bacterial Endosymbionts in Arbuscular Mycorrhizal Fungi Belonging to the Family Gigasporaceae. *Appl. Environ. Microbiol.*, **66**, 4503–4509.

Birtel, J., Walser, J.-C., Pichon, S., Bürgmann, H. and Matthews, B. (2015) Estimating Bacterial Diversity for Ecological Studies: Methods, Metrics, and Assumptions. *PLOS ONE*, **10**, e0125356.

Bodenhausen, N., Bortfeld-Miller, M., Ackermann, M. and Vorholt, J.A. (2014) A Synthetic Community Approach Reveals Plant Genotypes Affecting the Phyllosphere Microbiota. *PLOS Genetics*, **10**, e1004283.

Bodenhausen, N., Horton, M.W. and Bergelson, J. (2013) Bacterial Communities Associated with the Leaves and the Roots of *Arabidopsis thaliana*. *PLOS ONE*, **8**, e56329.

Bonfante, P. and Anca, I.-A. (2009) Plants, Mycorrhizal Fungi, and Bacteria: A Network of Interactions. *Annu. Rev. Microbiol.*, **63**, 363–383.

Bonfante, P. and Genre, A. (2010) Mechanisms underlying beneficial plant–fungus interactions in mycorrhizal symbiosis. *Nature Communications*, **1**, 48.

Bonito, G., Reynolds, H., Robeson, M.S., Nelson, J., Hodkinson, B.P., Tuskan, G., Schadt, C.W. and Vilgalys, R. (2014) Plant host and soil origin influence fungal and bacterial assemblages in the roots of woody plants. *Molecular Ecology*, **23**, 3356–3370.

Bonkowski, M. (2004) Protozoa and plant growth: the microbial loop in soil revisited. *New Phytologist*, **162**, 617–631.

Bordenstein, S.R. and Theis, K.R. (2015) Host Biology in Light of the Microbiome: Ten Principles of Holobionts and Hologenomes. *PLOS Biology*, **13**, e1002226.

Bouffaud, M.-L., Poirier, M.-A., Muller, D. and Moënne-Loccoz, Y. (2014) Root microbiome relates to plant host evolution in maize and other Poaceae. *Environmental Microbiology*, **16**, 2804–2814.

Boyes, D.C., Zayed, A.M., Ascenzi, R., McCaskill, A.J., Hoffman, N.E., Davis, K.R. and Görlach, J. (2001) Growth Stage–Based Phenotypic Analysis of *Arabidopsis*: A Model for High Throughput Functional Genomics in Plants. *The Plant Cell*, **13**, 1499–1510.

Bruez, E., Haidar, R., Alou, M.T., et al. (2015) Bacteria in a wood fungal disease: characterization of bacterial communities in wood tissues of esca-foliar symptomatic and asymptomatic grapevines. *Front. Microbiol.*, **6**.

Brune, A. (2014) Symbiotic digestion of lignocellulose in termite guts. *Nature Reviews Microbiology*, **12**, 168–180.

Buée, M., Boer, W. de, Martin, F., Overbeek, L. and Jurkevitch, E. (2009) The rhizosphere zoo: An overview of plant-associated communities of microorganisms, including phages, bacteria, archaea, and fungi, and of some of their structuring factors. *Plant and Soil*, **321**, 189–212.

Bulgarelli, D., Garrido-Oter, R., Münch, P.C., Weiman, A., Dröge, J., Pan, Y., McHardy, A.C. and Schulze-Lefert, P. (2015) Structure and Function of the Bacterial Root Microbiota in Wild and Domesticated Barley. *Cell Host Microbe*, **17**, 392–403.

Bulgarelli, D., Rott, M., Schlaeppi, K., *et al.* (2012) Revealing structure and assembly cues for *Arabidopsis* root-inhabiting bacterial microbiota. *Nature*, **488**, 91–95.

Bulgarelli, D., Schlaeppi, K., Spaepen, S., Themaat, E.V.L. van and Schulze-Lefert, P. (2013) Structure and Functions of the Bacterial Microbiota of Plants. *Annual Review of Plant Biology*, **64**, 807–838.

Busby, P.E., Peay, K.G. and Newcombe, G. (2016) Common foliar fungi of *Populus trichocarpa* modify *Melampsora* rust disease severity. *New Phytologist*, **209**, 1681–1692.

Bhuyan, S.K., Bandyopadhyay, P., Kumar, P., Mishra, D.K., Prasad, R., Kumari, A., Upadhyaya, K.C., Varma, A. and Yadava, P.K. (2015) Interaction of *Piriformospora indica* with *Azotobacter chroococcum*. *Scientific Reports*, **5**, 13911.

Caporaso, J. Gregory, Bittinger, K., Bushman, F.D., DeSantis, T.Z., Andersen, G.L. and Knight, R. (2010) PyNAST: a flexible tool for aligning sequences to a template alignment. *Bioinformatics*, **26**, 266–267.

Caporaso, J Gregory, Kuczynski, J., Stombaugh, J., *et al.* (2010) QIIME allows analysis of high-throughput community sequencing data. *Nat Methods*, **7**, 335–336.

Cardinale, M., Grube, M., Erlacher, A., Quehenberger, J. and Berg, G. (2015) Bacterial networks and co-occurrence relationships in the lettuce root microbiota. *Environmental Microbiology*, **17**, 239–252.

Carmona, M.A., Sautua, F.J., Grijalba, P.E., Cassina, M. and Pérez-Hernández, O. (2018) Effect of potassium and manganese phosphites in the control of *Pythium* damping-off in soybean: a feasible alternative to fungicide seed treatments. *Pest Manag. Sci.*, **74**, 366–374.

Castrillo, G., Teixeira, P.J.P.L., Paredes, S.H., et al. (2017) Root microbiota drive direct integration of phosphate stress and immunity. *Nature*, **543**, 513–518.

Cha, J.-Y., Han, S., Hong, H.-J., *et al.* (2016) Microbial and biochemical basis of a *Fusarium* wilt-suppressive soil. *ISME J*, **10**, 119–129.

Chaparro, J.M., Badri, D.V. and Vivanco, J.M. (2014) Rhizosphere microbiome assemblage is affected by plant development. *ISME J*, **8**, 790–803.

Chapelle, E., Mendes, R., Bakker, P.A.H. and Raaijmakers, J.M. (2016) Fungal invasion of the rhizosphere microbiome. *The ISME Journal*, **10**, 265–268.

Chinn, S.H.F. (1973) Prevalence of *Dendryphion nanum* in field soils in Saskatchewan with special reference to rape in the crop rotation. *Can. J. Bot.*, **51**, 2253–2258.

Coince, A., Caël, O., Bach, C., *et al.* (2013) Below-ground fine-scale distribution and soil versus fine root detection of fungal and soil oomycete communities in a French beech forest. *Fungal Ecology*, **6**, 223–235.

Coleman, D.C. (1994) The microbial loop concept as used in terrestrial soil ecology studies. *Microb Ecol*, **28**, 245–250.

Coleman, J.J., Ghosh, S., Okoli, I. and Mylonakis, E. (2011) Antifungal Activity of Microbial Secondary Metabolites. *PLOS ONE*, **6**, e25321.

Coleman-Derr, D., Desgarennes, D., Fonseca-Garcia, C., *et al.* (2016) Plant compartment and biogeography affect microbiome composition in cultivated and native *Agave* species. *New Phytologist*, **209**, 798–811.

Copeland, J.K., Yuan, L., Layeghifard, M., Wang, P.W. and Guttman, D.S. (2015) Seasonal Community Succession of the Phyllosphere Microbiome. *MPMI*, **28**, 274–285.

Cordier, T., Robin, C., Capdevielle, X., Fabreguettes, O., Desprez-Loustau, M.-L. and Vacher, C. (2012) The composition of phyllosphere fungal assemblages of European beech (*Fagus sylvatica*) varies significantly along an elevation gradient. *New Phytologist*, **196**, 510–519.

Cordovez, V., Carrion, V.J., Etalo, D.W., Mumm, R., Zhu, H., Wezel, G.P. van and Raaijmakers, J.M. (2015) Diversity and functions of volatile organic compounds produced by *Streptomyces* from a disease-suppressive soil. *Front Microbiol*, **6**, 1081.

Cusano, A.M., Burlinson, P., Deveau, A., Vion, P., Uroz, S., Preston, G.M. and Frey-Klett, P. (2011) *Pseudomonas fluorescens* BBc6R8 type III secretion mutants no longer promote ectomycorrhizal symbiosis. *Environmental Microbiology Reports*, **3**, 203–210.

Day, J.P., Wattier, R. a. M., Shaw, D.S. and Shattock, R.C. (2004) Phenotypic and genotypic diversity in *Phytophthora infestans* on potato in Great Britain, 1995–98. *Plant Pathology*, **53**, 303–315.

Boer, W. de, Leveau, J.H.J., Kowalchuk, G.A., Gunnewiek, P.J.A.K., Abeln, E.C.A., Figge, M.J., Sjollema, K., Janse, J.D. and Veen, J.A. van (2004) *Collimonas fungivorans* gen. nov., sp. nov., a chitinolytic soil bacterium with the ability to grow on living fungal hyphae. *International Journal of Systematic and Evolutionary Microbiology*, **54**, 857–864.

Delgado-Baquerizo, M., Oliverio, A.M., Brewer, T.E., Benavent-González, A., Eldridge, D.J., Bardgett, R.D., Maestre, F.T., Singh, B.K. and Fierer, N. (2018) A global atlas of the dominant bacteria found in soil. *Science*, **359**, 320–325.

DeSantis, T.Z., Hugenholtz, P., Larsen, N., *et al.* (2006) Greengenes, a Chimera-Checked 16S rRNA Gene Database and Workbench Compatible with ARB. *Appl. Environ. Microbiol.*, **72**, 5069–5072.

Deshpande, V., Wang, Q., Greenfield, P., Charleston, M., Porras-Alfaro, A., Kuske, C.R., Cole, J.R., Midgley, D.J. and Tran-Dinh, N. (2016) Fungal identification using a Bayesian classifier and the Warcup training set of internal transcribed spacer sequences. *Mycologia*, **108**, 1–5.

Desirò, A., Salvioli, A., Ngonkeu, E.L., Mondo, S.J., Epis, S., Faccio, A., Kaech, A., Pawlowska, T.E. and Bonfante, P. (2014) Detection of a novel intracellular microbiome hosted in arbuscular mycorrhizal fungi. *The ISME Journal*, **8**, 257–270.

Dittmar, E.L., Oakley, C.G., Ågren, J. and Schemske, D.W. (2014) Flowering time QTL in natural populations of *Arabidopsis thaliana* and implications for their adaptive value. *Molecular Ecology*, **23**, 4291–4303.

Dombrowski, N., Schlaeppi, K., Agler, M.T., Hacquard, S., Kemen, E., Garrido-Oter, R., Wunder, J., Coupland, G. and Schulze-Lefert, P. (2017) Root microbiota dynamics of perennial *Arabis alpina* are dependent on soil residence time but independent of flowering time. *ISME J*, **11**, 43–55.

Du, Z.-Y. and Wang, Q.-F. (2016) Phylogenetic tree of vascular plants reveals the origins of aquatic angiosperms. *Journal of Systematics and Evolution*, **54**, 342–348.

Dubinsky, E.A., Silver, W.L. and Firestone, M.K. (2010) Tropical forest soil microbial communities couple iron and carbon biogeochemistry. *Ecology*, **91**, 2604–2612.

Eberl, L. (1999) N-Acyl Homoserinelactone-mediated Gene Regulation in Gram-negative Bacteria. *Systematic and Applied Microbiology*, **22**, 493–506.

Edgar, R.C. (2010) Search and clustering orders of magnitude faster than BLAST. *Bioinformatics*, **26**, 2460–2461.

Edwards, J., Johnson, C., Santos-Medellín, C., Lurie, E., Podishetty, N.K., Bhatnagar, S., Eisen, J.A. and Sundaresan, V. (2015) Structure, variation, and assembly of the root-associated microbiomes of rice. *Proc. Natl. Acad. Sci. U.S.A.*, **112**, E911-920.

Edwards, J.A., Santos-Medellín, C.M., Liechty, Z.S., Nguyen, B., Lurie, E., Eason, S., Phillips, G. and Sundaresan, V. (2018) Compositional shifts in root-associated bacterial and archaeal microbiota track the plant life cycle in field-grown rice. *PLOS Biology*, **16**, e2003862.

Fierer, N., Bradford, M.A. and Jackson, R.B. (2007) Toward an Ecological Classification of Soil Bacteria. *Ecology*, **88**, 1354–1364.

Fierer, N. and Jackson, R.B. (2006) The diversity and biogeography of soil bacterial communities. *PNAS*, **103**, 626–631.

Fierer, N., Leff, J.W., Adams, B.J., *et al.* (2012) Cross-biome metagenomic analyses of soil microbial communities and their functional attributes. *PNAS*, **109**, 21390–21395.

Filion, M., St-Arnaud, M. and Fortin, J.A. (1999) Direct interaction between the arbuscular mycorrhizal fungus *Glomus intraradices* and different rhizosphere microorganisms. *New Phytologist*, **141**, 525–533.

Fitzpatrick, C.R., Copeland, J., Wang, P.W., Guttman, D.S., Kotanen, P.M. and Johnson, M.T.J. (2018) Assembly and ecological function of the root microbiome across angiosperm plant species. *PNAS*, 201717617.

Flues, S., Bass, D. and Bonkowski, M. (2017) Grazing of leaf-associated Cercomonads (Protists: Rhizaria: Cercozoa) structures bacterial community composition and function. *Environmental Microbiology*, **19**, 3297–3309.

Frey-Klett, P., Garbaye, J. and Tarkka, M. (2007) The mycorrhiza helper bacteria revisited. *New Phytol.*, **176**, 22–36.

Frey-Klett, P., Burlinson, P., Deveau, A., Barret, M., Tarkka, M. and Sarniguet, A. (2011) Bacterial-Fungal Interactions: Hyphens between Agricultural, Clinical, Environmental, and Food Microbiologists. *Microbiol. Mol. Biol. Rev.*, **75**, 583–609.

Glaeser, S.P., Imani, J., Alabid, I., et al. (2016) Non-pathogenic *Rhizobium radiobacter* F4 deploys plant beneficial activity independent of its host *Piriformospora indica*. *The ISME Journal*, **10**, 871–884.

Glynou, K., Ali, T., Buch, A.-K., Haghi Kia, S., Ploch, S., Xia, X., Çelik, A., Thines, M. and Maciá-Vicente, J.G. (2016) The local environment determines the assembly of root endophytic fungi at a continental scale. *Environ. Microbiol.*, **18**, 2418–2434.

Gürtler, H., Pedersen, R., Anthoni, U., Christophersen, C., Nielsen, P.H., Wellington, E.M., Pedersen, C. and Bock, K. (1994) Albaflavenone, a sesquiterpene ketone with a zizaene skeleton produced by a streptomycete with a new rope morphology. *J. Antibiot.*, **47**, 434–439.

Hacquard, S. (2016) Disentangling the factors shaping microbiota composition across the plant holobiont. *New Phytologist*, **209**, 454–457.

Hacquard, S., Garrido-Oter, R., González, A., *et al.* (2015) Microbiota and Host Nutrition across Plant and Animal Kingdoms. *Cell Host & Microbe*, **17**, 603–616.

Hacquard, S. and Schadt, C.W. (2015) Towards a holistic understanding of the beneficial interactions across the *Populus* microbiome. *New Phytologist*, **205**, 1424–1430.

Hacquard, S., Kracher, B., Hiruma, K., et al. (2016) Survival trade-offs in plant roots during colonization by closely related beneficial and pathogenic fungi. *Nat Commun*, **7**, 11362.

Hamonts, K., Trivedi, P., Garg, A., Janitz, C., Grinyer, J., Holford, P., Botha, F.C., Anderson, I.C. and Singh, B.K. (2018) Field study reveals core plant microbiota and relative importance of their drivers. *Environmental Microbiology*, **20**, 124–140.

Haney, C.H., Samuel, B.S., Bush, J. and Ausubel, F.M. (2015) Associations with rhizosphere bacteria can confer an adaptive advantage to plants. *Nature Plants*, **1**, 15051.

Harcombe, W. (2010) Novel Cooperation Experimentally Evolved Between Species. *Evolution*, **64**, 2166–2172.

Hardoim, P.R., Overbeek, L.S. van, Berg, G., Pirttilä, A.M., Compant, S., Campisano, A., Döring, M. and Sessitsch, A. (2015) The Hidden World within Plants: Ecological and Evolutionary Considerations for Defining Functioning of Microbial Endophytes. *Microbiol. Mol. Biol. Rev.*, **79**, 293–320.

Haas, D. and Défago, G. (2005) Biological control of soil-borne pathogens by fluorescent pseudomonads. *Nature Reviews Microbiology*, **3**, 307–319.

Hassani, M.A., Durán, P. and Hacquard, S. (2018) Microbial interactions within the plant holobiont. *Microbiome*, **6**, 58.

Heijden, M.G.A. van der, Bardgett, R.D. and Straalen, N.M. van (2008) The unseen majority: soil microbes as drivers of plant diversity and productivity in terrestrial ecosystems. *Ecol. Lett.*, **11**, 296–310

Heijden, M.G. van der, Bruin, S. de, Luckerhoff, L., Logtestijn, R.S. van and Schlaeppi, K. (2016) A widespread plant-fungal-bacterial symbiosis promotes plant biodiversity, plant nutrition and seedling recruitment. *The ISME Journal*, **10**, 389–399.

Heijden, M.G.A. van der and Schlaeppi, K. (2015) Root surface as a frontier for plant microbiome research. *PNAS*, **112**, 2299–2300.

Hiruma, K., Gerlach, N., Sacristán, S., *et al.* (2016) Root Endophyte *Colletotrichum tofieldiae* Confers Plant Fitness Benefits that Are Phosphate Status Dependent. *Cell*, **165**, 464–474.

Hoffman, M.T. and Arnold, A.E. (2010) Diverse Bacteria Inhabit Living Hyphae of Phylogenetically Diverse Fungal Endophytes. *Appl. Environ. Microbiol.*, **76**, 4063–4075.

Horton, M.W., Bodenhausen, N., Beilsmith, K., *et al.* (2014) Genome-wide association study of *Arabidopsis thaliana* leaf microbial community. *Nat Commun*, **5**, 5320.

Howell, C.R. (2003) Mechanisms Employed by Trichoderma Species in the Biological Control of Plant Diseases: The History and Evolution of Current Concepts. *Plant Disease*, **87**, 4–10.

Hu, J., Wei, Z., Friman, V.-P., *et al.* (2016) Probiotic Diversity Enhances Rhizosphere Microbiome Function and Plant Disease Suppression. *mBio*, **7**, e01790-16.

Hunter, P.J., Hand, P., Pink, D., Whipps, J.M. and Bending, G.D. (2010) Both Leaf Properties and Microbe-Microbe Interactions Influence Within-Species Variation in Bacterial Population Diversity and Structure in the Lettuce (*Lactuca* Species) Phyllosphere. *Appl. Environ. Microbiol.*, **76**, 8117–8125.

Ibekwe, A.M., Poss, J.A., Grattan, S.R., Grieve, C.M. and Suarez, D. (2010) Bacterial diversity in cucumber (*Cucumis sativus*) rhizosphere in response to salinity, soil pH, and boron. *Soil Biology and Biochemistry*, **42**, 567–575.

Ingle, R.A., Stoker, C., Stone, W., Adams, N., Smith, R., Grant, M., Carré, I., Roden, L.C. and Denby, K.J. (2015) Jasmonate signalling drives time-of-day differences in susceptibility of *Arabidopsis* to the fungal pathogen *Botrytis cinerea*. *Plant J.*, **84**, 937–948.

Jakuschkin, B., Fievet, V., Schwaller, L., Fort, T., Robin, C. and Vacher, C. (2016) Deciphering the Pathobiome: Intra- and Interkingdom Interactions Involving the Pathogen *Erysiphe alphitoides*. *Microb Ecol*, **72**, 870–880.

Jarosz, L.M., Ovchinnikova, E.S., Meijler, M.M. and Krom, B.P. (2011) Microbial Spy Games and Host Response: Roles of a *Pseudomonas aeruginosa* Small Molecule in Communication with Other Species. *PLOS Pathogens*, **7**, e1002312.

Joergensen, R.G. and Emmerling, C. (2006) Methods for evaluating human impact on soil microorganisms based on their activity, biomass, and diversity in agricultural soils. *Journal of Plant Nutrition and Soil Science*, **169**, 295–309.

Johansson, J.F., Paul, L.R. and Finlay, R.D. (2004) Microbial interactions in the mycorrhizosphere and their significance for sustainable agriculture. *FEMS Microbiol Ecol*, **48**, 1–13.

Joshi, F., Archana, G. and Desai, A. (2006) Siderophore Cross-Utilization Amongst Rhizospheric Bacteria and the Role of Their Differential Affinities for Fe^{3+} on Growth Stimulation Under Iron-Limited Conditions. *Curr Microbiol*, **53**, 141.

Jumpponen, A. and Jones, K.L. (2009) Massively parallel 454 sequencing indicates hyperdiverse fungal communities in temperate *Quercus macrocarpa* phyllosphere. *New Phytologist*, **184**, 438–448.

Jurkevitch, E., Minz, D., Ramati, B. and Barel, G. (2000) Prey Range Characterization, Ribotyping, and Diversity of Soil and Rhizosphere *Bdellovibrio spp*. Isolated on Phytopathogenic Bacteria. *Appl. Environ. Microbiol.*, **66**, 2365–2371.

Kamoun, S., Furzer, O., Jones, J.D.G., *et al.* (2015) The Top 10 oomycete pathogens in molecular plant pathology. *Molecular Plant Pathology*, **16**, 413–434.

Kamoun, S., Hraber, P., Sobral, B., Nuss, D. and Govers, F. (1999) Initial Assessment of Gene Diversity for the Oomycete Pathogen *Phytophthora infestans* Based on Expressed Sequences. *Fungal Genetics and Biology*, **28**, 94–106.

Kato, H., Mori, H., Maruyama, F., *et al.* (2015) Time-series metagenomic analysis reveals robustness of soil microbiome against chemical disturbance. *DNA Res*, **22**, 413–424.

Kembel, S.W., O'Connor, T.K., Arnold, H.K., Hubbell, S.P., Wright, S.J. and Green, J.L. (2014) Relationships between phyllosphere bacterial communities and plant functional traits in a neotropical forest. *PNAS*, **111**, 13715–13720.

Kemen, E. (2014) Microbe–microbe interactions determine oomycete and fungal host colonization. *Current Opinion in Plant Biology*, **20**, 75–81.

Kia, S.H., Glynou, K., Nau, T., Thines, M., Piepenbring, M. and Maciá-Vicente, J.G. (2017) Influence of phylogenetic conservatism and trait convergence on the interactions between fungal root endophytes and plants. *The ISME Journal*, **11**, 777–790.

Kobayashi, D.Y. and Crouch, J.A. (2009) Bacterial/Fungal Interactions: From Pathogens to Mutualistic Endosymbionts. *Annu. Rev. Phytopathol.*, **47**, 63–82.

Kohlmeier, S., Smits, T.H.M., Ford, R.M., Keel, C., Harms, H. and Wick, L.Y. (2005) Taking the Fungal Highway: Mobilization of Pollutant-Degrading Bacteria by Fungi. *Environ. Sci. Technol.*, **39**, 4640–4646.

Kremer, J.M., Paasch, B.C., Rhodes, D., Thireault, C., Froehlich, J.E., Schulze-Lefert, P., Tiedje, J.M. and He, S.Y. (2018) FlowPot axenic plant growth system for microbiota research. *bioRxiv*, 254953.

Krome, K., Rosenberg, K., Bonkowski, M. and Scheu, S. (2009) Grazing of protozoa on rhizosphere bacteria alters growth and reproduction of *Arabidopsis thaliana*. *Soil Biology and Biochemistry*, **41**, 1866–1873.

Labbé, J.L., Weston, D.J., Dunkirk, N., Pelletier, D.A. and Tuskan, G.A. (2014) Newly identified helper bacteria stimulate ectomycorrhizal formation in *Populus*. *Front Plant Sci*, **5**, 579.

Lackner, G., Moebius, N. and Hertweck, C. (2011) Endofungal bacterium controls its host by an *hrp* type III secretion system. *The ISME Journal*, **5**, 252–261.

Lascaris, D. and Deacon, J.W. (1991) Colonization of wheat roots from seed-applied spores of *Idriella* (*Microdochium*) *bolleyi*: A biocontrol agent of take-all. *Biocontrol Science and Technology*, **1**, 229–240.

Lauber, C.L., Hamady, M., Knight, R. and Fierer, N. (2009) Pyrosequencing-Based Assessment of Soil pH as a Predictor of Soil Bacterial Community Structure at the Continental Scale. *Appl. Environ. Microbiol.*, **75**, 5111–5120.

Layeghifard, M., Hwang, D.M. and Guttman, D.S. (2017) Disentangling Interactions in the Microbiome: A Network Perspective. *Trends in Microbiology*, **25**, 217–228.

Lebeis, S.L., Paredes, S.H., Lundberg, D.S., *et al.* (2015) Salicylic acid modulates colonization of the root microbiome by specific bacterial taxa. *Science*, **349**, 860–864.

Leff, J.W., Tredici, P.D., Friedman, W.E. and Fierer, N. (2015) Spatial structuring of bacterial communities within individual *Ginkgo biloba* trees. *Environmental Microbiology*, **17**, 2352–2361.

Lekberg, Y., Schnoor, T., Kjøller, R., Gibbons, S.M., Hansen, L.H., Al-Soud, W.A., Sørensen, S.J. and Rosendahl, S. (2012) 454-sequencing reveals stochastic local reassembly and high disturbance tolerance within arbuscular mycorrhizal fungal communities. *Journal of Ecology*, **100**, 151–160.

Leveau, J.H.J. and Preston, G.M. (2008) Bacterial mycophagy: definition and diagnosis of a unique bacterial–fungal interaction. *New Phytologist*, **177**, 859–876.

Lindahl, B.D., Nilsson, R.H., Tedersoo, L., *et al.* (2013) Fungal community analysis by high-throughput sequencing of amplified markers – a user's guide. *New Phytologist*, **199**, 288–299.

Links, M.G., Demeke, T., Gräfenhan, T., Hill, J.E., Hemmingsen, S.M. and Dumonceaux, T.J. (2014) Simultaneous profiling of seed-associated bacteria and fungi reveals antagonistic interactions between microorganisms within a shared epiphytic microbiome on Triticum and Brassica seeds. *New Phytologist*, **202**, 542–553.

Livak, K.J. and Schmittgen, T.D. (2001) Analysis of Relative Gene Expression Data Using Real-Time Quantitative PCR and the 2−ΔΔCT Method. *Methods*, **25**, 402–408.

Lozupone, C. and Knight, R. (2005) UniFrac: a New Phylogenetic Method for Comparing Microbial Communities. *Appl. Environ. Microbiol.*, **71**, 8228–8235.

Lundberg, D.S., Lebeis, S.L., Paredes, S.H., *et al.* (2012) Defining the core *Arabidopsis thaliana* root microbiome. *Nature*, **488**, 86–90.

Ma, L.-S., Hachani, A., Lin, J.-S., Filloux, A. and Lai, E.-M. (2014) *Agrobacterium tumefaciens* Deploys a Superfamily of Type VI Secretion DNase Effectors as Weapons for Interbacterial Competition In Planta. *Cell Host & Microbe*, **16**, 94–104.

Mackelprang, R., Waldrop, M.P., DeAngelis, K.M., David, M.M., Chavarria, K.L., Blazewicz, S.J., Rubin, E.M. and Jansson, J.K. (2011) Metagenomic analysis of a permafrost microbial community reveals a rapid response to thaw. *Nature*, **480**, 368–371.

Maida, I., Chiellini, C., Mengoni, A., Bosi, E., Firenzuoli, F., Fondi, M. and Fani, R. (2016) Antagonistic interactions between endophytic cultivable bacterial communities isolated from the medicinal plant Echinacea purpurea. *Environmental Microbiology*, **18**, 2357–2365.

Maignien, L., DeForce, E.A., Chafee, M.E., Eren, A.M. and Simmons, S.L. (2014) Ecological Succession and Stochastic Variation in the Assembly of *Arabidopsis thaliana* Phyllosphere Communities. *mBio*, **5**, e00682-13.

Marupakula, S., Mahmood, S. and Finlay, R.D. (2016) Analysis of single root tip microbiomes suggests that distinctive bacterial communities are selected by *Pinus sylvestris* roots colonized by different ectomycorrhizal fungi. *Environmental Microbiology*, **18**, 1470–1483.

Mendes, R., Kruijt, M., Bruijn, I. de, *et al.* (2011) Deciphering the Rhizosphere Microbiome for Disease-Suppressive Bacteria. *Science*, **332**, 1097–1100.

Mercado-Blanco, J. and Bakker, P.A.H.M. (2007) Interactions between plants and beneficial *Pseudomonas spp.*: exploiting bacterial traits for crop protection. *Antonie van Leeuwenhoek*, **92**, 367–389.

Moebius, N., Üzüm, Z., Dijksterhuis, J., Lackner, G. and Hertweck, C. (2014) Active invasion of bacteria into living fungal cells. *eLife Sciences*, **3**, e03007.

Moran, N.A. and Sloan, D.B. (2015) The Hologenome Concept: Helpful or Hollow? *PLOS Biology*, **13**, e1002311.

Morris, E.K., Caruso, T., Buscot, F., *et al.* (2014) Choosing and using diversity indices: insights for ecological applications from the German Biodiversity Exploratories. *Ecology and Evolution*, **4**, 3514–3524.

Morris, J.J., Lenski, R.E. and Zinser, E.R. (2012) The Black Queen Hypothesis: Evolution of Dependencies through Adaptive Gene Loss. *mBio*, **3**, e00036-12.

Mousa, W.K., Shearer, C., Limay-Rios, V., Ettinger, C.L., Eisen, J.A. and Raizada, M.N. (2016) Root-hair endophyte stacking in finger millet creates a physicochemical barrier to trap the fungal pathogen *Fusarium graminearum*. *Nat Microbiol*, **1**, 16167.

Murase, J., Noll, M. and Frenzel, P. (2006) Impact of Protists on the Activity and Structure of the Bacterial Community in a Rice Field Soil. *Appl Environ Microbiol*, **72**, 5436–5444.

Nadell, C.D., Xavier, J.B. and Foster, K.R. (2009) The sociobiology of biofilms. *FEMS Microbiol Rev*, **33**, 206–224.

Nagarajan, H., Embree, M., Rotaru, A.-E., Shrestha, P.M., Feist, A.M., Palsson, B.Ø., Lovley, D.R. and Zengler, K. (2013) Characterization and modelling of interspecies electron transfer mechanisms and microbial community dynamics of a syntrophic association. *Nature Communications*, **4**, 2809.

Naumann, M., Schüßler, A. and Bonfante, P. (2010) The obligate endobacteria of arbuscular mycorrhizal fungi are ancient heritable components related to the *Mollicutes*. *The ISME Journal*, **4**, 862–871.

Netzker, T., Fischer, J., Weber, J., Mattern, D.J., König, C.C., Valiante, V., Schroeckh, V. and Brakhage, A.A. (2015) Microbial communication leading to the activation of silent fungal secondary metabolite gene clusters. *Front. Microbiol.*, **6**

Nguyen, N.H. and Bruns, T.D. (2015) The Microbiome of *Pinus muricata* Ectomycorrhizae: Community Assemblages, Fungal Species Effects, and *Burkholderia* as Important Bacteria in Multipartnered Symbioses. *Microb Ecol*, **69**, 914–921.

Nilsson, R.H., Tedersoo, L., Ryberg, M., *et al.* (2015) A Comprehensive, Automatically Updated Fungal ITS Sequence Dataset for Reference-Based Chimera Control in Environmental Sequencing Efforts. *Microbes Environ*, **30**, 145–150.

Niu, B., Paulson, J.N., Zheng, X. and Kolter, R. (2017) Simplified and representative bacterial community of maize roots. *PNAS*, **114**, E2450–E2459.

Nobori, T., Velásquez, A.C., Wu, J., Kvitko, B.H., Kremer, J.M., Wang, Y., He, S.Y. and Tsuda, K. (2018) Transcriptome landscape of a bacterial pathogen under plant immunity. *PNAS*, 201800529.

Nuccio, E.E., Hodge, A., Pett-Ridge, J., Herman, D.J., Weber, P.K. and Firestone, M.K. (2013) An arbuscular mycorrhizal fungus significantly modifies the soil bacterial community and nitrogen cycling during litter decomposition. *Environmental Microbiology*, **15**, 1870–1881.

Nützmann, H.-W., Reyes-Dominguez, Y., Scherlach, K., et al. (2011) Bacteria-induced natural product formation in the fungus *Aspergillus nidulans* requires Saga/Ada-mediated histone acetylation. *PNAS*, **108**, 14282–14287.

Partida-Martinez, L.P. and Hertweck, C. (2005) Pathogenic fungus harbours endosymbiotic bacteria for toxin production. *Nature*, **437**, 884–888.

Partida-Martinez, L.P., Monajembashi, S., Greulich, K.-O. and Hertweck, C. (2007) Endosymbiont-Dependent Host Reproduction Maintains Bacterial-Fungal Mutualism. *Current Biology*, **17**, 773–777.

Paulson, J.N., Stine, O.C., Bravo, H.C. and Pop, M. (2013) Differential abundance analysis for microbial marker-gene surveys. *Nat. Methods*, **10**, 1200–1202.

Peay, K.G., Kennedy, P.G. and Talbot, J.M. (2016) Dimensions of biodiversity in the Earth mycobiome. *Nature Reviews Microbiology*, **14**, 434–447.

Peiffer, J.A., Spor, A., Koren, O., Jin, Z., Tringe, S.G., Dangl, J.L., Buckler, E.S. and Ley, R.E. (2013) Diversity and heritability of the maize rhizosphere microbiome under field conditions. *PNAS*, **110**, 6548–6553.

Peterson, S.B., Dunn, A.K., Klimowicz, A.K. and Handelsman, J. (2006) Peptidoglycan from *Bacillus cereus* Mediates Commensalism with Rhizosphere Bacteria from the Cytophaga-Flavobacterium Group. *Appl. Environ. Microbiol.*, **72**, 5421–5427.

Ploch, S., Rose, L.E., Bass, D. and Bonkowski, M. (2016) High Diversity Revealed in Leaf-Associated Protists (Rhizaria: Cercozoa) of Brassicaceae. *J Eukaryot Microbiol*, **63**, 635–641.

Ponomarova, O. and Patil, K.R. (2015) Metabolic interactions in microbial communities: untangling the Gordian knot. *Current Opinion in Microbiology*, **27**, 37–44.

Raaijmakers, J.M., Vlami, M. and Souza, J.T. de (2002) Antibiotic production by bacterial biocontrol agents. *Antonie Van Leeuwenhoek*, **81**, 537.

Rastogi, G., Coaker, G.L. and Leveau, J.H.J. (2013) New insights into the structure and function of phyllosphere microbiota through high-throughput molecular approaches. *FEMS Microbiol Lett*, **348**, 1–10.

Raynaud, X. and Nunan, N. (2014) Spatial Ecology of Bacteria at the Microscale in Soil. *PLOS ONE*, **9**, e87217.

Records, A.R. (2011) The Type VI Secretion System: A Multipurpose Delivery System with a Phage-Like Machinery. *MPMI*, **24**, 751–757.

Redford, A.J., Bowers, R.M., Knight, R., Linhart, Y. and Fierer, N. (2010) The ecology of the phyllosphere: geographic and phylogenetic variability in the distribution of bacteria on tree leaves. *Environ Microbiol*, **12**, 2885–2893.

Redford, A.J. and Fierer, N. (2009) Bacterial Succession on the Leaf Surface: A Novel System for Studying Successional Dynamics. *Microb Ecol*, **58**, 189–198.

Reinhold-Hurek, B., Bünger, W., Burbano, C.S., Sabale, M. and Hurek, T. (2015) Roots Shaping Their Microbiome: Global Hotspots for Microbial Activity. *Annual Review of Phytopathology*, **53**, 403–424.

Reis, P., Cabral, A., Nascimento, T., Oliveira, H. and Rego, C. (2013) Diversity of *Ilyonectria* species in a young vineyard affected by black foot disease. *Phytopathologia Mediterranea*, **52**, 335–346.

Rezki, S., Campion, C., Iacomi-Vasilescu, B., et al. (2016) Differences in stability of seed-associated microbial assemblages in response to invasion by phytopathogenic microorganisms. *PeerJ*, **4**, e1923.

Rezzonico, F., Binder, C., Défago, G. and Moënne-Loccoz, Y. (2005) The Type III Secretion System of Biocontrol *Pseudomonas fluorescens* KD Targets the Phytopathogenic Chromista *Pythium ultimum* and Promotes Cucumber Protection. *MPMI*, **18**, 991–1001.

Ritpitakphong, U., Falquet, L., Vimoltust, A., Berger, A., Métraux, J.-P. and L'Haridon, F. (2016a) The microbiome of the leaf surface of *Arabidopsis* protects against a fungal pathogen. *New Phytologist*, **210**, 1033–1043.

Rolli, E., Marasco, R., Vigani, G., *et al.* (2015) Improved plant resistance to drought is promoted by the root-associated microbiome as a water stress-dependent trait. *Environmental Microbiology*, **17**, 316–331.

Rosenberg, K., Bertaux, J., Krome, K., Hartmann, A., Scheu, S. and Bonkowski, M. (2009) Soil amoebae rapidly change bacterial community composition in the rhizosphere of *Arabidopsis thaliana*. *ISME J*, **3**, 675–684.

Rousk, J., Bååth, E., Brookes, P.C., Lauber, C.L., Lozupone, C., Caporaso, J.G., Knight, R. and Fierer, N. (2010) Soil bacterial and fungal communities across a pH gradient in an arable soil. *The ISME Journal*, **4**, 1340–1351.

Rudnick, M.B., Veen, J.A. van and Boer, W. de (2015) Baiting of rhizosphere bacteria with hyphae of common soil fungi reveals a diverse group of potentially mycophagous secondary consumers. *Soil Biology and Biochemistry*, **88**, 73–82.

Ruiz-Herrera, J., León-Ramírez, C., Vera-Nuñez, A., Sánchez-Arreguín, A., Ruiz-Medrano, R., Salgado-Lugo, H., Sánchez-Segura, L. and Peña-Cabriales, J.J. (2015) A novel intracellular nitrogen-fixing symbiosis made by *Ustilago maydis* and Bacillus spp. *New Phytologist*, **207**, 769–777.

Rypien, K.L., Ward, J.R. and Azam, F. (2010) Antagonistic interactions among coral-associated bacteria. *Environmental Microbiology*, **12**, 28–39.

Sanchez-Vallet, A., Ramos, B., Bednarek, P., López, G., Piślewska-Bednarek, M., Schulze-Lefert, P. and Molina, A. (2010) Tryptophan-derived secondary metabolites in *Arabidopsis thaliana* confer non-host resistance to necrotrophic *Plectosphaerella cucumerina* fungi. *The Plant Journal*, **63**, 115–127.

Santhanam, R., Luu, V.T., Weinhold, A., Goldberg, J., Oh, Y. and Baldwin, I.T. (2015) Native root-associated bacteria rescue a plant from a sudden-wilt disease that emerged during continuous cropping. *PNAS*, **112**, E5013–E5020.

Sapp, M., Ploch, S., Fiore-Donno, A.M., Bonkowski, M. and Rose, L.E. (2018) Protists are an integral part of the *Arabidopsis thaliana* microbiome. *Environmental Microbiology*, **20**, 30–43.

Sato, Y., Narisawa, K., Tsuruta, K., Umezu, M., Nishizawa, T., Tanaka, K., Yamaguchi, K., Komatsuzaki, M. and Ohta, H. (2010) Detection of Betaproteobacteria inside the Mycelium of the Fungus *Mortierella elongata*. *Microbes and Environments*, **25**, 321–324.

Schaad, N.W., Postnikova, E. and Randhawa, P. (2003) Emergence of *Acidovorax avenae* subsp*. citrulli* as a Crop Threatening Disease of Watermelon and Melon. In

N. S. Iacobellis, A. Collmer, S. W. Hutcheson, *et al.,* eds. *Pseudomonas syringae and related pathogens*. Springer Netherlands, pp. 573–581.

Schlaeppi, K., Dombrowski, N., Oter, R.G., Themaat, E.V.L. van and Schulze-Lefert, P. (2014) Quantitative divergence of the bacterial root microbiota in *Arabidopsis thaliana* relatives. *PNAS*, **111**, 585–592.

Schmidt, R., Etalo, D.W., Jager, V. de, Gerards, S., Zweers, H., Boer, W. de and Garbeva, P. (2016) Microbial Small Talk: Volatiles in Fungal–Bacterial Interactions. *Front. Microbiol.*, **6**.

Schroeckh, V., Scherlach, K., Nützmann, H.-W., Shelest, E., Schmidt-Heck, W., Schuemann, J., Martin, K., Hertweck, C. and Brakhage, A.A. (2009) Intimate bacterial-fungal interaction triggers biosynthesis of archetypal polyketides in *Aspergillus nidulans*. *Proc. Natl. Acad. Sci. U.S.A.*, **106**, 14558–14563.

Schulz-Bohm, K., Geisen, S., Wubs, E.R.J., Song, C., Boer, W. de and Garbeva, P. (2017) The prey's scent – Volatile organic compound mediated interactions between soil bacteria and their protist predators. *The ISME Journal*, **11**, 817–820.

Sender, R., Fuchs, S. and Milo, R. (2016) Are We Really Vastly Outnumbered? Revisiting the Ratio of Bacterial to Host Cells in Humans. *Cell*, **164**, 337–340.

Shabuer, G., Ishida, K., Pidot, S.J., Roth, M., Dahse, H.-M. and Hertweck, C. (2015) Plant pathogenic anaerobic bacteria use aromatic polyketides to access aerobic territory. *Science*, **350**, 670–674.

Shakya, M., Gottel, N., Castro, H., ***et al.*** (2013) A Multifactor Analysis of Fungal and Bacterial Community Structure in the Root Microbiome of Mature *Populus deltoides* Trees. *PLOS ONE*, **8**, e76382.

Sharma, M., Schmid, M., Rothballer, M., et al. (2008) Detection and identification of bacteria intimately associated with fungi of the order Sebacinales. *Cellular Microbiology*, **10**, 2235–2246.

Scheublin, T.R., Sanders, I.R., Keel, C. and Meer, J.R. van der (2010) Characterisation of microbial communities colonising the hyphal surfaces of arbuscular mycorrhizal fungi. *The ISME Journal*, **4**, 752–763.

Shi, S., Nuccio, E., Herman, D.J., ***et al.*** (2015) Successional Trajectories of Rhizosphere Bacterial Communities over Consecutive Seasons. *mBio*, **6**, e00746-15.

Song, C., Schmidt, R., Jager, V. de, et al. (2015) Exploring the genomic traits of fungus-feeding bacterial genus *Collimonas*. *BMC Genomics*, **16**, 1103.

Steidle, A., Sigl, K., Schuhegger, R., ***et al.*** (2001) Visualization of N-Acylhomoserine Lactone-Mediated Cell-Cell Communication between Bacteria Colonizing the Tomato Rhizosphere. *Appl. Environ. Microbiol.*, **67**, 5761–5770.

Stringlis, I.A., Proietti, S., Hickman, R., Verk, M.C.V., Zamioudis, C. and Pieterse, C.M.J. (2018) Root transcriptional dynamics induced by beneficial rhizobacteria and microbial immune elicitors reveal signatures of adaptation to mutualists. *The Plant Journal*, **93**, 166–180.

Svenningsen, N.B., Watts-Williams, S.J., Joner, E.J., Battini, F., Efthymiou, A., Cruz-Paredes, C., Nybroe, O. and Jakobsen, I. (2018) Suppression of the activity of arbuscular mycorrhizal fungi by the soil microbiota. *The ISME Journal*, **12**, 1296–1307.

Takken, F. and Rep, M. (2010) The arms race between tomato and *Fusarium oxysporum*. *Molecular Plant Pathology*, **11**, 309–314.

Talbot, J.M., Bruns, T.D., Taylor, J.W., ***et al.*** (2014) Endemism and functional convergence across the North American soil mycobiome. *PNAS*, **111**, 6341–6346.

Tedersoo, L., Bahram, M., Põlme, S., ***et al.*** (2014) Global diversity and geography of soil fungi. *Science*, **346**, 1256688.

Thompson, L.R., Sanders, J.G., McDonald, D., ***et al.*** (2017) A communal catalogue reveals Earth’s multiscale microbial diversity. *Nature*, **551**, 457–463.

Toju, H., Kishida, O., Katayama, N. and Takagi, K. (2016) Networks Depicting the Fine-Scale Co-Occurrences of Fungi in Soil Horizons. *PLoS ONE*, **11**, e0165987.

Toju, H., Sato, H., Yamamoto, S., Kadowaki, K., Tanabe, A.S., Yazawa, S., Nishimura, O. and Agata, K. (2013) How are plant and fungal communities linked to each other in belowground ecosystems? A massively parallel pyrosequencing analysis of the association specificity of root-associated fungi and their host plants. *Ecol Evol*, **3**, 3112–3124.

Toljander, J.F., Lindahl, B.D., Paul, L.R., Elfstrand, M. and Finlay, R.D. (2007) Influence of arbuscular mycorrhizal mycelial exudates on soil bacterial growth and community structure. *FEMS Microbiol Ecol*, **61**, 295–304.

Tyc, O., Berg, M. van den, Gerards, S., Veen, J.A. van, Raaijmakers, J.M., Boer, W. de and Garbeva, P. (2014) Impact of interspecific interactions on antimicrobial activity among soil bacteria. *Front Microbiol*, **5**, 567.

Tyc, Olaf, Song, C., Dickschat, J.S., Vos, M. and Garbeva, P. (2017) The Ecological Role of Volatile and Soluble Secondary Metabolites Produced by Soil Bacteria. *Trends in Microbiology*, **25**, 280–292.

Uroz, S., Oger, P., Morin, E. and Frey-Klett, P. (2012) Distinct Ectomycorrhizospheres Share Similar Bacterial Communities as Revealed by Pyrosequencing-Based Analysis of 16S rRNA Genes. *Appl. Environ. Microbiol.*, **78**, 3020–3024.

Van Acker, H., Van Dijck, P. and Coenye, T. (2014) Molecular mechanisms of antimicrobial tolerance and resistance in bacterial and fungal biofilms. *Trends in Microbiology*, **22**, 326–333.

Van Buyten, E. and Höfte, M. (2013) *Pythium* species from rice roots differ in virulence, host colonization and nutritional profile. *BMC Plant Biology*, **13**, 203.

Van der Ent, S., Van Wees, S.C.M. and Pieterse, C.M.J. (2009) Jasmonate signaling in plant interactions with resistance-inducing beneficial microbes. *Phytochemistry*, **70**, 1581–1588.

Vandenkoornhuyse, P., Quaiser, A., Duhamel, M., Van, A.L. and Dufresne, A. (2015) The importance of the microbiome of the plant holobiont. *New Phytologist*, **206**, 1196–1206.

Vik, U., Logares, R., Blaalid, R., Halvorsen, R., Carlsen, T., Bakke, I., Kolstø, A.-B., Økstad, O.A. and Kauserud, H. (2013) Different bacterial communities in ectomycorrhizae and surrounding soil. *Scientific Reports*, **3**, 3471.

Vorholt, J.A., Vogel, C., Carlström, C.I. and Müller, D.B. (2017) Establishing Causality: Opportunities of Synthetic Communities for Plant Microbiome Research. *Cell Host & Microbe*, **22**, 142–155.

Wagner, M.R., Lundberg, D.S., Del Rio, T.G., Tringe, S.G., Dangl, J.L. and Mitchell-Olds, T. (2016) Host genotype and age shape the leaf and root microbiomes of a wild perennial plant. *Nat Commun*, **7**, 12151.

Wandersman, C. and Delepelaire, P. (2004) Bacterial Iron Sources: From Siderophores to Hemophores. *Annu. Rev. Microbiol.*, **58**, 611–647.

Wang, J., Shen, J., Wu, Y., *et al.* (2013) Phylogenetic beta diversity in bacterial assemblages across ecosystems: deterministic versus stochastic processes. *The ISME Journal*, **7**, 1310–1321.

Wang, Q., Garrity, G.M., Tiedje, J.M. and Cole, J.R. (2007) Naïve Bayesian Classifier for Rapid Assignment of rRNA Sequences into the New Bacterial Taxonomy. *Appl. Environ. Microbiol.*, **73**, 5261–5267.

Wang, S., Sun, B., Tu, J. and Lu, Z. (2016) Improving the microbial community reconstruction at the genus level by multiple 16S rRNA regions. *J Theor Biol*, **398**, 1–8.

Ward, N.L., Challacombe, J.F., Janssen, P.H., *et al.* (2009) Three Genomes from the Phylum Acidobacteria Provide Insight into the Lifestyles of These Microorganisms in Soils. *Appl. Environ. Microbiol.*, **75**, 2046–2056.

Warmink, J.A., Nazir, R. and Elsas, J.D.V. (2009) Universal and species-specific bacterial ‘fungiphiles’ in the mycospheres of different basidiomycetous fungi. *Environmental Microbiology*, **11**, 300–312.

Warmink, J.A. and Elsas, J.D. van (2009) Migratory Response of Soil Bacteria to Lyophyllum sp. Strain Karsten in Soil Microcosms. *Appl. Environ. Microbiol.*, **75**, 2820–2830.

Wei, Z., Yang, T., Friman, V.-P., Xu, Y., Shen, Q. and Jousset, A. (2015) Trophic network architecture of root-associated bacterial communities determines pathogen invasion and plant health. *Nature Communications*, **6**, 8413.

Whipps, J.M. (2001) Microbial interactions and biocontrol in the rhizosphere. *J Exp Bot*, **52**, 487–511.

Wick, L.Y., Remer, R., Würz, B., Reichenbach, J., Braun, S., Schäfer, F. and Harms, H. (2007) Effect of Fungal Hyphae on the Access of Bacteria to Phenanthrene in Soil. *Environ. Sci. Technol.*, **41**, 500–505.

Worrich, A., König, S., Miltner, A., *et al.* (2016) Mycelium-Like Networks Increase Bacterial Dispersal, Growth, and Biodegradation in a Model Ecosystem at Various Water Potentials. *Appl. Environ. Microbiol.*, **82**, 2902–2908.

Xin, X.-F. and He, S.Y. (2013) *Pseudomonas syringae pv. tomato* DC3000: A Model Pathogen for Probing Disease Susceptibility and Hormone Signaling in Plants. *Annual Review of Phytopathology*, **51**, 473–498.

Xu, L., Naylor, D., Dong, Z., *et al.* (2018) Drought delays development of the sorghum root microbiome and enriches for monoderm bacteria. *PNAS*, 201717308.

Xue, C., Penton, C.R., Shen, Z., Zhang, R., Huang, Q., Li, R., Ruan, Y. and Shen, Q. (2015) Manipulating the banana rhizosphere microbiome for biological control of Panama disease. *Scientific Reports*, **5**, 11124.

Yang, P., Zhang, M., Warmink, J.A., Wang, M. and Elsas, J.D. van (2016) The type three secretion system facilitates migration of *Burkholderia terrae* BS001 in the mycosphere of two soil-borne fungi. *Biol Fertil Soils*, **52**, 1037–1046.

Yeoh, Y.K., Dennis, P.G., Paungfoo-Lonhienne, C., Weber, L., Brackin, R., Ragan, M.A., Schmidt, S. and Hugenholtz, P. (2017) Evolutionary conservation of a core root microbiome across plant phyla along a tropical soil chronosequence. *Nature Communications*, **8**, 215.

Youle, M., Knowlton, N., Rohwer, F., Gordon, J. and Relman, D.A. (2013) Superorganisms and Holobionts: Looking for a term for the functional entity formed by a macrobe and its associated symbiotic microbes and viruses? The term is “holobiont.” *Microbe Magazine*, **8**, 152–153.

Zamioudis, C., Korteland, J., Pelt, J.A.V., *et al.* (2015) Rhizobacterial volatiles and photosynthesis-related signals coordinate MYB72 expression in *Arabidopsis* roots during onset of induced systemic resistance and iron-deficiency responses. *The Plant Journal*, **84**, 309–322.

Zarraonaindia, I., Owens, S.M., Weisenhorn, P., *et al.* (2015) The Soil Microbiome Influences Grapevine-Associated Microbiota. *mBio*, **6**, e02527-14.

Zelezniak, A., Andrejev, S., Ponomarova, O., Mende, D.R., Bork, P. and Patil, K.R. (2015) Metabolic dependencies drive species co-occurrence in diverse microbial communities. *PNAS*, **112**, 6449–6454.

Zhalnina, K., Louie, K.B., Hao, Z., *et al.* (2018) Dynamic root exudate chemistry and microbial substrate preferences drive patterns in rhizosphere microbial community assembly. *Nature Microbiology*, **3**, 470–480.

Zhang, J., Zhang, N., Liu, Y.-X., *et al.* (2018) Root microbiota shift in rice correlates with resident time in the field and developmental stage. *Sci. China Life Sci.*, 1–9.

Zhang, L., Xu, M., Liu, Y., Zhang, F., Hodge, A. and Feng, G. (2016) Carbon and phosphorus exchange may enable cooperation between an arbuscular mycorrhizal fungus and a phosphate-solubilizing bacterium. *New Phytologist*, **210**, 1022–1032.

Zhang, M., Silva, P. e, C, M. de, De Mares Maryam, C., Elsas, V. and Dirk, J. (2014) The mycosphere constitutes an arena for horizontal gene transfer with strong evolutionary implications for bacterial-fungal interactions. *FEMS Microbiol Ecol*, **89**, 516–526.

Zhang, Y., Kastman, E.K., Guasto, J.S. and Wolfe, B.E. (2018) Fungal networks shape dynamics of bacterial dispersal and community assembly in cheese rind microbiomes. *Nature Communications*, **9**, 336.

Supplementary figures and tables

Supplementary Figure 1

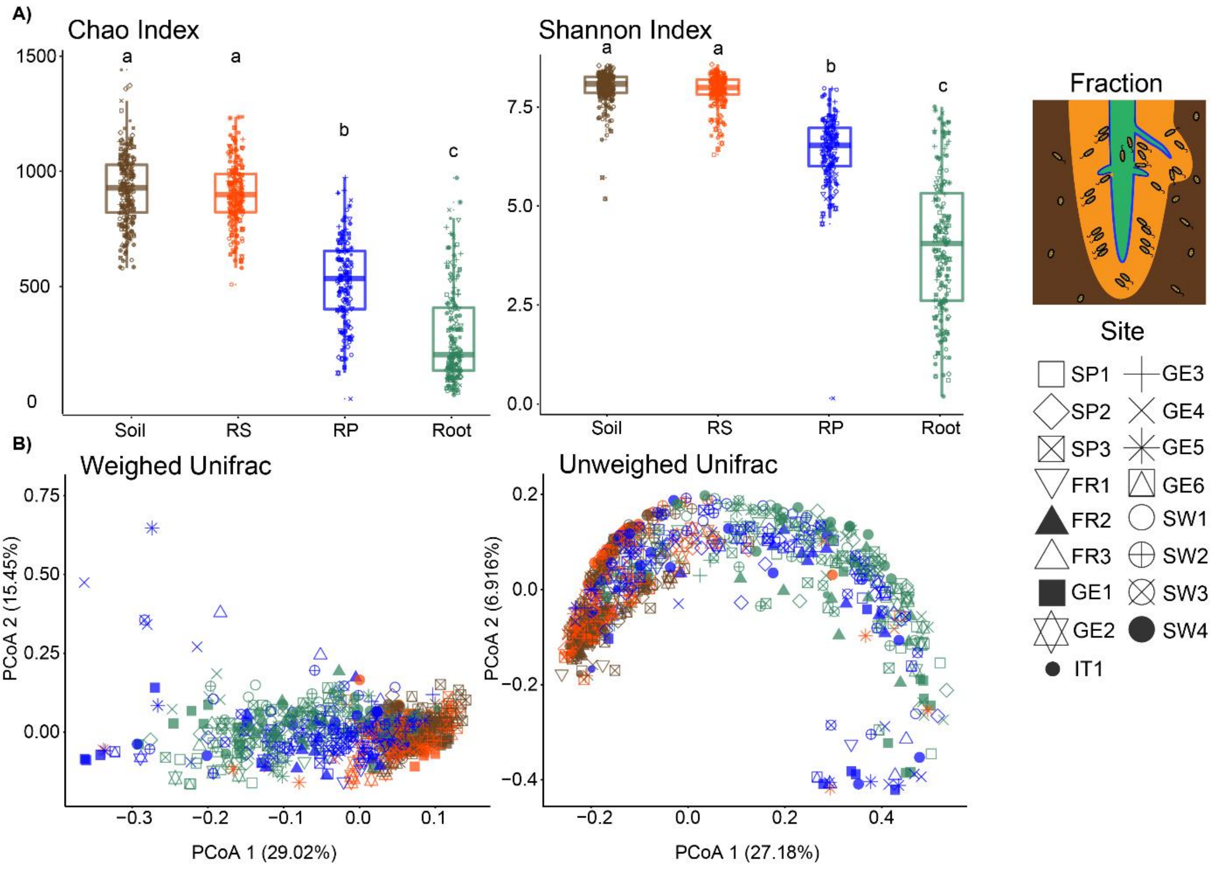

Supplementary Figure 1: Alternative methods to describe alpha- and beta-diversities in bacterial communities. A) Two additional alpha-diversity indices are shown here for all samples: Chao Index (indicates the predicted number of taxa by accounting for the rare taxa potentially missing due to under-sampling) and the Shannon Index (accounts for microbial abundance and evenness of the species). Significantly different values are depicted with different letters (Kruskal Wallis, Dunn test *post-hoc*, $p<0.05$). **B)** Two additional beta-diversity indices are shown here for all samples: Weighted Unifrac (quantifies the composition dissimilarity between two samples, based on counts on each sample and microbial taxonomy) and Unweighted Unifrac (accounts for taxonomy and absence/presence of certain OTUs). Samples are colored by fraction (Soil, RS, RP and Root), matching the cartoon in the right, and shaped by site.

Supplementary Figure 2

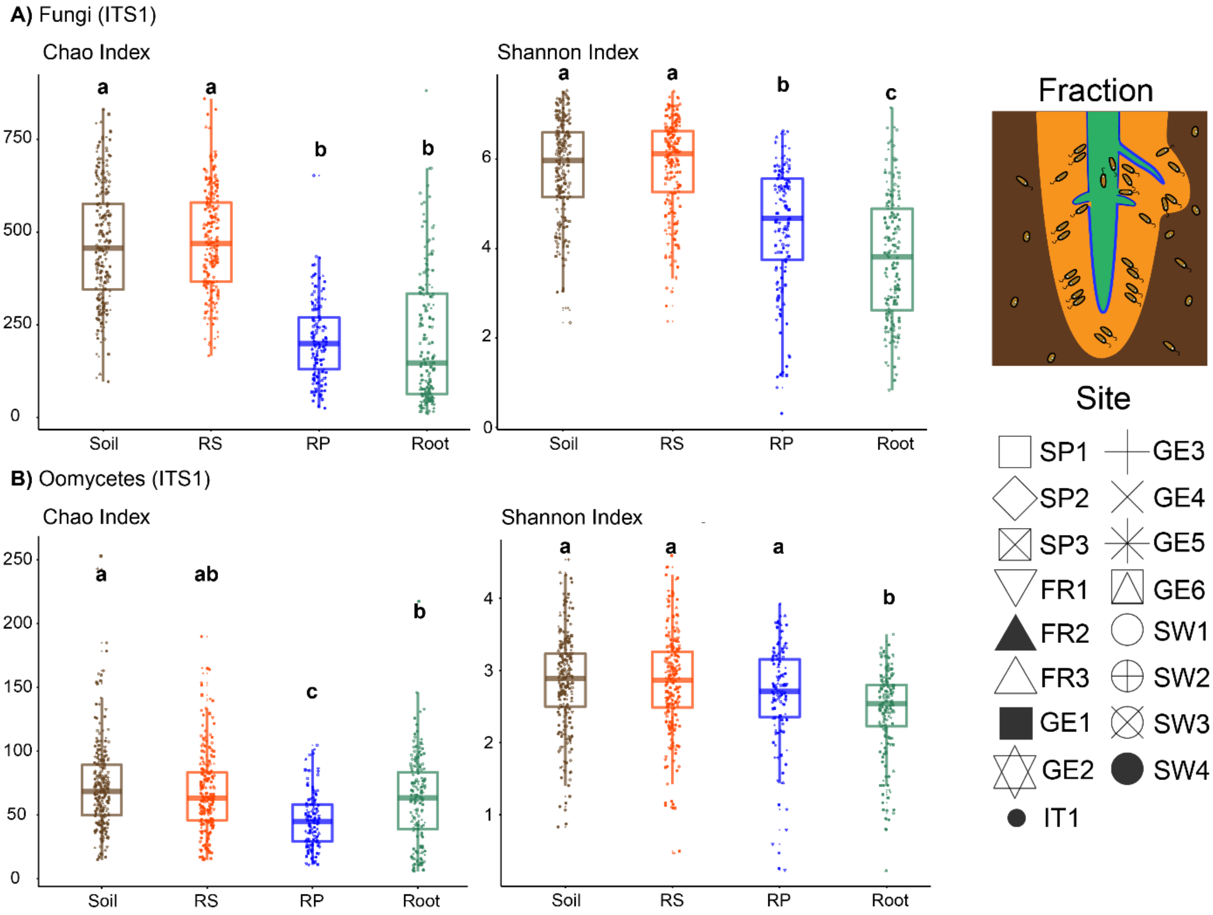

Supplementary Figure 2: Alternative methods to describe alpha-diversities in fungal and oomycetal communities. Two additional alpha-diversity indices are shown here for all samples: Chao Index (indicates the predicted number of taxa by accounting for the rare taxa potentially missing due to under-sampling) and the Shannon Index (accounts for microbial abundance and evenness of the species), for fungal **(A)** and oomycetal **(B)** communities. Significantly different values are depicted with different letters (Kruskal Wallis, Dunn test *post-hoc*, $p<0.05$). Samples are colored by the fraction they belong to, matching the cartoon on the right side, and shaped by the site.

Supplementary Figure 3

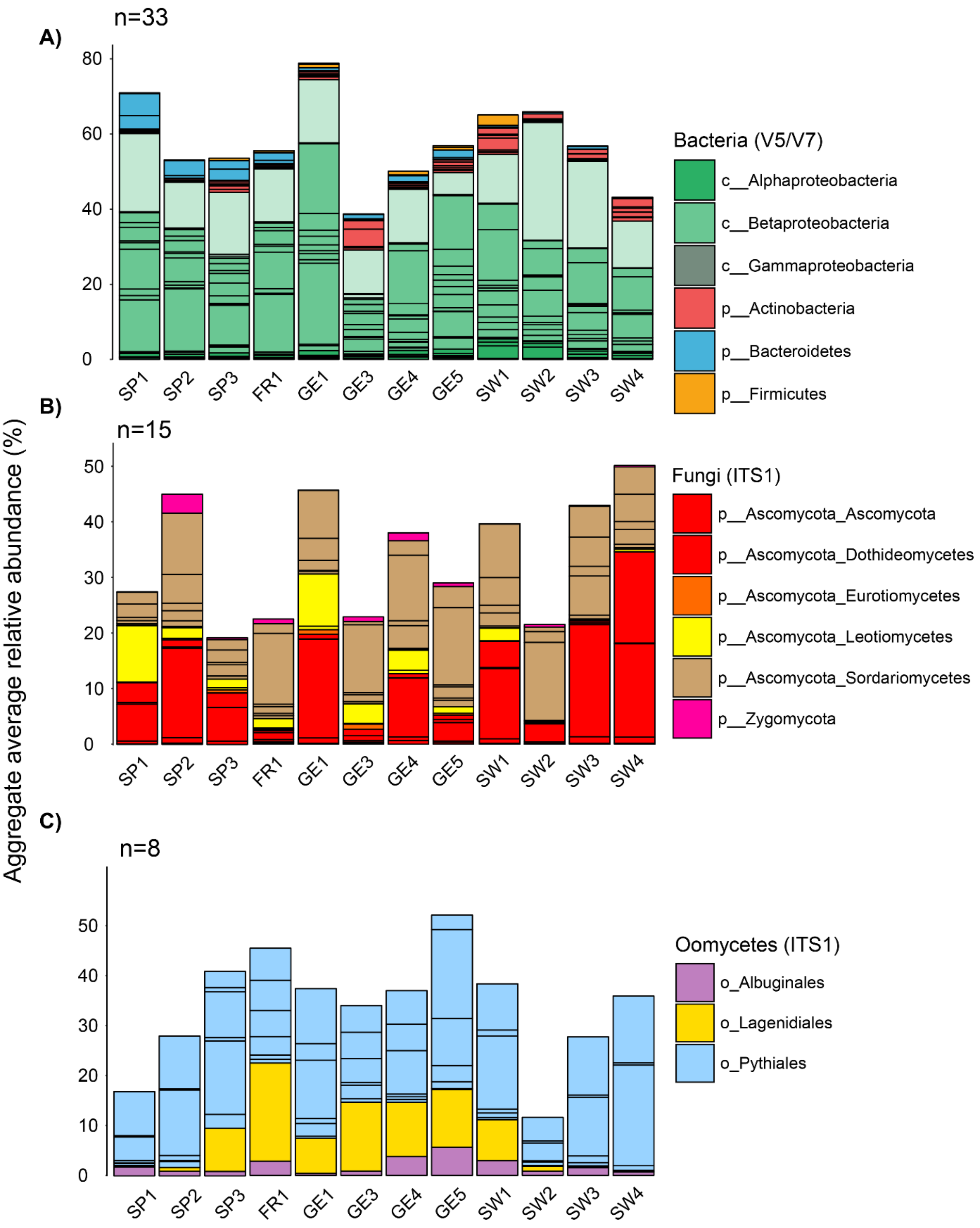

Supplementary Figure 3: **The Arabidopsis root core microbiota across Europe (2).** Aggregate average relative abundance of the bacterial **(A)**, fungal **(B)** and oomycetal **(C)** OTUs present all harvested years and in at least 50% of the samples in 75% of the sites (i.e.: at least in 9 sites out of 12). (”n” represents the number of OTUs that are present in all sites per microbial group). Each OTU (blocks within each bar) is colored by their taxonomic assignment, at phylum and class level for bacterial and fungal OTUs, and order level for oomycetal OTUs.

Supplementary Figure 4

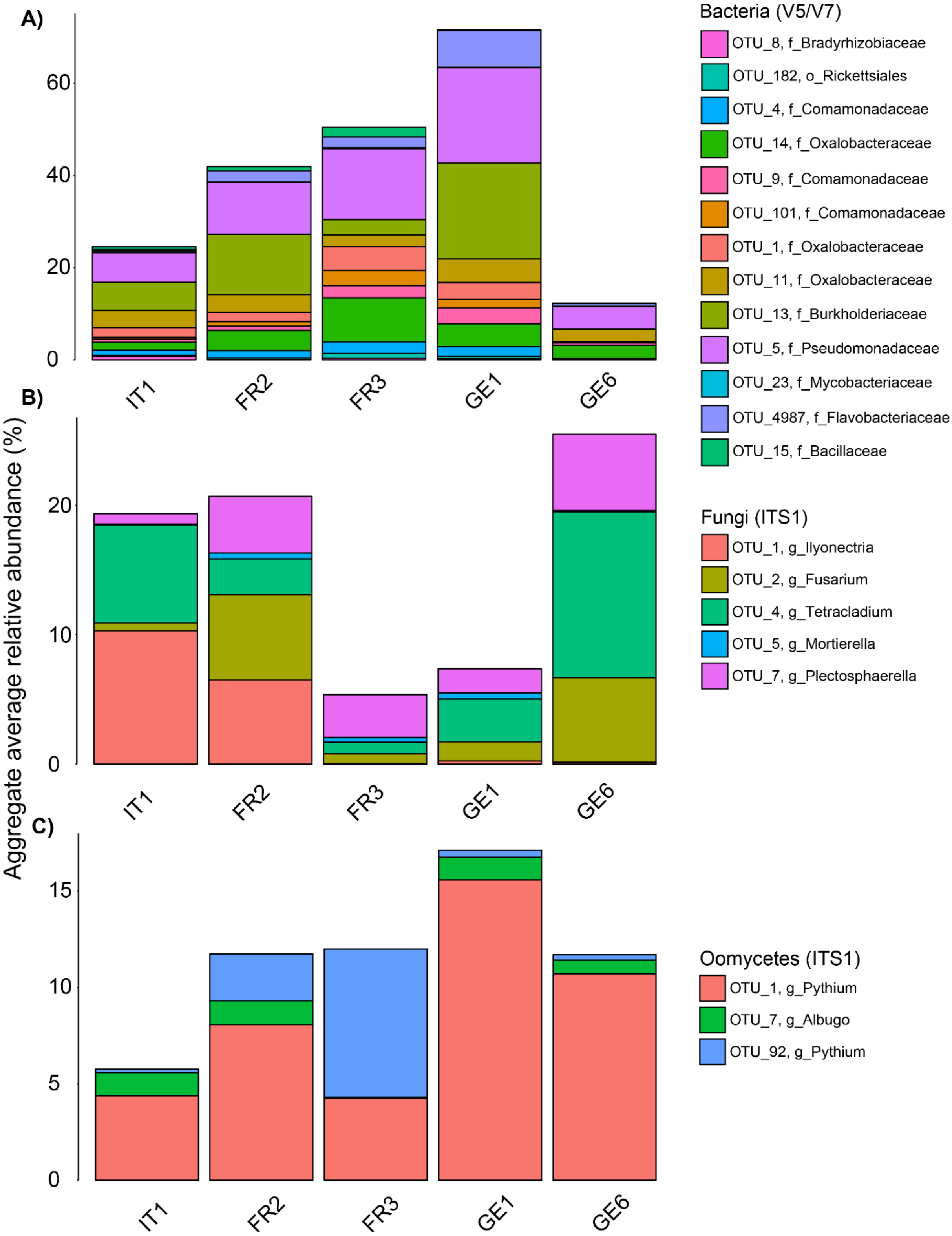

Supplementary Figure 4: The Arabidopsis root core microbiota across Europe (3). Aggregate average relative abundance of the bacterial **(A)**, fungal **(B)** and oomycetal **(C)** OTUs consistently found across root samples harvested all years and in at least half of the samples in each site (**Figure 8**). Here, these OTUs are also represented in the sites that were not harvested across three years (IT1, FR2, FR3, GE1 and GE6)

Supplementary Figure 5

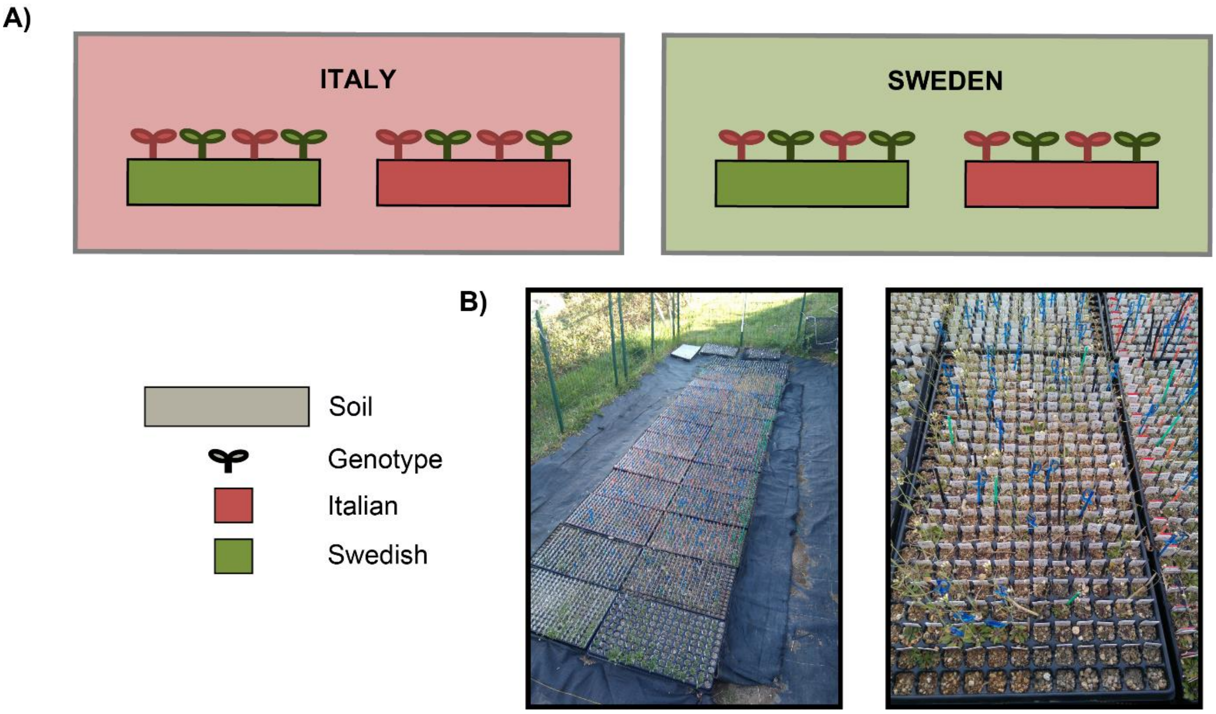

Supplementary Figure 5: *In-situ* common-garden experiment. In order to understand the role of climatic conditions and genotype-driven changes on soil and root-associated microbial communities, soils were planted with their adapted genotype (It15, It24, It32, It41, for Italian soil, and Sw7, Sw11, Sw43, Sw47 for Swedish soil) and the reciprocal genotypes, in IT1 (Castelnuovo di Porto, Italy) and in SW4 (Rödåsen, Sweden), as shown in the cartoon in (**A**). (**B**) shows how the trays looked like on site. *A.thaliana* plants underwent a full life cycle (from October 2016 to March 2017 in Italy, and to May 2017 in Sweden). After this period, plants and their surrounding soil were harvested for community profiling of bacterial, fungal and oomycetal communities. Also, plant fitness was assessed by scoring mature fruit production at the end of the experiment.

Supplementary Figure 6

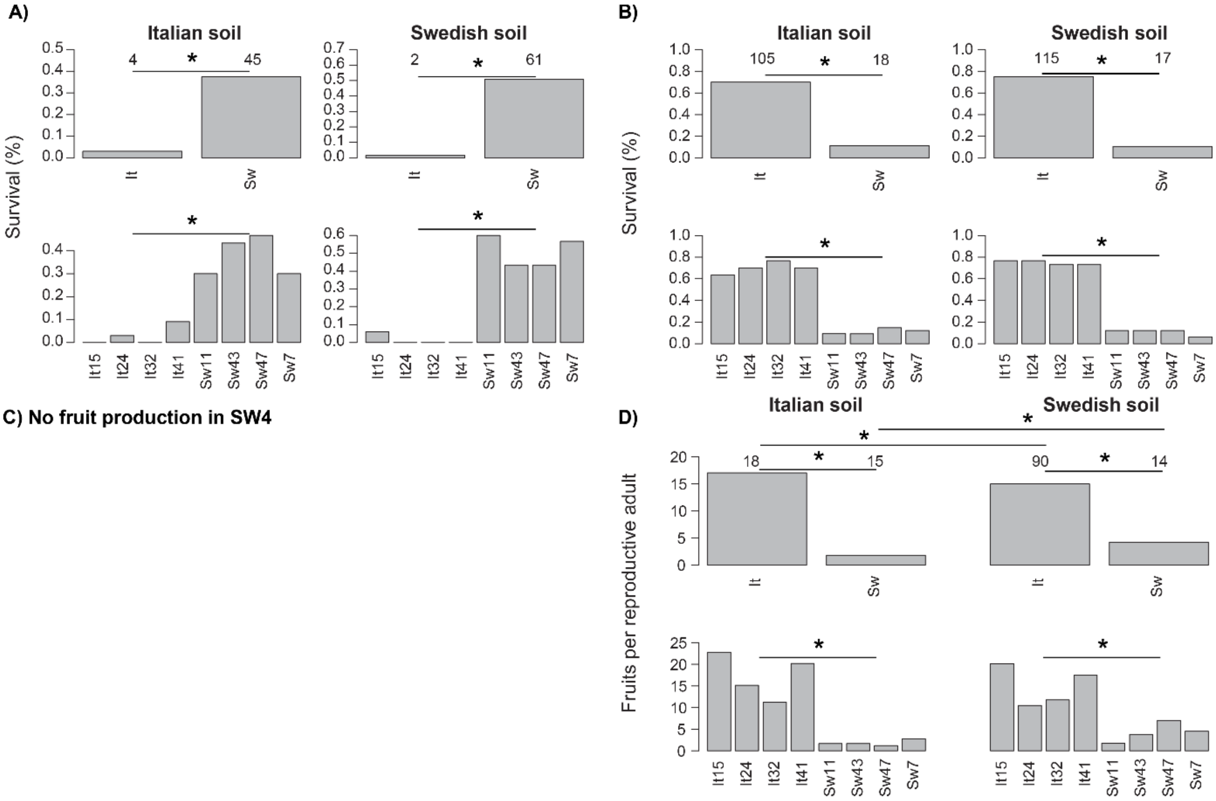

Supplementary Figure 6: Plant survival and fitness in common-garden experiment. Survival rate was calculated at the two sites (SW4, **A**; and IT1, **B**), as the percentage of plants that survived after winter compared to the number of plants established before winter time, pooling all parental lines (upper plot) and each parental lines separately (lower plot). In both sites, local *A. thaliana* accession had a higher survival than the foreign accession, but with no soil-driven effect (Generalized Linear Model, p-value<0.001). **C)** No Italian-genotype plants survived to fruit production stage and very few Swedish-genotype did. Therefore, no data was recorded for this site. **D)** Fruit number score at end-time of the experiment (only in IT1 April 2017) showed a significant advance for Italian parental lines compared to Swedish parental lines, especially in their own soil (Generalized Linear Model, p-value<0.001). Number on top of the bars indicate the number of plants evaluated. Analysis and figures by Dr. Thomas Ellis, University of Uppsala.

Supplementary Figure 7

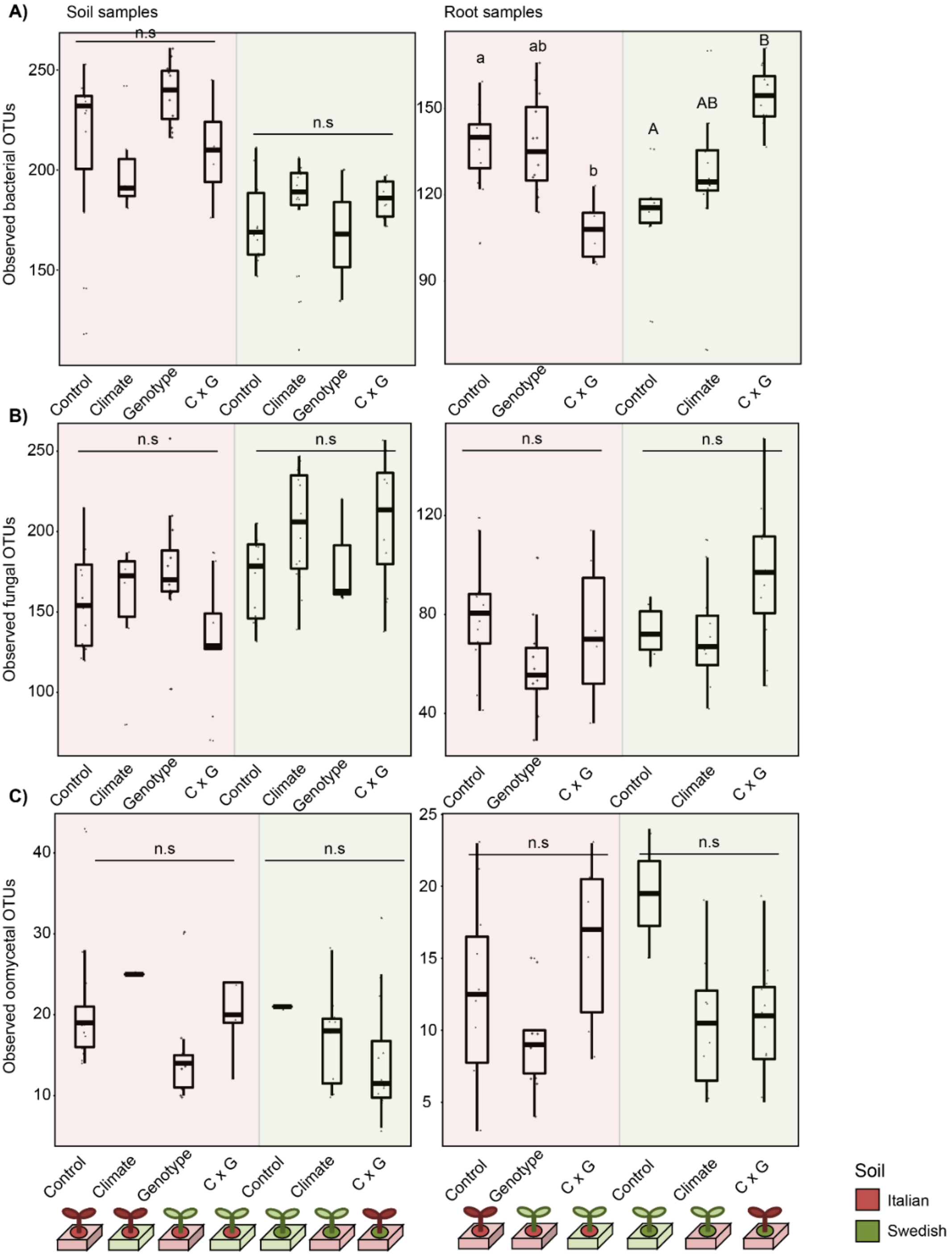

Supplementary Figure 7: Microbial alpha-diversity in the common-garden experiment. Plots depicting the Observed OTUs for bacterial **(A)**, fungal **(B)** and oomycetal **(C)** profiles, separated by fraction (soil samples, left panels; root samples, right panels) and by soil type (red background, Italian soil; green background, Swedish soil). Cartoons at the bottom show which conditions are changed, while soil (either Italian -red- or Swedish -green-) remains as the constant factor. Significantly different values are represented with different letters (note that statistical comparison are done within soil type, not across soil types. ANOVA, Tukey *post-hoc* test, p-value-<0.05).

Supplementary Figure 8

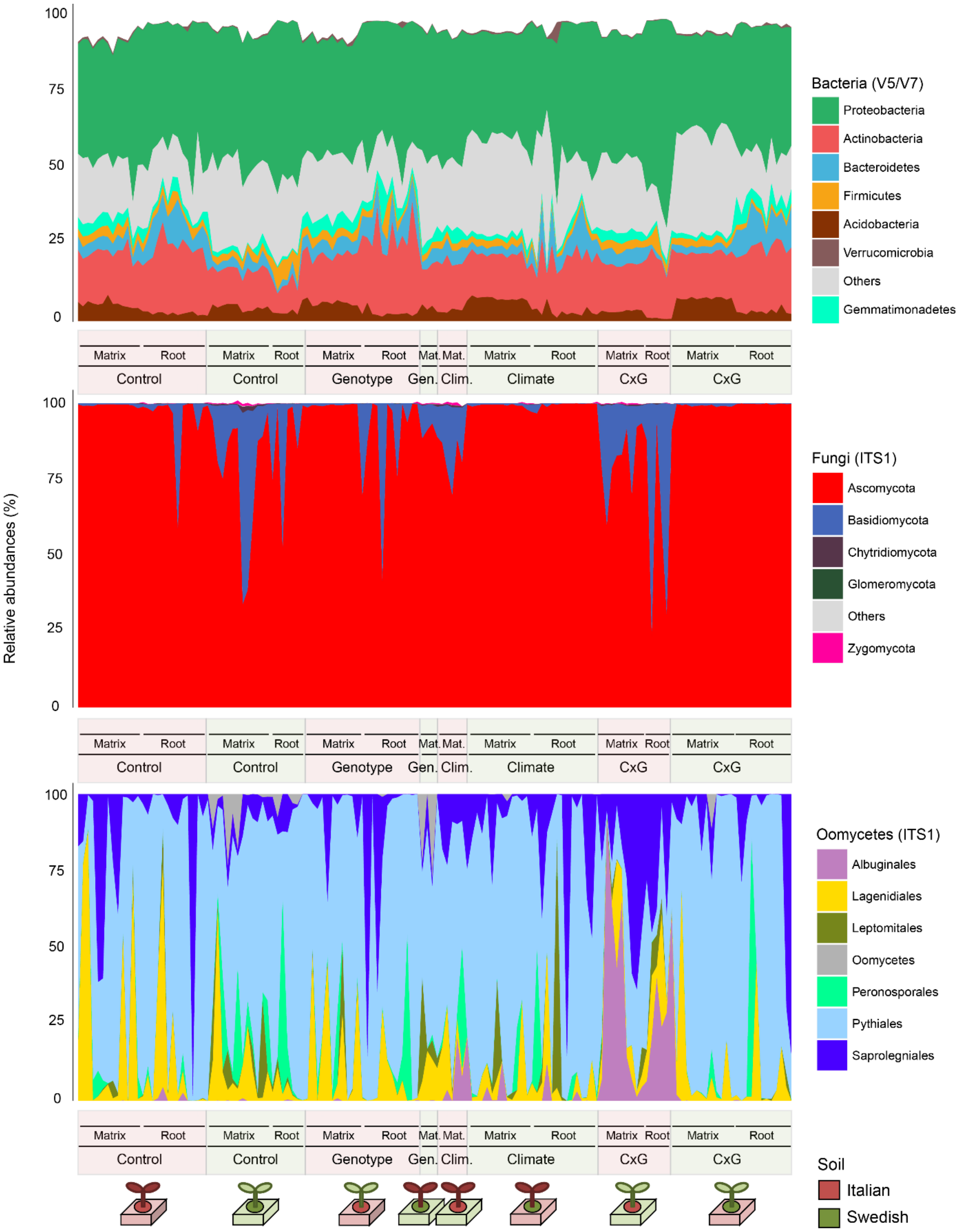

Supplementary Figure 8: Microbial relative abundances in common-garden experiment. Relative abundances plots are shown here of OTUs with an abundance of >0.01%, for bacterial **(A)**, fungal **(B)** and oomycetal **(C)** communities, colored by their taxonomic assignment (phylum level for bacterial and fungal profiles, and order level for oomycetal profiles). Colored boxes at the x axis' labels represent the soil which is being compared (red, Italian; green, Swedish) and the cartoons at the bottom represent the conditions that are represented in the plot.

Supplementary Figure 9

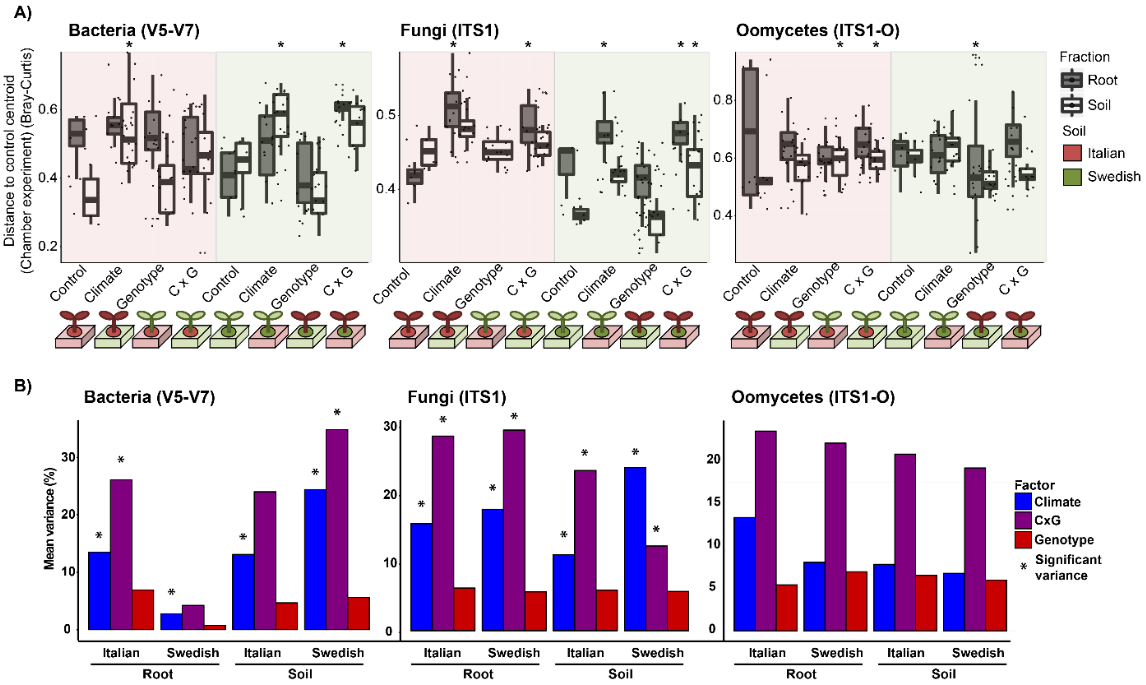

Supplementary Figure 9: Transplantation experiment under controlled conditions (climatic chambers). A) Plots depicting average Bray-Curtis distances between clusters of conditions (x axis) compared to the distance of the control cluster within itself, in bacterial, fungal and oomycetal profiles. Cartoons show which conditions are changed, while soil (either Italian -red- or Swedish -green-) remains as the constant factor. Asterisks indicate in which conditions microbial communities are significantly apart from the control cluster (Kruskal-Wallis, Dunn test *post-hoc*, p<0.05). **B)** Variance explained in microbial communities due to changing the Climate, Genotype or CxG. Due to the high variability in the samples and the very high impact of “Soil” and “Fraction” factors (not shown), data was subsetted and the variance was calculated as the average variance per factor (PERMANOVA, 95% interval of confidence, p-value<0.05).

Supplementary Figure 10

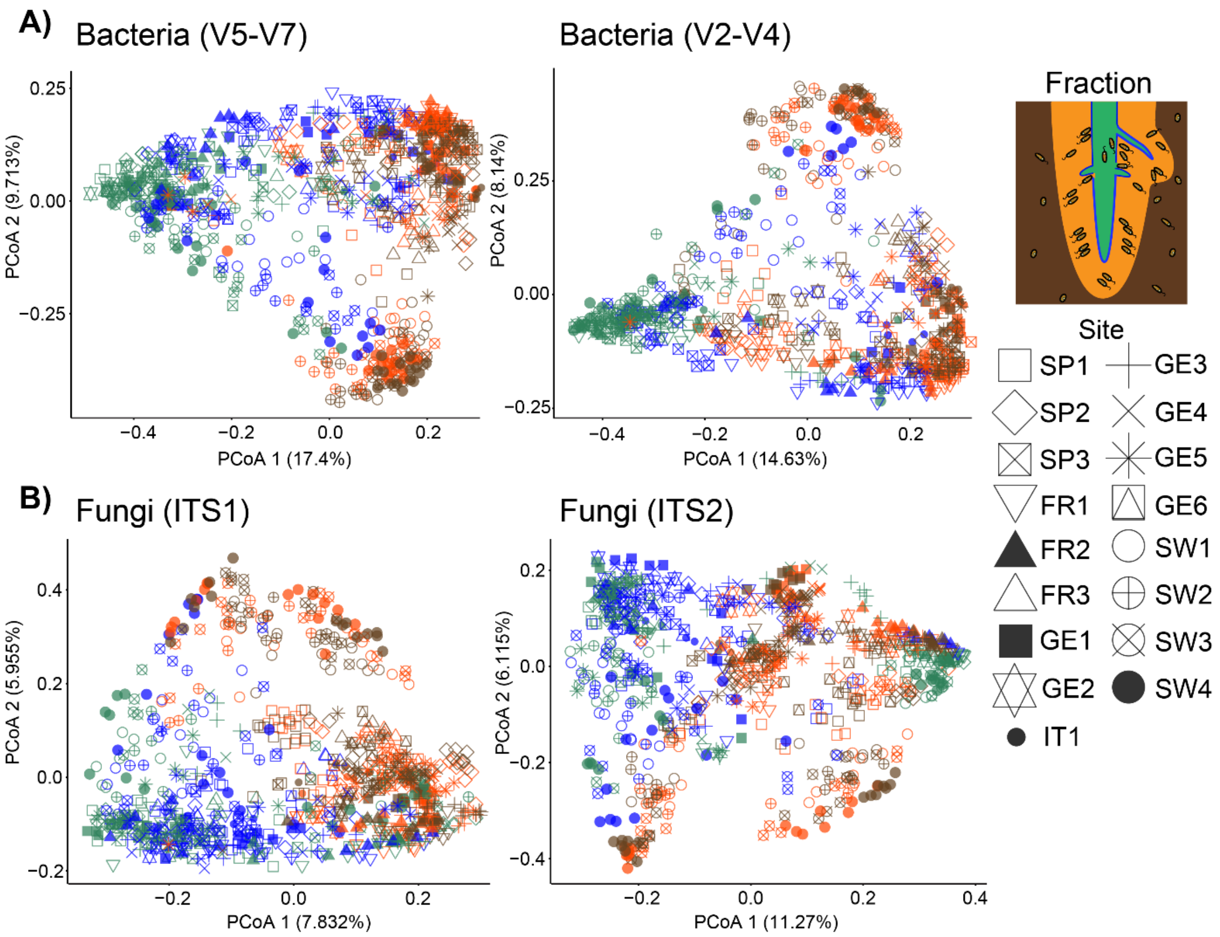

Supplementary Figure 10: Structure of bacterial and fungal communities using other DNA amplification regions. PCoA plots depicting Bray-Curtis dissimilarities between samples of the full dataset, comparing sample distribution using another DNA amplification region for bacteria (V5/V7 versus V2/V4, **A**) and for fungi (ITS1 versus ITS2). **B**). Samples are colored by the fraction they belong to, matching the cartoon on the right side, and shaped by site.

Supplementary Figure 11

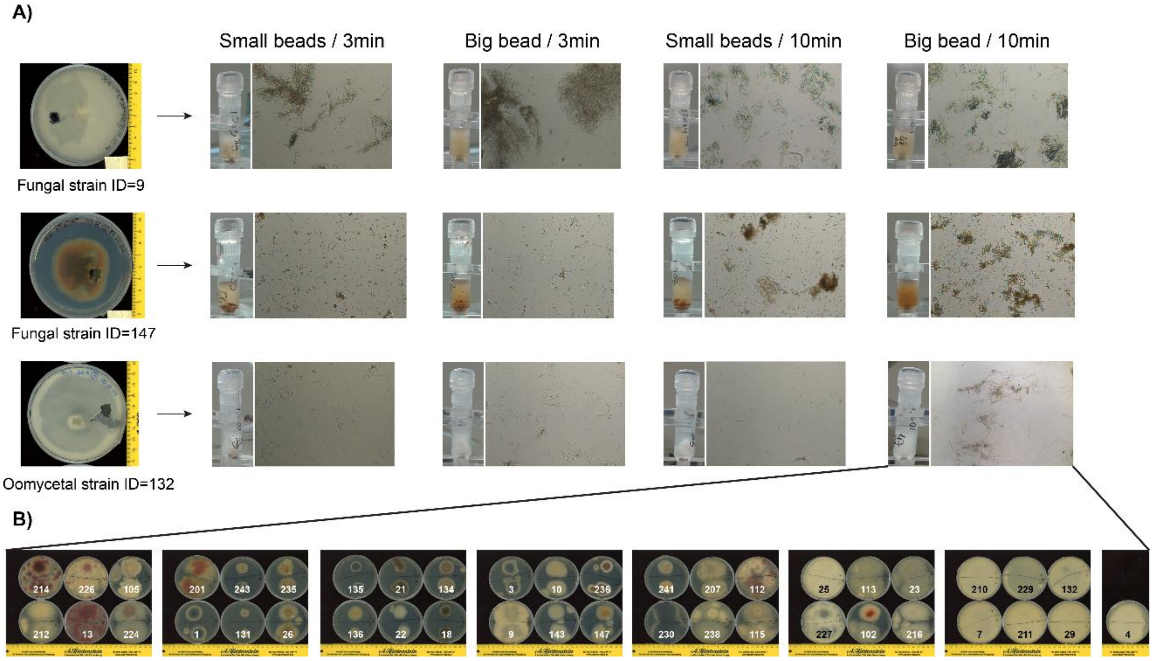
A)
Small beads / 3min
Big bead / 3min
Small beads / 10min
Big bead / 10min
Fungal strain ID=9
Fungal strain ID=147
Oomycetal strain ID=132
B)
214
226
105
212
13
224
201
243
235
1
131
26
135
21
134
136
22
18
3
10
236
9
143
147
241
207
112
230
238
115
25
113
23
227
102
216
210
229
132
7
211
29
4

Supplementary Figure 11: Grinding protocol development for filamentous microbe's inoculation. A) Three morphologically diverse fungal and oomycetes were tested (*Chaetomium megalocarpum*, 9; *Ilyonectria macrodidyma*, 147; *Pythium sylvaticum*, 132) with four grinding techniques (two beads sizes and two durations, with 1 mL of 10 mM $MgCl_2$). Each condition is depicted by the homogenate appearance in the tube and later observation of hyphae disaggregation under bright field microscope (5x). **B)** After selection of the last method (one big bead beating for 10 minutes), each of the microbes utilized for later experiments was tested for survival 7 days after the bead-beating and plated on PGA (white-labelled plates are fungal strains; black-labelled plates are oomycetal strains).

Supplementary Figure 12

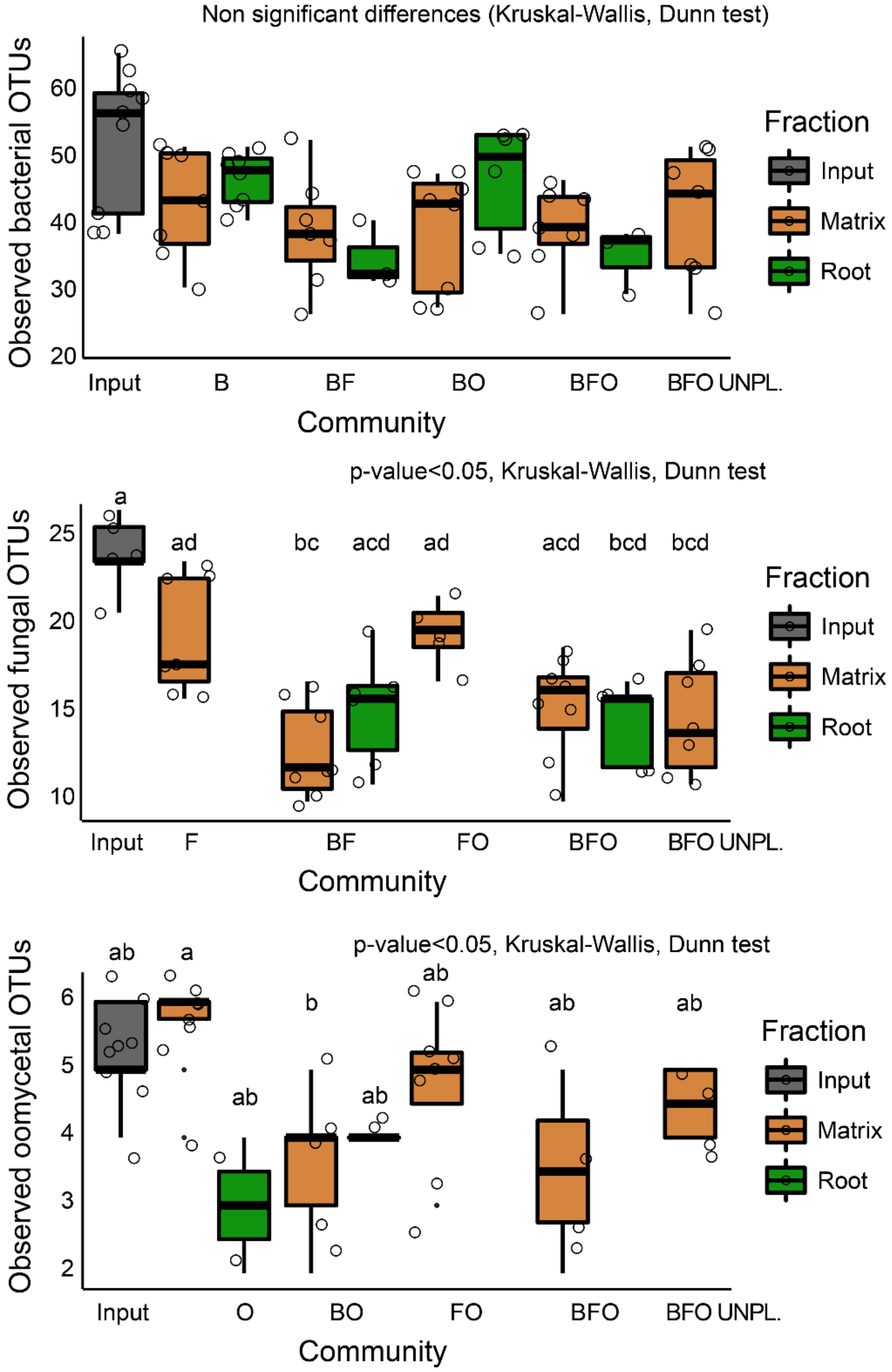

Supplementary Figure 12: Observed species in each microbial combination co-inoculated with *A.thaliana* Col-0 and unplanted control, compared to Input community. Plots depicting the observed OTUs in root and matrix samples, compared to initial OTUs in “Input” samples (in grey), for bacterial (**A**), fungal (**B**) and oomycetal (**C**) communities, in each microbial combination (B: Bacteria only, F: Fungi only, O: Oomycetes only, BO: Bacteria and oomycetes, BF: Bacteria and fungi, FO: Fungi and oomycetes, BFO: full microbial community, BFO UNPL.: full microbial community without host plant), in matrix (brown) and root (green samples). Significant differences are depicted with different letters (Kruskal-Wallis, Dunn test *post-hoc*, p<0.05)

Supplementary Figure 13

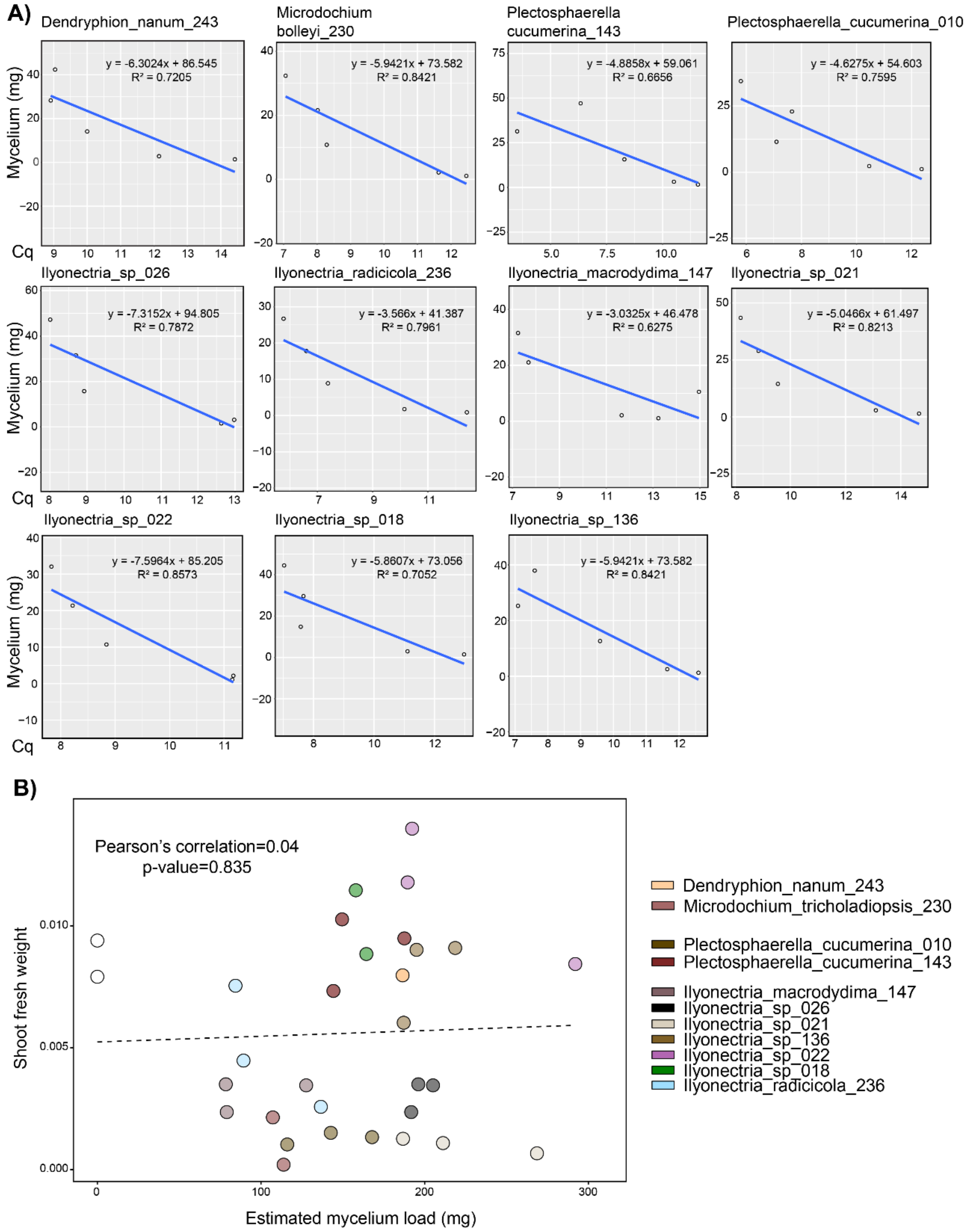

Supplementary Figure 13: Correlation between plant growth and fungal load. A) 50 mg of mycelium of each fungal strain was weighted and DNA was isolated. DNA concentration was correlated with Cq reads (using ITS1 as amplification region), in order to estimate mycelium load in gnotobiotic experiments (see **Methods**). **B)** Regression plot correlating plant shoot fresh weight with the estimated mycelium load in matrix samples, using standard curves in (**A**) (Pearson's correlation, non-significant, p-value= 0.835). Work performed together with Nick Dunken (Bachelor student, University of Cologne).

Supplementary Figure 14

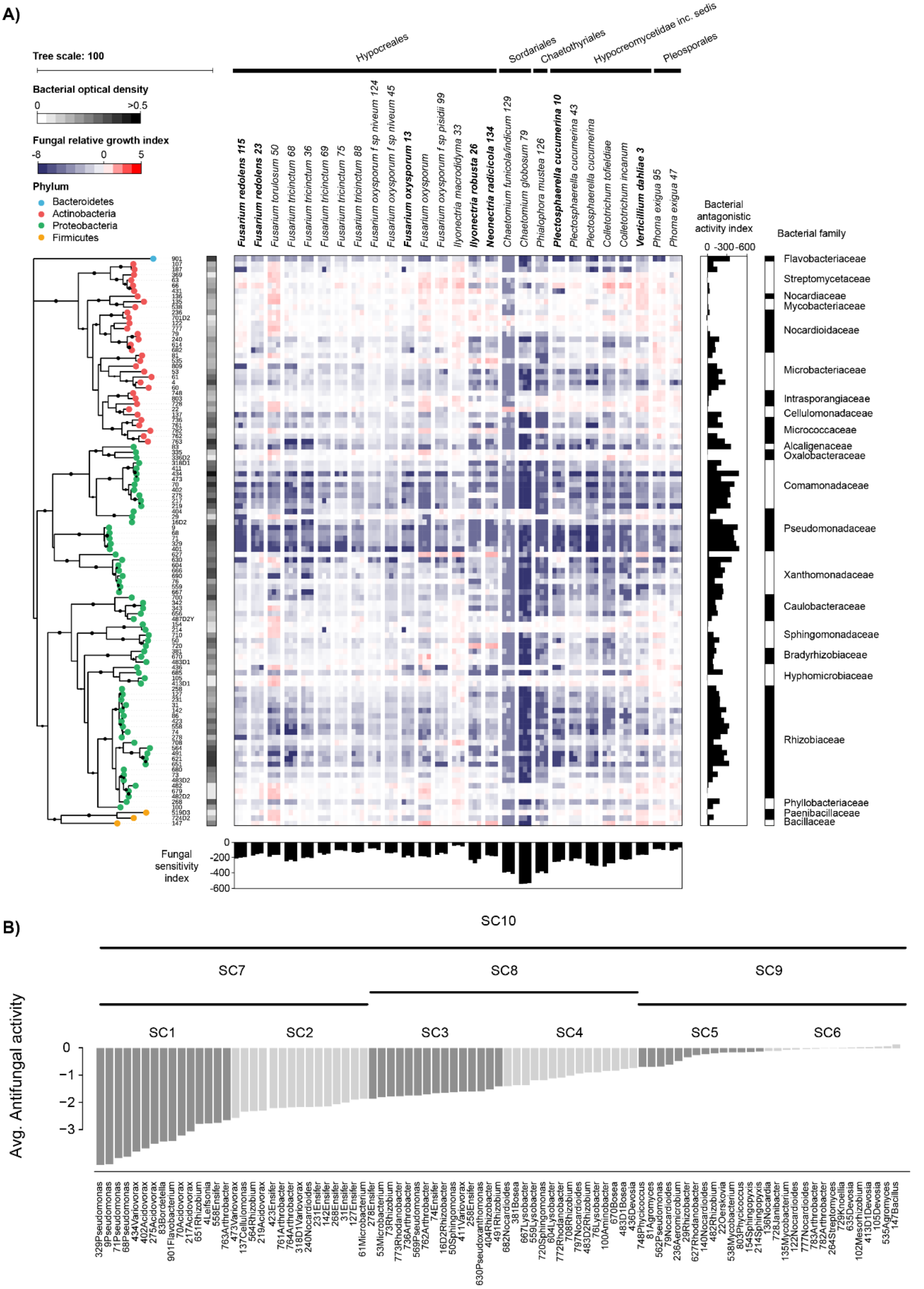

Supplementary Figure 14: Prediction of bacterial communities' antagonism to fungi based on binary interactions. A) (Results and figure by Dr. Stéphane Hacquard). Alteration of fungal growth upon interaction with phylogenetically diverse members of the bacterial root microbiota. The heat map depicts the log2 fungal relative growth index (presence *versus* absence of bacterial competitors) measured by fluorescence using a chitin binding assay against WGA (Wheat Germ Agglutinin), Alexa Fluor 488 conjugate. The phylogenetic tree was constructed based on the full bacterial 16S rRNA gene sequences and bootstrap values are depicted with black circles. Vertical- and horizontal-bar plots indicate the cumulative antagonistic activity for each bacterial strain and the cumulative sensitivity score for each fungal isolate, respectively. Alternation of white and black colors are used to distinguish the bacterial families. All bacteria presented and 7/34 fungi (highlighted in bold) were used for EXP1. **B)** Experimental set-up scheme in order to assess bacterial antagonism against fungi in a community context. Low-diversity subsets of the full bacterial community (SC10) are separated following a fungal antagonism gradient, based on (**A**) (SC1 to SC6, from more to less antagonistic). In order to exclude the possibility that bacterial diversity/load is important for fungal control, higher diversity groups were also selected, following the same gradient (SC7, SC8 and SC9). Bacterial SynComs were inoculated individually or together with the full fungal community, and with sterile *A.thaliana* Col-0 seeds in the FlowPots system, and incubated for three weeks. After this period, shoot fresh weight was assessed as indirect proxy of bacterial antagonism, and root and matrix samples harvested to estimate microbial load in each condition.

Supplementary Figure 15

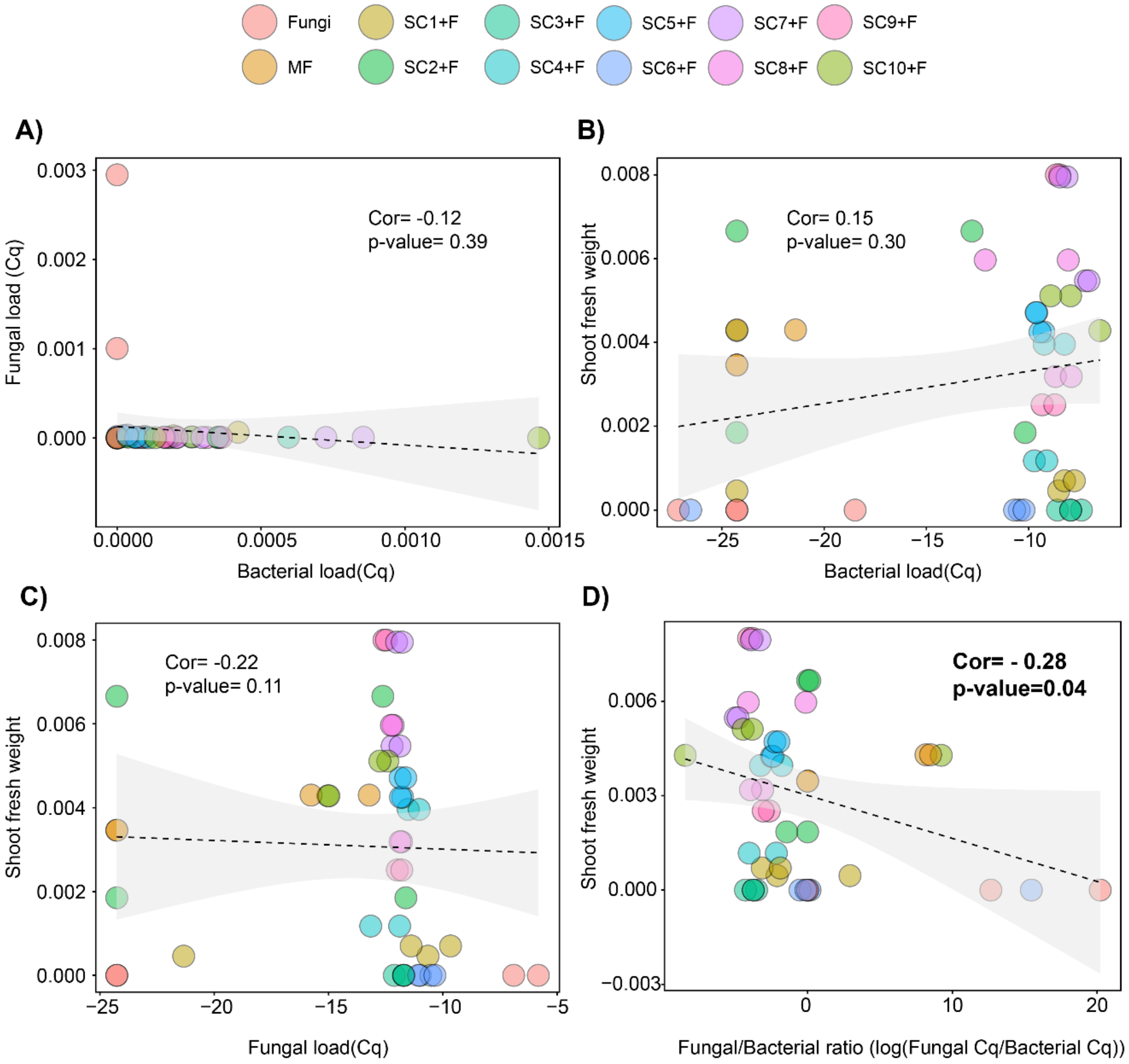

Supplementary Figure 15: Correlations between fungal load, bacterial load and shoot fresh weight. Microbial load was estimated in matrix samples from PERT2 by amplifying by qPCR the 16s rRNA V5/V7 region and ITS1 for bacterial and fungal communities, respectively. Cq values were then normalized to the microbe-free values (MF=1). Here, plots depict the correlation between bacterial and fungal load (**A**), between bacterial load (log(Cq)) and shoot fresh weight (**B**), between fungal load (log(Cq)) and shoot fresh weight (**C**), and between the ratio fungal/bacterial loads (log(Fungal Cq/Bacterial Cq)) and shoot fresh weight (**D**) (Pearson's correlation, non-significant in **A**, **B** and **C**, p-value=0.04 in **D**). Colored dots represent matrix samples from different SynComs (MF=Microbe-free).

Supplementary Figure 16

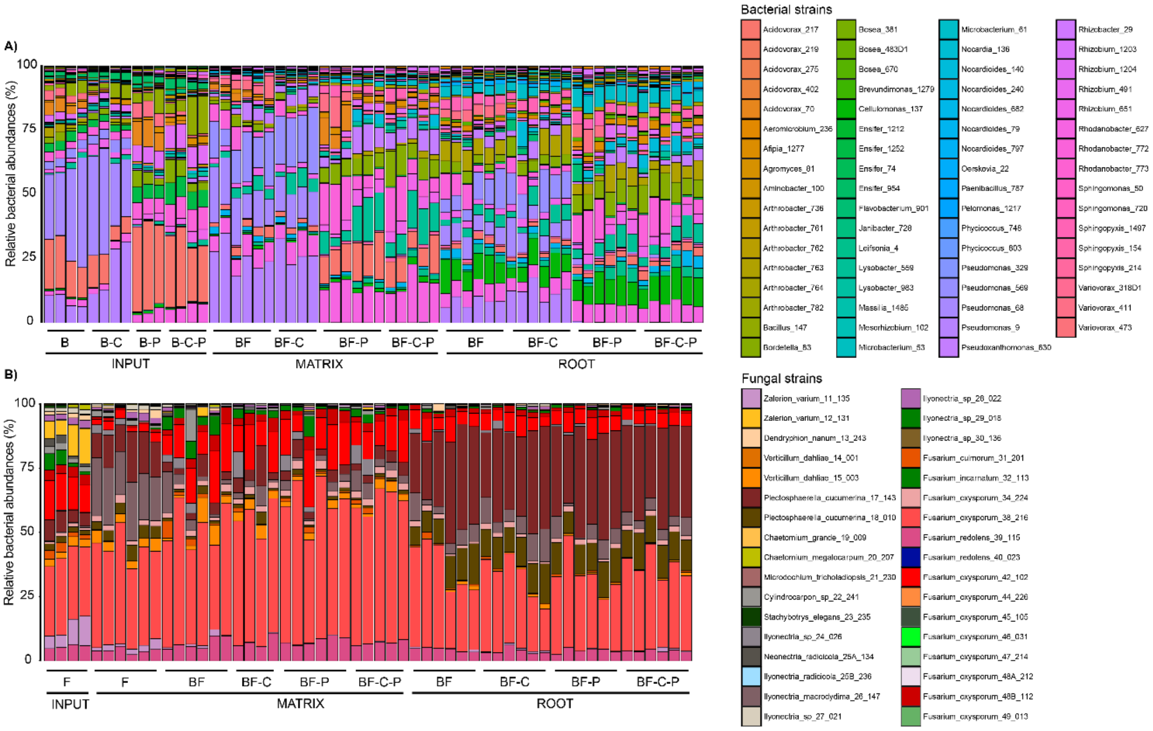

Supplementary Figure 16: Perturbed bacterial communities in PERT3. Relative abundances of bacterial (**A**) and fungal (**B**) strains in each microbial combination of the depletion experiment in input and output matrix and root samples four weeks after inoculation in the Flowpots system. *In-silico* depletion of removed members shows no significant differences from the full bacterial community to different perturbed conditions (Generalized Linear Model, p.adj.method=FDR).

Supplementary Figure 17

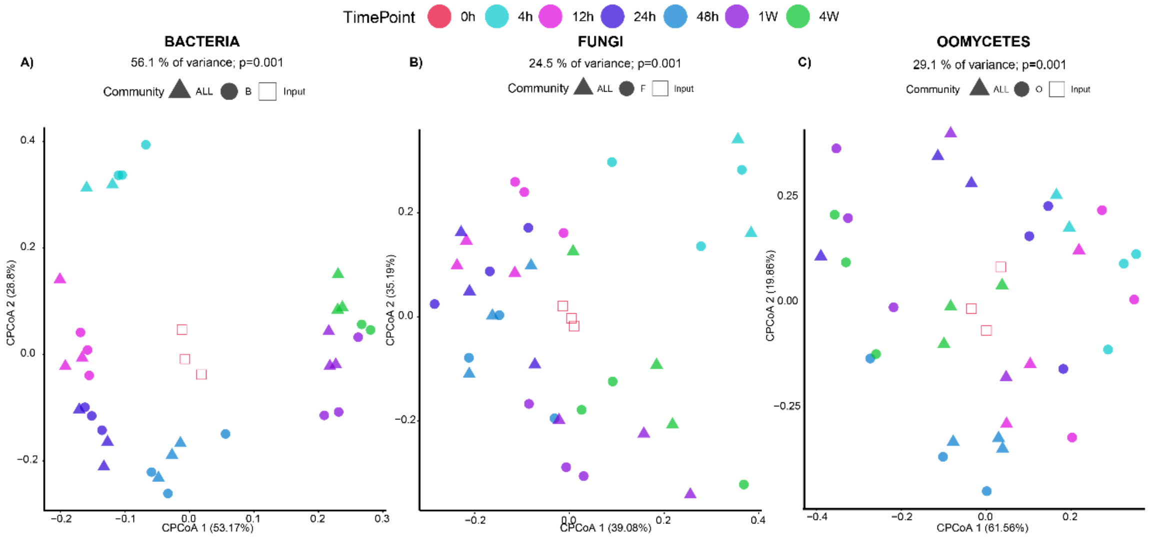

Supplementary Figure 17: Microbial communities' time-dependency. Bray-Curtis distances of matrix samples, plotted in a PCoA plot and constrained by the time-point in which they were harvested (PERMANOVA, percentage of the variance explained by the constrained factor is shown on top of the plot, p-value<0.001). Here, unplanted samples are plotted (TIME1), for bacterial (**A**), fungal (**B**) and oomycetes (**C**) profiles, including single community inoculations (circles) and full community inoculations (triangles), as well as input communities (squares). Different colors represent each time point at which samples were harvested. Here, one technical replicate is shown per each of the three biological replicates.

Supplementary Table 2

Factor	Fraction	Bacteria (V2/V4)	Fungi (ITS2)
Site	All	12.51	14.82
	Soil	43.5	30.82
	Rhizosphere	41.26	33.13
	Rhizoplane	19.96	18.59
	Root	16.64	33.36
Fraction		38.24	5.33
Single/Pooled	All	0.39	0.81
	Soil	0.11	0.17
	Rhizosphere	0.1	0.29
	Rhizoplane	10.27	1.12
	Root	0.67	1.17
Year	All	1.35	9.9
	Soil	3.69	3.2
	Rhizosphere	1.4	2.86
	Rhizoplane	1.45	3.4
	Root	8.2	9.68
Species (*Arabidopsis*/ Neighbors)	Soil	0.68	1.98
	Rhizosphere	0.58	1.77
	Rhizoplane	9.12	9.94
	Root	2.94	1.19

Supplementary Table 5: PERMANOVA analysis of bacterial V2/V4 and fungal ITS2. Permutation analysis of different microbial genomic regions (bacterial 16s rRNA V2/V4 and fungal ITS2). PERMANOVA analysis (999 permutations, p-value< 0.001). Full dataset was used to calculate "Site", "Fraction" and "Single/Pooled" effects; only samples harvested three consecutive years were used to calculate "Year" effect; a subset of single and neighboring plants was used to calculate "Species" effect.

Supplementary Table 5

A) Unplanted matrix samples								
Bacteria			**Fungi**			**Oomycetes**		
Factor	**Var. (%)**	**p-val**	**Factor**	**Var (%)**	**p-val**	**Factor**	**Var (%)**	**p-va**
Community	1.30	0.227	**Community**	1.24	0.491	**Community**	7.94	0.014
TimePoint	63.84	0.001	**TimePoint**	31.81	0.001	**TimePoint**	39.27	0.001
Experiment	1.35	0.674	**Experiment**	3.74	0.253	**Experiment**	1.2	0.905
B) Planted variance								
Bacteria			**Fungi**			**Oomycetes**		
Factor	**Var. (%)**	**p-val**	**Factor**	**Var (%)**	**p-val**	**Factor**	**Var (%)**	**p-va**
Community	2.38	0.026	**Community**	4.17	0.006	**Community**	7.37	0.002
TimePoint	18.47	0.001	**TimePoint**	12.77	0.001	**TimePoint**	4.97	0.189
Experiment	1.98	0.187	**Experiment**	5.15	0.02	**Experiment**	0.7	0.668
Fraction	16.20	0.001	**Fraction**	5.43	0.001	**Fraction**	25.49	0.001

Supplementary Table 5: PERMANOVA analysis of TIME1 and TIME2. Factors driving microbial communities' variance in a time-series experiment, in unplanted matrix samples (**A**) and planted samples (**B**). Factors tested are the effect of other microbial members present, time-dependency, technical variation and fraction (TIME2). PERMANOVA analysis (999 permutations).

Erklaerung

Ich versichere, dass ich die von mir vorgelegte Dissertation selbständig angefertigt, die benutzten Quellen und Hilfsmittel vollständig angegeben und die Stellen der Arbeit - einschließlich Tabellen, Karten und Abbildungen -, die anderen Werken im Wortlaut oder dem Sinn nach entnommen sind, in jedem Einzelfall als Entlehnung kenntlich gemacht habe; dass diese Dissertation noch keiner anderen Fakultät oder Universität zur Prüfung vorgelegen hat; dass sie - abgesehen von unten angegebenen Teilpublikationen - noch nicht veröffentlicht worden ist sowie, dass ich eine solche Veröffentlichung vor Abschluss des Promotionsverfahrens nicht vornehmen werde.

Die Bestimmungen der Promotionsordnung sind mir bekannt. Die von mir vorgelegte Dissertation ist von Prof. Dr. Paul Schulze-Lefert und Dr. Stéphane Hacquard betreut worden.

Köln, Juli 2019

Paloma Durán

Teilpublikationen

Hassani, M.A., Durán, P. and Hacquard, S. (2018) Microbial interactions within the plant holobiont. *Microbiome*, **6**, 58.

Duran, P., Thiergart, T., Garrido-Oter, R., Agler, M., Kemen, E., Schulze-Lefert, P., & Hacquard, S. (2018). Microbial interkingdom interactions in roots promote Arabidopsis survival. *Cell*, **175**(4), 973-983.

Thiergart, T., Duran, P., Ellis, T., Garrido-Oter, R., Kemen, E., Roux, F., ... & Hacquard, S. (2019). Root microbiota assembly and adaptive differentiation among European Arabidopsis populations. *bioRxiv*, 640623.

Acknowledgements

I would like to take this opportunity to thank everybody that has made this thesis possible. First of all, to Stéphane and Paul, for handing me such cool projects to develop and for all the guidance and supervision during these three years. Also, thank you to Marcel Bucher and Juliana Almario for being part of my TAC, and Gunther Döhlemann and Rubén Garrido-Oter for being part of my defense committee.

I would also like to thank Thorsten and Rubén, for the immense help they have given me to analyze all these data, and, more importantly, for all the patience with my not-so-bright questions and for still using R Studio, even though I have been told (repeatedly) not to.

A big thanks goes also to all the collaborators across Europe (Carlos Alonso Blanco, Fabrice Roux, Eric Kemen, Jon Agren, Tom Ellis, and the people in their labs) for a great project together, but specially for hosting us and for all their help in the field. Also, I would like to thank James Kremer for creating the FlowPots, the system that changed everything! Also, Thorsten, Kathrin and Patrick for double-checking the German parts of this thesis.

Also, I want to thank Alfredo, for all the trips together, for all the ups and downs across Europe, for making all the harvestings way more enjoyable and, of course, for the Eurotrip soundtrack.

I would like to thank all the people in the Rooters, Hacquard and RGO groups, because I could not have wished for a better working environment and to be surrounded by so many brilliant minds. But more importantly, I would like to thank you for all the lab outings, the Friday lunches, the scientific and non-so-scientific discussions and all the after-work beers drinks. I would also like to thank Felix and Nick, for the great work and for teaching me just as much as I taught you.

I would like to specially thank the Coffee Breakers: the former members (Simone, Nina, Eva, Amine, Rafal) and the present ones (Amélia, CJ, Rubén, Eik, Rui, Nathan, Kathrin). Even if it all started because of a caffeine and sugar need after lunch, it has become one of the greatest times of the working day. You brought so much laughter and very-much-needed craziness during all this time.

Me gustaría agradecer a Chidi y Cristina, por convertirse en mi segunda familia en el extranjero, por todos los planes guays y por lo muchísimo que nos hemos reído juntos, por aguantar a Kayla y mis calendarios, por la República Checa, por Croacia, y por todo lo que está por venir.

Una de las personas que más ha contribuido a esta tesis y que me gustaría agradecer es Miguel, no sólo por todos los “harvesting” que se ha comido, sino también por aguantarme todos estos años y por decidir que emigrar conmigo merecía la pena.

También me gustaría agradecer a mi familia, la de verdad y la de acogida, por estar siempre ahí, aún en la distancia, apoyándome a lo largo de todo el camino.

Finalmente, me gustaría agradecer a la Fundación de Huérfanos del Cuerpo de la Policía Nacional, por todo el apoyo y oportunidades que me han brindado a lo largo de los años.

Gracias a todos/ Thank you very much!

Curriculum vitae

Persönliche Daten

Name	Paloma Durán Ballesteros
Anschrift	Vogelsangerstrasse 482, 50829 Köln
Geburtsdatum	02.08.1990

Akademische Ausbildung

Seit 10.2014	**Promotionsstudent** am Max-Planck-Institut für Pflanzenzüchtungsforschung, Köln (Deutschland), in der Arbeitsgruppe von Prof. Dr. Paul Schulze-Lefert Thema: “Dissecting the multispecies interaction network at the *A. thaliana* root-soil interface"
2013-2014	**Masterarbeit** an der Universidad de Granada, Granada (Spanien), in der Arbeitsgruppe von Dr. María José Soto Misfutt, CSIC-EEZ Thema: “Effect of the biopesticide 2-TDC (2-tridecanone) on the colonization and molecular communication between the bacterium *Ensifer meliloti* GR4 and alfalfa (*Medicago sativa*). "
2013	**Erasmus Praktikum** am Max-Planck-Institut für Pflanzenzüchtungsforschung, Köln (Deutschland) in der Arbeitsgruppe von Prof. Dr. Seth Davis Thema: "Plant circadian clock and its interplay with phytohormones, using the model plant *Arabidopis thaliana*"
2011-2012	**Erasmus Stipendium** an der Universität Würzburg, Würzburg (Deutschland), in der Arbeitsgruppe von Dr. Frank Waller Thema: "Research of the tripartite interaction between *Serendipita indica-Pseudomonas-Arabidopsis thaliana*"
2008-2013	**Studium der Biologie** an der Universidad de Salamanca, Salamanca (Spanien)

Schulische Ausbildung

2007-2008	**Austauschstudent** an der New London-Spicer Highschool in New London, Minnesota, USA
2004-2007	Gymnasium Wenceslao Benítez, San Fernando, Cádiz (Spanien)

Annex

Due to the size limitations, raw data, as well as **Table 1**, **Table 2**, **Supplementary Table 1**, **Supplementary Table 3** and **Supplementary Table 4**, can be found under:

http://www.at-sphere.com/downloads/Thesis_PDuran_2018.tar.gz